UNIVERSITY OF LEEDS

Effect of Openings on Long-Term Flexural Behaviour of Partially Cracked Reinforced Concrete Slabs

Mohammed Ahmed Abdulrahman

Submitted in accordance with the requirements for the degree of
Doctor of Philosophy

The University of Leeds
School of Civil Engineering

August, 2019

Declaration of Originality

The candidate confirms that the work submitted is his own and that appropriate credit has been given within thesis where reference has been made to the work of others.

This copy has been supplied on the understanding that it is copyright material and that no quotation from the thesis may be published without proper acknowledgement.

The right of **Mohammed Ahmed Abdulrahman** to be identified as Author of this work has been asserted by him in accordance with the Copyright, Designs and Patents Act 1988.

Acknowledgements

First, I owe the successful completion of this work to my **God** who granted me the strength to undertake this work at the weakness and hard times.

The research reported in this thesis was undertaken in the School of Civil Engineering at the University of Leeds, Leeds. My sincere gratitude and profound thanks to my supervisors **Professor John P. Forth** and **Dr Emilio Garcia-Taengua** for their valued contribution and advice. They provided continuous support and motivation during the period of my PhD and related research. I am also thankful to the former tutor **Dr Miller Alonso Camargo-Valero** for his appreciated advice and support.

I would like to express my deepest grateful to the technical staff **Mr. Norman Harmon, Mr. Peter Flatt, Mr. Marvin Wilman, Mr. Stephen Holmes and Mr. Robert Clarke** at the George Earl Laboratory for their continued assistance and support in carrying out of the experimental work. I would like to thank the staff at the **Engineering Graduate Office (EGO)** for their consistent hard working and support throughout the research period. I also express my deep appreciation to those who they developed the computing powerful tools and office word software, without which this research work would not have been completed satisfactorily.

I wish to thank my Iraqi government at **Higher Committee for Education Development in Iraq (HCED)** for giving me the opportunity and assistance to accomplish the PhD studies.

Finally, I would like to express my deepest gratitude to my family for their patience, support and encouragement throughout this PhD research while I was thousands of miles away from home.

Dedication

I dedicate this research work to those motivate me in this world;

To

The soul of my father

Ahmed

To

My beloved mother

To

My dear brothers and sisters

To

All the members of my family

who have been and will always be a source of happiness, motivation and inspiration

Abstract

Slabs are structural members that are primarily subjected to bending and torsion. The analysis of slabs is difficult to perform even if linear elastic behaviour can be assumed. The analysis of slabs arises the difficulty of solving complex governing differential equation. Often slabs can be partially cracked. Load, creep and shrinkage all contribute to deformation and cracking in slabs. The combined effects of these problems complicate the analysis of slabs. Meanwhile, different models in available guidance have been proposed to represent these problems in the analysis with different degree of simplifications. They have been derived originally for beams and one-way spanning slabs. These models in general approximate the deformation without providing an insight into the short-term and long-term behaviour of the members under bending, particularly in the case of slabs. The case is more problematic when openings exist, wherein the existence of such openings will complicate the already complex analysis of slabs. Their influence has not been addressed critically under sustained loading. Accordingly, a more sophisticated method of analysis, considering the effects of these problems, is required.

This thesis presents a new numerical analysis procedure for the nonlinear analysis of reinforced concrete slabs. The layered cross-sectional analysis approach, based on fundamentals of Kirchhoff thin plate theory, is used together with the finite difference method for modelling of slab behaviour. The layered approach permits to include the nonlinear variation of material properties through the depth of the slab, which particularly aims to explore the role of tensile creep. The effects of cracking, tension stiffening, creep and shrinkage of the concrete are considered. The uniaxial stress-strain relationships for concrete and steel are used to model the nonlinear material behaviour, whereas the cracked tensile concrete is modelled as a linear brittle material. A maximum stress criterion has been adopted to represent the onset of cracking. A fixed smeared crack concept is utilized to simulate the crack orientation and propagation. Perfect bond is assumed between concrete and reinforcement. The reinforcement is smeared into a layer between concrete layers. The creep and shrinkage effects have been modelled as additional strains acting gradually on a concrete cross-section, with considering the effect of internal restraint provided by reinforcements.

The accuracy and efficiency of the proposed procedure are then demonstrated by comparisons with the results obtained from experimental tests on full-scale slabs at the University of Leeds. The short-term behaviour of the slabs was monitored until failure, while the long-term behaviour was recorded for a period of 90 days. The proposed procedure showed a reasonable agreement in predicting the load-deflection behaviour of solid slab. On the other hand, for slab with opening, the numerical results were found to have good correlation with test results within the service load range. Based on long-term analysis findings, for slabs with the opening, the method exhibited good agreement with those obtained from the experimental time-deflection curves when the tensile creep is equal to the compressive creep. Conversely, and as unexpectedly, the method presented fit better results with the experimental time-deflection curves of solid slab when the creep coefficient in tension is equal to seven times the creep coefficient in compression.

The verified procedure is used to conduct a parametric study to investigate the effect of different opening sizes on the behaviour of partially cracked slabs under sustained loading. The results showed that when the opening size increases, the instantaneous and long-term deflections increase significantly. On the other hand, the models offered by the CEB-FIP 2010 and Eurocode 2 (BSI, 2004) were also analysed critically. Results revealed that the approaches can predict with reasonable accuracy the load-deflection response and the long-term deflection of the solid slab, but in general the approaches overestimated the theoretical short-term and long-term deflections of the slab with opening. Notwithstanding, the theoretical results based on these approaches showed satisfactory agreement with the measured load-deflection curves within service load range.

Table of Contents

Chapter 1 Introduction 1

1.1 Research Background 1

1.2 Research Significance 4

1.3 Aims and Objectives of the Research Work 5

1.4 Layout of Thesis 6

Chapter 2 Literature Review 7

2.1 Introduction 7

2.2 Types of Slabs 8

2.3 Theoretical Methods for the Analysis of Slabs 9

2.3.1 Finite Element Method 11

2.3.2 Finite Difference Method 14

2.4 Theoretical Background of Thin Plate Theory 15

2.5 Behaviour of Slabs under Combined Effects of Bending, Torsion and Shear Stresses 17

2.5.1 Behaviour of Beams Subjected to Pure Bending Moment 17

2.5.2 Behaviour of slabs 19

2.6 Effect of Openings on the Slab Behaviour 20

2.7 Influence of Openings on Shear Strength of Slabs 27

2.8 Response of Members Post-Cracking 34

2.8.1 Tension Stiffening 36

2.8.2 Tension Stiffening Approaches 38

2.8.3 Factors Influencing Tension Stiffening 43

2.9 Bond-Slip Behaviour 47

2.10 Nonlinear Modelling of Reinforced Concrete Behaviour 49

2.10.1 Smeared Crack Approach 50

2.10.2 Discrete Crack Approach 52

2.10.3 Layered Approach 53

2.11 Time-Dependent Behaviour of Plain Concrete 54

2.11.1 Creep of Concrete 55

2.11.2 Shrinkage of Concrete 57

2.12 Prediction of Creep and Free Shrinkage for Plain Concrete 58

2.12.1 Predictions of Shrinkage and Creep Deformation by CEB-FIP-MC2010 Model 59

2.12.2 Predictions of Shrinkage and Creep Deformation by ACI 209.2R-08 Model 61
2.13 Loss of Tension Stiffening 63
2.14 Tensile Stresses Caused by Restraint to Shrinkage Strains 67
2.15 Modelling of Creep and Shrinkage Curvatures 68
2.16 Instantaneous and Long-term Deflections of Reinforced Concrete Flexural Members 80
2.16.1 Instantaneous Deflection 81
2.16.2 Long-Term Deflection 81
2.17 Summary and Conclusions 83
Chapter 3 Experimental Work 86
3.1 Introduction 86
3.2 Test Set up and Loading 86
3.3 Measurements and Data Processing 90
3.4 Steel Reinforcement 93
3.5 Concrete Mix Proportion and Material Properties 95
3.6 Short-term and Long-term Tests of Small Specimens. 96
3.6.1 Compressive Strength of Concrete 99
3.6.2 Modulus of Elasticity of Concrete 100
3.6.3 Splitting Tensile Strength of Concrete 102
3.7 Creep and Shrinkage Deformations 104
3.8 Summary 109
Chapter 4 Numerical Modelling of Reinforced Concrete Slabs 110
4.1 Introduction 110
4.2 Finite Difference Method 110
4.3 Materials Modelling 112
4.3.1 Uniaxial Compression of Concrete 112
4.3.2 Uniaxial Tension of Concrete 115
4.3.3 Modelling of Long- term Properties of Plain Concrete 116
4.3.4 Steel Reinforcement 118
4.4 Creep Superposition of Concrete 120
4.5 Modelling of Creep and Shrinkage in Reinforced Concrete Sections under Flexural 121
4.6 Modelling of Boundary Conditions and Loads 125
4.7 Mesh Sizes and Convergence Analysis 127
4.8 Assumptions 128

4.8.1 Assumptions of Short-term Analysis....128
4.8.2 Assumptions of Long-term Analysis....129
4.9 Numerical Analysis Procedure....130
4.9.1 Short-term Analysis....131
4.9.2 Long-term Analysis....136
Chapter 5 Results and discussion....139
5.1 Introduction....139
5.2 Experimental Results of Load- Steel Strain....139
5.3 Convergence Analysis....144
5.4 Verification of Short-term Deformation Results with the Proposed Procedure....145
5.4.1 Solid Slab S0....146
5.4.2 Slab S5....153
5.5 Sustained Load Level....161
5.6 Verification of Long-term Movements with the Proposed Procedure....162
5.6.1 Deflection Development with Time....162
5.6.2 Concrete surface tensile strain development with time....174
5.7 Summary....179
5.8 Code-based Models....180
5.8.1 Short-term Deflection....181
5.8.2 Long-term Deflection....183
5.9 Parametric Studies....186
5.9.1 Parameters Considered....186
5.9.2 Influence of Opening Sizes on Deflections....190
Chapter 6 Conclusions and Recommendations....193
6.1 Summary....193
6.2 Conclusions....193
6.2.1 Conclusions Based on the verifications of the numerical method....193
6.2.2 Conclusions Based on the Evaluation of Code-based models....194
6.2.3 Conclusions Based on the Parametric Study....195
6.3 Recommendations and Future Research....196
6.4 References....197

List of Figures

Figure 2-1. Types of slabs 8
Figure 2-2. Discrete modelling of reinforced concrete slab 12
Figure 2-3. Layered modelling of reinforced concrete slab 12
Figure 2-4. Proposed new finite element by (Phuvoravan and Sotelino, 2005) 13
Figure 2-5. Bond stress and changes in neutral axis position in cracked sections. 17
Figure 2-6. Typical moment-curvature diagram for singly reinforced concrete flexural sections 18
Figure 2-7. Typical crack pattern in flat plate slabs (a) at top (b) at bottom by (Subramanian,2013) 19
Figure 2-8. Slabs details 24
Figure 2-9. Uniformly loaded square slab with central opening 25
Figure 2-10. Yield lines and deformations of a simply-supported square slab with an opening at the centre (Ng et al., 2008)....26
Figure 2-11. Yield lines and deformations of a fixed-end square slab with an opening at the centre (Ng et al., 2008) 27
Figure 2-12. Typical punching shear failure 28
Figure 2-13. Experimental tests carried out by (Talbot, 1913) 29
Figure 2-14. Control shear perimeter proposed by different codes 30
Figure 2-15. Schematic drawing of edge slabs with openings 33
Figure 2-16. Cracking propagation of slabs SF0, SF1, and SF3: (a) 40% of ultimate load; (b) 80% of ultimate load; and (c) at ultimate load. 34
Figure 2-17. Moment- average relationship for a reinforced concrete member without shrinkage prior to loading (Gilbert and Ranzi, 2010) 35
Figure 2-18. Member deformation for axial member (Bischoff, 2005)....37
Figure 2-19. Cracks formation at the interface between concrete and reinforcement (Goto, 1971)....38
Figure 2-20 Average tensile stress-strain response of cracked reinforced concrete....39
Figure 2-21. Measured tension stiffening bond factor β response curve (Bischoff and Paixao, 2004)....40
Figure 2-22. Effect of shrinkage on tension stiffening results for 20M bonded specimens ($\rho = 1.9\%$) (Bischoff, 2001)....45
Figure 2-23. Effect of reinforcement ratio on tension stiffening results for $\varepsilon sh = -230\ \mu\varepsilon$ (Bischoff, 2001)....45
Figure 2-24. Moment versus curvature with shrinkage prior loading (Gilbert,2011)....46

Figure 2-25. Influence of creep on bond-slip relationship 48
Figure 2-26. Comparison of FEM and experimental time-dependent midspan deflections 49
Figure 2-27: Tensile stress vs. crack strain diagram (Rots et al., 1985) 51
Figure 2-28. Smeared approaches to crack propagation without remeshing 51
Figure 2-29: Tensile stress of a fracture zone vs. concrete strain (Rots et al., 1985).....52
Figure 2-30. Discrete crack modelling.....52
Figure 2-31. Tensile stress vs. crack opening displacement diagram (Rots et al., 1985).....53
Figure 2-32. Concrete strain components under sustained stress (Gilbert & Ranzi, 2010) 55
Figure 2-33. Schematic diagram of effect of tensile creep on initial concrete stress (Beeby & Scott, 2006) 65
Figure 2-34. Reinforcement inside poured fresh concrete 68
Figure 2-35: Neutral axis depth in un-cracked and gross section 69
Figure 2-36. Neutral axis depth in fully-cracked and gross section.....70
Figure 2-37. Effects of Creep on the stresses and strains with time under constant bending moment fully-cracked (CEB-FIP-MC2010, 2010) 70
Figure 2-38. Restraint provided by symmetrically reinforcement (Gilbert, 2017) 72
Figure 2-39. Shrinkage stresses and curvatures in a sections restrained by a single reinforcement (Gilbert & Ranzi, 2010) 73
Figure 2-40. Shrinkage-induced deformations of plain concrete and symmetrically reinforced members 74
Figure 2-41. Shrinkage-induced deformations of unsymmetrically reinforced member.....74
Figure 2-42. Gradient of shrinkage (Parakash,2018).....75
Figure 2-43. Definition of symbols in introduced by (Ghali, Favre, & Elbadry, 2002) for analysis of effects of creep and shrinkage 77
Figure 2-44. Reinforced concrete (RC) flat slabs under tests (Gilbert & Guo, 2005).....83
Figure 3-1. Testing of short-term specimens: (a) solid slab; (b) slab with opening.....88
Figure 3-2. Long-term test of slabs 89
Figure 3-3. Typical Strain gauge positions for all specimens 90
Figure 3-4. Typical locations of VWG in the tension side for solid slab.....91
Figure 3-5. Typical locations of VWG in the tension side for slabs containing opening.....91
Figure 3-6. locations of LVDT for long-term tested slabs 92

Figure 3-7. Locations of LVDT for short-term tested slabs.....92
Figure 3-8. Average stress-strain curve for steel 93
Figure 3-9. Details of reinforcing steel bars 94
Figure 3-10. Arrangements of reinforcement bars 94
Figure 3-11. Sample preparations of each tested slab.....96
Figure 3-12. Slab specimen being poured and cured 96
Figure 3-13. Creep and shrinkage small specimens 97
Figure 3-14. Relative humidity and temperature for solid slab S1.....98
Figure 3-15. Relative humidity and temperature for all slabs containing opening.....99
Figure 3-16. Modulus of elasticity test of cylinder 101
Figure 3-17. Splitting tensile strength test.....103
Figure 3-18. Comparison of measured and predicted long-term deformation of shrinkage and creep of solid slab S1 105
Figure 3-19. Comparison of measured and predicted long-term deformation of shrinkage and creep of slab S2 106
Figure 3-20. Comparison of measured and predicted long-term deformation of shrinkage and creep of slab S3 107
Figure 3-21. Comparison of measured and predicted long term deformation of shrinkage and creep of slab S4 108
Figure 4-1. Finite difference mesh and nodes.....111
Figure 4-2. Typical uniaxial compressive stress-strain curve and modulus of concrete.....113
Figure 4-3. Uniaxial stress-strain curve for concrete proposed by (Hognestad, 1951).....114
Figure 4-4. Biaxial strength and stress-strain enhancement factor of concrete (Kupfer and Hilsdorf, 1969).....114
Figure 4-5. Uniaxial tensile stress-strain curve of concrete.....115
Figure 4-6. Uniaxial stress-strain curve for typical reinforcement 118
Figure 4-7. Idealized of stress-strain curves of steel.....119
Figure 4-8. Sectional properties of unreinforced and reinforced concrete.....122
Figure 4-9. Shrinkage action at plane element (a), and restraint to shrinkage provided by reinforcement (b) 123
Figure 4-10. Shrinkage and creep action of plane element (a) and changes in curvature and neutral axis at age t (b).....125
Figure 4-11. Representation of boundary conditions for finite differences method by (Szilard, 2004).....126
Figure 4-12. Convergence of FDM (Szilard, 2004) 128

Figure 4-13. Plane stress state of ith element (a), and associated layered transformed cross-section subjected to biaxial bending moment (b) 133
Figure 4-14. Algorithms of current numerical analysis (short-term)..... 135
Figure 4-15. Computation algorithms for current numerical analysis (long-term) 138
Figure 5-1. Measured tensile steel strains for slabs with and without opening 143
Figure 5-2. Load-deflection relationship for different mesh sizes of slab with opening 400x400 145
Figure 5-3. Comparison of measured and predicted deflections of solid slab S0 148
Figure 5-4. Comparison of measured and predicted steel strains of solid slab S0..... 152
Figure 5-5: Comparison of measured and predicted deflections of slab S5..... 157
Figure 5-6. Comparison of measured and predicted tensile steel strains of slab S5..... 161
Figure 5-7. Comparison of long-term deflections of solid slab S1 163
Figure 5-8. Comparison of measured and predicted long term deflections of slab S2..... 167
Figure 5-9. Comparison of measured and predicted long term deflections of slab S3..... 170
Figure 5-10. Comparison of measured and predicted long term deflections of slab S4..... 173
Figure 5-11. Comparison of measured and predicted long-term concrete surface tensile strain of solid slab S1..... 175
Figure 5-12. Comparison of measured and predicted long-term concrete surface tensile strain of slab S2 177
Figure 5-13. Comparison of measured and predicted long-term concrete surface tensile strain of slab S3 178
Figure 5-14. Comparison of measured and predicted long-term concrete surface tensile strain of slab S4 179
Figure 5-15. Comparison between measured and calculated short-term deflections for slab S0. 182
Figure 5-16. Comparison between measured and calculated short-term deflections for slab S5. 182
Figure 5-17. Comparison between measured and calculated long-term deflections for slab S1. 183
Figure 5-18.Comparison between measured and calculated long-term deflections for slab S2. 184
Figure 5-19. Comparison between measured and calculated long-term deflections for slab S3. 185

Figure 5-20. Comparison between measured and calculated short-term deflections for slab S4. 185
Figure 5-21. Creep coefficient based on CEB-FIP MC-90 187
Figure 5-22. Shrinkage strain based on CEB-FIP MC-90 187
Figure 5-23. Schematic of reference slab 189
Figure 5-24: Schematic of slabs with different opening sizes 190
Figure 5-25. long-term deflections of slabs 191
Figure 5-26. Instantaneous and long-term deflections of slabs 192

List of Tables

Table 3-1: Experimental results for concrete mechanical properties.....87
Table 3-2: Properties of steel reinforcement bars 93
Table 3-3 : Proportions of concrete mix. 95
Table 3-4: Experimental results for concrete compressive strength test.....100
Table 3-5: Measured and estimated results for concrete modulus of elasticity. 102
Table 3-6: Measured and estimated results for concrete spitting tensile strength. 104
Table 5-1: Parametric study considerations. 188

Chapter 1 Introduction

1.1 Research Background

Slabs are the most commonly used structural members in a building; they support and transmit the vertical loads to the supporting systems. The design of reinforced concrete slabs is incomplete until all strength and serviceability criteria are satisfied. As slabs are thin compared to beams, the serviceability limit state of deflection is usually critical in the design rather than the ultimate limit states. In addition, the change in design philosophy and the introduction of high strength materials lead to smaller sections, having less stiffness that can result in higher stresses and larger deflections. Moreover, one of the most important considerations that come into play in the design process of slabs is the existence of the opening, which will complicate the already complex slab behaviour. Opening reduces the slab stiffness and, in turn, this usually leads to increase in initial stress and deflection. As a result of the aforementioned aspects, a sound understanding of the deflection behaviour of slabs at the service loads is extremely important.

The deflection of a flexural member increases with increasing external load. The degree of cracking will also have a significant effect on deflections. Concrete cracks at relatively low load levels, wherever and whenever the tensile stresses exceed the concrete tensile strength, causing a nonlinear structural response. However, only parts of the length of member are usually cracked. The ability of the active tensile concrete, however, between the cracks to contribute to the overall post-cracking stiffness of a member is known as tension stiffening. In addition to the aforementioned reasons, creep, shrinkage (in the case of asymmetric reinforced cross-section) and tensile stress loss of concrete are the main factors that effectively increase the deflection of the flexural member under sustained load. Meanwhile, different expressions in available codes have been proposed for modelling these problems in deflection calculations with different degree of simplifications. Most of these expressions are based on empirical and semi-empirical formulations, and hence they do not have a strong theoretical basis. Furthermore, the creep effect in flexural members has been modelled on

the basis of creep in tension and compression are the same; in fact, it has recently been shown that they are not equal.

Deflection of the slabs is almost always the governing design consideration that should be controlled. In several design codes, including (BS8110-1:1997; Eurocode2, 2004), there are two basic approaches for deflection control; the provisions of allowable span-depth ratios, and calculation of deflection. Furthermore, the (ACI 318-14) code provides two methods for deflection control; the simplest method is deflection control of members by satisfying the provisions of minimum thickness, and by the calculation of deflection that is limited to a specified value. However, the provisions provided in the design codes usually involve simplified and predefined values of certain relevant design parameters, as well as they do not consider the most important parameters that play significant roles on the long-term behaviour of the members. Such provisions may not be suitable for all design situations. They are not suitable for unusual structural arrangements, such as irregular patterns of loading or presence of openings in flat slabs, or when an accurate assessment of deflection is required (Concrete Society, 2005). Therefore, the designer may choose to calculate the deflections and then check that these deflections are less than specified allowable limits. However, the calculation of deflections for slabs is challenging even if linear elastic behaviour can be assumed (ACI 318-14).

Design codes usually provide methods that are based on the calculation of effective stiffness or effective curvature of the members between un-cracked and fully-cracked states in order to calculate instantaneous and long-term deflections, except ACI 318-14 multiplier approach, for cracked beams and one-way spanning slabs. A critical review of previous research revealed that the behaviour of beams is very different from that two-way slabs. The calculation of two-way slab deflections creates the dual difficulties of solving complex governing differential equation as well as considering the effects of cracking, creep and shrinkage. Instead, a number of approximate methods are available to calculate the deflections of two-way slabs, based on crossing-beam analogy, by considering separately the slab deformations in each direction. The contributions of deflection in each direction are then added to obtain the total deflection. While often methods are suitable for design purposes, they do not adequately provide

an insight into the realistic flexural behaviour resulting from the variation of material properties throughout the cross-section. In addition, such methods are not suitable for possible design situations- of particular importance here is the existence of opening in the slabs. However, the development of high speed digital powerful tools has made it possible to solve such problems numerically.

Finite element models have been developed to account for long-term deflections of reinforced concrete members (ASCE,1982). Nevertheless, it is not straightforward to obtain realistic estimates of deflections using linear elastic finite element analysis since cracking increases long-term deflections in addition to shrinkage and creep (Concrete Society, 2005). Although several available finite element software packages provide nonlinear cracking analysis, the calculation procedures for shrinkage and creep are not performed with such analysis. Furthermore, the finite element analysis does not take into consideration the effect of tensile stresses, before loading, due to shrinkage constrained by bonded reinforcement. In addition, it does not consider the inequality between tensile and compressive creep development under similar sustained stress. Alternatively, the need for a reliable and appropriate techniques for modelling the various factors that affect the slab behaviour is essentially required. The most general method to assess deformations is to perform a nonlinear analysis capable of computing the instantaneous and long-term deformations, taking into consideration the effects of applied load, the nonlinear behaviour of steel and concrete, and time-dependent material deformations due to creep and shrinkage of concrete (CEB-FIP Model Code 2010).

Over the last 60 years, a great deal of experimental and theoretical works has been carried out to identify the deflection behaviour of beams and one-way spanning slabs. The great majority of this work has been related to the short-term flexural behaviour. In addition, a number of studies have investigated the flexural strength, cracking and deflection of two-way slabs, but this is not so for long-term behaviour which is usually of importance in practice rather than the short-term behaviour, and hence this is the area where a better understanding would be of value. Relatively few studies have been carried out to provide an understanding of the long-term behaviour of slabs. However, no attempt has been done to establish the long-term behaviour of slabs with existence of the opening. In

reality, experimental investigations alone will not therefore sufficiently distinguish the influence of each relevant parameter on the long-term behaviour.

Therefore, this thesis presents a new method that can be used to model and analyse the slabs by using the finite difference method along with the layered approach. The application of this new method in the present study does involve the use of existing principles in a way that has not been previously reported. The method avoids the oversimplification in the existing structural design codes that can significantly affect the accuracy of the analysis. An experimental program has been carried out in order to verify the accuracy of the proposed method. The study presented in this thesis will give a valuable understanding of identifying the role of tensile to compressive creep ratio on the long-term movements at possible design situations. Furthermore, it will contribute to offering a clear picture of the influence of the opening on the slab behaviour in the case where the current recommended models and provisions do not address the sensitivity of slab deflections with such problems.

1.2 Research Significance

The structural design codes usually involve simplified approaches to model the long-term effects that influencing the member behaviour. In addition, codes provide simplified models for estimating the slab deformations that are suitable for simple configurations. So far, no specific analysis related to the effect of the opening in reinforced concrete slabs is known to the author. This calls for further attempts for modelling the slabs with incorporation of long-term effects, taking into consideration the existence of the opening. The key focus in this research is to contribute to knowledge by introducing a proper numerical analysis technique. The technique is capable of modelling and analysing the slabs with complex design situations, that is, the existence of the opening. This technique can be considered as a basis for the next generations of models that deal with cracking and long-term effects on the slab behaviour.

1.3 Aims and Objectives of the Research Work

The aim of this research is to introduce a new numerical analysis procedure that can accurately predict the short-term and long-term behaviour of partially cracked reinforced concrete slabs under potential design conditions. In particular, the emphasis is to identify the influence of the opening on the slab behaviour under sustained loading. The research also is aimed to address the influence of tensile to compressive creep ratio on the long-term behaviour of slabs. The following objectives are summarized to achieve the general aims of this research:

- Carry out a review on the current state of the literature on the behaviour of slabs with and without openings. Moreover, to further focus on the main phenomena that affect the long-term behaviour of reinforced concrete members, i.e. the effect of time-dependent cracking, tension stiffening, creep and shrinkage of concrete. Also, to conduct a brief review on finite difference and finite element methods.
- Design the experimental set-up, i.e. to determine the size of the slab and reinforcement, sizes and desired location of openings, the experimental loading frame and the instrumentation.
- Introduce a new numerical analysis procedure that is capable of simulating the slab behaviour together with the incorporation of the main relevant phenomena that reflects the effect of tension stiffening, time-dependent cracking, creep and shrinkage of concrete.
- Conduct experimental tests on full-scale reinforced concrete slabs to demonstrate the applicability of the presented procedure by comparisons the solutions with the laboratory data.
- Perform a series of numerical experiments by using the verified method to investigate the effect of various opening sizes on the long-term deflections of partially cracked reinforced concrete slabs.
- Evaluate the effectiveness of the existing expressions proposed by design codes (CEB-FIP-MC2010, 2010) and (Eurocode2, 2004) for estimating the deflections of cracked two-way slabs.
- Introduce a set of recommendations to establish further relevant researches.

1.4 Layout of Thesis

Chapter 1 – General background of the research program, highlights the research significance and outlines key aims and objectives.

Chapter 2 – Based on the research area, this chapter presents a brief review of current literature on the behaviour of reinforced concrete slabs with openings. Moreover, it gives a brief review of current literature on the parameters that influencing the member behaviour such as cracking, tension stiffening, creep and shrinkage of concrete. Moreover, provides various types of concrete cracking models.

Chapter 3 – Gives detailed description of the experimental program, details of the specimens, the test set up, mechanical properties, long-term creep and shrinkage tests of concrete specimens.

Chapter 4 – Presents the details of the numerical modelling of the reinforced concrete slabs. The methods for modelling of short-term and long-term material properties are included. The procedure of modelling creep and shrinkage deformation for reinforced concrete slab is presented. The numerical analysis procedure carried out as a part of this study is given.

Chapter 5 – The detailed behaviour of each tested slab is presented individually. The accuracy of the numerical analysis procedure is examined under worst design scenario by verifying the numerical results with the laboratory data, both in terms of load-deformation and long-term movements, towards fulfilment the set of the objectives. The effectiveness of building code models for prediction of short-term and long-term deflections are introduced. Parametric study to identify the influence of openings of varying aspect ratios subjected to sustained load is also presented.

Chapter 6 –The conclusions drawn from the present study as well as recommendations for future studies are summarized.

Chapter 2 Literature Review

2.1 Introduction

Reinforced concrete is a composite material that consists of steel and concrete. Unfortunately, the nature of reinforced concrete alters with time and with loading, and this will therefore affect the member stiffness and deformation. Over the last few decades, a considerable deal of interest has been made to investigate the short-term and long-term behaviour of beams and one-way slabs, and nowadays there is much ongoing research on the subject but there is a little research published in literature to provide an understanding on the behaviour of slabs.

However, no attempt has been reported about the long-term behaviour of slabs with the existence of opening. When the openings in reinforced concrete slabs are introduced, the large difference exists between the distribution of elastic theory moments and the distribution of design moments. Hence, to correctly understand and analyse the complex problem ascertained by the presence of openings, it is important first to understand the behaviour of slabs with and without openings, and second to understand thoroughly the response of reinforced concrete members post-cracking and the concrete properties with time as well as their effects on the flexural members.

In this chapter, a review on the slab types and the effect of the opening on their behaviour have been included. Brief review on the theory of elasticity, and the assumptions of classical thin plate theory have been presented. The response of reinforced concrete members post-cracking has been discussed. The development of creep, shrinkage, loss of tension stiffening and their effect on the flexural members have been presented. The review of different methods for modelling the concrete cracking in the analysis has been introduced. Finally, a summary from those studies, which are reviewed in this chapter, is provided to highlight the existing gaps in knowledge.

2.2 Types of Slabs

A reinforced concrete structure has several members in the form of columns, beams, slabs, and walls that are connected to form a structural frame. Slabs are the most widely used structural elements whose thickness is much smaller than their other dimensions. They are often used as roofs and floors in buildings. Depending on their dimensions and support conditions, they are classified as one-way or two-way slabs. Two-way slabs are those in which the load is carried on both spans, while in one-way slabs the load is mainly carried on the shorter span. Slabs are generally categorized into flat slabs, flat plates, waffle slabs, and two-way solid slabs supported by beams as shown in Figure 2-1.

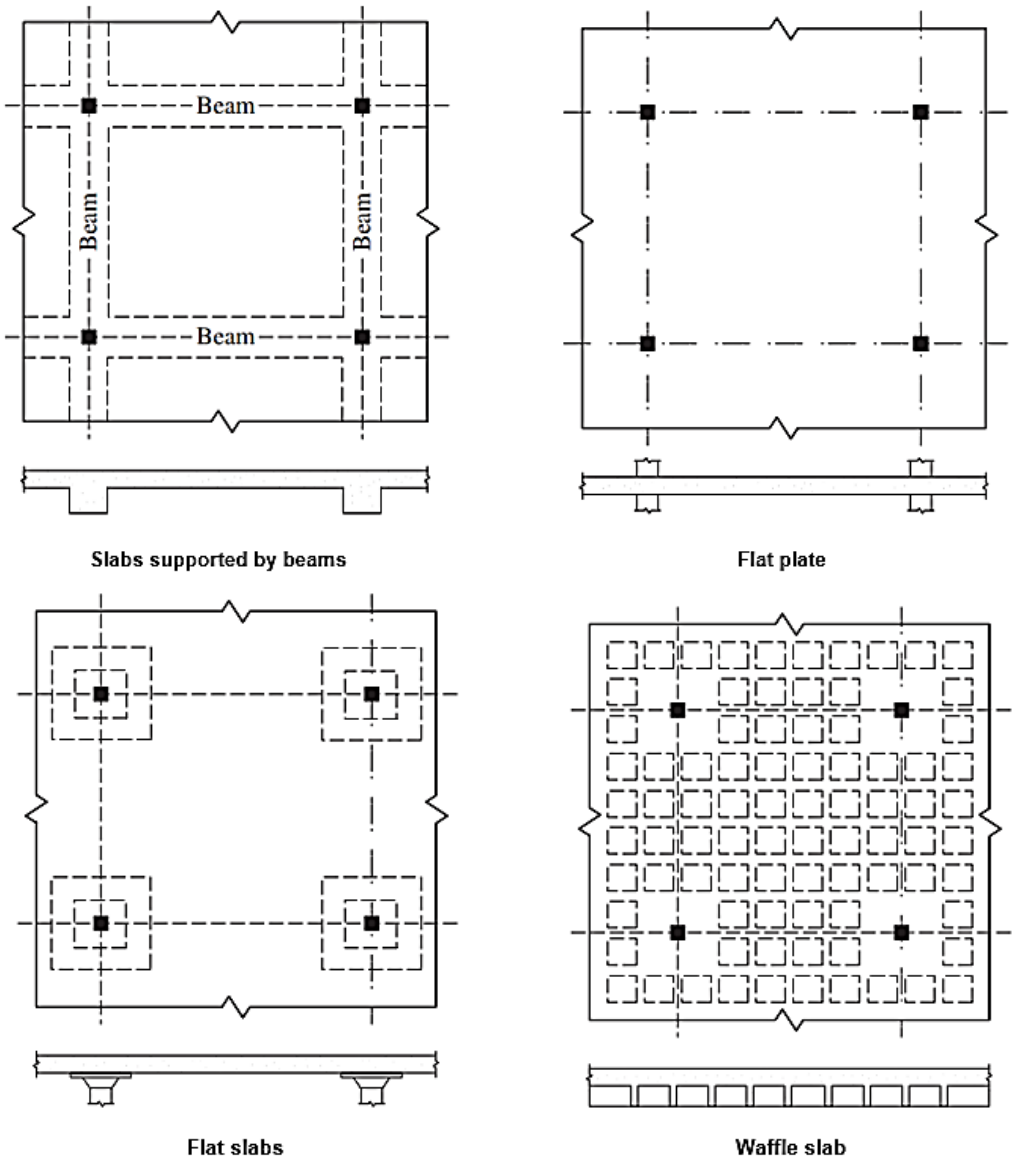

Figure 2-1. Types of slabs

The flat plate is an extremely simple structure which supported directly on columns without beams, while flat slab is supported on columns with existing of drop panels or column capitals. Although their low stiffness, they are one of the most popular and efficient floor systems and, however, they are difficult to analyse. Slabs supported on beams on all sides are generally referred to two-way slabs supported on beams. When a slab is supported other than on two opposite sides only, the precise amount and distribution of the load taken by each support, and consequently the bending and torsional moments, are not easily computed. Determination of these forces acting on the slabs, with various loading and boundary conditions, is very important during the design stages. Normally, the first step in design process is to perform ultimate limit state analysis; then the serviceability limit state is verified. Slabs are particularly designed to resist bending and torsional moments and shearing forces. In many cases, however, the serviceability limit state of deflection is usually critical in the slab design rather than the ultimate limit states. In order to determine the deformation and internal forces that are used to design the slab, approximate theoretical analyses are generally required.

2.3 Theoretical Methods for the Analysis of Slabs

Usually, analysis results of slabs depend primarily on the geometry, boundary conditions, sectional properties and load pattern. Analysis of slab means the determination of deflection, stress, bending and torsional moment distribution at various points of interest. Generally, the exact analysis of a slab, having an arbitrary support conditions and geometry, due to a general arrangement of loading is extremely complex. Therefore, there are a number of possible approaches to the analysis of two-way slab systems, which including the following:

- Linear elastic analysis for plates (classical solutions, finite difference method).
- Plastic or limit analysis (yield-line theory).
- Finite element method (FEM).
- Equivalent frame method (EFM).

- Simplified methods of analysis (moment coefficient method, direct design method).
- Modifications to elastic and limit analysis theory.

Most of the analysis and design procedures for slabs are frequently based on empirical or semi-empirical considerations, particularly, equivalent frame method and direct design method. These procedures were derived particularly from the elastic theory in combination with limit analysis and experimental data. When the realistic representation of the behaviour of slabs at the ultimate limit state is required, the yield-line theory is more suitable to adopt.

Yield-line is a limit analysis method derived for the slab design. The method requires the designer to postulate collapse mechanisms, for calculating ultimate limit load of a given slab system. The most informative contributions to the collapse analyses of reinforced concrete slabs have been made by British researchers, in particular the work of Wood at the Building Research Station (McNeice,1967). Although such method enables the maximum resistance moment for a given pattern of failure to be determined, they do not consider whether the yield-line pattern is the critical one. Yield-line theory alone cannot predict serviceability limit state behaviour, deflections and associated crack widths may be increased significantly (Concrete Society, 2005). In the Johansson's method, the torsional moments on the slab of each yield-line are assumed to be zero. Despite these disadvantages, yield-line theory is extremely useful and easy to solve problems. Moreover, the theory may be useful for designing slabs of unusual shapes or boundary conditions.

Basically, plate theory and yield line theory are commonly used to analyse slabs spanning in two-way directions. Theory of plate is based on linear elastic analysis, while yield-line theory denotes the behaviour of the slab is considered as collapse state. The so-called exact theory of the elastic bending of plates is derived originally from the work of Lagrange in 1811, who produced the governing differential equation for bending in plates. Among most contributors in the derivation of plate theory, Kirchhoff's classical thin plate theory yields sufficiently accurate results (Szilard,2004).Solutions of the plate equation for specific geometries and boundary conditions have been given by (Timoshenko and

Woinowsky-Krieger,1959).Unfortunately, the analytical solutions of the governing differential equations are limited to simple design situations while in many realistic cases such equations are difficult to solve analytically. However, several numerical methods have been devised to solve such problems; finite element and finite difference methods are most widely used.

2.3.1 Finite Element Method

The finite element method is a numerical application that can be used to obtain solutions to various engineering problems. Principal researchers into the development and application of finite elements have been (Clough,1965) in the United States and (Zienkiewicz,1965; Zienkiewicz,1967) in the United Kingdom. The finite element method gives an exact mathematical solution to an approximate continuum. It applies a physical discretization in which the actual continuum is replaced by an assembly of discrete elements, referred to as finite elements, connected together to form two-dimensional or three-dimensional structure. It is used to replicate the real structure by idealizing a three-dimensional system in order to simulate the actual behaviour under experimental conditions. The finite element procedure produces many simultaneous linear or nonlinear algebraic equations which are generally solved by powerful tools to determine nodal displacements. Hence, the use of finite element method will generate a coefficient matrix that is much large with many unknowns and results in errors. Few plate bending problems had been attempted until 1964 when British academics began examining the method and applying it to slab problems. Subsequently, the first application of finite element method to elastic-plastic plate bending analysis has been made by (McNeice, 1967).

Finite element procedures for the three-dimensional analysis of reinforced concrete structures have been available for several years. The analysis of reinforced concrete slabs using this method has been the subject of intensive investigation since 1970s. The most informative contribution to the bending analysis of reinforced concrete slabs by the finite element method has been introduced by (Jofriet and McNeice,1971). Extensive research has been done in recent years on finite element representations to replicate reinforced concrete elements. In general, two techniques exist for modelling of reinforced concrete, namely the discrete modelling and the layered modelling. With respect to former,

concrete is modelled by three-dimensional solid elements while the reinforcing steel is modelled by one-dimensional truss elements as shown in Figure 2-2

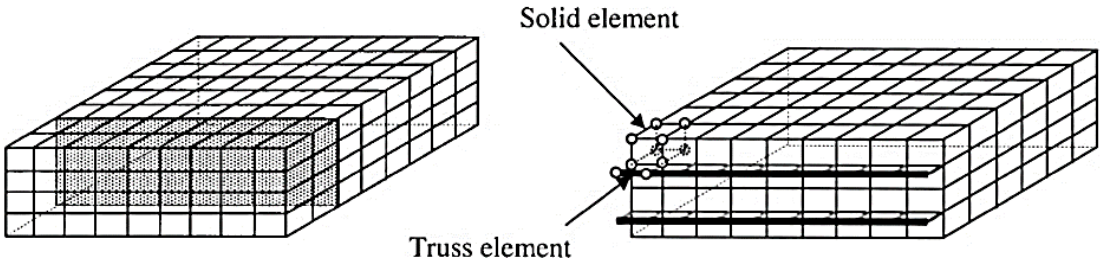

Figure 2-2. Discrete modelling of reinforced concrete slab

A major disadvantage of discrete modelling technique is that the mesh boundary of the concrete element must overlap the direction and location of the steel reinforcement. Therefore, the layered modeling comes into play now. In this case, concrete is divided into a set of parallel layers along the thickness of plate, while the reinforcing steel is assumed to be smeared into a layer between concrete layers as shown Figure 2-3. Then, the total stiffness of a layered element consists of the stiffness of the concrete and the stiffness of the steel reinforcement. With smeared concept, the reinforcement is often described by the reinforcement ratio and it has stiffness only in the direction of reinforcement. When the reinforcement is assumed to be smeared, a full compatibility between concrete and steel is naturally enforced. Thus, it does not permit the interface behavior such as bond-slip to be explicitly modelled. The main advantage of this technique is that the three-dimensional slab is simulated as a set of two-dimensional layers. Moreover, the variation of stress along the slab thickness can be modeled.

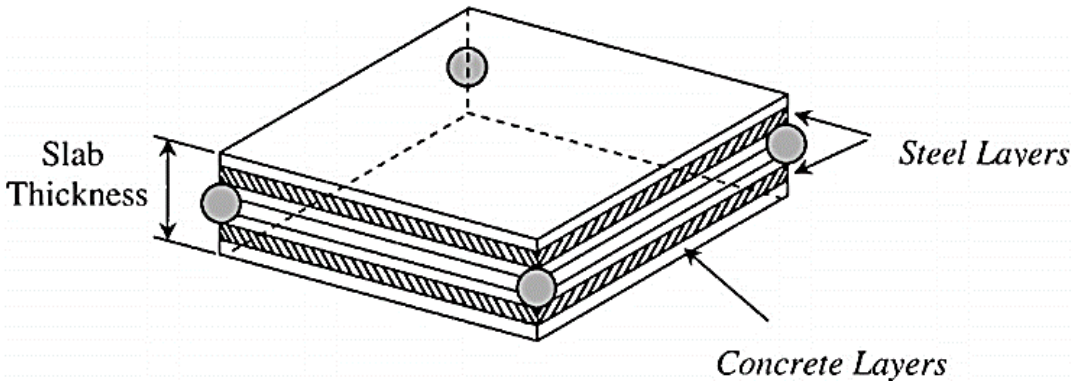

Figure 2-3. Layered modelling of reinforced concrete slab

More recently, a new finite element based on combination of two elements was developed by (Phuvoravan and Sotelino, 2005) to model reinforced concrete slab. The concrete was modelled using four-node Kirchhoff shell element, while the reinforcement bars was modelled using two-node Euler beam element as illustrated in Figure 2-4. The connectivity between concrete shell element and reinforcement beam element was achieved by means of rigid link. The stiffness and resisting forces from the reinforcement were implicitly included in this new finite element.

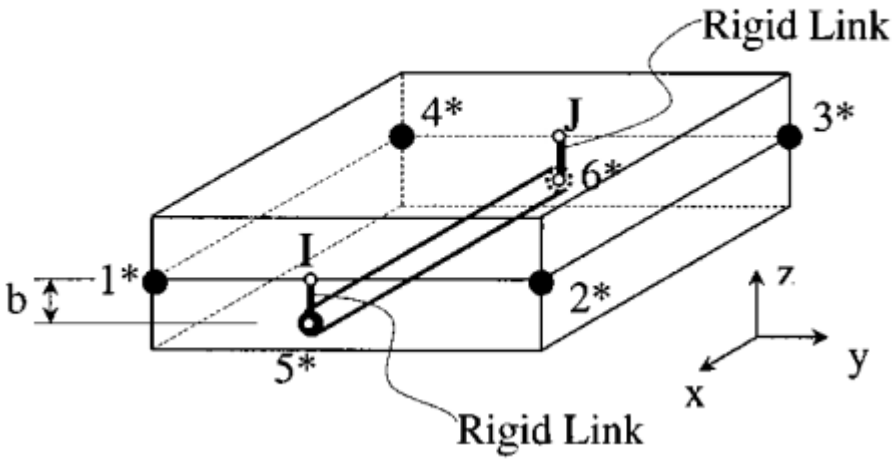

Figure 2-4. Proposed new finite element by (Phuvoravan and Sotelino, 2005)

It is seen from the foregoing features of finite element method that it is possible to analyse the members under various load pattern and geometry. Unfortunately, the nature of reinforced concrete changes with loading and with time. Therefore, it is not straightforward to obtain a realistic estimate of deformations using linear elastic finite element analysis since cracking increases the deformations in addition to material nonlinearity. Finite element method provides an option to include the changes in the section properties due to cracking and material nonlinearities using the stiffness modification procedures. In spite of these advantages, this method is not suitable for design as it is time-consuming, since a large number of degrees freedom is required. In general, finite element method is particularly useful in the assessment of deflections or checking structural performance of slab systems when there are irregular geometries and/or holes

(Concrete Society, 2005). However, any such analysis that does not include the effect of cracked section stiffness will considerably underestimate the deflections.

As already stated, the reinforced concrete characteristics change with loading and with time. Some finite element programs modify the global plate stiffness to account for cracking, creep and shrinkage effects (Concrete Society, 2005). Although the available finite element software packages provide nonlinear cracking analysis, the calculation procedures for shrinkage and creep are not performed with nonlinear cracking analysis. Furthermore, the finite element analysis does not take into consideration the restraint stresses due to early shrinkage restraint by reinforcement. In addition, such analysis method does not consider the variation of concrete creep through the depth of flexural sections.

2.3.2 Finite Difference Method

The finite difference method is another common approach of oldest numerical methods for solving partial differential equations. It is the most general and clear, particularly, in the problems of plate bending analysis. The finite difference method gives an approximate mathematical solution to the exact continuum. It operates directly by replacing the set of differential equations into a series of simultaneous linear algebraic equations at each node. The finite difference method has been used in solving differential equations for structural analysis of continuous beams or plates loaded out of plane or in plane. As a computational method, the finite difference method together with finite element method originated in the engineering literature in the since 1950s. Using this method, a complete structural modelling and analysis can be carried out based on linear elastic theory. Usually, the use of finite difference method generates a coefficient matrix that is fewer than that generated using the finite element method. Recent studies have demonstrated the capability of the finite difference method in the analysis of reinforced concrete structures using physical or geometrical nonlinearity approach to evaluate the cracking, ultimate load, steel-concrete bond-slip, deflection and buckling (Lima et al.,2014). The studies indicated that the comparisons with experimental tests confirm the validity of the method as well as the finite difference analysis procedure is both accurate and fast running, and most suitable for design office application, combining the speed of analysis and the accuracy of finite element analysis (Jones et al., 2009).

2.4 Theoretical Background of Thin Plate Theory

The classical theory of plates is an important and special application of the theory of elasticity, which formulates and solves equations of plate problems from a rigorous mathematical analysis. Mathematically, exact stress analysis of the plates loaded normal to their surface requires solution of the differential equations of three-dimensional (Flugge, 1962). Among most contributors in the derivation of plate theories, Kirchhoff's classical theory of thin plates gives sufficiently accurate results without three-dimensional stress analysis (ignoring transverse shear stresses). The governing fourth order differential equation for thin plate deflection analysis has been derived based on Kirchhoff's assumptions. The main assumptions used in the derivation of the differential equation of thin plate are based on the following:

- The plate is initially flat.
- The material of plate is homogenous, linear elastic and isotropic
- The thickness of plate is small compared to other lateral dimensions, the smallest lateral dimension of the plate is at least ten times larger than its thickness.
- The transverse deflections are small compared to the plate thickness $(\omega \leq 0.2\mathrm{h})$.
- The deflection of the plate is produced by displacement of points normal to its horizontal plane.
- Deformations due to transverse shear are neglected $\sigma_z \& \epsilon_z = 0$.
- The deformations are, initially normal to the middle surface, remain straight and normal to the middle plane before and after deformation.

The distribution of moment for Kirchhoff's thin plate theory can be obtained from the following expression:

$$\frac{\partial^2 \mathrm{m_x}}{\partial \mathrm{x}^2} + 2\,\frac{\partial^2 \mathrm{m_{xy}}}{\partial \mathrm{x}\;\partial \mathrm{y}} + \frac{\partial^2 \mathrm{m_y}}{\partial \mathrm{y}^2} = -\mathrm{p_z}(\mathrm{x},\mathrm{y}) \qquad (2\text{-}1)$$

In the thin plate theory, the normal stresses can be expressed in terms of displacement as in the following equations:

$$\sigma_x = \frac{E}{1-v^2}\left(\frac{\partial^2 w}{\partial x^2} + v\frac{\partial^2 w}{\partial y^2}\right) \quad (2\text{-}2)$$

$$\sigma_y = \frac{E}{1-v^2}\left(\frac{\partial^2 w}{\partial y^2} + v\frac{\partial^2 w}{\partial x^2}\right) \quad (2\text{-}3)$$

Thus, the resulting moment can be obtained in term of displacements by integration of equations (2-2) and (**2-3**) through the plate thickness. Therefore, the moment-curvature relationship can be obtained from the following equations:

$$m_x = -\frac{E\,h^3}{12(1-v^2)}\left(\frac{\partial^2 w}{\partial x^2} + v\frac{\partial^2 w}{\partial y^2}\right) = -D\left(\frac{\partial^2 w}{\partial x^2} + v\frac{\partial^2 w}{\partial y^2}\right) \quad (2\text{-}4)$$

$$m_y = -D\left(\frac{\partial^2 w}{\partial y^2} + v\frac{\partial^2 w}{\partial x^2}\right) \quad (2\text{-}5)$$

$$m_{xy} = m_{yx} = -(1-v)\,D\frac{\partial^2 w}{\partial x\,\partial y} \quad (2\text{-}6)$$

Where D represents the flexural rigidity of plate according to the following expression:

$$D = \frac{E\,h^3}{12(1-v^2)} \quad (2\text{-}7)$$

By substituting the equations (2-4), (2-5) ,and (2-6) into equation (2-1), then the governing fourth order differential equation (2-8 for thin plate can be obtained.

$$\frac{\partial^4 w}{\partial x^4} + 2\frac{\partial^2 w}{\partial x^2\,\partial y^2} + \frac{\partial^4 w}{\partial y^4} = \frac{P_z(x,y)}{D} \quad (2\text{-}8)$$

2.5 Behaviour of Slabs under Combined Effects of Bending, Torsion and Shear Stresses

Over the past few decades, understanding the behaviour of members at all stages of loading has become more important, particularly when they are designed based on the strength design method. Before understanding the behaviour of the slab, it is important first to know the behaviour of the beam.

2.5.1 Behaviour of Beams Subjected to Pure Bending Moment

For simplicity, consider a singly reinforced beam subjected to pure bending as shown in Figure 2-5. At low moment levels, the beam is uncracked, and the material stress-strain relationships behave as linear elastic, thus, the deformations can be calculated from elastic theory using the uncracked flexural rigidity. When the tensile stresses exceed the tensile strength of the concrete, new cracks start to form in the highly stressed regions, but much of the beam sections remain uncracked. Simultaneously, the neutral axis position moves towards the compressive area and the length and width of an already formed cracks increase with increasing load. At this stage, the moment of inertia of the sections containing the crack decreases, and this leads to decreasing in flexural stiffness.

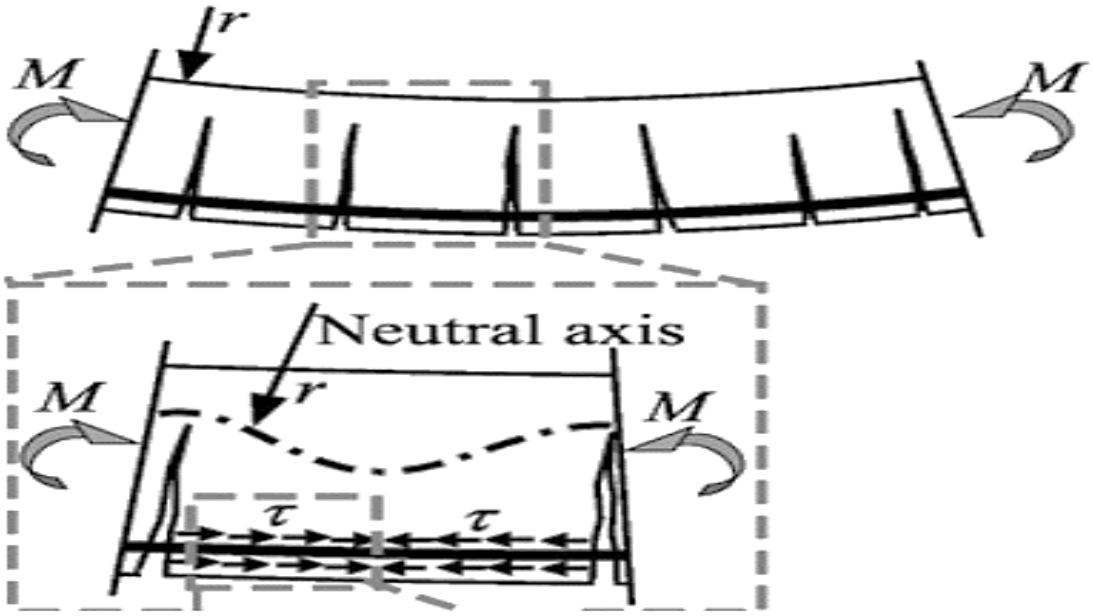

Figure 2-5. Bond stress and changes in neutral axis position in cracked sections.

According to this process, the moment-curvature relationship is no longer proportional to the moment of inertia of the uncracked transformed section as shown in Figure 2-6. After cracking the bond stress in the tensile zone between the cracks deteriorates dramatically, specifically at high bending regions. As the load increases, more cracks form and much of the sections over the beam begin to enter nonlinear range as a result of the nonlinear behaviour of materials at high stress levels. Hence, the flexural stiffness of those sections decreases further. Eventually, when the load approaches the ultimate capacity, the curvature increases significantly with little change in the moment. Hence, the slope of the moment-curvature relationship becomes very low.

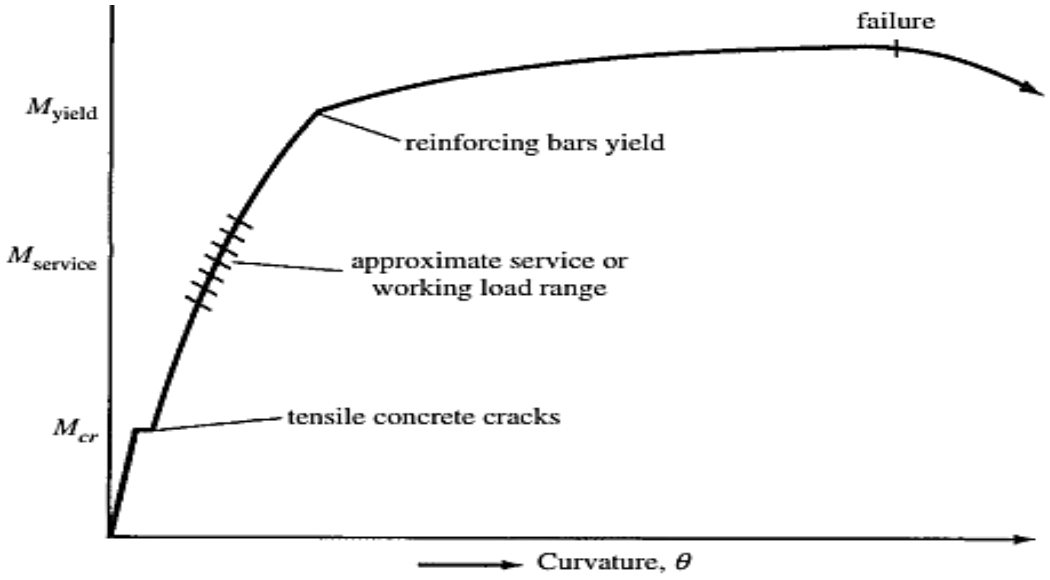

Figure 2-6. Typical moment-curvature diagram for singly reinforced concrete flexural sections

It is evident that full analysis of the members for determining the complete behaviour at all levels of loading is lengthy and can be achieved successfully only with the aid of powerful computational tools. Such a computational tool would be valuable to evaluate the structural performance at all range of loading, including the service load. Understanding the complete behaviour of slabs is not straightforward, particularly after cracking, since most member responses are drawn from uniaxial tension members. Tension members are subjected to normal stress while the slab members are subjected to bending, torsion and shear stresses.

2.5.2 Behaviour of slabs

Usually, the flooring system has different slab panels that are categorized into one-way and two-way slabs depending on the way they support the loads. For two-way slabs, unlike one-way spanning slabs, load sharing is in two directions and hence main reinforcements must be provided in these directions to resist bending moments. The actual behaviour of a two-way slab is very complex. Initially, at low load levels, the entire slab area is uncracked, then the slab response behaves as linear elastic. When the load on a slab is increased beyond the cracking load, the zones of highest bending moments will crack first particularly in the mid-span and adjacent the column; wherever the flexural tensile stress exceeds the concrete tensile strength. Thereafter, the slab stiffness decreases, and the load-deformation response becomes nonlinear. After first cracking, the crack pattern of two-way slab is not similar to one-way slabs. Increasing the loads further will increase the length, width and the number of the cracks and the material yielding will take place. At the same time, the already formed cracks at the top surface around the central column develop radially and orthogonally. Concurrently, the formation of inclined shear cracks around the columns occurs when the punching shear stress is exceeded. These cracks start to form near the column edges, then they develop through the thickness at an angle of 20^0-45^0 to the bottom of the slab. When the loads reach the slab capacity, the cracks tend to migrate to the boundaries of the slab, as shown in Figure 2-7, and the reinforcement passing through the cracks may yield.

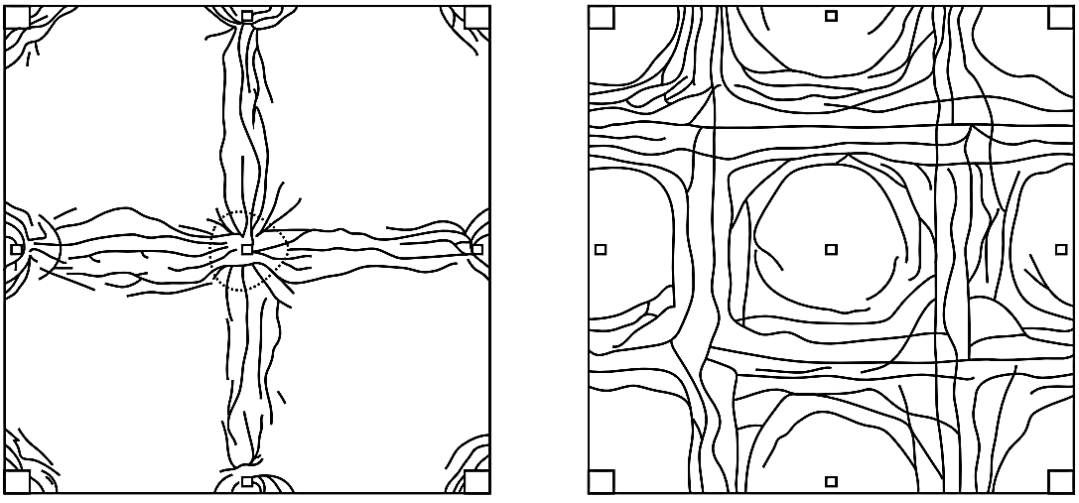

(a) (b)

Figure 2-7. Typical crack pattern in flat plate slabs (a) at top (b) at bottom by (Subramanian,2013)

When the slab containing opening, the case will be more difficult. Usually, the presence of such openings in the slab reduces the slab stiffness, and in tun increases the deflections and stresses. Although slabs usually contain openings, the behaviour of that type is not completely addressed in literature. Next sections will give clear picture on how such openings have an effect on the slab behaviour.

2.6 Effect of Openings on the Slab Behaviour

Understanding the behaviour of reinforced concrete members under different design situations, particularly here is the existence of openings in slabs, is vital to obtain a comprehensive knowledge to design an adequate structure. Slabs often contain openings of considerable size for accommodating utility services. The existence of openings changes the behaviour of the slab to a more complex one. Openings reduce the slab stiffness and lead to increase in deflection, particularly near the opening (Concrete Society, 2005). Although numerous shapes of openings are possible, rectangular and square openings are most common. The area within the solid slab experiences stresses due to an external static load; in the case when the slab contains an opening these stresses become higher, specifically in the remaining slab area, which may lead to more cracking. In other words, the opening reduces the volume of reinforced concrete sustaining stresses. Accordingly, the slab is not able to carry load over the region of the opening and thereby the total load capacity is usually smaller than a slab without the opening. Openings tend to attract yield-lines formation, since they represent regions of zero flexural strength in the slab (Park & Gamble, 2000).

In the design of reinforced concrete slabs with openings, the design codes usually propose instructions that are not supported by the underlying theories or reliable data. Usually, the existence of openings in the slab makes the analysis difficult to perform even if the slab is analysed based on linear elastic theory. Therefore, the usual design practice trend is to neglect the opening and, hence, a large difference will exist between the distribution of elastic theory moments and the distribution of design moments. Design codes, including (ACI-318, 2014), clearly stated that openings of any size shall be permitted in slab systems if shown by analysis that all serviceability and strength requirements, including the limits on deflections are satisfied. As an alternative to the previous provision, the ACI 318

code provides special situations regarding with opening sizes and locations, and the design of such slabs are generally based on the assumption that the total amount of reinforcement for the slab without opening on both directions must be maintained. Hence, a quantity of reinforcement equivalent to that interrupted by an opening shall be added on the sides of the opening. Otherwise, yield-line methods of analysis and nonlinear finite element methods may be adopted to design of such slabs.

There are several methods to analyse the slabs. Of these, experimental testing is one of the most reliable methods to understand the behaviour accurately Relatively little research has been published in literature on the behaviour of slabs with openings, primarily due to the mathematical difficulties. Nevertheless, several studies regarding the effect of openings on the elastic behaviour of metal plates were conducted by using numerical methods.

In 1960, (Fluhr et al.,1960) conducted theoretical investigation on plate with the effects of rectangular and square openings on the bending moments and deflections with fixed edges. The investigation was divided into three series as follows: five plates with rectangular openings of different sizes; five plates with square openings of different sizes; three plates with multiple openings. In the series with square openings, two of the plates had openings at one corner and three had openings at the centre. In the series with rectangular openings, the openings were located at the centre and had varying lengths and constant widths. In the series with multiple openings, one of the plates had two rectangular openings located on the X-axis; another had two square openings located on the X-axis; and the third plate had four square openings located on the diagonal of the plate. Two types of loading conditions were investigated: a uniform load on the remaining surface of plate with openings while for solid plates the uniform load was distributed over the area of the plate except in the area previously occupied by the opening ; and a uniform load on the remaining surface of the plate plus a uniformly distributed line load on the perimeter of the opening while for solid slab the load was distributed over the area of the plate except in the area previously occupied by the opening and hence the total line load equal to the total load on the area removed by opening. Therefore, the total load for each plate loaded uniformly plus line load on perimeter of openings is the same as the total

uniform load of solid plate. They found that the position of maximum deflections was at the centre of the plate for all solid plates. However, the maximum deflections of plates with openings depending on the shape of opening itself. For plate loaded uniformly with the square openings located in the centre of the plate, the maximum deflections of plate were smaller than solid plate. The same thing was true for plates with openings and loaded uniformly plus line load on perimeter of openings except for the smallest openings which gave a slight increase in deflection. For the openings located in one corner of the plates, the maximum value of deflections was larger than solid plate for both kinds of loading. For rectangular openings series, the maximum deflections for uniformly loaded were smaller than those of solid plate. While, the maximum deflections were larger than solid plates for uniformly plus line loading on the perimeter of opening. For multiple opening series, the maximum deflections were approximately the same as the solid plate loaded uniformly. While the deflections were larger than solid slab for uniformly loaded plus line load around the opening.

In 1961, (Prescott et al.,1961) presented the theoretical investigation on plate with the effects of different size of square openings at the centre of plates to study the effects of such openings on deflections and bending moments in fixed edge square plates. Moreover, to study the effects of adding stiffening beams at the perimeter of the opening. The edges of openings being stiffened with beams having various degrees and combinations of torsional and flexural stiffness. Two types of loading conditions were investigated: a uniform over entire area; and uniformly distributed line load on the perimeter of the opening. They concluded that for plates with openings, the maximum deflections were at the edges of openings. For the conditions of uniformly distributed load, maximum deflections for plate with small opening exceed the plate with the larger opening. For distributed line load around the opening, the maximum deflection of plate with large opening size are greater than of plate with smaller square opening when the flexural stiffness of the stiffened beams around the opening is small, while the deflection of plate with smaller square opening greater than of plate with larger square opening when the value of the flexural stiffness becomes large.

In 2015, (Roknuzzaman et al.,2015) conducted theoretical analysis of steel plate with opening in the centre. In their study, a finite difference method (FDM) is

proposed to analyse a rectangular steel plate. The plate is considered to be subjected to a lateral uniformly distributed loading (out of plane) and is considered to be clamped at the two opposite edges, and free at the other two edges. Firstly, the plate is analysed considering it to be solid completely and then it was re-analysed considering a rectangular opening at its centre. The governing differential equation was solved by the ordinary finite difference method. The results indicated that the maximum deflection of plate with opening in the centre are greater than of solid plate specifically in the perimeter of opening.

A numerical study was carried out by (Bhatti et al.,1996) on the effects of openings of different sizes on deflection and strength of reinforced concrete slabs under distributed and concentrated load cases. Both simply supported and fixed end conditions have been studied. Cracking and crushing of concrete, and plasticity of both concrete and reinforcement have been considered and included in their nonlinear finite element model using three-dimensional brick elements. Their numerical outcomes were validated first against the slab tested by (McNeice,1967). They found that openings do not affect the deflections and collapse load significantly in the case of simply supported slabs subjected to uniformly distributed loads. The conclusion was that as the openings are getting larger, the total applied load on the slab is getting smaller and thereby the overall behaviour is not affected much by opening. They reported that the openings can usually be neglected in the design since the deflections, at a given distributed load, do not vary significantly in the service load range when the opening size increases. When there were simply supported slabs subjected to concentrated load, deflection increased and both collapse and cracking load decreased rapidly, as the size of the opening was increased. The slabs were also analysed again with distributed load and under fixed end condition. Similar to the simply supported case, the overall behaviour is not affected significantly by the opening. The results revealed that under concentrated load a significant loss in slab strength was noticed as a result of openings in the slab.

(Boon et al., 2009) carried out an experimental work of one-way reinforced concrete slabs to determine the structural performance with rectangular opening under four points tests. Five types of RC slab which consist of two panels for each type were tested. The dimension of the slabs is 1100 x 300 x 75 mm. These slabs

include one control slab S1 without opening and other four slabs S2, S3, S4, and S5 with rectangular opening at the centre. A 150 x 300 mm rectangular opening was located at the centre of slab. Slabs were provided with additional rectangular and diagonal bars at the edges of openings as shown in Figure 2-8.The experiments showed that the presence of openings generally reduced the flexural strength of the slabs 36.6% compared with slabs without openings. Furthermore, the presence of additional reinforcements around the edge of openings increases the flexural capacity of the slabs compared with slabs without additional reinforcements around the openings. Moreover, from the experimental observations, the cracking pattern found in the slabs show a high concentration stress occurred at the corner of the opening.

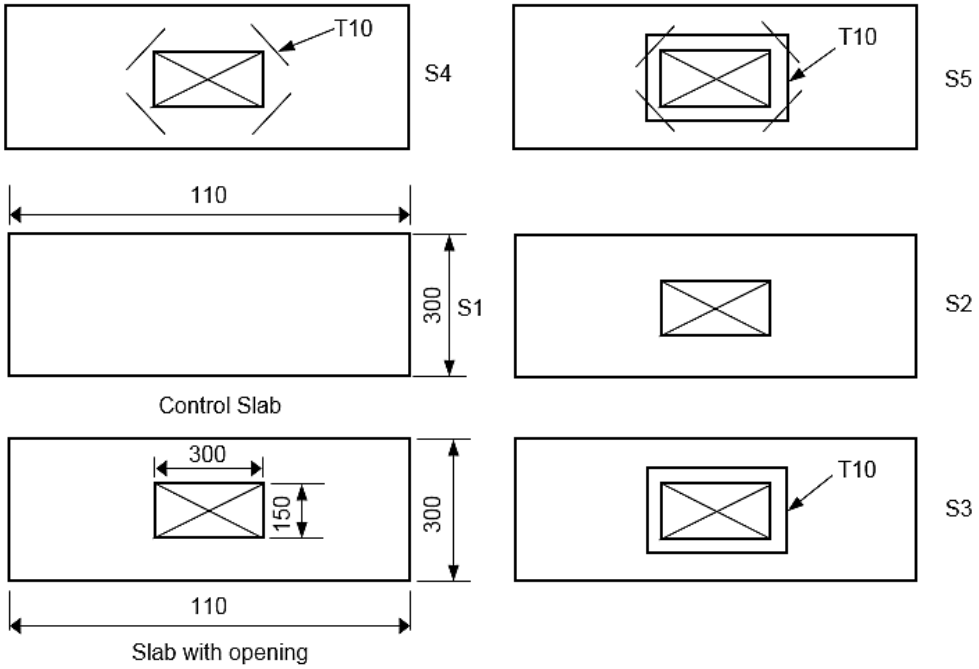

Figure 2-8. Slabs details

In 2014, (Sheetal & Itti, 2014) performed an modelling of RC slab with and without opening by ANSYS FEA software. The dimension of the slabs is 2000x3000x120 mm and the uniform distributed load has been applied on the slab area with 12 kN/m^2. Four different boundary conditions were considered: slab with fixed support on all four edges; slab simply supported on two adjacent edges; slab is simply supported on two edges and fixed supported on other two supports; and slab with simple support on all four edges. They found that the presence of opening in the centre of slab with different boundary conditions increases the

deflections significantly compared with slab without opening. They concluded that the deflection in the slab fixed on all the edges with opening is 13 % higher than the slab without opening with same boundary condition, but the deflection in slab with opening is higher 17.75% higher than the slab without opening with the same boundary condition which fixed on adjacent two edges and simply support on adjacent opposite two edges. However, the deflection in slab having fix support on opposite edges and other opposite edges simply supported is 18.36% higher than the slab without opening. Finally, the deflection in slab which simply supported on all four edges is 18.02% higher than the slab without opening with same boundary condition.

(Park & Gamble, 2000) conducted a theoretical yield-line analysis of uniformly distributed load on reinforced concrete square slab with a central square opening as shown in Figure 2-9. The size of opening is defined by the value k and the slab was fixed around the outside edge. From the results, for simply supported condition, the opening causes a maximum reduction in the ultimate load of about 11% when $k = 0.2$ to $= 0.3$, and when $k = 0.5$ or greater, there is no significant reduction in the load carried. For fixed edge slabs, they found that in general the reduction is less than for simply supported slabs.

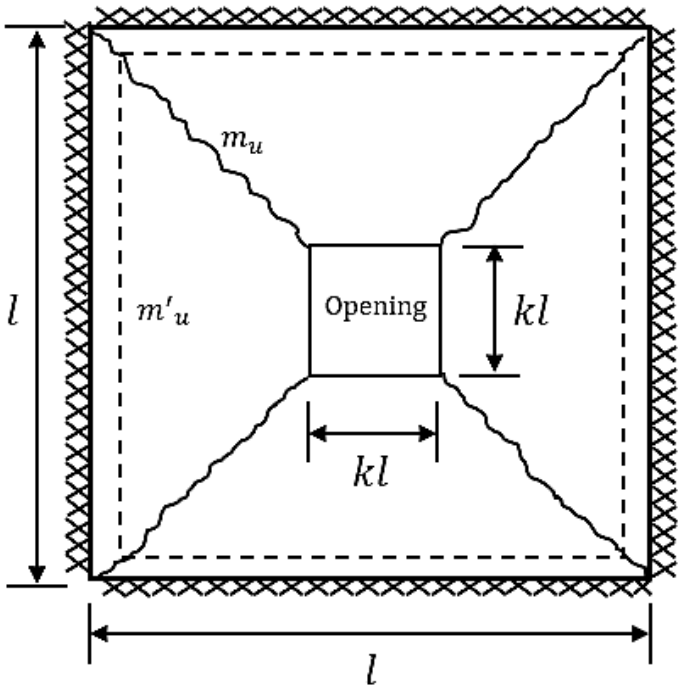

Figure 2-9. Uniformly loaded square slab with central opening

(Ng et al., 2008) carried out a theoretical yield-line study, a study on_simply-supported and fixed-end, square slabs with opening at ultimate limit state using the yield line method as shown in Figure 2-10 and Figure 2-11. A study on the effect of opening on the load carrying capacity of simply supported and fixed-end slabs was presented. After their analysis they came to a conclusion that, since most of the slabs have small opening of size up to 0.3 times the slab dimension, a simply supported slab would have a reduction in ultimate area load of up to 11% and a reduction of ultimate total load of up to 19% and a fixed-end slab would experience less significant reduction in both ultimate area load and ultimate total load capacities of 4% and 7%, respectively. They also presented charts in normalized load capacity and opening size which could be e used as guidelines for predicting the load capacity of simply- supported and fixed-end slabs with openings.

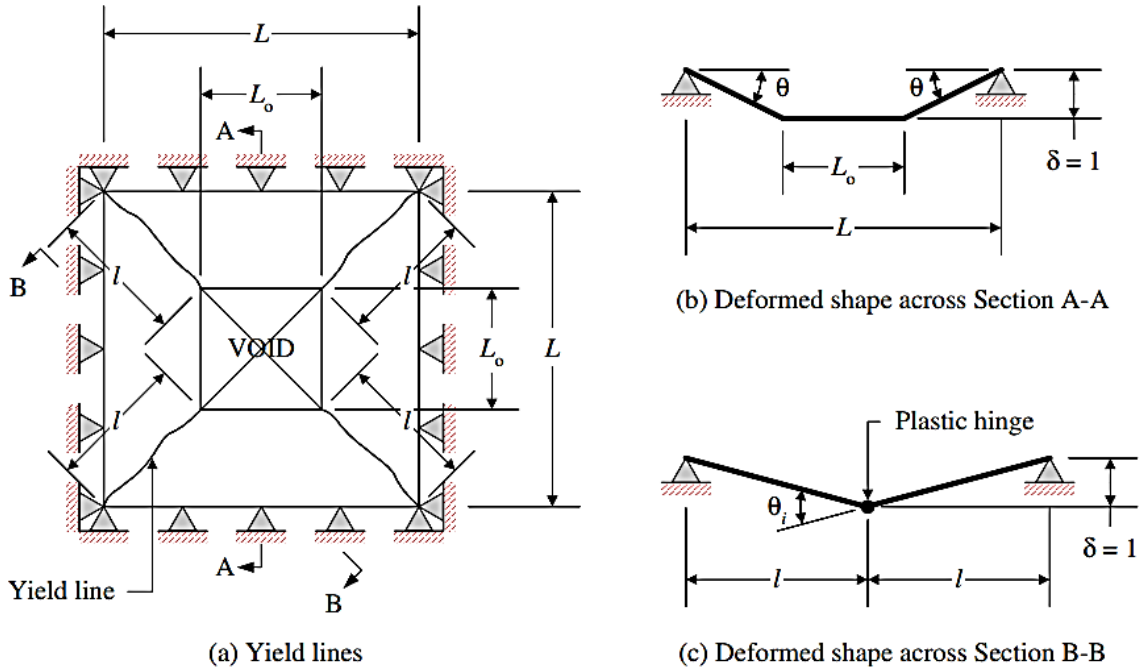

Figure 2-10. Yield lines and deformations of a simply-supported square slab with an opening at the centre (Ng et al., 2008)

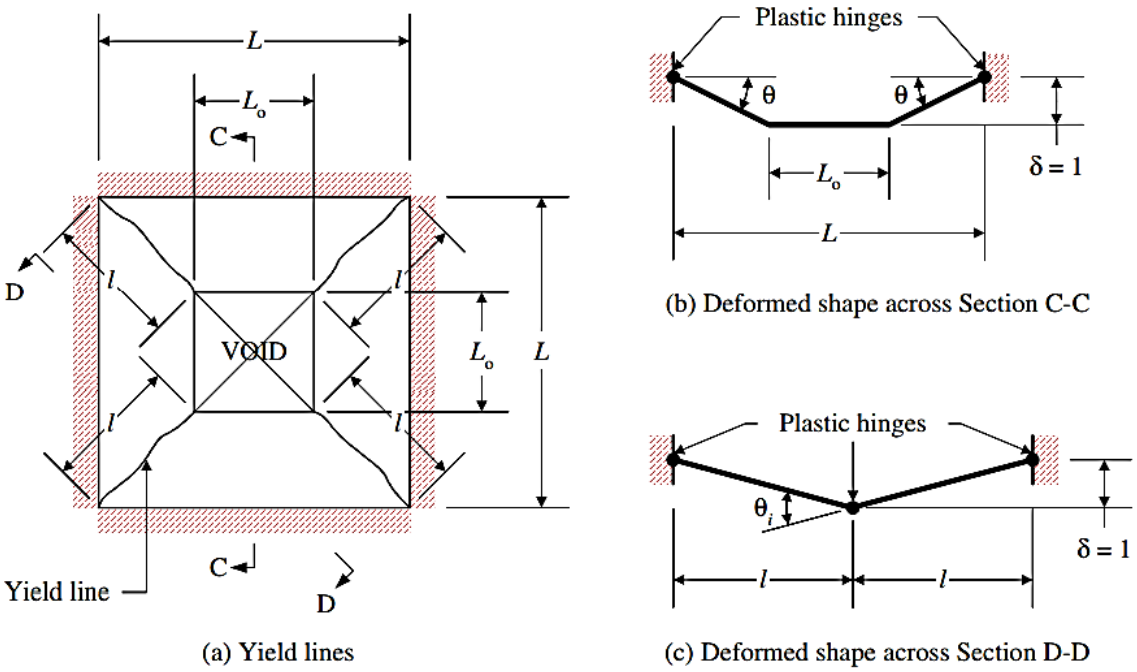

Figure 2-11. Yield lines and deformations of a fixed-end square slab with an opening at the centre (Ng et al., 2008)

2.7 Influence of Openings on Shear Strength of Slabs

The existence of openings changes the behaviour of the slab to a more complex one. Even though several codes contain detailed provisions for openings in floor slabs, however, they are derived based on experimental tests. The openings must be placed in such a way that no potential failure could develop. Among the available methods that can offer a suitable option to analyse the slabs, the experimental method represents a reliable way to analyse and understand the behaviour of slabs thoroughly.

Reinforced concrete slabs that supported directly on columns without beams are usually common structural systems. The construction of such system started in the beginning of the 20th century in the Europe and North America. Flat plates are one of the most popular and economical floor systems and provides many advantages. In contrast, these slabs generally have low flexural stiffness compared with the conventional concrete slab-beam system. Such type of slabs develops high shear stresses near the column or concentrated load. Once these shear stresses exceed the shear capacity of slab, punching shear failure occurs with little or no warning as shown in Figure 2-12. These shear stresses become higher when openings are introduced. Openings in slabs are one of the critical

factors that influence the punching shear strength of flat plate systems and govern its thickness in the vicinity of the slab-column zone.

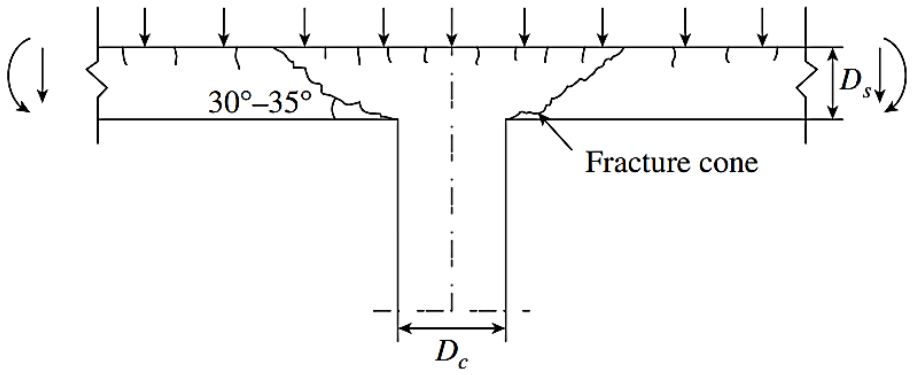

Figure 2-12. Typical punching shear failure

Extensive researches have been carried out on punching shear strength. Therefore, several analytical models have been proposed for prediction of punching shear capacity. Tests for punching shear strength started at the beginning of the 20th century. Generally, in all slab tests, the slab is considered as isolated specimen representing the portion of slab around the column extending to the line of contra-flexure. The first study of shear strength of footings was reported by (Talbot, 1913). He carried out experimental tests of 114 thick wall footings and 83 thick column footings tested to failure as shown in Figure 2-13. Of these tests, approximately 20 specimens failed in shear. Based on his experimental results, the formula for shear strength at the footing was proposed, and therefore, these results found not adequate for prediction punching shear capacity of slabs (Genikomsou, 2015), thus, experimental investigation on concrete flat slabs started to be considered. However, this formula is still widely used, after developments, in several design codes. In his research, the concept of the critical shear perimeter was first considered. The test observations presented by (Talbot, 1913) led to the first concepts and recommendations for punching shear which was published in 1925 in American Concrete Institute Code.

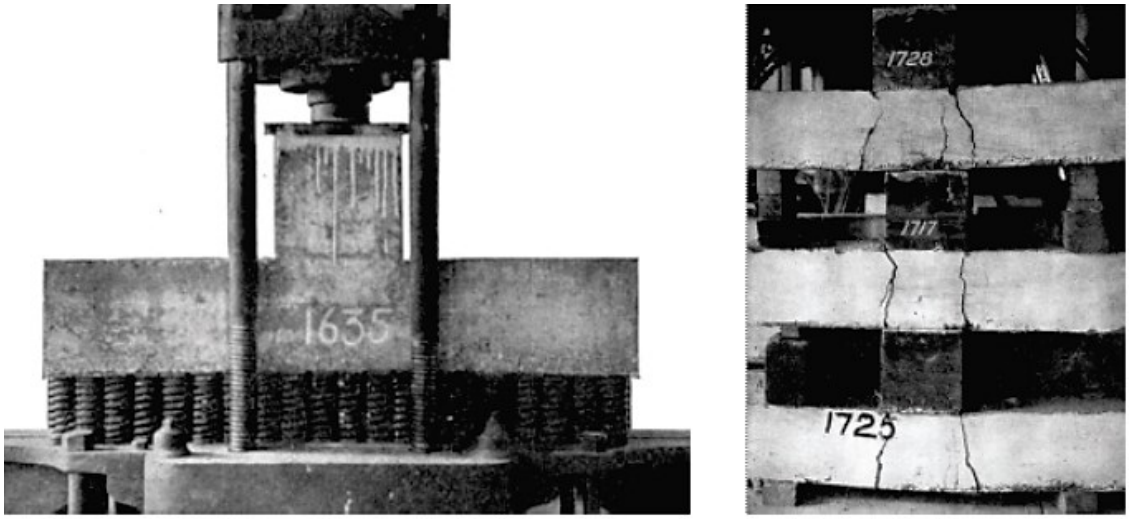

Figure 2-13. Experimental tests carried out by (Talbot, 1913)

In 1915, (Bach & Graf, 1915) tested a large number of slabs which were designed mainly to examine the flexural strength. Nevertheless, few slabs failed in shear. In 1933, (Graf, 1933) carried out a series of experimental tests on slabs subjected to concentrated loads near the supports. He derived a formula for predicting nominal shear stress. Important early contributions in understanding the shearing strength of slabs came from (Elstner & Hognested, 1956) , they tested 39 slabs to estimate the influence of the concrete strength, percentage of flexural tension and compression reinforcement, size of column, conditions of support and loading, distribution of tension reinforcement, and amount and position of shear reinforcement on the punching shear strength of the slabs. For 34 slabs, final failure was in shear by the column punching shear through the slab. The test findings from their estimations show that all these factors have significant influence on the ultimate shearing strength of slabs, except the compressive reinforcement that had no effect on the ultimate shearing strength of the slabs. The test findings confirm the outcomes of the re-evaluation conducted by (Hognestad, 1953) of (Richart, 1948) footing investigation, to the effect that the ultimate shearing strength is a function of concrete strength as well as of several other variables. Furthermore, their studies have shown that a critical shear stress exists at the periphery of the column.

Pioneering work of Moe (Moe, 1961) first derived an empirical expression to predict the ultimate shearing strength of slabs under vertical loading. The main

variables were concrete strength, column dimensions, shear reinforcement and concrete strength. He found that the ultimate shear strength is a function of the square root of the concrete compressive strength. Moreover, he suggested that the critical section perimeter governing shear strength is located at the face of column. After analysing significant number of tests, he included the influence of the unbalanced moments in the slab-column connections. His work remains until now the basis for the ACI code 318. However, (ACI-ASCE Committee 326, 1962) suggested that critical shear section to be taken at the distance d/2 from the face of the column, where d denotes the effective depth of the slab. Based on critical shear section perimeter consideration on ultimate shearing strength of slabs, (ACI-318, 2014) and (FIP Model Code, 2010) propose the critical shear perimeter at distance of $d/2$ from the column face to predict the punching shear strength, while (Eurocode2, 2004) considers the perimeter of critical shear at distance of $2d$ from the column face as shown in Figure 2-14, where d is the effective depth of the slab. Both (Eurocode2, 2004) and (FIP Model Code, 2010) assume the critical shear perimeter zone with circular edges.

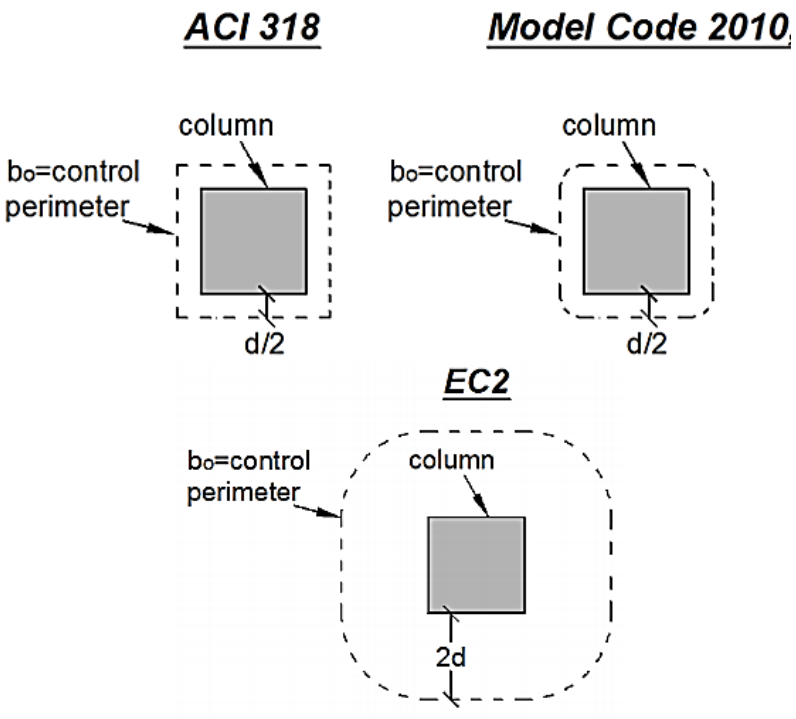

Figure 2-14. Control shear perimeter proposed by different codes

Based on the experimental observations on punching shear tests, several empirical equations have been derived. In 1960, (Kinnunen & Nylander, 1960) presented a mechanical model based upon observations of 61 tests on circular slabs supported centrally by circular columns to predict the punching shear failure of slab-column connection without shear reinforcement and to explain the punching shear failure mechanism. This valuable study of shear failure of slabs was offered the first real attempt to establish a theoretical method of analysis. The main variables were the amount and type of flexural reinforcement and the diameter of the column. The model was derived based on the formation of shear cracks and bending moment cracks. This method was a relevant original contribution and was first reliable theory presented. However, the model was considered complex.

In 2008, (Muttoni, 2008) presented the most recent theoretical approach well-known as Critical Shear Crack Theory (CSCT) for estimating the punching shear strength for members without transverse reinforcement by adopting the approach that a single shear crack localizes the strains in the critical shear zone. The (CSCT) assumes that the punching shear resistance decreases as the rotation ψ of the slab increases. The approach correlates between thickness of slab, rotation, and critical shear crack opening. This theoretical approach has recently been adopted in the first draft of the (FIP Model Code, 2010). Then in 2009, (Fernandez & Muttoni, 2009) proposed a physical model based on CSCT that allows to reliable estimate the contribution of concrete and shear reinforcement to the punching shear strength.

Again, the existence of openings in flat slabs decreases punching shear strength by increasing shear stresses around the opening zone. A review of the literature reveals that studies of slabs with openings are quite limited and focus on the effects of openings on the flexural strength of slabs. The earliest study for slabs with openings near supporting column seems to be reported by (Kinnunen & Nylander, 1960) (Moe, 1961) (Hognestad et al., 1964; Mowrer & Vanderbilt, 1967;Regan,1974). In the research works done by (Kinnunen & Nylander, 1960), (Moe, 1961), and (Regan, 1974), they proposed the principle of the reduction of critical shear perimeter due to the existence of opening near column, its critical shear perimeter is reduced and an ineffective part is ignored. The reduction of

critical shear perimeter was first considered in the (ACI ASCE Committee-326, 1962), which was assumed to be at d/2 from the loaded area. More recently, the current building codes adopts the reduction of the critical perimeter principle with a similar way. However, the codes (ACI-318, 2014; Eurocode2, 2004; FIP Model Code, 2010) proposed simplified models for prediction of shear strength by reducing control shear perimeter depending on the size and location of opening. According to the (ACI-318, 2014), if the edge of opening is located at a distance of less than 10 times the slab thickness from a column face, the critical perimeter is reduced by excluding the ineffective part. The provisions in (Eurocode2, 2004; FIP Model Code, 2010) recommend that if the opening is located at a distance of less than $6d$ or $5d$ from a column face, the perimeter is reduced and the new effective perimeter is considered.

A number of publications have been investigated the punching shear behaviour of slabs with openings again started in the 1990_s by recent researchers (El-Salakawy et al., 1999) and more recently by (Aikaterini et al., 2017; Borgas et al., 2013; Ha et al., 2015; Teng et al., 2004,Balomenos et al.,2019). Generally, their results confirm that the punching shear resistance decreases due to the existence of openings, and it is generally proportional to the size and location of opening from the column, as its usually critical shear perimeter is reduced by opening existence (Ha et al., 2015).

In 2014, (Anil et al., 2014) conducted an experimental study on eight reinforced concrete slab specimens with openings at different positions and a control specimen without opening. Two-way square slabs (2000 x 2000 x 120 mm) were tested by applying an axial load from the top of a square column (200 x 200 mm) positioned at the centre of the slab. The test specimens studied had different opening sizes (300 x 300 mm and 500 x 500 mm) and positions: each size of opening was positioned in parallel and diagonal positions adjacent to the column and 300 mm from the column. In the test specimens, Ø 10 mm tensile and compressive reinforcements were used and placed in the same ratio in each direction. They found from the tests that the punching shear resistance decreases with an increase in opening size and it notably decreases for openings adjacent to the column compared with openings located away from the column.

In 2017, (Aikaterini et al., 2017) carried out finite element analysis effect of openings and their locations on crack propagation and punching shear strength of slab-column edge connections. These slabs had the same geometry, material properties, and reinforcement ratio. Moreover, the slabs had the same opening size (150x250) mm but with different distance from the column face as shown in Figure 2-15. As they stated, the opening effect is examined at the front of the column and not beside it since this is found as the worst scenario in both the tests and numerical results. The crack patterns of slabs SF0, SF1, and SF2 are presented as shown in Figure 2-16. They presented the crack patterns into three loading stages 40%, 80%, and up to ultimate load, respectively. Up to 40% of the ultimate load, the cracking is concentrated around the column with some radial cracks on the tension side on the diagonal. At the 80% of the ultimate load, the shear cracks have already developed and extended further, and tangential cracks have developed and continued to the diagonal of the slab. At this load stage, more radial cracks become visible. They found that the propagation of cracks in the slabs with openings next to column propagate starting from the column and around the opening (SF0). While in the case of slabs SF1 and SF2, respectively, secondary cracks form and start to propagate from the corners of the openings and extend away from the columns. They also confirmed that similar observations have been noticed for the interior slab-column connections.

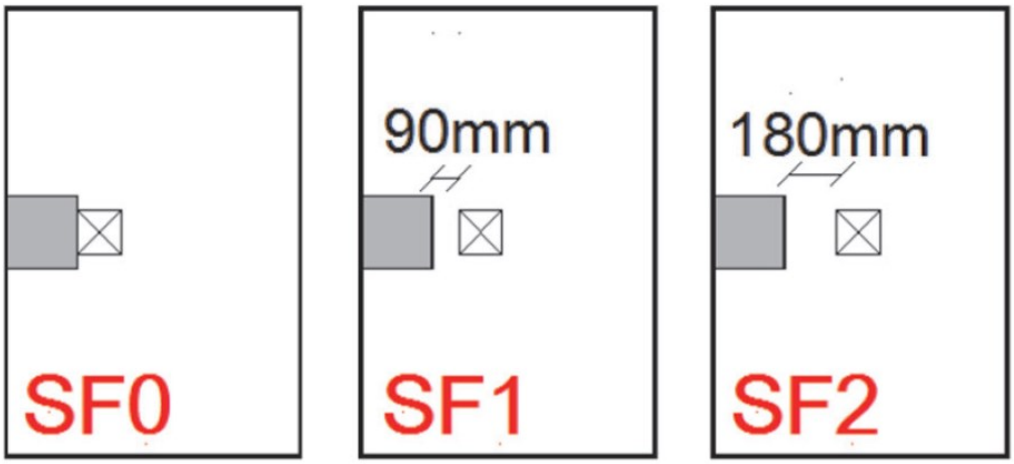

Figure 2-15. Schematic drawing of edge slabs with openings

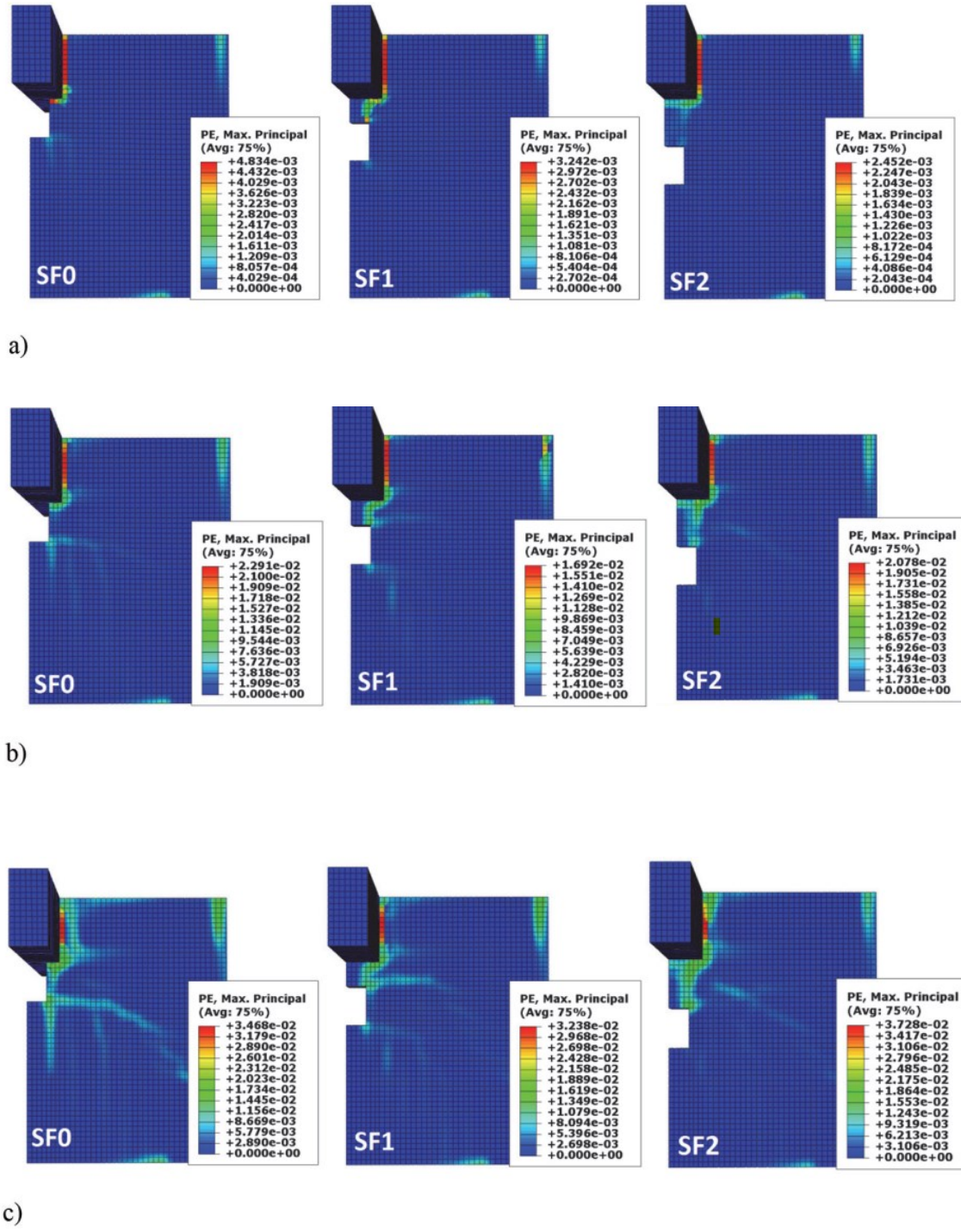

Figure 2-16. Cracking propagation of slabs SF0, SF1, and SF3: (a) 40% of ultimate load; (b) 80% of ultimate load; and (c) at ultimate load.

2.8 Response of Members Post-Cracking

In this section the behaviour of member post cracking is presented briefly. The flexural stiffness of a member EI is the product of two variables: the moment of inertia I; and the material modulus of elasticity E. In the reinforced concrete

members, both variables are subject to change whether initially or with time. The change in the material modulus of concrete depends on the material nonlinearity of the stress-strain curve beyond the elastic limits, while the change in the moment of inertia depends on the amount of cracking that has been taken place in the member. Cracking significantly affects the behaviour of reinforced concrete structures. Usually, the member is initially uncracked and thereby the response is governed more by the concrete than the steel reinforcement. When the bending moment anywhere at a cross section reaches cracking moment, the first crack starts to form. As the moment at different sections increases above the cracking moment, more cracks develop at discrete intervals along the member and the actual response of the member follows the curve *AB* and then tends toward the fully-cracked response as depicted in Figure 2-17. Traditionally, it is assumed in the strength design of reinforced concrete that the tensile capacity of concrete is neglected. Thus, the contribution of beneficial tensile concrete to the member stiffness is ignored. The flexural stiffness of reinforced concrete member then consists of the contribution of concrete in compression and reinforcement provided in the section. In practice, it is found that the concrete is still able to carry some tensile stresses between cracks through bond action, even after cracking, and this adds to the stiffness. The contribution of active tensile concrete is known as tension stiffening. Tension stiffening plays an important role in nonlinear analysis of reinforced concrete.

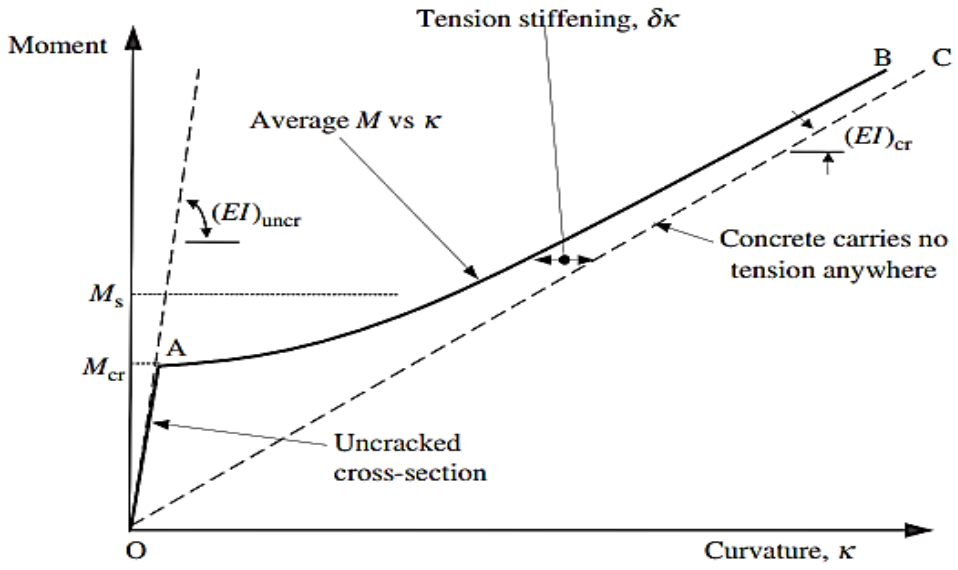

Figure 2-17. Moment- average relationship for a reinforced concrete member without shrinkage prior to loading (Gilbert and Ranzi, 2010)

2.8.1 Tension Stiffening

Often members can be partially cracked. A section of a member is deemed to be cracked if the allowable tensile stress is exceeded. In such a case, only parts of the length of member are cracked. The cracked parts in a section are ineffective in resisting forces; however, the active concrete between cracks continues to carry tensile stresses due to the transfer of forces from the reinforcement into the concrete through bond action. This phenomenon is called tension stiffening or tension stiffens, and it has an effect on member stiffness, deflection, and crack widths under service load conditions (Bischoff, 2005; Gilbert and Ranzi, 2010; Gilbert and Warner, 1978; Concrete Society, 2005, Gilbert, 2007). Although tension stiffening has only a relatively minor effect on the deflection of heavily reinforced beams, it is found to have very significant effect in lightly reinforced members, particularly in the case of slabs, where the flexural stiffness of a fully-cracked section is many times smaller than that of an un-cracked section (Gilbert, 2007). Tension stiffening, on average, contributes more than 50% of the instantaneous stiffness of a lightly reinforced concrete slab (typically $\rho < 0.003$) after cracking at service load (Gilbert, 2007).

Unfortunately, the assessment of short-term tension stiffening in flexural members is fraught with problems (Scott & Beeby, 2005). Even though it is possible to measure the strains in flexural members with reasonable accuracy, the assessment of the internal forces producing these strains can only be indirectly achieved. Therefore, tension stiffening is best understood by considering the axial response of a reinforced concrete tension member (Bischoff, 2005).

Consider the load-strain response of a singly reinforced concrete member shown in Figure 2-18. At load less than the cracking load P_{cr} , the member is initially un-cracked and hence the response is governed more by the concrete section than reinforcement. Consequently, the applied load is then shared between the concrete and steel in relation to their respective rigidities. Once the concrete cracks at discrete locations, when the load greater than P_{cr},the actual member response is intermediate between the uncracked and fully cracked limits and it is affected by the stiffness of reinforcing bar and follows a gradual transition toward

the bare bar response, as more and more cracks develop in the member. Cracking is accompanied then by a gradual reduction in the average load carried by the active concrete as more cracks develop. The amount of tension transferred to the concrete (between cracks) depends to a large extent on the bond between the concrete and steel in relation to the crack spacing which develops as the member cracks (Bischoff, 2001).

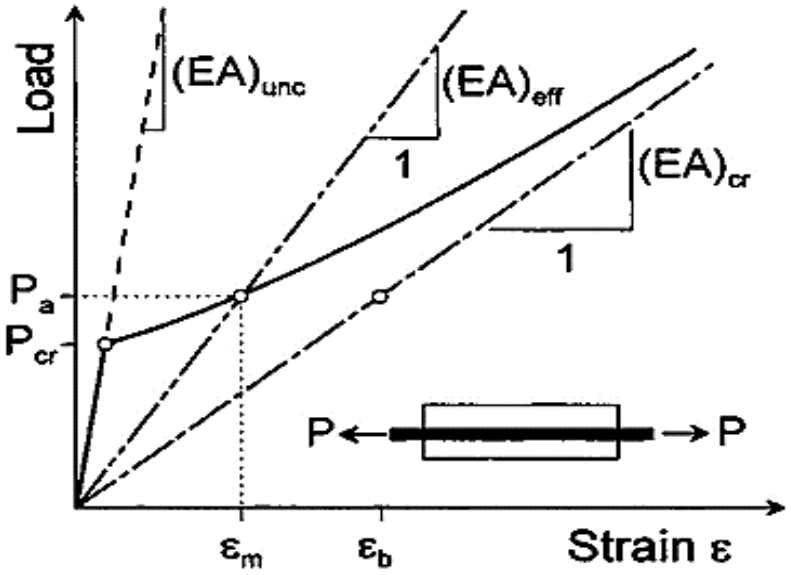

Figure 2-18. Member deformation for axial member (Bischoff, 2005)

At the cracked section, the stress in the concrete drops to zero and all tension is then carried by the steel reinforcement, while some tensile stresses are, however, present in the concrete between the cracks as a result of bond action. Therefore, the tensile strain in the steel midway between the cracks is lower than the steel strain at the crack location. Once cracking has stabilized, the load carried by the concrete continues to decrease as internal cracks develop between the primary cracks (Goto, 1971; Bischoff, 2001), as shown in Figure 2-19. (Goto, 1971) was able to observe the pattern of internal cracking around a deformed bar by injecting red ink into a duct running parallel to a bar in tension specimen. The relationship between the load and the average strain for member after cracking is given by:

$$P = (\mathrm{EA})_e \varepsilon_m \tag{2-9}$$

The term $(\mathrm{EA})_e$ can be referred to as the effective stiffness of the member.

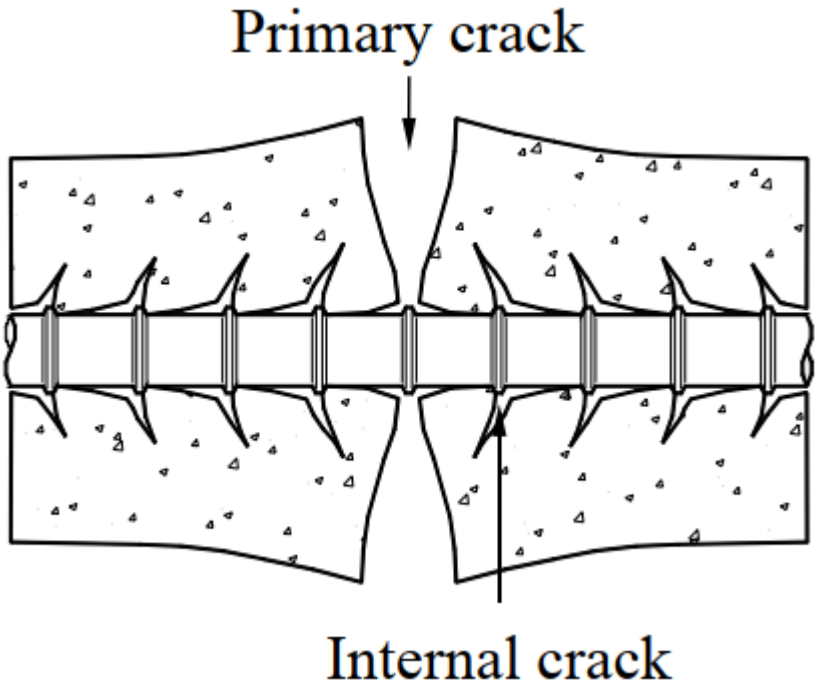

Figure 2-19. Cracks formation at the interface between concrete and reinforcement (Goto, 1971)

2.8.2 Tension Stiffening Approaches

Modelling of tension stiffening phenomenon is important in studying the load-deformation characteristics of reinforced concrete members in the post-cracking range. Numerous empirical approaches have been proposed in a number of different ways to reflect the effective stiffness $(\mathrm{EA})_e$ in a cracked reinforced concrete member. Three basic approaches are available and have been included in (ACI 224.2R-92). The first approach is based on effective modulus (E_b) of embedded reinforcement and the actual area of reinforcement. This method ignores the concrete tensile stress but increases the apparent reinforcement stiffness to account for the concrete stress between cracks. It has been used in finite element analysis to compute the response of reinforced concrete slabs (Gilbert and Warner, 1978). The second approach is to write the effective stiffness $(\mathrm{EA})_e$ in terms of the modulus of elasticity of the concrete and an effective (reduced) area of concrete. This approach is analogous to the effective moment of inertia concept developed by (Branson,1965). A third approach that has been employed in finite element analysis of concrete structures involves a progressive reduction of the effective modulus of elasticity of concrete with increasing cracking. This approach is equivalent with the approach that accounts

for the tensile contribution of the concrete between cracks based on an average stress–strain response with a descending branch after cracking, as depicted in Figure 2-20.

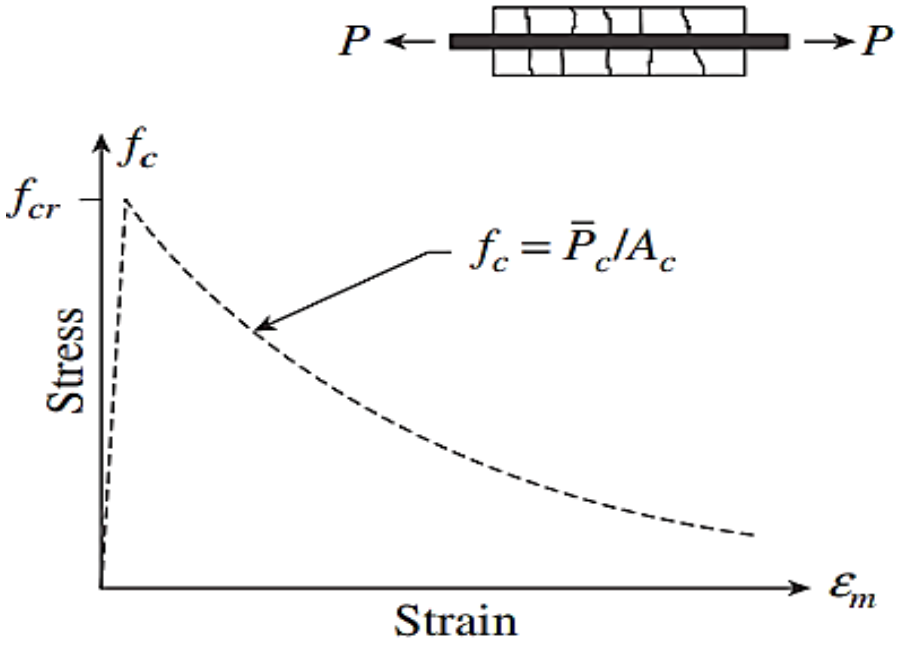

Figure 2-20 Average tensile stress-strain response of cracked reinforced concrete

The idea of effective modulus of elasticity of concrete has been used by (Scanlon & Murray, 1982) for calculating deflections of slabs with the aid of finite element program, where the modulus of elasticity of concrete in both directions is modified based on Branson's effective moment of inertia equation to reflect the reduction in stiffness due to cracking. The only reason to employ this procedure is to modify the cross-sectional flexural stiffness using a linear elastic orthotropic finite element plate bending program. The analysis is then repeated using the reduced modulus of elasticity. A comparison between computed and measured deflections shown good agreement at each load level. Similar to the Scanlon and Murray proposed method, (Jofriet and McNeice, 1971) presented a nonlinear finite element analysis of reinforced concrete slab based on modified stiffness. The nonlinear behaviour due to progressive cracking of the slab has been considered in the analysis to include the effect of tension stiffening. In their analysis, a bilinear moment-curvature relationship based on an empirically determined effective moment of inertia of the cracked slab section was used to reflect the reduction in flexural stiffness in each direction.

Further to the aforementioned methods, the tensile contribution of concrete can be represented by tension stiffening factor β (or bond factor) that accounts for the variation of stress within the concrete between cracks, representing the average tensile stress f_c carried by the cracked concrete with respect to the cracking strength f_{cr}. This then gives β= f_c/f_{cr} as shown in Figure 2-21. The factor β varies between one (just before cracking) and zero for the special case of no bond exists after cracking. Several different proposals have been made for tension stiffening factor β. (Rao,1966; Rostasy et al.,1976) proposed using an expression of β= f_{sr}/f_s , which varies inversely with the stress in the reinforcement. Earlier research indicates that β decreases exponentially as the member strain ε_m increases (Fields and Bischoff, 2004). The following expression for β is proposed by (Bischoff and Paixao, 2004), where ε_{cr} is the concrete strain at cracking.

$$\beta = \exp[-800\ (\varepsilon_m - \varepsilon_{cr})] \qquad (2\text{-}10)$$

Test results showed that the predicted response using the expression β provides a reasonable comparison with the measured response of members reinforced with either GFRP or steel bars with different ratios (Bischoff and Paixao, 2004).

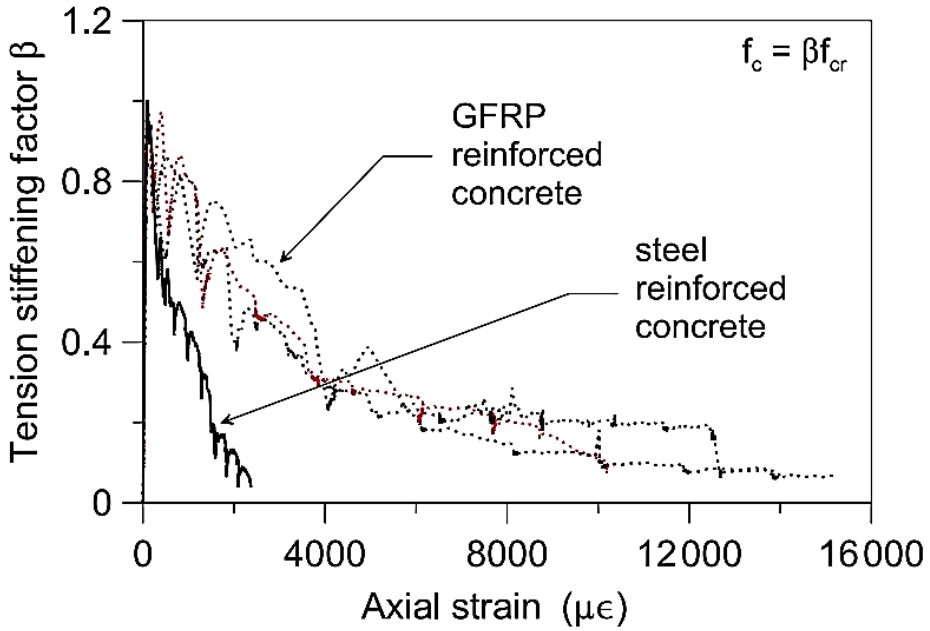

Figure 2-21. Measured tension stiffening bond factor β response curve (Bischoff and Paixao, 2004)

A more realistic method for reflecting the tension stiffening effect is to use a suitable bond-slip relationship at the concrete-steel interface. The action of bond produces tensile stress in the concrete around the bar. (Balazs, 1993) used the ascending branch of the bond-slip relationship from CEB-FIP Code to describe the bond zone and obtain the steel stress distribution between the cracks. However, the formula that he gives to calculate crack spacing or crack width is not computationally friendly (Wu, 2010). The tension chord model developed by (Marti et al., 1998) assumes that the bond stress is constant and hence the steel stress distribution along the tension element is linear. The model assumes that the concrete stresses are zero at the crack, and away from the cracks tensile force is transferred from the reinforcement to the surrounding concrete by bond. Although these models provide a realistic description of the tension stiffening effect, modelling of cracking and the steel-concrete interaction, however, gives rise to numerical difficulties and computational instability of the system and hence convergence problems.

In the practical design situations of flexural members, tension stiffening effect is often taken into account with the effective moment of inertia for flexural members. After cracking, I_{uncr} and I_{cr} are often combined empirically to approximate the average properties of the partially cracked members, I_e, and hence to reflect the tension stiffening effect. Several empirical relationships are available to calculate the effective moment of inertia I_e. (Branson, 1965) proposed a well-known empirical relationship to express a gradual transition from gross moment of inertia to a fully cracked moment of inertia that is to be used for deflection calculations. In many cases, I_g is replaced by I_{uncr} , when the member is heavily reinforced. The intent of this equation is to account for the effects of cracking and reinforcement on member stiffness under increasing load. The effective moment of inertia with this method is highly dependent on the as the ratio of I_g/I_{cr} as well as on the level of the service moment relative to the cracking moment. This equation developed originally for beams, however, it only works well for flexure members with an I_g/I_{cr} ratio less than approximately 3, and this corresponds to beams and slabs with a steel reinforcing ratio greater than 1% (Bischoff and Scanlon, 2007). The equation has been adopted by several building codes including ACI 318-14 and is given by the following expression:

$$\mathrm{I_e} = \left(\frac{\mathrm{M_{cr}}}{\mathrm{M_a}}\right)^3 \mathrm{I_g} + \left[1 - \left(\frac{\mathrm{M_{cr}}}{\mathrm{M_a}}\right)^3\right] \mathrm{I_{cr}} \leq \mathrm{I_g} \qquad (2\text{-}11)$$

Where I_{cr} is the moment of inertia of the fully-cracked transformed section about an axis through centroid, I_g is the moment of inertia of the gross section about an axis through centroid, M_{cr} is the cracking moment of the section, and M_a is the maximum moment under service load.

(Bischoff, 2005) demonstrates that Branson's equation grossly overestimates the average stiffness of reinforced concrete member with small quantities of steel reinforcement ratios less than 1% and thereby gives a member deflection less than predicted. Therefore, (Bischoff, 2005) proposed an alternative expression for calculating effective moment of inertia I_e as given in Equation (2-12). It gives a rational approach that incorporates a tension stiffening model adopted in Eurocode 2 approach. The expression is independent of I_g/I_{cr} and works equally well for either steel or FRP reinforced concrete.

$$\mathrm{I_e} = \frac{\mathrm{I_{cr}}}{1 - \left(1 - \frac{\mathrm{I_{cr}}}{\mathrm{I_g}}\right)\left(\frac{\mathrm{M_{cr}}}{\mathrm{M_s}}\right)^2} \leq \mathrm{I_g} \qquad (2\text{-}12)$$

Where $\mathrm{I_g}$ the gross moment of inertia is, $\mathrm{I_{cr}}$ the fully-cracked moment of inertia.

On the other hand, (BS8110 part 2, 1985) includes for some concrete stress in tension below the neutral axis position to incorporate a tension stiffening phenomenon, while (Eurocode2, 2004) and (FIP Model Code, 2010) give an expression between the un-cracked and fully-cracked condition. It interpolates the curvature between the un-cracked and the fully-cracked stages to estimate the intermediate curvature. For members subjected mainly to flexure, the curvature of a section after cracking is calculated using the following expression:

$$\mathrm{k} = (1 - \xi)\,\mathrm{k_{un}} + \xi\,\mathrm{k_{cr}} \qquad (2\text{-}13)$$

Where ξ is a distribution coefficient (allowing for tension stiffening) that accounts for the moment level and the degree of cracks; and k is the deformation

parameter considered which may be, for example, a strain, a curvature, or a rotation. (As a simplification, $\boldsymbol{k}$ may also be taken as a deflection).

$$\xi = 1 - \beta \left(\frac{M_{cr}}{M_a}\right)^2 \quad (2\text{-}14)$$

$$M_{cr} = f_r \frac{I_g}{y_t} \quad (2\text{-}15)$$

Where β is coefficient to account the effects of duration of loading or repeated loading, $\beta = 1$ for short-term, $\beta = 0.5$ for sustained loads (allowing for loss of tension stiffening) or many cycles of repeated loading; f_r modulus of rupture; M_{cr} is the cracking moment; M_a is the maximum moment under service load.

2.8.3 Factors Influencing Tension Stiffening

There are several factors that affect the tension stiffening estimation. Changes in the steel reinforcement ratio or distribution could affect this value if there is a corresponding change to the area of concrete affected by the reinforcement (Bischoff, 2001). Other factors, such as concrete cover (Collins & Mitchell, 1991) and the presence of transverse reinforcement (Rizkalla et al., 1983), can also have an influence on crack spacing, which may affect tension stiffening (Bischoff, 2001). Early experimental work by (Clark & Cranstown, 1979) showed that the decrease of tension stiffening under short-term loading is not only a function of strain but also bar spacing in reinforced concrete slabs. They suggested that the decay of tension stiffening was greater when the bars were widely spaced in slabs. This is more significant when the bar spacing exceeds a critical value of 1.5 times the slab depth. Furthermore, the experimental study by (Sooriyaarachchi et al., 2005) showed that there was no significant influence on tension stiffening when the bar diameter was varied provided the reinforcement ratio remained unchanged.

On the other hand, (Chong, 2004) concluded that the contact surface area between the tensile steel and the concrete in a reinforced concrete member is an important factor affecting the overall bond characteristic in the tension zone of the member. Thus, larger concrete-steel contact surface area can improve the bond characteristic of a member. Based on the experiments conducted by

(Abrishami & Mitchell, 1996) they concluded that the use of high-strength concrete can increase tension stiffening, mainly in the linear elastic stage and at the crack formation stage. However, they found that this influence decreases gradually during the crack stabilisation stage. They also indicated that crack spacing in high strength concrete specimens is larger than in normal strength concrete specimens. A similar conclusion was reported by (Ouyang et al., 1997) who found that the tension stiffening effect declines faster in high-strength concrete members than in the normal-strength members as the average strain increases. They suggested that this may be attributed to the more brittle cracking process in high-strength concrete.

Another factor that could affect the tension stiffening is initial shrinkage prior to loading. Several tests have been carried out to examine the instantaneous response of reinforced concrete members after cracking. Most of these tests have not considered the influence of initial concrete shrinkage prior to loading. Test results show that estimates of tension stiffening, which represent the contribution from concrete to member stiffness, are influenced by shrinkage and will lead to an underestimation of this value if the initial member shortening caused by shrinkage is not included in the member response calculations (Bischoff, 2001). Therefore, shrinkage must be included in analysis of the member response to evaluate tension stiffening effect correctly (Fields and Bischoff, 2004).

From test observations conducted by (Bischoff, 2001) to investigate the effect of shrinkage on tension stiffening for tension members, he concluded that the apparent bond factor β_{exp} decreases considerably as the shrinkage increases for the same reinforcement ratio as shown in Figure 2-22. Furthermore, he exhibited that for the same amount of shrinkage the apparent loss of tension stiffening becomes worse as the reinforcing percentage increases as shown in Figure 2-23. He also stated that the shrinkage effects are certainly significant for reinforcing percentages greater than at least 1%. Moreover, he concluded that shrinkage does not have much effect on measured crack widths, assuming that crack widths are directly related to both the crack spacing and the difference in strain between the steel and concrete.

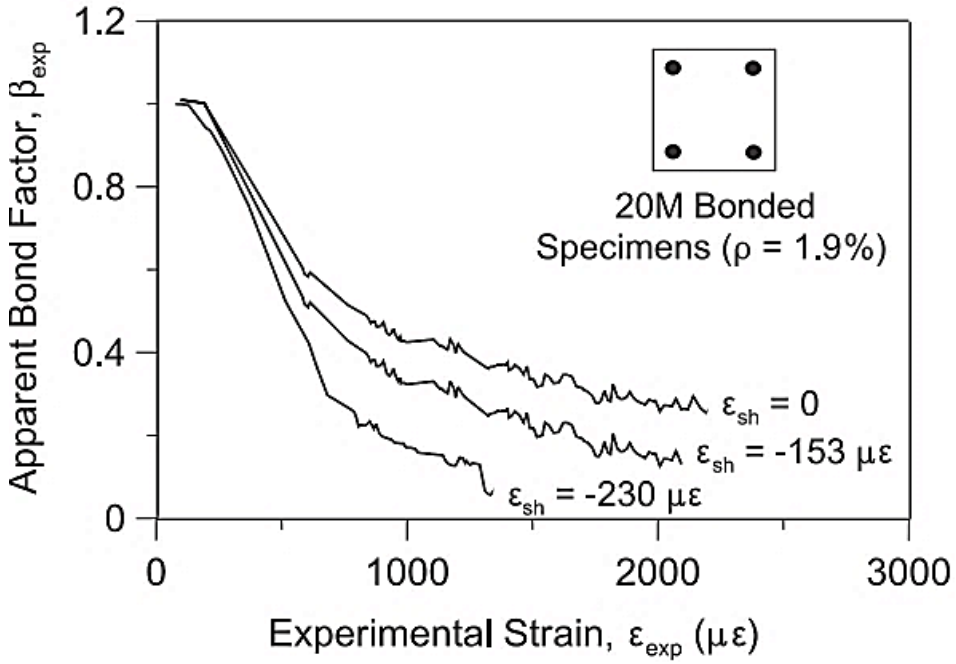

Figure 2-22. Effect of shrinkage on tension stiffening results for 20M bonded specimens ($\boldsymbol{\rho = 1.9\%}$) (Bischoff, 2001)

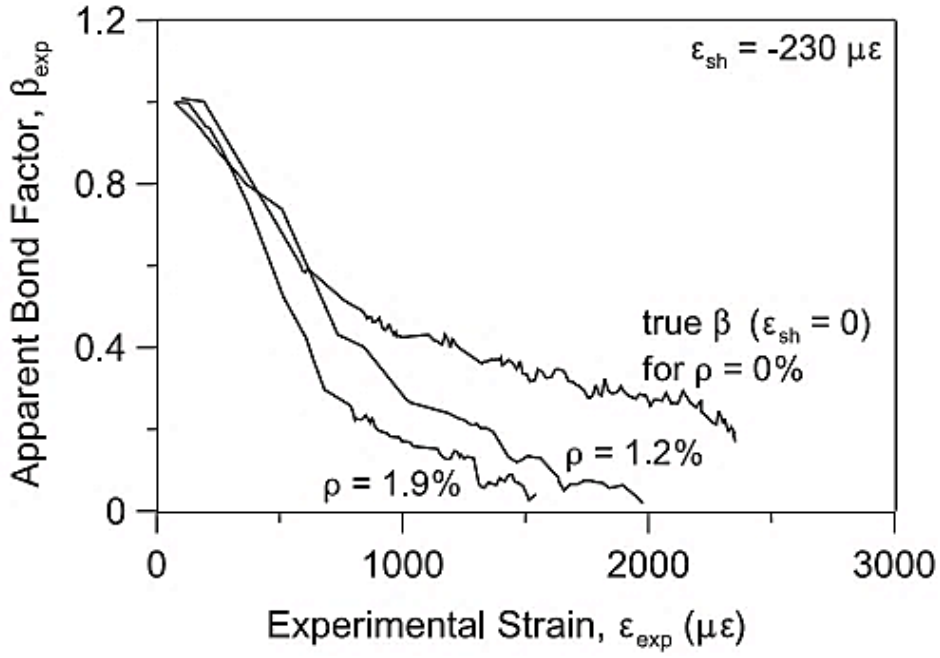

Figure 2-23. Effect of reinforcement ratio on tension stiffening results for $\boldsymbol{\varepsilon_{sh} = -230\ \mu\varepsilon}$ (Bischoff, 2001)

It has to be noted that the previous proposed empirical expressions for estimating tension stiffening have not addressed the influence of the shrinkage that occurred prior to loading. Generally, analysis of results from past work has assumed in

most cases that the response of a reinforced concrete tension member begins at zero deformation before the load is applied.

In the reinforced concrete flexural members, the average moment-curvature relationship is significantly affected if shrinkage occurs prior to loading as shown in Figure 2-24. As can be seen, the initial curvature of the fully cracked section is significantly larger than that of the uncracked section. For unsymmetrical reinforced concrete member, curvature and restraint stresses develop due to drying shrinkage even if the external load is still zero. Thus, the moment required to cause first cracking M_{crsh0} will be less than cracking moment M_{cr} as a result of restraint tensile stresses.

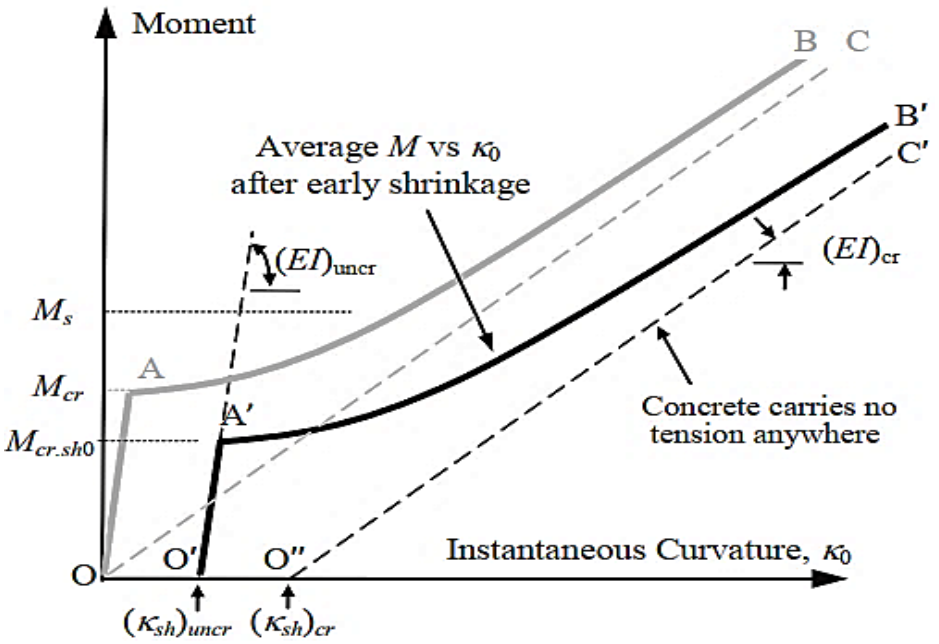

Figure 2-24. Moment versus curvature with shrinkage prior loading (Gilbert,2011)

Because the cracking moment is reduced, it is likely that early shrinkage prior to loading affects the magnitude of tension stiffening (Gilbert, 2011) but this is yet to be confirmed. As stated previously, (Bischoff, 2001) has only confirmed that the amount of tension stiffening will be underestimated if the early shrinkage is not included in the member response calculations. However, this effect does not account in the procedures of available finite element analysis FEA software packages.

Since early shrinkage of concrete is generally restrained, it would seem appropriate to account for restraint stresses when predicting member response. The restraint is provided by a combination of embedded reinforcement, attachment to structural supports, and lower shrinkage rates of previously placed adjacent panels when slab panels are placed at different times. Several methods have been proposed to account for restraint stress effect. A more general approach was proposed by (Scanlon and Murray, 1982) to include the effect of restraint cracking by introducing a restraint stress which effectively reduces the modulus of rupture. Instead of using this procedure, a value of $0.33\sqrt{f'_c}$,or about half of the code-specified value, was proposed for the reduced effective modulus of rupture. This approach was investigated by (Tam and Scanlon, 1986) and has found to give good correlation between calculated and measured field deflections. In 1987, (Ghali, 1987) has also used the idea of reduced modulus of rupture and exhibits the calculation of restraint stress due to embedded reinforcement with presence of uniform shrinkage strain profile.

2.9 Bond-Slip Behaviour

The behaviour of reinforced concrete members is strongly influenced by bond between the reinforcement and surrounding concrete, which in turn strongly affects the cracking performance. The magnitude and distribution of the bond stress determines the distribution of tensile stress in the concrete and steel between the cracks. At crack locations, slip reaches its peak and bond stress drops to zero. The bond-slip relationship between the steel and the concrete greatly affects the transfer of tension to the concrete and the contribution of the tensile concrete to the member's stiffness. Therefore, the bond-slip relationship plays an important role in the determination of service load behaviour including the deflection, widths and spacing of cracks both in the short-term and in the long-term. The bond between the steel and concrete ensures strain compatibility and thus the composite action of concrete and steel. Proper bond also ensures that there is no slip between the steel bars relative to the surrounding concrete under service load.

The correct prediction of cracking depends on a realistic modelling of the steel-concrete bond action. In fact, there is a degree of confusion regarding the

significance of the modelling of bond between concrete and reinforcing steel. The influence of bond is not important if the primary interest is to obtain a monotonic load-deflection response of a reinforced concrete member (Darwin, 1993). Stevens et al. (1991) concluded that the global load-deflection behaviour of a reinforced concrete member was not sensitive to bond-slip except for cases where bond failure was critical. However, if crack widths and crack spacings are of primary interest, the modelling of bond-slip is crucial. The importance of the bond-slip interface elements will be seen subsequently when it comes to determining the crack opening of the specimens. (Chong, 2004) stated that the crack pattern computed without using the bond-slip interface elements is unobjective. He also concluded that although localized cracking was computed, the spacing of the cracks is evidently incorrect compared to the experimental crack pattern.

The bond-slip behaviour presented above is related to short-term loading. Overtime, however, creep causes a gradual increase in slip and this phenomenon is known as bond creep. The consequences of bond creep are the reduction of slope of the bond-slip relationship as shown in Figure 2-25.

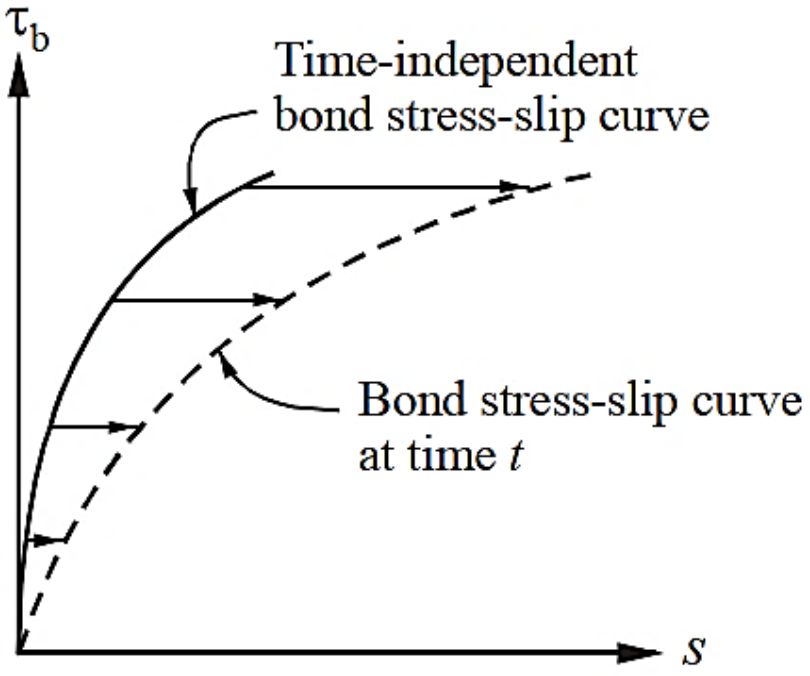

Figure 2-25. Influence of creep on bond-slip relationship

(Chong, 2004) found that the calculated long-term midspan defection for beam with a perfect steel-concrete bond assumption, is similar from those calculated using bond-slip interface elements as depicted in Figure 2-26.

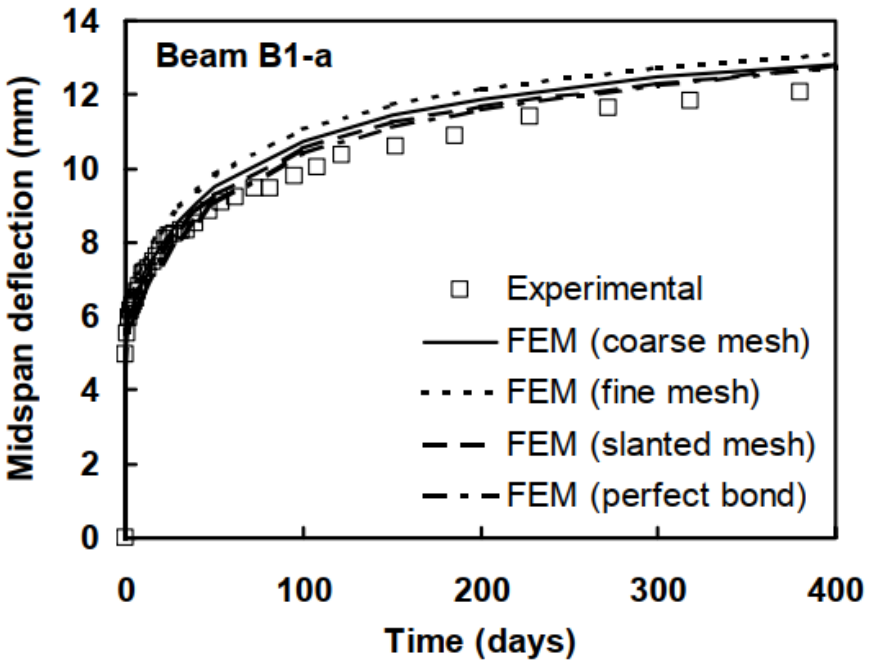

Figure 2-26. Comparison of FEM and experimental time-dependent midspan deflections

2.10 Nonlinear Modelling of Reinforced Concrete Behaviour

Cracking of concrete is considered the most important contribution to nonlinear behaviour in reinforced concrete structures. Nonlinear analysis of reinforced concrete structures has become important increasingly over the last few decades. Correct modelling of the post-cracking response of concrete in tension is needed to obtain realistic predictions of structural performance. Despite significant progress having been made in the development of computational methods, the accurate prediction of overall deformational of reinforced concrete slabs and their ultimate loads remains a difficult task since the mechanical behaviour of such members is very complicated and is extremely difficult, if not impossible, to model precisely (Jiang and Mirza, 1997).

As a criterion for cracking, two theories are known: the maximum stress theory and maximum strain theory. With regard to the former the cracking in concrete occurs whenever the maximum principal stress exceeds the tensile strength of

concrete. The first theory, however, is more popular than the second. (Phillips, 1973) found that the second theory, i.e. maximum strain theory, predicts stiffer behaviour than the first theory. So far, two basic approaches are available in the literature for the modelling of tensile cracking in concrete structures, namely the smeared crack approach and discrete crack approach. The selection of a cracking model depends on the purpose of the analysis. If overall load-deflection behaviour is of primary interest, the smeared crack model is probably the best choice. If detailed local behaviour is of interest, the adoption of the discrete crack model might be necessary.

In this section the smeared and discrete crack approaches are presented. In addition, the layered approach for sectional analysis has been also presented.

2.10.1 Smeared Crack Approach

This approach was proposed by (Rashid, 1968) and then it has been adopted and evaluated by DIANA Finite Element Software by considering three parameters: the softening behaviour, the tension failure criterion, and the shear retention. The smeared crack approach is a concept that developed for simulating crack propagation and fracture in concrete. This approach comes directly from computational continuum mechanics. This means that the criteria for crack propagation and, eventually, the prediction of the direction of propagation came directly from this theory, which is, mostly, based on failure criteria expressed in terms of stresses or strains (Cervera & Chiumenti, 2006). Because a smeared crack model is used, the reduced stiffness affects the entire clement, which causes a significant drop in the overall stiffness of the model (Bhatti et al.,1996).

In the smeared crack approach, one of the most important advantages that is do not account for discontinuities of the mesh topology. With such an approach, the geometric of local discontinuities due to cracking is treated as continuous by spreading the local discontinuity from the cracks over the entire element width as shown in Figure 2-27. Hence, the cracked material is assumed to remain a continuum and the mechanical properties (stiffness and strength) are modified to reflect the effect of cracking, therefore, remeshing is unnecessary as shown in Figure 2-28.

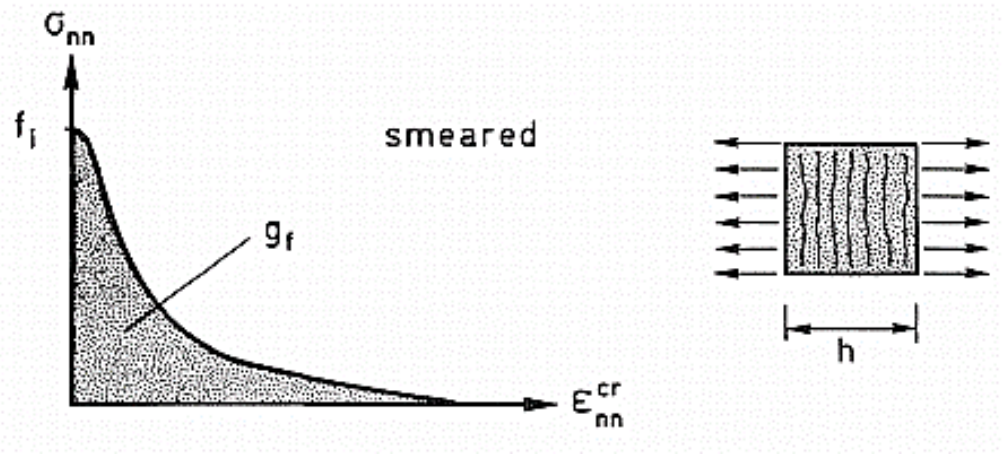

Figure 2-27: Tensile stress vs. crack strain diagram (Rots et al., 1985)

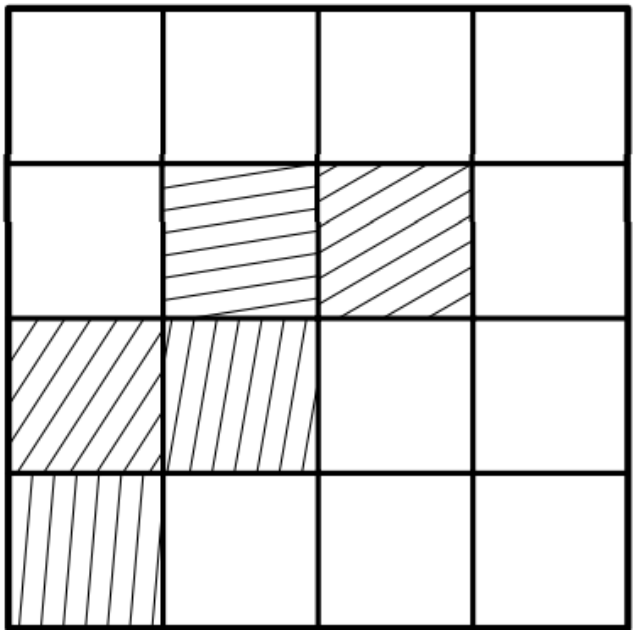

Figure 2-28. Smeared approaches to crack propagation without remeshing

Within the fracture zone, the stress decreases gradually while the strain increases as shown in Figure 2-29. This behaviour is known as tensile strain-softening. Consequently, cracking strain localization is accompanied by unloading of the material outside the fracture zone, thus, the cracks outside the fracture zone are closed or even recovered. In the smeared crack approach, the propagation of cracks can be described as rotating or fixed. In fixed crack, the crack formation normal to the major principal stress and has a fixed orientation along the entire element. In rotating crack model, the crack propagation rotates with the principal stress during the entire element.

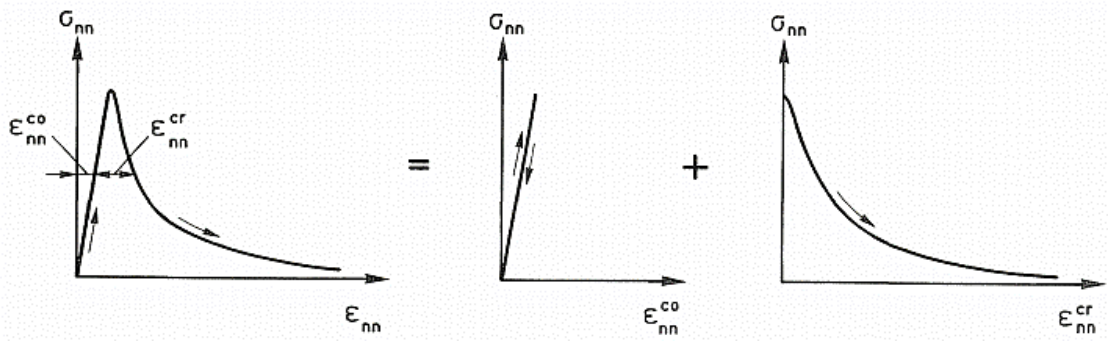

Figure 2-29: Tensile stress of a fracture zone vs. concrete strain (Rots et al., 1985)

2.10.2 Discrete Crack Approach

In the earliest applications of the finite element method to concrete structures 1960s, cracks were modelled by so-called discrete crack model, by separation of nodal points in fracture zone (Clough, 1962;Ngo & Scordelis, 1967;Nilson, 1968; Blaauwendraad & Grootenboer, 1981;Hillerborg, 1985). The node is assumed to split into two nodes, i.e. when the tensile strength criterion is violated at this node, and the tip of the crack is assumed to propagate to the next node as sketched in Figure 2-30. The discrete crack approach in its original form several disadvantages, for instance, cracks are forced to propagate along element boundaries, so that a mesh bias is introduced.

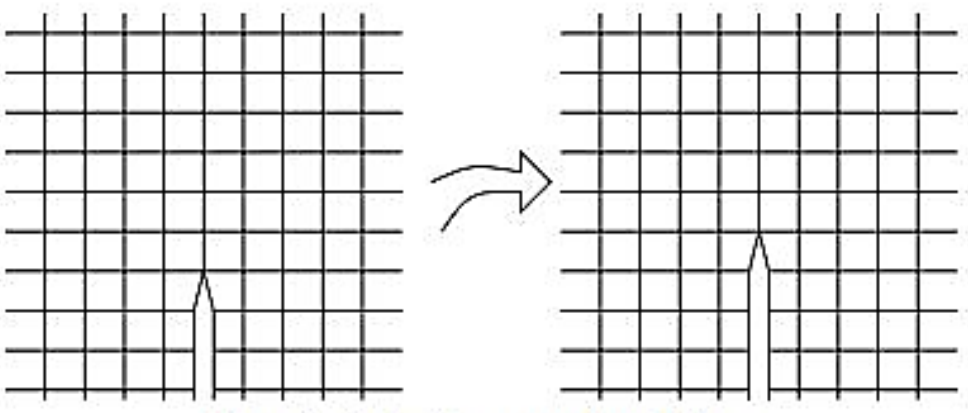

Figure 2-30. Discrete crack modelling

With such an approach, the cracks are modelled as a changing in geometrical discontinuity in a structure. Thus, the response is mesh dependent strongly and re-meshing procedure is necessary. Furthermore, when a crack propagates, the

mesh geometry is changed, and the updating process are time consuming. In this approach, the local fracture zone due to cracking is treated by modelling the local discontinuity from the cracks with stress-crack opening relation as shown in Figure 2-31.

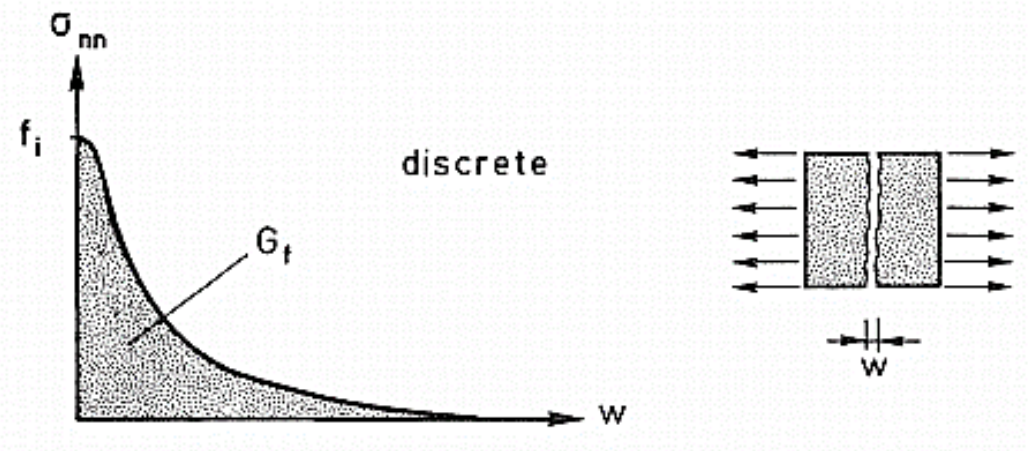

Figure 2-31. Tensile stress vs. crack opening displacement diagram (Rots et al., 1985)

This approach is the localized cracking approach, in which concrete fracture models are used in conjunction with bond-slip interface elements to model stress transfer between concrete and steel, which actually takes into account the relative displacement of the reinforcing steel and the adjacent concrete. Fracture behaviour of plain concrete at a discrete crack is characterized by strain softening and has little influence on the tension stiffening response (Bischoff and Paixao, 2004). The discrete crack model was later replaced by the smeared crack approach which is more attractive in a variety of computational aspects (Chong,2004).

2.10.3 Layered Approach

Layered approach provides a suitable way to deal with complex issues such as cracking of concrete and tension stiffening as well as creep and shrinkage. The approach uses the material stress-strain relationships used for modelling the behaviour of materials.

The forming of cracks is generally considered to be the most important factor governing the nonlinear behaviour of reinforced concrete flexural members (Rots

et al., 1985; Szilard, 2004). Therefore, several efforts have been made to simulate the tensile cracks. Some of these efforts have been discussed earlier. Theoretically, to trace the cracking propagation and changes in the properties of cracked zones, it is convenient to subdivide the concrete into layers. For bending analysis of reinforced concrete slabs, probably the use of layered finite element analysis appears to be the most convenient.

This approach has been widely used for the finite element analysis of reinforced concrete structure (Hand, 1972; Hand,1973; Lin and Scordelis,1975; Scanlon, 1971). It has been demonstrated to be effective, particularly, ultimate behaviour in bending and shear (Guan and Loo, 1997).

2.11 Time-Dependent Behaviour of Plain Concrete

The first step in design is usually to perform ultimate limit state (ULS) analysis; the serviceability limit state (SLS) is then verified. In many cases, however, serviceability (i.e. deflection) is critical and it is this limit state, particularly in the case of reinforced concrete (RC) flat slabs and flat plates which are typically thin in relation to their spans. As the properties of concrete develop with age, the serviceability of a member is affected – it will behave time dependently.

Under a sustained stress, the concrete specimen exhibits an immediate deformation at the time of loading; then a long-term deformation, which gradually increases with time at a rate dependent on the applied stress and the environmental conditions. The total strain of a plain concrete that loaded uni-axially at time t_0 with a constant stress may be expressed as total strain produced by instantaneous, creep, shrinkage, and thermal strains (CEB-FIP-MC2010, 2010). Creep strain is induced by sustained stress, while free shrinkage strain is stress independent. Creep and shrinkage are inherent properties of concrete. Furthermore, they are dependent phenomena. Figure 2-32 illustrates the total concrete strain components with time under sustained stress and constant temperature.

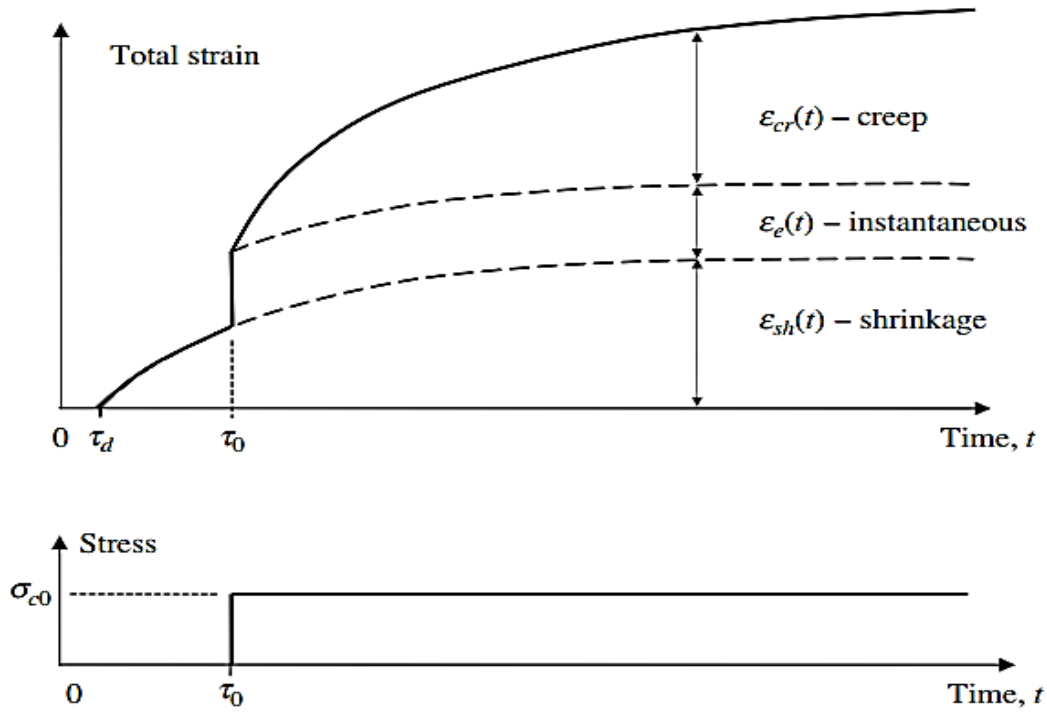

Figure 2-32. Concrete strain components under sustained stress (Gilbert & Ranzi, 2010)

Among the time-dependent properties of concrete that are of interest to the structural engineer are creep and shrinkage. In a flexural member, there are three basic phenomena that lead to an increase in deflection with time over instantaneous deflection. These are development of shrinkage, creep, and loss of tension stiffening with time.

2.11.1 Creep of Concrete

If concrete specimen is subjected to a sustained stress, it continues to deform further with time. This phenomenon was discovered by (Hatt, 1907). It is now commonly known as creep. Creep is caused by several different and complex mechanisms that are not yet fully understood. In 1983, (Neville, Dilger, & Brooks, 1983) identified the mechanisms of creep are caused by : sliding the cement gel between layers of absorbed water (viscous flow);decomposition of the interlayer water within the cement gel, elastic deformation of the aggregate and the gel crystals (delayed elasticity); local fracture within the gel involving the breakdown of bonds (micro-cracking); mechanical deformation theory; and plastic flow. Perhaps 75% of the total creep will occur during the first year (McCromac and Brown,2015). About 50 per cent of the final creep develops in the first 2–3 months and about 90 per cent after 2–3 years (Gilbert and Ranzi, 2010). After several

years under load, the rate of change of creep with time is very small. Several factors that influence the magnitude and rate of creep development such as effect of concrete mix proportions, size and shape of member, relative humidity and temperature, applied stress level, curing condition, the age at loading (ACI-209.1R, 2005). The amount of creep is largely dependent on the amount of stress. It is almost directly proportional to stress as long as the sustained stress is not greater than about one-half of f'_c. Beyond this level, creep will increase rapidly. High strength concretes have less creep than do lower strength concretes (McCromac and Brown,2015). Large creep members, i.e. those with large volume to surface ratios, will creep proportionally less than smaller thin members where the free water has smaller distances to travel (McCromac and Brown,2015).

Early work by (Hansen and Mattock, 1966) showed that the size and shape of concrete member affect, at all ages, both creep and shrinkage stored under drying conditions. Hence, both the rate and final values of creep and shrinkage decrease as the member becomes larger. They indicated that the creep approaches the value of basic creep corresponding to a sealed specimen when the member is very large since the moisture path would be expected to be low. They were used the volume /surface ratio to correlate shrinkage with change in size and shape, and hence this ratio could then reasonably be used to correlate the drying creep with change in size and shape. Since basic creep is unaffected by size and shape of member, the volume / surface ratio could also be used to study the total creep occurring under drying conditions (Hansen and Mattock, 1966). In1994, (Bazant and Xi, 1994) demonstrated that the drying creep larger than the sum of the separately observed basic creep and shrinkage. As the size and the shape of the member influence the rate of shrinkage and creep, the size effect has been considered by using correction coefficients proposed by several guidance and codes.

Creep occurs under both compressive and tensile stresses (Neville et al., 1983). However, previous research on creep has mostly been focused on concrete in compression. Despite research having been undertaken on tensile creep, the mechanisms are still uncertain and measuring the magnitude and rate of development of tensile creep is complicated by the inevitable difficulties encountered in isolating the small tensile creep strain from the concurrent

shrinkage strain, which may be many times larger (R.I. Gilbert, 1988). Nevertheless, the creep of concrete in tension is different than creep in compression. Tensile creep also plays a significant role in the analysis of RC members. Little attention has been devoted to the study of tensile creep (ACI-209.2R, 2008) . It is accepted that the analytical models for creep prediction in compression also extend to concrete in tensile(CEB-FIP-MC2010, 2010).

Some experimental observations indicate similar behaviour between tensile creep and compressive creep while other observations suggest that tensile creep is higher than compressive creep at similar stress levels. In 2014, (Forth, 2014) conducted experimental test on series of experimental specimens to investigate the tensile creep behaviour of concrete. On the basis of equal stresses, tensile creep is on average between 2 and 3 times greater than compressive creep, the maximum ratio is in excess of 8. The use of the compressive creep to the tensile creep ratio in calculation of long-term deflections of beam has been applied successfully by (Z. P. Bazant & Oh, 1984; Branson, 1977; Chu & Carreira, 1986). They have multiplied the measured compression creep coefficients by factors to predict equivalent coefficient describing tensile creep. They have found that the deflection of beams gives fit better results with time when the tensile creep coefficient ranged of 1 to 3 compressive creep. While tensile creep can cause a negative effect on the behaviour of a concrete structure it can also act positively, it can relieve induced stresses caused by the restraint of imposed strains (e.g. shrinkage, early thermal movement).

2.11.2 Shrinkage of Concrete

Shrinkage of concrete is the unrestrained unloaded volume decreases associated with chemical changes and loss of moisture from the concrete. Shrinkage strain is stress independent. Shrinkage can be divided into plastic shrinkage, thermal shrinkage, autogenous shrinkage, and drying shrinkage. Plastic shrinkage occurs in the first few hours, whereas drying, and thermal shrinkage all occur in after setting in the hardened concrete. Autogenous shrinkage, some called it hydration shrinkage. The drying shrinkage is the reduction in volume principally caused by the loss of moisture to the environment during the drying. Drying shrinkage increases with time at a gradually decreasing rate and continuous in the months and years after casting (R.I. Gilbert & Ranzi,

2010). The drying shrinkage also depend on several factors such effect of mix proportions, the relative humidity and temperature, curing condition, the size and the shape of the member (ACI-209.1R, 2005). If the drying conditions are the same the top and bottom surfaces, the total strain is uniform over the depth. But, if drying is different from the top and bottom surfaces, the total strain distribution is no longer uniform over the depth of the section. Thus, a curvature develops on the unreinforced section (R.I. Gilbert & Ranzi, 2010). All concrete members are subject to volume change in varying degrees. Uniform volume change will not produce internal stresses and cracking if the concrete is relatively free to change in all directions. This case is rarely for massive concrete members since size alone usually causes non-uniform change and there is often sufficient restraint either internally or externally to produce stresses and then cracking (ACI-207.2R, 2002).

2.12 Prediction of Creep and Free Shrinkage for Plain Concrete

Accuracy of predictions of creep and shrinkage deformations leads to the accuracy of structural behaviour modelling and predictions. Very extensive attempts have been carried out in the past for estimating the long-term creep and shrinkage of concrete. Several authors suggested models to predict the long-term creep and shrinkage deformation. Such models are included in (ACI-209.2R, 2008; Z.P. Bazant & Baweja, 1995, 2000; CEB-FIP-MC2010, 2010; CEB-FIP, 1990; Gardner & Lockman, 2001). Moreover, (Neville & Brooks, 1975) proposed equations for predicting shrinkage and creep at one year from measured values at 7 and 28 days. For periods longer than 1 year, the prediction is also possible with those equations. In 2005, (Brooks, 2005) conducted experimental investigation on creep and shrinkage deformation during 30 years, he stated that most methods fail to recognize the influence of strength of concrete and type of aggregate on creep coefficient , which ranged from 1.2 to 9.2. Unlike the other models, the CEB model method does account for the influence of concrete strength.

2.12.1 Predictions of Shrinkage and Creep Deformation by CEB-FIP-MC2010 Model

If the concrete specimen is subjected to sustained loads with constant temperature, it continuous to deform further with time. This phenomenon was discovered in 1907 by (Hatt, 1907). It is now commonly known as creep. The creep coefficient at any time t, $\emptyset(t, t_0)$ can be estimated using model proposed in (CEB-FIP-MC2010, 2010). These analytical equations are valid for stress level $\sigma_c < 0.4\, f_{cm_{(t_0)}}$ and exposed to mean relative humidity in the range 40 to 100 % and mean temperature $5^{\circ}C$ to$30^{\circ}C$. The creep coefficient can be found from following:

$$\emptyset(t, t_0) = \emptyset_0 \beta_c(t - t_0) \tag{2-16}$$

$$\emptyset_0 = \emptyset_{RH}\, \beta(f_{cm})\, \beta(t_0) \tag{2-17}$$

$$\emptyset_{RH} = \left[1 + \frac{1 - RH/RH_0}{0.1\sqrt[3]{(h/h_0)}} . \alpha_1\right] . \alpha_2 \tag{2-18}$$

$$\alpha_1 = \left[\frac{35}{f_{cm}}\right]^{0.7}, \qquad \alpha_2 = \left[\frac{35}{f_{cm}}\right]^{0.2} \tag{2-19}$$

$$\beta(f_{cm}) = \frac{16.8}{\sqrt{(f_{cm})}} \tag{2-20}$$

$$\beta(t_0) = \frac{1}{0.1 + (t_0)^{0.2}} \tag{2-21}$$

The development of time-ratio of creep is given by:

$$\beta_c(t - t_0) = \left[\frac{(t - t_0)/t_1}{\beta_H + (t - t_0)}\right]^{0.3} \tag{2-22}$$

$$\beta_H = 1.5\ x\ h\ x \left\{1 + (1.2\frac{RH}{RH_0})^{18}\right\} + 250\ \alpha_3 \ll 1500\ \alpha_3 \quad (2\text{-}23)$$

$$\alpha_3 = \left[\frac{35}{\mathrm{f_{cm}}}\right]^{0.5} \quad (2\text{-}24)$$

$$\mathrm{f_{cm}} = \mathrm{f_{ck}} + 8\ \mathrm{MPa} \quad (2\text{-}25)$$

Where $\emptyset(t, t_0)$ is the creep coefficient ;$\emptyset_0$ is the notional creep coefficient ;β_c is the coefficient to describe the development of creep with time after loading ; t is the age of concrete (days) since pouring day ; t_0 is the age of concrete at loading (days) ;$h = 2A_c/u$ is the notional size of member (mm), where A_c is the cross-section and u is the perimeter of the member in contact with atmosphere; f_{cm} is the mean compressive strength of concrete at the age of 28 days (MPa); f_{ck} refer to characteristic strength; $f'c$ is the concrete compressive strength at age 28 days; $f_{cm0} = 10$ MPa; RH is the ambient relative humidity (%); $RH_0 = 100\%$; $h_0 =$ 100 mm.

Free shrinkage strain is stress independent. The reduction in volume principally caused by the loss of water during the drying known as drying shrinkage. The total shrinkage strain is composed of two components, the autogenous shrinkage strain and the drying shrinkage strain. The drying shrinkage strain develops slowly, since it is a function of the loss of the water through the hardened concrete, while the autogenous shrinkage strain develops during hardening process: therefore, the major part develops in the early days after casting. The free shrinkage strain at any time t, $\varepsilon_{sh}\,(t, t_c)$ can be estimated using the model proposed in (CEB-FIP-MC2010, 2010) as following:

$$\varepsilon_{\mathrm{cs}}(\mathrm{t}, \mathrm{t_s}) = \varepsilon_{\mathrm{cas}}(\mathrm{t}) + \varepsilon_{\mathrm{cds}}(\mathrm{t}, \mathrm{t_s}) \quad (2\text{-}26)$$

Where shrinkage is subdivided into the autogenous $\varepsilon_{\mathrm{cas}}(\mathrm{t})$ shrinkage and drying shrinkage $\varepsilon_{\mathrm{cds}}(\mathrm{t}, \mathrm{t_s})$.

$$\varepsilon_{\mathrm{cas}}(\mathrm{t}) = \varepsilon_{\mathrm{cas0}} \cdot \beta_{\mathrm{as}}(\mathrm{t}) \quad (2\text{-}27)$$

$$\varepsilon_{cds}(t, t_s) = \varepsilon_{cds0}\,(f_{cm}).\,\beta_{RH}\,(RH).\,\beta_{ds}(t - t_s) \quad (2\text{-}28)$$

$$\varepsilon_{cas0}\,(f_{cm}) = -\alpha_{as}\left(\frac{f_{cm}/10}{6 + f_{cm}/10}\right)^{2.5}.10^{-6} \quad (2\text{-}29)$$

$$\beta_{as}(t) = 1 - \exp\left(-0.2\,.\sqrt{t}\right) \quad (2\text{-}30)$$

$$\varepsilon_{cds0}\,(f_{cm}) = [(220 + 110.\,\alpha_{ds1}\,).\exp(-\alpha_{ds2}\,.f_{cm}).10^{-6}] \quad (2\text{-}31)$$

$$\beta_{RH} = -1.55\left[1 - \frac{RH}{100}\right]^{3} \quad \text{for } 40 \le RH \le 99\ \%.\,\beta_{s1} \quad (2\text{-}32)$$

$$\beta_{s1} = \left[\frac{35}{f_{cm}}\right]^{0.1}$$

$$\beta_{ds}(t - t_s) = \left(\frac{(t - t_s)}{0.035\ h^2 + (t - t_s)}\right)^{0.5} \quad (2\text{-}33)$$

Where f_{cm} is the mean compressive strength of concrete at the age of 28 days (MPa); α_{as} , α_{ds1} , α_{ds2} are a coefficients dependent on the type of cement (for current study α_{as} , α_{ds1} , α_{ds2} are 600, 6,0.012 respectively); $\beta_{ds}(t - t_s)$ describing the time-development; t is the age of concrete (days); t_s is the age of concrete (days) at the beginning of shrinkage or swelling; $h = 2A_c/u$, is the notional size of member (mm).

2.12.2 Predictions of Shrinkage and Creep Deformation by ACI 209.2R-08 Model

Due to the properties of concrete, concrete exhibits a long-term deformation. Among the long term properties of concrete that are of interest to the structural engineer are the shrinkage and creep. (ACI-209.2R, 2008) recommends a procedure and set of analytical models for predicting creep and shrinkage deformations. Under standard conditions the creep coefficients can be determined from:

$$\emptyset_{(t,t_0)} = \frac{(t - t_0)^{0.6}}{d + (t - t_0)^{0.6}} . \emptyset_u \quad (2\text{-}34)$$

Where $\emptyset_{(t,t_0)}$ is the creep coefficient at concrete age t due to a load applied at the aget_0; d (in days)

For the standard conditions, in the absence of specific creep data for local aggregates and conditions, the average value proposed for the ultimate creep coefficient $\emptyset_u$=2.35. For conditions other than the standard conditions, the value of the ultimate creep coefficient needs to be modified by correction factors as shown in equations (**2-35** and (**2-36**.

$$\emptyset_u = 2.35\, \gamma_c \quad (2\text{-}35)$$

$$\gamma_c = \gamma_{c,t_0} \gamma_{c,RH} \gamma_{c,vs} \gamma_{c,s} \gamma_{c,\psi} \gamma_{c,\alpha} \quad (2\text{-}36)$$

Where γ_c represent the cumulative product of the applicable correction factors. The correction factors are age at loading γ_{c,t_0} , ambient relative humidity $\gamma_{c,RH}$, size of the member $\gamma_{c,vs}$, slump of fresh concrete $\gamma_{c,s}$, ratio of fine aggregate factor $\gamma_{c,\psi}$, air content percentage $\gamma_{c,\alpha}$.

(ACI-209.2R, 2008) also recommends a procedure and set of analytical models for predicting shrinkage deformations. The shrinkage strain against time can be estimated by the following expression:

$$\varepsilon_{sh_{(t,t_c)}} = \frac{(t - t_c)^{35}}{f + (t - t_c)^{35}} . \varepsilon_{shu} \quad (2\text{-}37)$$

Under standard conditions, in the absence of specific shrinkage data for local aggregates and at ambient relative humidity of 40%, the average value suggested for the ultimate shrinkage strain ε_{shu}= 780×10^{-6} mm/mm. For conditions other than the standard conditions, the average value of the ultimate

shrinkage ε_{shu} needs to be modified by correction factors as shown in equations (**2-38** and (**2-39**.

$$\varepsilon_{\mathrm{shu}} = \gamma_{\mathrm{sh}}\, 780 \times 10^{-6} \tag{2-38}$$

$$\gamma_{\mathrm{sh}} = \gamma_{\mathrm{sh,t_c}}\gamma_{\mathrm{sh,RH}}\gamma_{\mathrm{sh,vs}}\gamma_{\mathrm{sh,s}}\gamma_{\mathrm{sh,\psi}}\gamma_{\mathrm{sh,\alpha}}\gamma_{\mathrm{sh,c}} \tag{2-39}$$

Another type of shrinkage occurring in the concrete is so called autogenous shrinkage. It is occurring in the absence of moisture exchange due to the hydration reactions taking place in the cement matrix. Until recently, autogenous shrinkage was not considered significant because, in most cases, it did not exceed 150 micro-strains (ACI-209.2R, 2008). For concretes with water-cement ratios (w/c) less than 0.4, mean compressive strengths greater than 60 MPa, or both, autogenous shrinkage may be a major component of the shrinkage strain. Some models separate total shrinkage into its autogenous and drying shrinkage components as mentioned in (CEB-FIP-MC2010, 2010), whereas (ACI-209.2R, 2008) only introduces total shrinkage strain with no distinguishing of autogenous and drying shrinkage. Most test programs consider the measurement of strains from the start of drying. It is assumed that the restrained stresses due to autogenous shrinkage and swelling are negligible because of the large creep strains and stress reduction of the concrete at early ages (ACI-209.2R, 2008). For normal-strength concrete, it is usually assumed that the entire shrinkage strain is from drying shrinkage, and any contribution from autogenous shrinkage is neglected (ACI-209.1R, 2005).

2.13 Loss of Tension Stiffening

As explained previously, there are three main phenomena that lead to an increase in deformation with time under sustained load. These are loss of tension stiffening, shrinkage and creep. Shrinkage and creep have been studied extensively over the years, but this is not so for tension stiffening phenomenon which is a structural problem related to the loss of beneficial stiffness with time. To date, no formulae exist to predict how tension stiffening changes as a function of time. A very limited number of studies have been devoted to the investigation

of the actual mechanisms that cause the reduction of tension stiffening under long-term loading. It has been concluded that the major mechanism controlling the long-term loss of tension stiffening is the development of cumulative damage which occurs mainly from either the formation or extension of existing surface cracks or the extension or formation of internal cracks (Beeby & Scott, 2006). Over time, however, the internal cracking will lead then to a reduction in the stiffness of the connection between the reinforcement and the surrounding concrete and hence decreasing the stress transferred to the concrete over the transfer length. According to the investigations carried out by (Beeby & Scott, 2006), it was suggested that there are three most likely possibilities that are related to internal cracking. These are increase in the length of internal cracks, increase in the number of internal cracks and breaking through of the internal cracks nearest to crack surface into the cracks. With respect to the latter possibility, Beeby and Scott stated that if the internal crack, as shown in Figure 2-19, nearest to the primary crack extends, it is possibly to break through into the crack face. When this mechanism happens, the reinforcement has become detached from the body of the concrete and will thus no stress transfer between the reinforcement and the concrete within this zone.

More recently, (Scott & Beeby, 2005) stated that the internal events, such as crack development around reinforcement or slip between the reinforcement and the concrete, will lead to a reduction in tension stiffening. In 2004, (Gilbert, 2004) and others have shown that the tension stiffening effect reduces with time under sustained loads, probably due to the combined effects of shrinkage induced micro-cracking around the steel bars and tensile creep rupture. (Gilbert, 2007) has also come to this conclusion. He concluded that the tension stiffening decreases with time, possibly due to the combined effects of tensile creep, shrinkage cracking and creep rupture. Furthermore,(Gilbert & Wu, 2009) indicated that the loss of tension stiffening is primarily attributed to cracking and bond breakdown caused by drying shrinkage and, to a lesser extent, due to tensile creep. Based on their experimental findings at the obtained variation in concrete stress along a bar, (Beeby & Scott, 2006) concluded that the effect of tensile creep would be expected to be a reduction in the initial peak stress as shown in Figure 2-33. However, despite the effect of tensile creep on the initial

concrete stress, Beeby and Scott proposed that the contribution of tensile creep plays an insignificant role in the changes in tension stiffening with time.

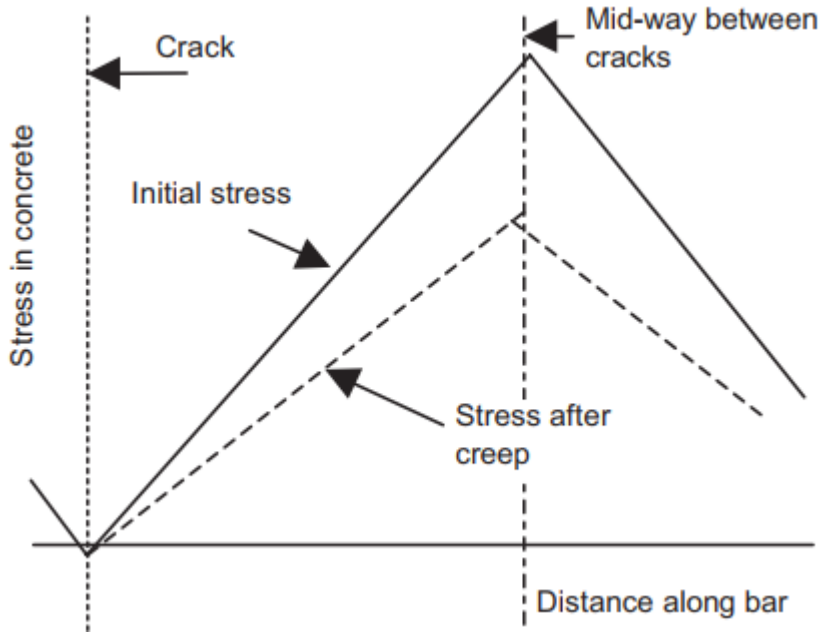

Figure 2-33. Schematic diagram of effect of tensile creep on initial concrete stress (Beeby & Scott, 2006)

As mentioned earlier, tension stiffening in a reinforced concrete member arises from a certain amount of tensile stresses carried by the concrete due to the bond between the steel and concrete. Since bond creep is a mechanism of long-term deformation, the effect of such a phenomena would be to reduce the gradient of the stress change adjacent to a crack (Beeby and Scott, 2006) and hence a reduction in tension stiffening. The effect of this would be indistinguishable from that shown in Figure 2-33. In reality, the consequence of normal creep will be a reduction in the shear stresses (i.e. bond stresses) at the steel-concrete interface (Beeby and Scott, 2006).

Further to the previous reasons, the long-term loss of tension stiffening is also influenced by the reduction in tensile strength with time. It is well known that the tensile strength of concrete decreases under constant load with time. (Beeby and Scott, 2006) found that the tensile strength reduces by about 35% over a period of around 1 to 10 days, which is similar to the period which tension stiffening is

lost. This led Beeby and Scott to suggest that the increase in cumulative damage wth time, and hence the loss of tension stiffening, results from the reduction in tensile strength of the concrete surrounding the reinforcement with time under constant load. They also suggested that the high strength concrete suffers a greater loss of tensile strength of concrete with time under constant load than does the normal strength concrete.

There is a minimal published information on the rate of decreasing of tension stiffening. The assessment of tension stiffening with flexural members is fraught with problems. Most tests used square prisms with a singly reinforcement placed centrally, loaded in pure uniaxial tension. In addition, a small number of slabs were tested to check the capability of the tensile results to flexural situation. In reality, the assessment of long -term loss of tension stiffening in flexural members is further complicated by the development of creep in the compression zone and shrinkage. In 2004, (Scott & Beeby, 2004) have shown that the tension stiffening decayed much rapidly more than was previously thought, they concluded that tension stiffening decreases to about half the initial value in a period 20 day or sooner after loading; the stiffening effect then remains constant for a constantly applied load. How rapidly this reduction occurs has not been studied. A similar conclusion was reported by (Scott & Beeby, 2005) who found that the tension stiffening decays faster in the first 20 days after loading. However, they did not adequately identify the effects of shrinkage in the assessment of the experimental test results. They also did not report the effect of shrinkage that occurred prior to loading. In 2008, (R. Gilbert, 2008) stated that tension stiffening decreases gradually with time but not rapidly as reported by (Scott & Beeby, 2004) and (Scott & Beeby, 2005). In 2002, (Vollum, 2002) found that tension stiffening rapidly lost more after loading than predicted by models accounted loss of tension stiffening to shrinkage. In addition, he concluded that the tension stiffening is lost quicker in slabs that crack significantly forms on loading than in slabs that cracks mainly form after loading due to shrinkage. Furthermore, the study also showed that shrinkage does not contribute significantly to loss of tension stiffening in cracked members after loading.

Due to the lack of understanding of the long-term loss of tension stiffening, several models represent tension stiffening based on empirical equations. The

codes (FIP Model Code, 2010) and (Eurocode2, 2004) propose that the loss of tension stiffening can be modelled by take factor $\beta_2 = 0.5$. In 2013, (Forth et al., 2013) they stated that the Eurocode 2 equation predicts the shrinkage curvature reasonably well assuming mean-unfixed distribution factor ζ with $\beta_2 = 1$, particularly at early ages (up to 60 days), whereas assuming fixed ζ with $\beta_2 = 0.5$ significantly overestimates the curvature of a cracked beam. An alternative equation was proposed by (Gilbert, 2011) for modelling the loss of tension stiffening with time. This equation was derived originally by (Bischoff, 2005) for modelling effective moment of inertia, and then modified by Gilbert to reflect the loss of tension stiffening based on the term β as in the following equation:

$$\mathrm{I_{ef}} = \frac{\mathrm{I_{cr}}}{1 - \beta\left(1 - \frac{\mathrm{I_{cr}}}{\mathrm{I_{uncr}}}\right)\left(\frac{\mathrm{M_{cr}}}{\mathrm{M_s}}\right)^2} \leq 0.6\mathrm{I_{uncr}} \qquad (2\text{-}40)$$

Where $I_g$the gross moment of inertia is, $\mathrm{I_{cr}}$ the fully-cracked moment of inertia, $\mathrm{I_{ef}}$ the effective moment of inertia. The term β in equation is used to account for both shrinkages induced cracking and the reduction of tension stiffening with time. If shrinkage has not occurred before first cracking, a value of $\beta = 1$ can be used. However, in practice, the shrinkage usually occurs before first loading, and thereby the value β is less than 1. A value of $\beta = 0.7$ is recommended at early ages less than 28 days; and $\beta = 0.5$ is recommended at ages greater than 6 months.

2.14 Tensile Stresses Caused by Restraint to Shrinkage Strains

In concrete structures, unrestrained volume changes are unusual. Generally, all concrete members are subject to volume change in varying degrees due to shrinkage as a result of moisture loss. When the concrete member is not free to exhibit the volume changes (e.g., external restraint, restraint caused by the bonded reinforcement as shown in Figure 2-34), tensile stresses develop in the concrete member. Reinforcement embedded in a concrete member provides restraint to shrinkage, leading to a compressive stress in the reinforcement as well as a tensile stress in the concrete with time. This internal tensile restraining

stress is often significant enough to cause time-dependent cracking (Gilbert & Ranzi, 2010). After cracking, further shrinkage induced deformation causes significant increases in crack widths with time (Gilbert, 2017). In other words, shrinkage causes a gradual widening of flexure cracks and a gradual tension in the uncracked zones that may lead to additional cracking (Gilbert & Ranzi, 2010). Phenomenon of restrained shrinkage cracking is not merely an early age problem. It has recently shown that the drying shrinkage can play a significant role in the development of cracks beyond early age (Shehzad, 2018). It is well known that restrained shrinkage cracking of concrete depends on combinations of a variety of factors including the degree of restraint, rate and magnitude of shrinkage, mechanical property development, creep and stress relaxation, and fracture resistance of the concrete (Weiss, 1999). In most sustained loading cases, the time-dependent opening of cracks is largely dependent on the ability of a concrete to shrink (Chong, 2004).

Figure 2-34. Reinforcement inside poured fresh concrete

2.15 Modelling of Creep and Shrinkage Curvatures

In the flexural members, if the reinforcement is not symmetrically placed in the section or placed just in tension, uniform shrinkage will induce a curvature in the

cross section. Creep also induces curvature with time in the cross section. Therefore, the long-term analysis is required which incorporates the effects of shrinkage and creep within the cross section. The combination between creep and shrinkage actions are very complex physical phenomena. The distinguish between creep and shrinkage deformations in reinforced concrete member is not straightforward. Accordingly, most of derived analytical methods considers the creep and shrinkage actions are independently.

In the uncracked section with singly reinforced and under sustained moment, immediately after load application, the gradual development of creep strain on reinforced concrete section causes an increase in curvature as illustrated in Figure 2-35. In the tensile zone, creep is restrained by reinforcement. Because of strain compatibility, the tensile steel strain increases as the concrete tensile strain increases at the reinforcement level. Therefore, due to the force equilibrium, this will lead to lowering of the neutral axis depth. Depending on the quantity of steel and section properties, the increase in curvature due to creep is proportional to a large fraction of the creep coefficient (Gilbert & Ranzi, 2010). Obviously, the addition of reinforcing steel in the compression area of concrete will greatly reduce creep and, hence, the creep curvature decreases as quantity of compression reinforcement increases. Creep can be expected to be greater in members loaded at a level only just above cracking load since the tensile stresses will be higher than for members loaded at higher levels (Beeby and Scott,2006).

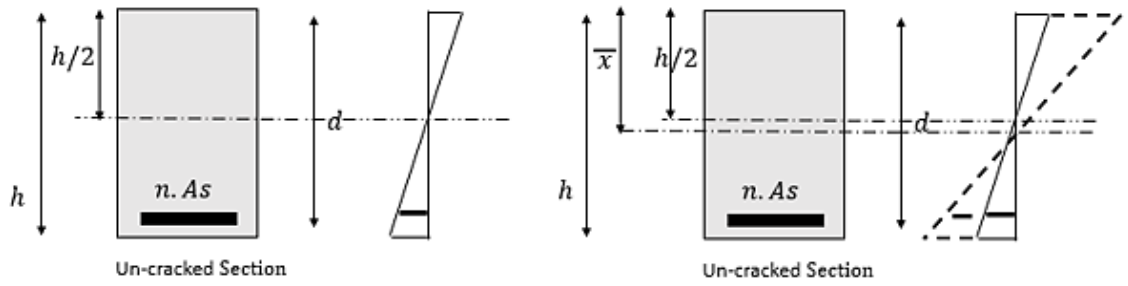

Figure 2-35: Neutral axis depth in un-cracked and gross section

In fully-cracked sections with singly reinforced and under sustained moment, as illustrated in Figure 2-36, the initial curvature is relatively large and the tensile concrete below the neutral axis is ignored and therefore does not creep. Thus,

the increase in curvature of the fully-cracked sections is proportional to a small fraction of the creep coefficient. As the creep strain increases in the compressive zone and due to the force equilibrium in the cross-section, the strain of the tensile reinforcement bars should be maintaining the balance. Consequently, the neutral axis depth moves downwards and thereby the compression depth increases with decreases in concrete compressive stress.

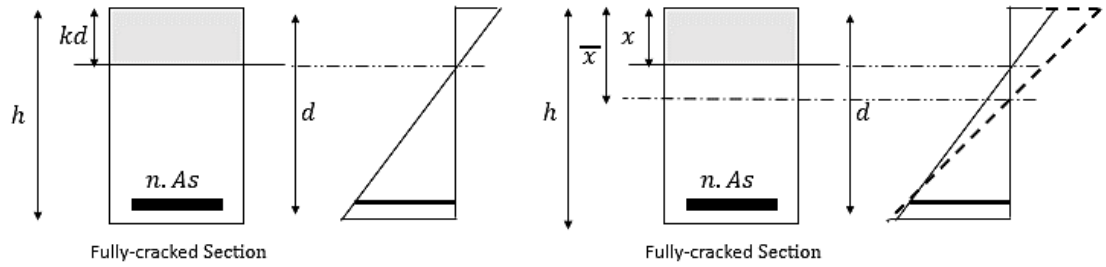

Figure 2-36. Neutral axis depth in fully-cracked and gross section

The gradual development of creep strain causes an increase in curvature. In the tensile zone, creep is restrained by reinforcement. Thereby, the neutral axis moves downward. Accordingly, the compression area increases and the extreme fibre stress decreases noticeably (Rusch et al., 1983). (CEB-FIP-MC2010, 2010) also stated that the changes in the stresses, strains and position of neutral axis occur due to creep, as shown in Figure 2-37, and shrinkage under constant moment. The effect of stress reduction with time is not accounted for the current code approaches and in most of the available analytical models.

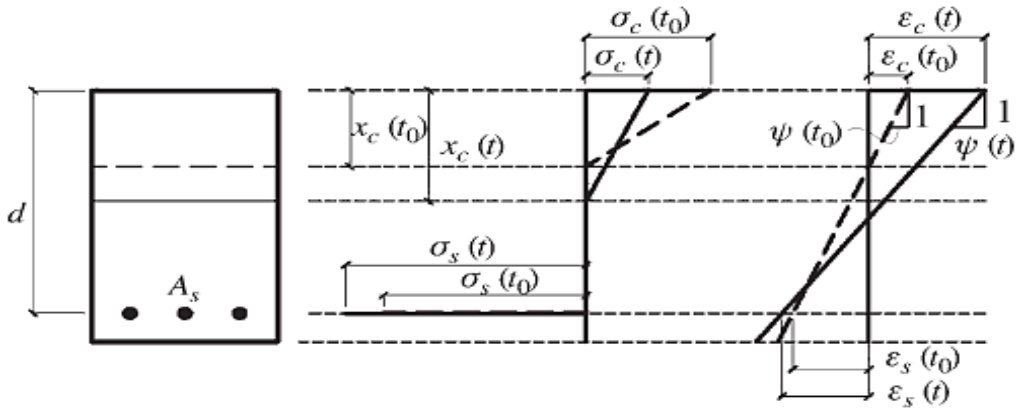

Figure 2-37. Effects of Creep on the stresses and strains with time under constant bending moment fully-cracked (CEB-FIP-MC2010, 2010)

Over time, the short-term modulus of elasticity of concrete decreases because of creep. Several methods have been proposed to include the effects of concrete creep, ranging from rheological models to simple effective modulus methods. However, the analyses could be carried out for member just as easily using any of these methods. Such methods are effective modulus method (EMM) and age-adjusted effective modulus method (AEMM). The effective modulus method is simplest and oldest technique to treat the effects of creep on concrete. This method was developed by (Faber, 1927). This method is approximated by assuming that the applied stress-dependent deformations are produced only by a sustained stress. Thus, the reduction of stress with time has been ignored and it depends only on the current stress. In such cases, the EMM may be unsuitable and more accurate method of analysis is required. In 1967 (Trost, 1967) was proposed a simple expansion to the effective modulus method EMM to account for the ageing of concrete. Then, this method was more formulated rigorously and further development was proposed by (Dilger & Neville, 1971).

In concrete structures, free contraction and rotation are unusual. Hence, when the member is not free to deform (e.g., because of external restraint, restraint caused by the embedded steel reinforcement and the geometrical properties of the cross-section), the imposed strains causes curvature and internal stresses as well as compressive force in reinforcement. Meanwhile, different concepts have been proposed to represent shrinkage in the analysis of reinforced concrete (RC) members with different degree of simplification. The simplest approach is based on equilibrium and compatibility of strains under the conditions of perfect bond. An alternative approach has been proposed by (Gilbert & Ranzi, 2010) to deal with shrinkage based on the equivalent force action for unloaded symmetrically and unsymmetrically reinforced concrete (RC) members as shown in Figure 2-38 and Figure 2-39, respectively. This approach is based on shortening of the unloaded concrete member. A gradual shortening in the unrestrained unreinforced concrete would cause the member to shorten by an amount $\varepsilon_{\mathrm{free}} l$ as shown in Figure 2-38a. On the other hand, the shortening $\varepsilon_{\mathrm{free}} l$ of the concrete in the reinforced concrete (RC) member, as shown in Figure 2-38b, causes a gradual compression in the bonded reinforcement and this is opposed by an equal and opposite tensile force $\Delta \mathrm{F_t}$ applied at the concrete cross-section that could possibly result in, or contribute to, cracking in concrete. Furthermore, for

unsymmetrically reinforced members the tensile force ΔF_t acting at some eccentricity to the centroid of the concrete cross-section produces elastic and creep strains and would be expected to result in curvature with time as shown in Figure 2-39. The curvature caused by ΔF_t obviously depends on the quantity and position of the reinforcement and on whether or not the cross-section has cracked. Again, reinforcement embedded in the concrete provides restraint to shrinkage, therefore, the stresses in steel and concrete are based on restraint factor R $(0 \leq R \leq 1)$, that depends on the amount of reinforcement.

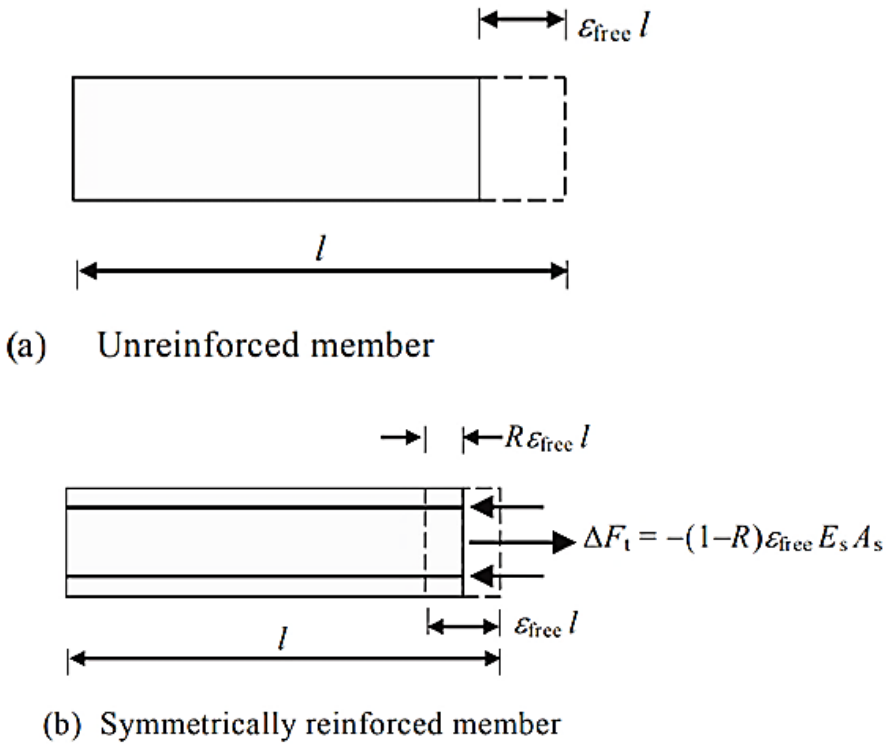

Figure 2-38. Restraint provided by symmetrically reinforcement (Gilbert, 2017)

.

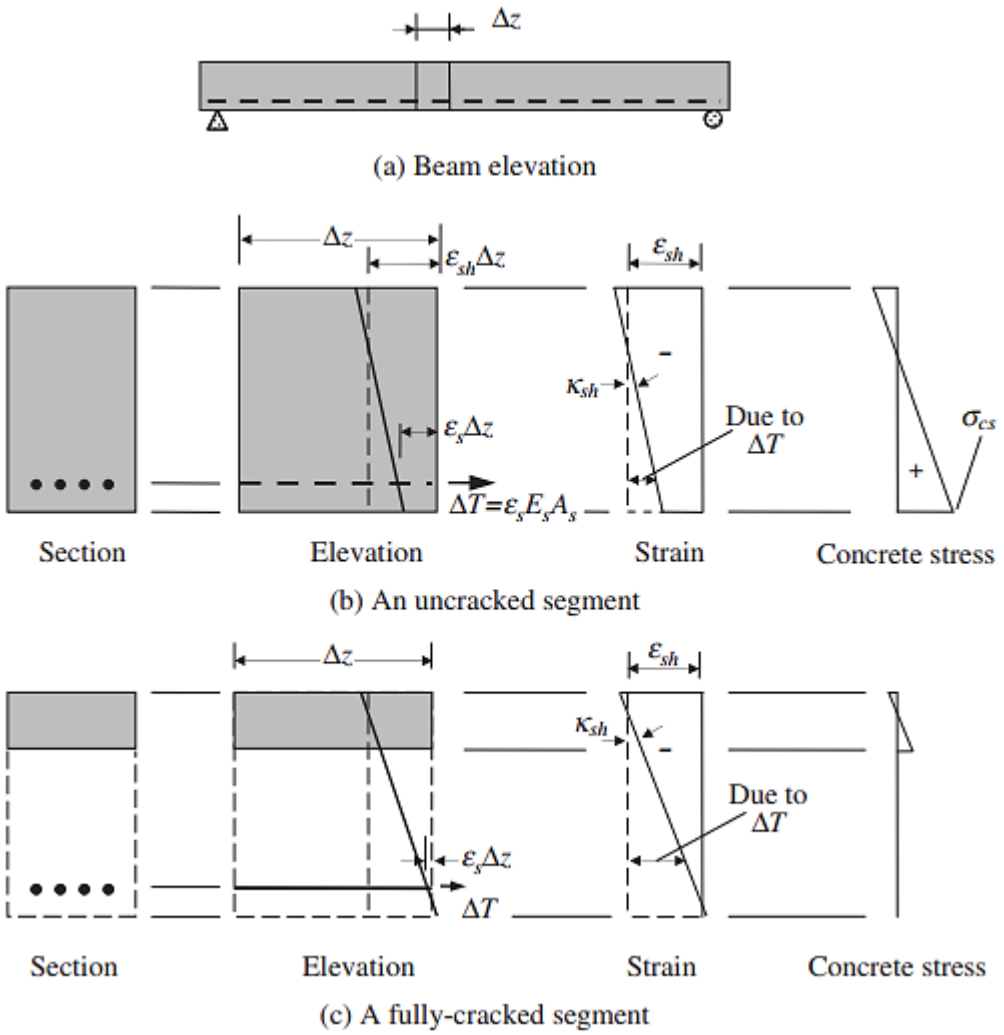

Figure 2-39. Shrinkage stresses and curvatures in a sections restrained by a single reinforcement (Gilbert & Ranzi, 2010)

From above, the shrinkage-induced curvature on the fully-cracked section is comparatively different than un-cracked sections. Although shrinkage deformation is stress-independent, it appears that curvature induced by shrinkage is dependent on the amount of external load applied. It seems that shrinkage curvature in fully-cracked section is significantly greater than shrinkage curvature in un-cracked section (Gilbert & Ranzi, 2010).

Another approach has been proposed based on the fictitious action conception act on unloaded shrunk member (Kaklauskas et al., 2009) ;Kaklauskas & Gribniak, 2011). It introduces a fictitious axial force $N_{cs\,(t,t_0)}$ acting at the centroid of the concrete net section to impose an axial strain $\varepsilon_{cs\,(t,t_0)}$ to a plain concrete member as shown in (Figure 2-40 a-c). Embedded reinforcement provides

restraint to shrinkage causes compressive forces in reinforcement and tensile stresses in concrete as shown in (Figure 2-40 d-e). Thereby, these forces produce elastic and creep strains and would be expected to relieve shrinkage stress as given in (Figure 2-40 f). Similarly, in an unsymmetrically reinforced member, shrinkage effect can also be modelled by means of the fictitious actions N_{cs} and M_{cs}. When the shrinkage fictitious force N_{cs} acting at the centroid of the concrete net section, the distance between the centroid of the concrete section and the centroid of reinforced concrete section causes a shrinkage curvature as shown in (Figure 2-41 c-e).

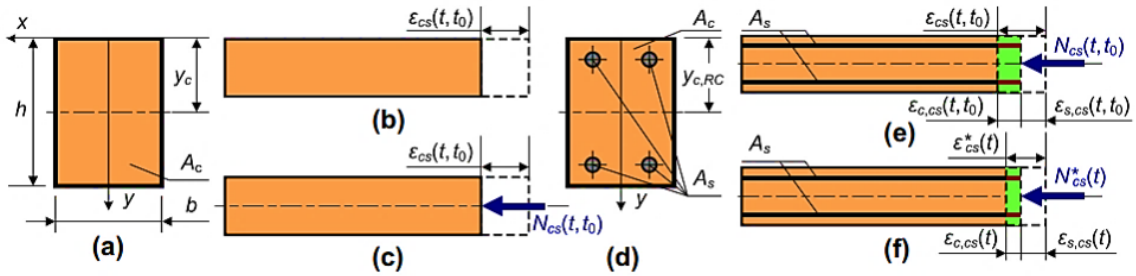

Figure 2-40. Shrinkage-induced deformations of plain concrete and symmetrically reinforced members

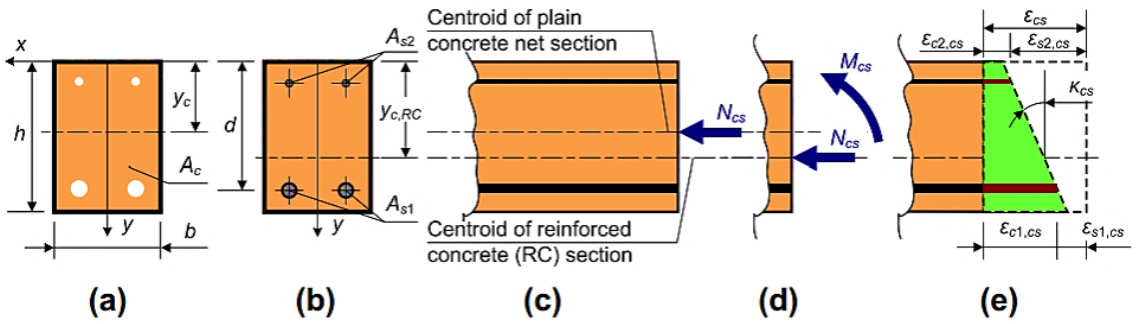

Figure 2-41. Shrinkage-induced deformations of unsymmetrically reinforced member

In 2018, (Prakash, 2018) conducted a nonlinear finite element analysis to predict cracking for slabs on ground due to gradient shrinkage strain as a result of moisture gradient on both surfaces. He modelled the shrinkage strain as initial strain, and its behaviour is modelled as a load effect as shown in Figure 2-42 . A uniformly distributed load is considered as the external applied load on the surface of the slab.

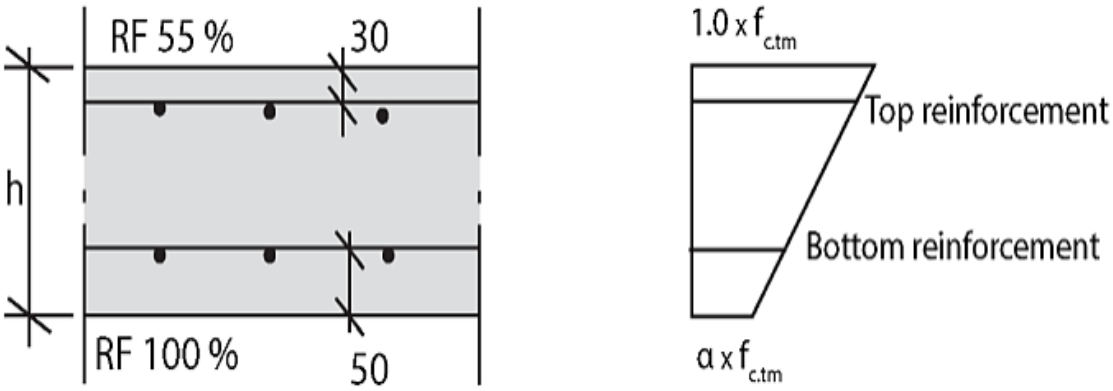

Figure 2-42. Gradient of shrinkage (Parakash,2018)

A two-dimensional continuum based finite element model has been developed by (Wu, 2010). The model incorporates instantaneous and time-dependent constitutive laws for concrete, steel and bond interface between them. A shrinkage-related bond model has been proposed to accurately model the loss of tension stiffening under long-term loading. In 2004, (Chong, 2004) carried out a numerical modelling on time-dependent cracking and deformation. Creep of concrete has been incorporated into the model by developing the principle of superposition. Both creep and shrinkage were treated as inelastic, pre-strain and applied to the discretized structure as equivalent nodal force.

In 2002, an analytical model for creep and shrinkage curvatures was presented by (Ghali et al., 2002) as shown in equations (2-41) to (2-46). The changes in stresses due to creep and shrinkage with time also developed with this model. The model applicable for sections subjected with combined bending moment M and normal force N or purely bending moment M, the internal forces are assumed to have been introduced at age t_0 (time of load application) as shown in Figure 2-43. Additionally, a reference point O is chosen arbitrarily, it depends on the section whether cracked or not and whether subjected to combined bending moment M and normal force N or only pure moment M. Possibly, a reference point O can be chosen at the centroid of the age-adjusted transformed section (Ghali et al., 2002). In fully-cracked section, only the part of effective concrete in compression zone creeps. Estimation the changes of axial strain at O, stresses and curvature due to creep and shrinkage as following expressions from Equation:

$$\Delta\varepsilon_o = \frac{A_c}{\bar{A}}[\varphi\,(t,t_o)(\varepsilon_o + \psi\, y_c) + \varepsilon_{cs}(t,t_o)] \qquad (2\text{-}41)$$

$$(\Delta\psi)_\varphi = \psi_{t_o}\,\varphi(t,t_0)\,k_\varphi \qquad (2\text{-}42)$$

$$(\Delta\psi)_{cs} = -\frac{\varepsilon_{cs}\,(t,t_0)}{d}\;k_{cs} \qquad (2\text{-}43)$$

$$k_\varphi = \frac{I_c + A_c\; y_c\; \Delta_y}{\bar{I}} \qquad (2\text{-}44)$$

$$k_{cs} = -\frac{A_c\; y_c\; d}{\bar{I}} \qquad (2\text{-}45)$$

The changes in stresses at any fibre due to creep and shrinkage with time also derived as following equation:

$$\Delta\sigma_c = \bar{E}_c\,[-\varphi\,(t,t_o)(\varepsilon_o + \psi y) - \varepsilon_{cs}(t,t_o) + \Delta\varepsilon_o + \Delta\psi y] \qquad (2\text{-}46)$$

Where:

ε_o, ψ are the axial strain at O and the curvature at time t_0 immediately after load application, $\varphi\,(t,t_o)$ is coefficient for creep at time t for age at loading t_0, $\varepsilon_{cs}\,(t,t_o)$ is free shrinkage strain, y_c is the y-coordinate of the centroid of the A_c and it is measured downward from O (is negative value), y is the fibre coordinate, measured from the centroid of the age-adjusted transformed section, Δy is the y-coordinate of the centroid of the age-adjusted transformed section measured downward from the centroid of the transformed section at t_0 , $(\Delta\psi)_\varphi$ is the curvature changes caused by creep, $(\Delta\psi)_{cs}$ is and shrinkage, k_φ is are the creep coefficient, k_{cs} is the shrinkage coefficient, A_c is are the area of compression zone, I_c is the moment of inertia of concrete section about an axis through O, and $\bar{I}$ is the moment of inertia about an axis through O of an age-adjusted transformed section.

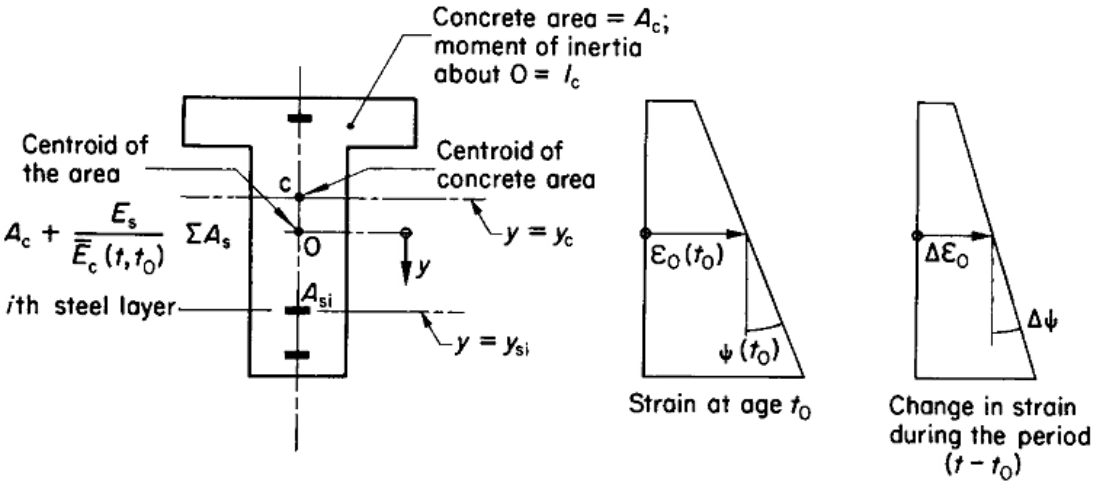

Figure 2-43. Definition of symbols in introduced by (Ghali, Favre, & Elbadry, 2002) for analysis of effects of creep and shrinkage

An analytical model was developed by (Gilbert, 2001) to estimate creep and shrinkage curvatures The proposed model have been developed as an empirical equation to the results gained from a parametric study of the creep and shrinkage induced changes in curvature on different cases of reinforced and pre-stressed concrete cross sections under constant sustained internal actions using the age-adjusted effective modulus method (AEMM). The creep $\mathrm{k_{creep}}$ and shrinkage $\mathrm{k_{sh}}$ curvatures can be estimated from the equations (2-47) and (2-48), respectively. These equations account for the effect of the restraining action of the reinforcement and cracking. As a basic assumption to derive the empirical equations, it is assumed that the drying process takes place on both sides and that the shrinkage strain profile through the thickness is uniform.

$$\mathrm{k_{creep}} = \mathrm{k_{i.sus}} \frac{\varphi(\mathrm{t}, \mathrm{t_0})}{\alpha} \qquad (2\text{-}47)$$

$$\mathrm{k_{sh}} = \frac{\mathrm{k_r} \,.\, \varepsilon_{\mathrm{sh}}}{\mathrm{D}} \qquad (2\text{-}48)$$

Where $k_{i.sus}$ is the instantons curvature under sustained load at time of load application $\mathrm{t_0}$, $\varphi(\mathrm{t}, \mathrm{t_0})$ is the creep coefficient, α is a creep modification factor that accounts for the effects of cracking state (un-cracked or fully-cracked) and the

braking action of the reinforcement on creep, D is the overall depth of the section, k_r is factor depend on the quantity and location of bonded reinforcement. , ε_{sh} is the free shrinkage strain.

several building codes have been adopted different models to deal with creep and shrinkage. Codes (FIP Model Code, 2010;BS8110, 1985;Eurocode2, 2004) have suggested that the total deformation including creep can be obtained by using an effective modulus of elasticity of concrete in the stiffness for both un-cracked and fully-cracked sections. While the shrinkage curvature for cracked sections may be determined by the following equation:

$$\frac{1}{r_{cs}} = \varepsilon_{cs}.n.\frac{S}{I} \qquad (2\text{-}49)$$

Where $\frac{1}{r_{cs}}$ is the curvature due to shrinkage, ε_{cs} is the free shrinkage strain, S is the first moment of area of reinforcement about the centroid of the section, I is the second moment of area of section, n is the effective modular ration (E_s/E_{ceff})

As stated in earlier work (Mu et al., 2008) , the shrinkage curvature proposed by (BS8110, 1985) has been originally derived based on the un-cracked section condition. However, it gives an option to use with fully-cracked section throughout first and second moment of area about the centroid of the cracked section. while in (Eurocode2, 2004), the shrinkage curvature also has been derived based on un-cracked section, However, the model can be used to predict mean shrinkage curvature between un-cracked and fully-cracked sections.

In 1979, (Hobbs, 1979) proposed an analytical model to estimate shrinkage curvature as given in equation (2-50). Again, this model was originally derived for un-cracked section. Hobbs also proposed that this formula was suitable for the shrinkage curvature of fully-cracked sections.

$$\frac{1}{r_{cs}} = \frac{(1+\psi)\varepsilon_{cs}\, E_s[A_s\,(d-x) - A_{s'}\,(x-d')]}{E_c I} \qquad (2\text{-}50)$$

Where ε_{cs} is the free shrinkage strain, ψ is the creep coefficient, E_s is the modulus of steel reinforcement, E_c is the modulus of concrete, I is the second moment of area of the un-cracked or fully-cracked section about an axis of age-adjusted transformed section.

Very few attempts have been carried out to verify the above analytical equations with experimental tests. In 2008, a method for modelling of the shrinkage curvature of sections with fully cracked due to an external applied bending moment has been developed by (Mu et al., 2008).This method is based on the mechanical equilibrium with basic assumptions of beam theory. The method based on divided the section into a number of strips with ignoring the tensile concrete zone. The change in neutral axis position and curvature were numerically determined by iteration. This model was originally derived to verify the accuracy of the calculation of shrinkage curvature adopted by codes (BS8110, 1985; Eurocode2, 2004) of for fully cracked section. They verified the calculations with experimental findings. Thus, the results showed that the model proposed in their investigation for a fully-cracked section predicts adequately the creep and shrinkage curvature of the experimental beams. Moreover, comparing the shrinkage curvatures calculated using the codes (BS8110,1985;Eurocode2, 2004) and in calculations using their investigation with the curvatures of the measured beams, the code methods are suitably accurate for cracked beams.

In 2013, an alternative theoretical approach proposed by (Forth et al., 2013) to experimentally and theoretically verify the shrinkage curvature models presented in (BS8110,1985;Eurocode2,2004). In the theoretical model, the effect of creep, shrinkage, and neutral axis position were considered. The stresses calculated in the concrete and steel at a cracked section according to this theoretical model were then applied to a finite element (FE). Experimentally, two beams were cast and subjected to a flexural loading to produce a stabilized crack pattern in the maximum-moment zone. For theoretical purposes, one beam was cast with low shrinkage concrete and the other with high shrinkage concrete. The shrinkage curvature was computed experimentally from strain profile on the beam side for up to 180 days. These experimentally obtained curvatures were compared with the mean curvatures obtained from the FE analysis. The comparison showed reasonable agreement. The results were also compared with uncracked and fully

cracked curvatures predicted by the codes. They concluded that, the curvatures derived from their theoretical approach fell within the boundaries of the uncracked and cracked curvatures predicted by the codes and, for the fully cracked case, the curvatures were closer to the uncracked boundary.

All previous analytical methods were considered the shrinkage and creep independent. Moreover, the shrinkage deformation was considered as uniform through the depth because of procedures for making reliable estimates of the variation of shrinkage strain within the depth of a section are at present are unavailable (Gilbert & Ranzi, 2010). Moreover, the internal stresses were assumed to be constant. Another technique for long term analysis can be provided by finite element method FEM. Most of finite element analysis technique provides elastic analysis with time. Although commercial software packages such as FEA provide nonlinear cracking analysis, the calculation procedure for shrinkage and creep are not actually performed with nonlinear cracking analysis.

2.16 Instantaneous and Long-term Deflections of Reinforced Concrete Flexural Members

As stated at the outset, deflection is one of the serviceability limit states to be satisfied in the limit state design of structures. In slab design, the serviceability limit state of defection is normally critical rather than ultimate limit state. Over the last few decades, consideration of deflections, both instantaneous and long-term, has become more important because the adoption of the strength design method and the use of higher strength concrete and high-grade steel and this, in turn, will lead therefore to shallower member sections and less reinforcement. Building codes provide two methods for deflection control: span to depth ratio (or minimum thickness requirements) and deflection calculations. The calculation of two-way slab deflections poses the dual difficulties of solving complex governing differential equations and considering the effects of material non-linearity, i.e. cracking, shrinkage and creep. The total deflections including instantaneous depend primarily on the development of creep, shrinkage, tension stiffening, and time-dependent cracking that affect the magnitude of tension stiffening.

2.16.1 Instantaneous Deflection

It is accepted practice in many building codes and recommendations to estimate deflections at mid-span of a cracked flexural member using standard elastic deflection formula of prismatic beam theory, incorporating the effective stiffness for the entire member. For simplicity, BS8110 part 2 gives a simplified approach (soft method) for deflection calculation, using an appropriate bending moment diagram shape coefficient. Meanwhile, several approaches have been derived to predict the deflection in cracked members. The majority of these methods are based on the calculation of the effective stiffness or effective curvature of the member that between uncracked and fully cracked state to account for tension stiffening phenomena. These approaches have been derived for beams and one-way slabs.

A method for calculation slab deflections based on the equivalent frame method of the ACI Code was proposed by Nilson and Walters. In addition, there are several approximate approaches have been proposed for estimation the deflection of slabs for each direction, some of these approaches were summarized in (ACI435.1R-95; Beeby,2000). Again, these approaches are not suitable for unusual structural arrangements, such as presence of openings in flat slabs, significant concentrated loads and this may lead to oversimplify the problem. These methods are primarily applicable for members subjected to a specific loading type and for simple boundary conditions such as cantilever, simply-supported beam and one-way slab. For reinforced concrete flat slabs and flat plates, they are difficult to analyse, as they require a two-dimensional approach. Thus, the rigorous approach is required by integrating the curvatures along the entire span (Ghali, 1993; Ghali et al., 2011).

2.16.2 Long-Term Deflection

The behaviour of reinforced concrete slabs in bending under a sustained load is complicated. Calculating the additional deflections due to shrinkage, creep, and the consequent redistribution of stresses is extremely difficult (Gardner, 2011) Shrinkage, creep and loss of tension stiffening all contribute essentially to an increase in deflection with time under sustained load. Several methods have been proposed to estimate the deflections with time. Many of these methods are

based on the estimation of tension stiffening based on crude assumptions as well as calculation of the creep and shrinkage curvatures of the member separately. Reliable prediction of long-term deflections is not straightforward. Calculating the additional deflections due to shrinkage, creep, and the consequent redistribution of stresses is extremely difficult (Gardner, 2011). As a convenient way, ACI 318 code proposed simplified approach for calculating long-term deflections by multiplying the instantaneous deflection caused by the sustained load by a multiplier factor. However, it does not include any allowance explicitly for shrinkage and creep as well as the loss of stiffness.

Relatively, few data have been published in literature on the effect of creep, shrinkage, and loss of tension stiffening on long-term deflection of reinforced concrete slabs. Thus, the available reliable data in literature concerns basically with the experimental tests of long-term deflection of slabs. In 1961, (Blakey, 1961) conducted an experimental study on the flat plate structure to measure the deflection with time. He has observed that the long-term deflections which were seven times the initial deflections. In 1969, (Taylor, 1969) has measured the deflections for several flat plate and flat slabs structures. He has fond that the long-term deflections from six to eight times the initial deflections. In 1977, (Taylor & Heiman, 1977) measured the deflections of several actual slabs for up to 9 years, and the results were compared with calculated values. It was found that the measured values were up to five times the values calculated by normal methods.

In 2005, (Gilbert & Guo, 2005) conducted an experimental program of long-term testing of large scale RC flat slab. Seven coniferous flat slab specimens were presented and was subjected to sustained service loads for periods up to 750 days as shown in Figure 2-44. The deflections, strains, extent of cracking were measured. They found that the measured long-term deflection is many times the initial deflection, due to the combined effect of transverse load and loss of stiffness associated with long-term cracking. Moreover, the results confirmed that long term cracking greatly affects the serviceability of flat slabs. In all specimens, new cracking observed with time and existing cracks widened (usually on the top surface) and extended. The extent of shrinkage cracking and its effect on the behaviour of concrete slabs was great and tended to be the most important factor

influencing long-term behaviour. This effect is not accounted for sufficiently in the current code approaches for deflection calculation and control.

Figure 2-44. Reinforced concrete (RC) flat slabs under tests (Gilbert & Guo, 2005)

2.17 Summary and Conclusions

Critical review of the previous research presented in this Chapter was aimed at identifying the gaps in current state of knowledge regarding the influence of openings on the behaviour of slabs and the effect of time-dependent properties of concrete on the behaviour of reinforced concrete members. A review of the literature regarding the types of slabs has been presented. Available theoretical approaches for the analysis of two-way slab systems has been summarized and compared to identify the suitable and efficient method that can be utilized. Previous experimental research on the Influences of openings on the flexural behaviour, deflections, and shear strength of slabs have been introduced to understand and identify the effect of openings on the behaviour of slabs. A critical review of the literature regarding the response of members post-cracking, factors influencing the tension stiffening, and current methods for modelling tension stiffening have been included. Detailed review of the literature regarding the time-dependent properties of concrete, methods for prediction of concrete creep and shrinkage, previous experimental research on the development of tensile/compressive creep coefficients, loss of tension stiffening, and cracking

caused by restraint to shrinkage strain have been presented. Available approaches for modelling creep and shrinkage deformations in reinforced concrete members have also been included to understand their influence on the reinforced cross section and hence to propose the suitable method can be utilized in this research. Brief review of the available literature regarding with long-term deflection of reinforced concrete slabs has been introduced. Finally, the available approaches for the modelling of concrete cracking have been discussed and presented to identify the suitable approach for simulating nonlinear cracking analysis.

Based on the critical review, the experimental fundamentals were designed. The experimental parameters such as reinforcement ratio and diameter, neglecting the compression reinforcement, suitable slab thickness, opening position, loading age, magnitude of initial shrinkage prior to loading, water-cement ratio, and mechanical properties of concrete were specified in order to gain optimal results, and the experimental details are presented in Chapter 3. Furthermore, based on the available approaches for modelling concrete response post-cracking which reviewed critically, the smeared fixed crack approach was adopted in the present study. Moreover, the layered approach and finite differences method were selected, and the theoretical details are presented in Chapter 4. From the reviewed literature, the following important conclusions which addresses the gaps in the current state of knowledge can be drawn:

- Tension stiffening is often derived from average tension uniaxial reinforced concrete members.
- Different models have been derived to represent average tension stiffening in the analysis of cracked members. However, they have not been evaluated critically at worst design scenario.
- Meanwhile, several methods have been proposed to model creep and shrinkage phenomena. The majority of methods are based on the calculation of the curvatures (uncracked and fully cracked) separately, whereas other approaches are based on finite element formulations which deal with creep and shrinkage as pre-strains acting at the nodes as nodal forces.

- Although tensile creep relives tensile stresses caused by restraint to shrinkage strain and hence the curvature will be affected, however, there is no attempts to model their influence dependently in the flexural reinforced cross section.
- In practice, it is commonly assumed that creep in tension and compression are the same. However, their influence has not been analysed and verified with experimental findings at possible design situations.
- A literature review revealed that the finite difference method has shown to be more general and efficient, particularly in the problems of plate bending analysis. So far, the use of layered approach with finite difference method for modelling and analysis the slab has not been published in literature.
- Long-term assessment of reinforced concrete slabs under possible design situation has not been performed before.
- The majority of the research involves with the influence of openings on strength criteria in term of ultimate limit states. Furthermore, several attempts have been carried out to analyse metal plates. However, it is worth noting that there is no clear picture about the response of partially cracked reinforced concrete slabs with associated potential design situations-particularly the presence of openings with possible load pattern.
- Although some codes permit openings of any size in slab systems, if shown by analysis that all strength and serviceability requirements are satisfied, including the limits on deflections. So far, no specific analysis of the effect of openings on short-term and long-term behaviour under possible design situation is known.
- Although the existing building code procedures provide provisions and guidance for deflection control, however, these provisions do not address the effect of material properties with time-particularly here is a relative tensile to compressive creep development under potential design situation.

Chapter 3 Experimental Work

3.1 Introduction

An experimental program consisting of reinforced concrete slabs was performed for achieving one of the main objectives of present study. The test program was designed to verify the proposed numerical analysis procedure under worst design situation. Furthermore, these tests will provide a useful reference for those who have attempted to verify their proposed models. To attain the aim of this study, six full-scale reinforced concrete slabs were tested, and the results are presented in this Chapter. Of these, two reinforced concrete slabs were tested up to failure, and four reinforced concrete slabs were tested under sustained loading with period 90 days. For slabs under sustained loading; three slabs contain different opening sizes, and one slab without opening.

This chapter describes the methodology of the experimental. Details regarding the test set up of the reinforced concrete slab are presented. The geometry of the slabs, concrete mix proportion, short-term and long-term material properties, instrumentation employed to measure the deformations and the reinforcement details are included.

3.2 Test Set up and Loading

As part of this study, an experimental testing program consisting of reinforced concrete slab slabs was performed for achieving the main objectives of current study. Six reinforced concrete slabs were tested. Of these, two reinforced concrete slabs were tested until failure four reinforced concrete slabs were tested under sustained load. The slab details, ages at loading, and the load magnitudes are given in Table 3-1. As has already been mentioned, the experimental method represents a reliable way to analyse and understand the behaviour of slabs thoroughly. Therefore, the current experimental program started by testing two reinforced concrete slabs, as shown in Figure 3-1, to monitor the behaviour and to record the ultimate load capacity. Ascertaining the load carrying capacity of the slab is very important in order to determine the suitable sustained load level. Based on the results of the tested slabs, the magnitude of the sustained loading

was chosen and then the remaining four slabs were tested for a period of 90 days as shown in Figure 3-2. Of these, three slabs contain different opening sizes, and one specimen without opening (reference specimen). A sustained loading of 80 kN was chosen for reinforced concrete solid slab, and the sustained loading of 60 of kN was chosen for the slabs with an opening. The details regarding the selection of the sustained loading level are explained in Chapter 5 (section 5.5). The long-term slabs were tested and monitored under sustained loading with a period of 90 days. The load was monitored and adjusted frequently to ensure that it remained constant. All slabs were supported by four sides rigid supports (square frame arrangement of I- beam sections). The simply supported manner was chosen in order to identify the effect of the relevant parameter without the complications and uncertainty associated with the analysis of complex support conditions.

Table 3-1: Experimental results for concrete mechanical properties.

Slab specimens	Opening size (mm)	Age of concrete at loading (days)	Sustained load level (kN)	Failure load kN
S1	Without opening	75	80	-
S0	Without opening	62	-	200
S2	150x250	41	60	-
S3	150x150	43	60	-
S4	200x200	51	60	-
S5	150x250	28		178.8

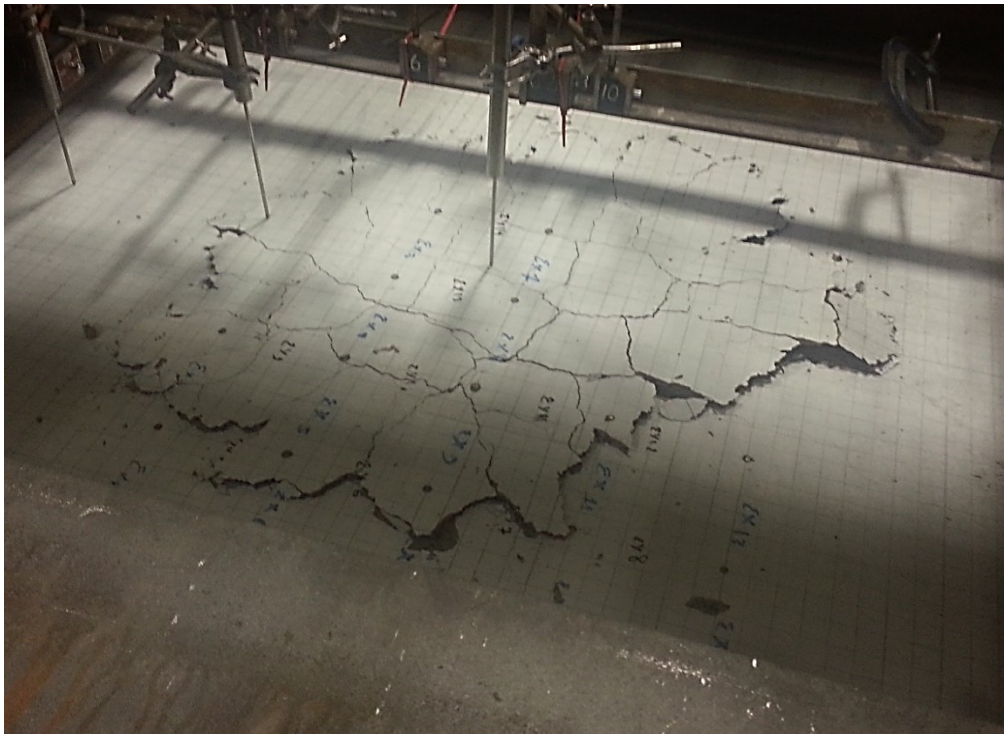

(a)

(b)

Figure 3-1. Testing of short-term specimens: (a) solid slab; (b) slab with opening

All specimens had the same overall full-scale dimensions with 1600x1600x125 mm. The loaded area (column stub) had a dimension of 200 x 200 mm and height 200 mm. It was decided to introduce the opening next to loaded area, adjacent to column, to replicate the worst design scenario (as it has been presented in the literature Chapter 2 sections 2.6 and 2.7).

Figure 3-2. Long-term test of slabs

3.3 Measurements and Data Processing

For the short-term tests, deflection and steel strain values are measured at different positions. For the long-term tests, the development of deflection and the surface concrete strains in tension with time are also monitored at different positions. To attain this, internal and external instruments were used during each test for measuring parameters at best locations in the slabs. Six internal strain gauges were used to measure strains in the reinforcements as illustrated in Figure 3-3. Externally, VWG (vibrating wire gauge) was used to measure concrete surface strains in tension as shown in Figure 3-4 and Figure 3-5. For measuring displacements, a linear variable differential transformer (LVDT) was placed underneath of the slab to record the deflections. The position of LVDT, geometric details of the slabs, and opening sizes and location are illustrated in the Figure 3-6 and Figure 3-7. The LVDTs and VWGs were positioned at the points which possibly gives the maximum deformations for short-term and long-term tests. For instance, the maximum strain concentrates in the diagonal zones from the edge of the column toward the corners while the maximum deformation concentrates around the openings and near load actions. In addition, the rebar strain gauges were positioned in the zones which possibly gives the maximum tensile strain values. A data logger was used to record output data of the test results to the computer as a Microsoft Excel sheet.

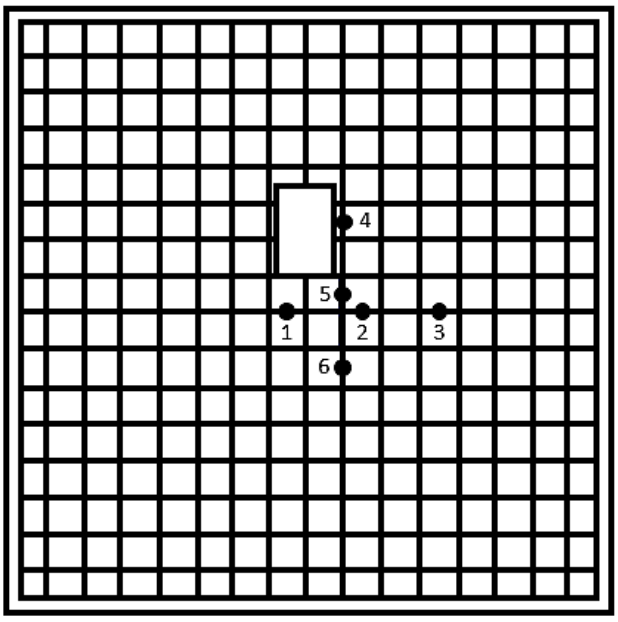

Figure 3-3. Typical Strain gauge positions for all specimens

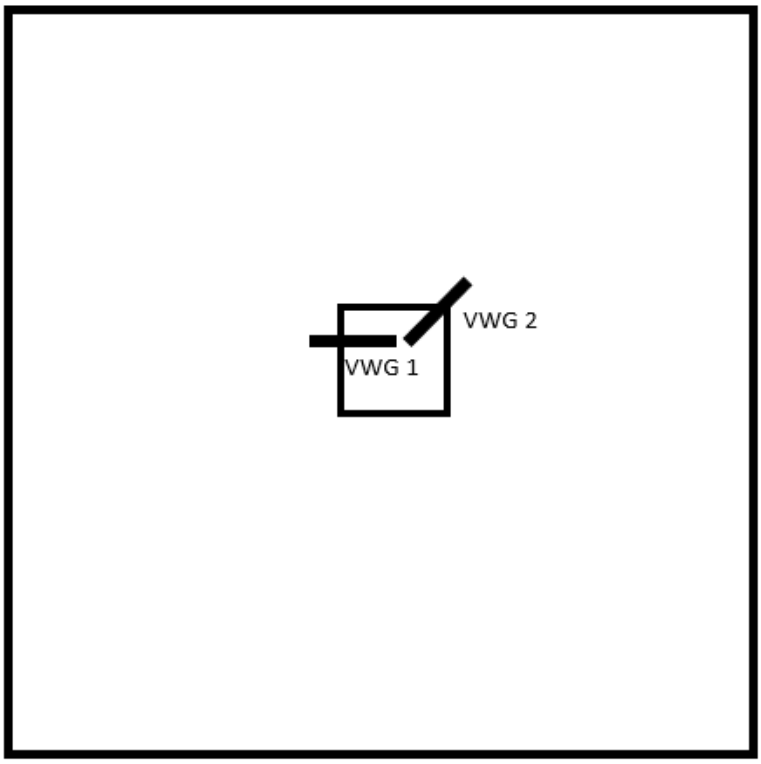

Figure 3-4. Typical locations of VWG in the tension side for solid slab

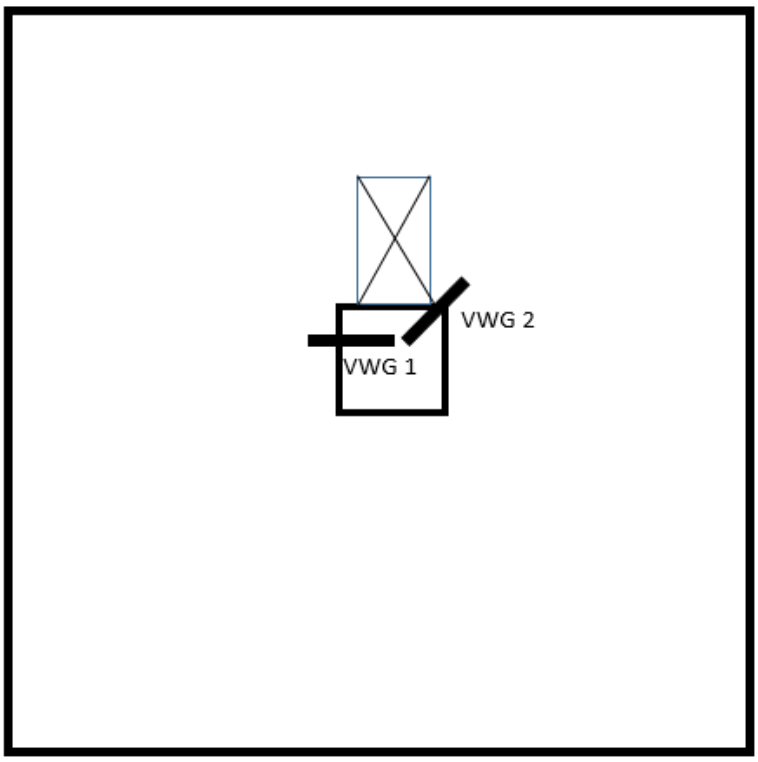

Figure 3-5. Typical locations of VWG in the tension side for slabs containing opening

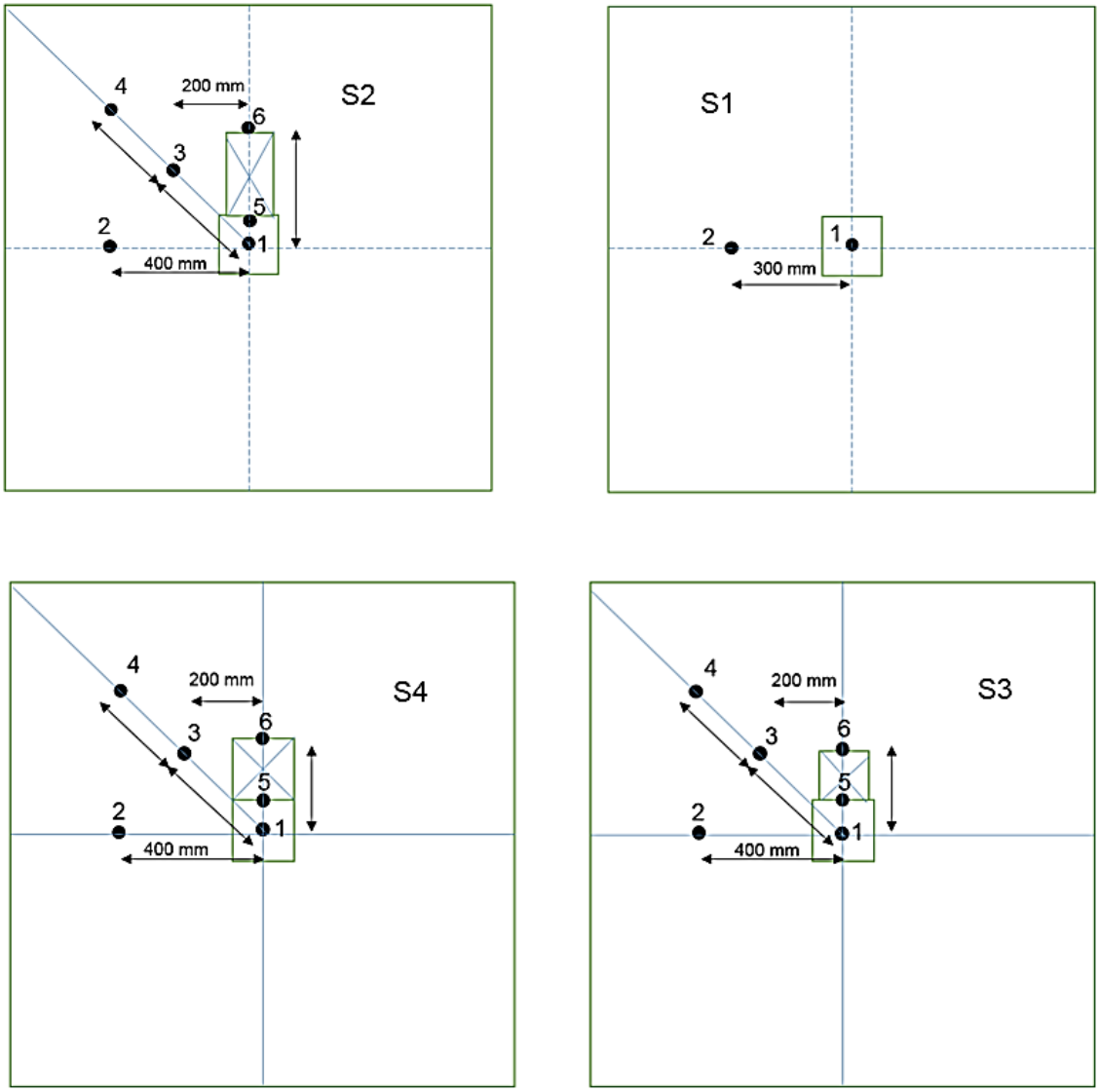

Figure 3-6. locations of LVDT for long-term tested slabs

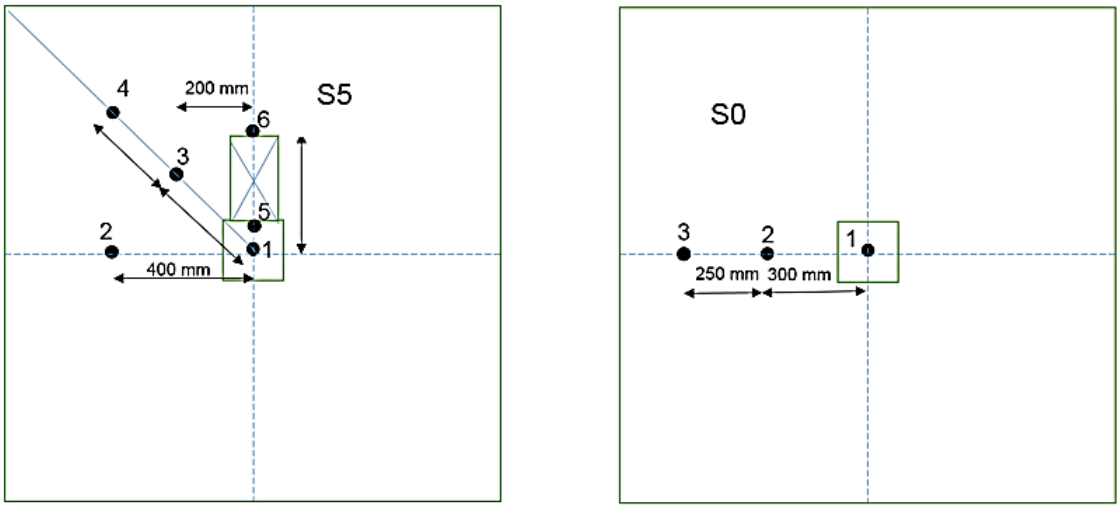

Figure 3-7. Locations of LVDT for short-term tested slabs

3.4 Steel Reinforcement

The flexural reinforcement for all slabs is placed orthogonally, that is, in two perpendicular directions. The same reinforcement quantity is provided in each direction. The reinforcement of 8 mm diameter was used. The properties of deformed bars reinforcement are illustrated in Table 3-2. The average yield strength of the steel bar was 600 MPa. The calculated percentage of lower reinforcement bars was ($\rho = 0.00528$), while for the upper reinforcement bars the calculated percentage was ($\rho = 0.00574$). The stress-strain relationship for deformed steel bars was obtained and presented in Figure 3-8. Six Electric Resistance Strain (ERS) gauges were placed on the reinforcing bars and connected to a data logger in order to record steel strains.

Table 3-2: Properties of steel reinforcement bars

Nominal diameter (mm)	Area (mm^2)	Modulus of elasticity (MPa)	Yield stress (MPa)
8	50.26	210000	600

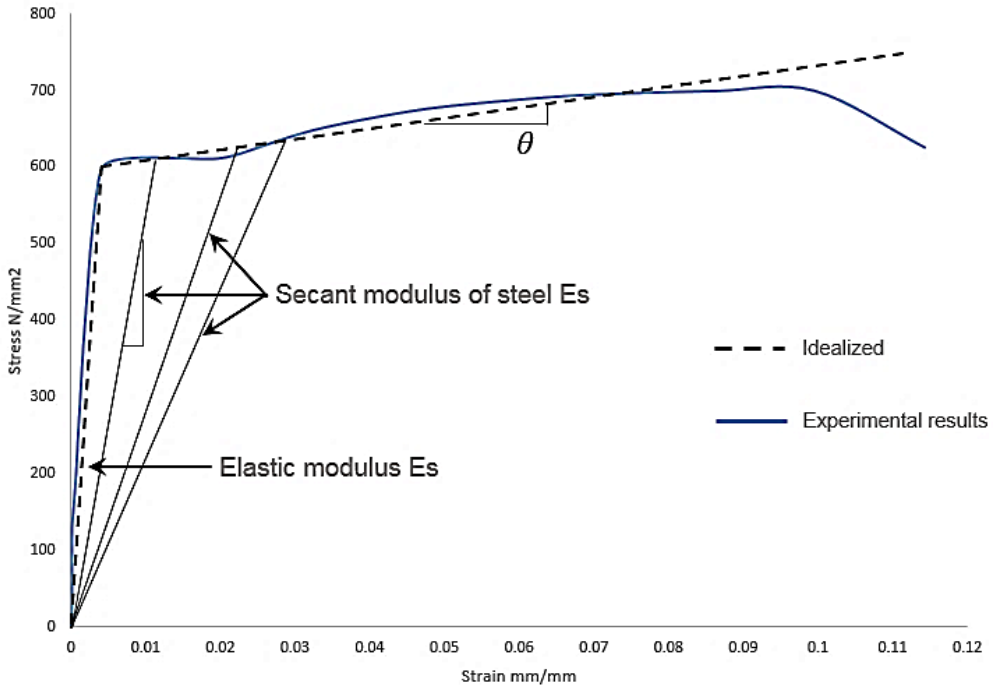

Figure 3-8. Average stress-strain curve for steel

All reinforcement bars were placed in the bottom of the slab with clear spacing 95 mm c/c at each direction. The reinforcement details and arrangements are shown in Figure 3-9 and Figure 3-10.

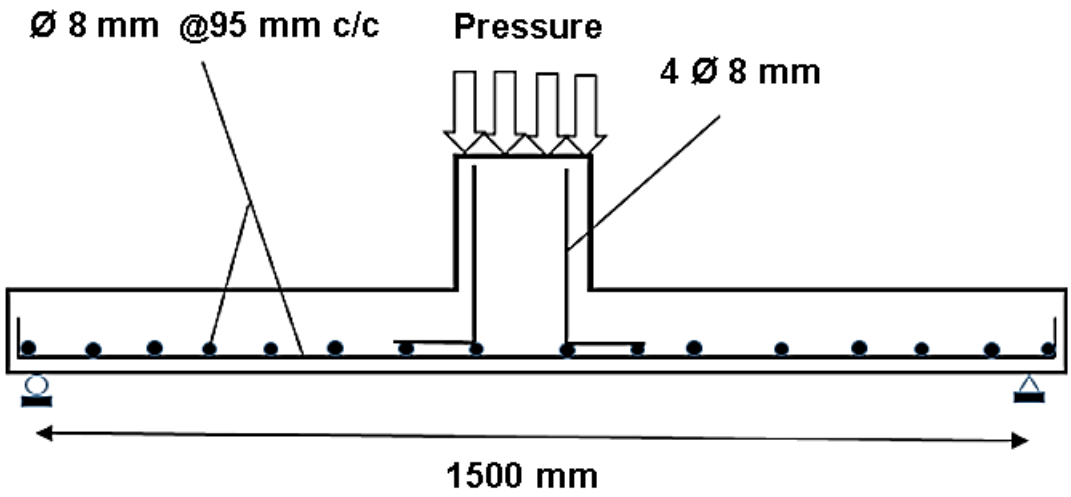

Figure 3-9. Details of reinforcing steel bars

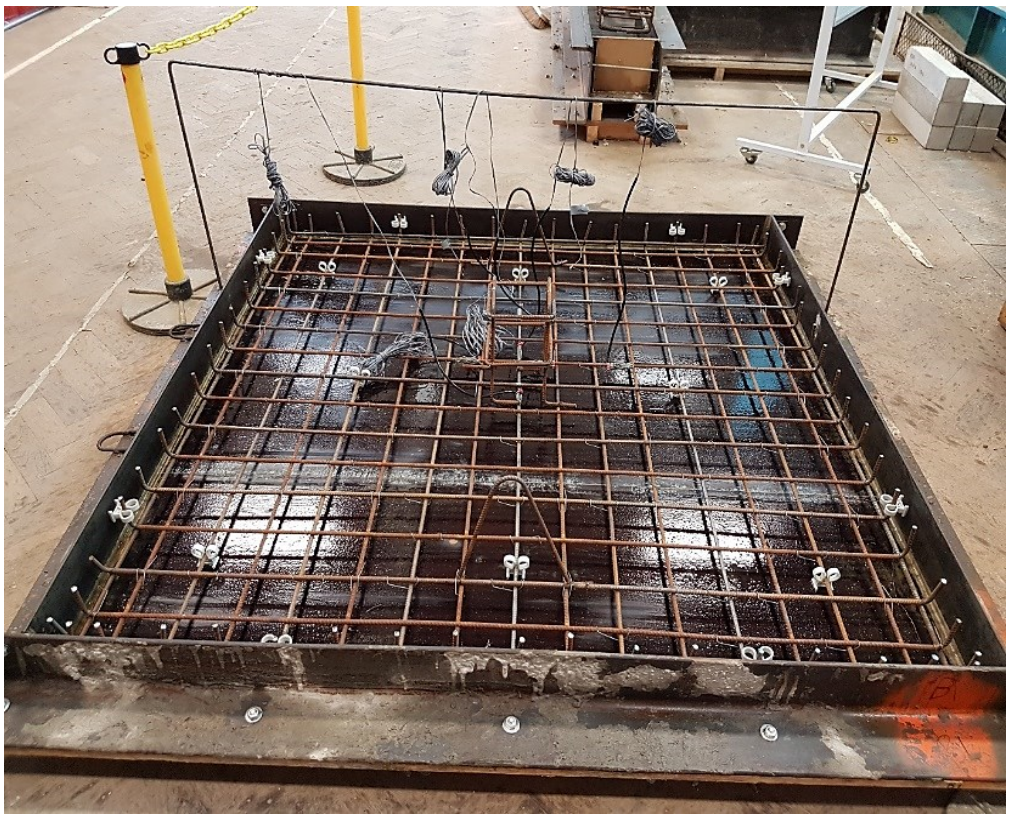

Figure 3-10. Arrangements of reinforcement bars

3.5 Concrete Mix Proportion and Material Properties

Concrete mix for the tests was designed according to the mix design standards in accordance with BS EN 206 (2013). Several trial concrete mixes were carried out according to the design procedures. The proportions of the final concrete mix are shown in Table 3-3.

Table 3-3 : Proportions of concrete mix

Water (Kg/m3)	Cement (Kg/m3)	Fine Aggregate (Kg/m3)	Coarse Aggregate (Kg/m3)	Slump (mm)
210	420	750	1020	110

The concrete mix consists of water, cement, fine and coarse aggregate. The cement used in the mixes was cement 52.5N obtained from the Hanson Group. This cement is complied with the requirements of BS EN 197-1 (2011). Natural fine aggregate with a maximum particle size of 5 mm was used in the mixes. The grading results of fine aggregate comply with standard requirement limits according to BS 882 (1992). The crushed coarse natural aggregate with a maximum size of 10 mm was used in the mixes. The grading of coarse aggregate conformed to standard limit requirements of BS 882 (1992). The same proportion of fine aggregate and coarse aggregate were used for all mixes of tested slabs. Potable water which meets the standards BS EN 1008 (2002) was used in the mixes. All mixes had the same water-to-cement ratio of W/C =0.5. Each reinforced concrete slab requires three batches to be poured. Thus, three samples of compressive strength, splitting tensile strength, and modulus of elasticity for each batch were poured, as shown in Figure 3-11, and cured in order to measure the concrete properties. Moreover, small prisms and cylinders for each batch were poured and cured to measure long-term concrete properties, i.e. creep and shrinkage strains. After casting, all specimens were cured in moulds and covered with wet burlap and plastic sheeting until an age of 20 days as shown in Figure 3-12.

Figure 3-11. Sample preparations of each tested slab

Figure 3-12. Slab specimen being poured and cured

3.6 Short-term and Long-term Tests of Small Specimens.

To determine short-term and long-term properties of concrete compressive cylinder strength, cube strength, splitting tensile strength, free shrinkages and creep strain were measured from samples. Creep strains were measured on two small cylinders with size 75x265 mm as shown in Figure 3-13. The cylinders in each creep rig were subjected to constant sustained stress of 9 MPa where$\sigma_c \leq 0.4\, f_{cm}\,(t_0)$. The constant compressive stress was applied on these small

cylinders at the same age of slab loading. To measure the unrestrained strain with time, free shrinkage strains were measured on three prisms for each slab with size (75x75x200 mm) as shown in Figure 3-13. The strain readings were taken from the samples directly through DEMEC points on both sides. The creep strain was determined by subtracting the sum of the measured instantaneous and shrinkage strain from the total strain measured on the creep cylinders. The creep coefficients at any time φ is obtained as the measured creep strain divided by the instantaneous strain.

Figure 3-13. Creep and shrinkage small specimens

All creep and shrinkage samples were cured and kept in moisture room until an age of 20 days. The development of drying shrinkage strain was measured at age of concrete when drying starts, typically at end of moist curing. These specimens then were placed in the laboratory near the slab and exposed to the same environmental conditions. Tests were conducted inside the laboratory at the University of Leeds. The relative humidity and temperature in the laboratory were monitored during the test and the average readings were later incorporated in the creep and shrinkage calculations using different prediction models. The comparison of the measured and predicted shrinkage and creep deformations are given in section 3.7. The recorded relative humidity and temperature in the laboratory near the tested slabs are shown Figure 3-14 and Figure 3-15. From the temperature and relative humidity records, the average relative humidity of

the solid slab S1 is 60% while the average relative humidity of all slab containing openings is 70%.

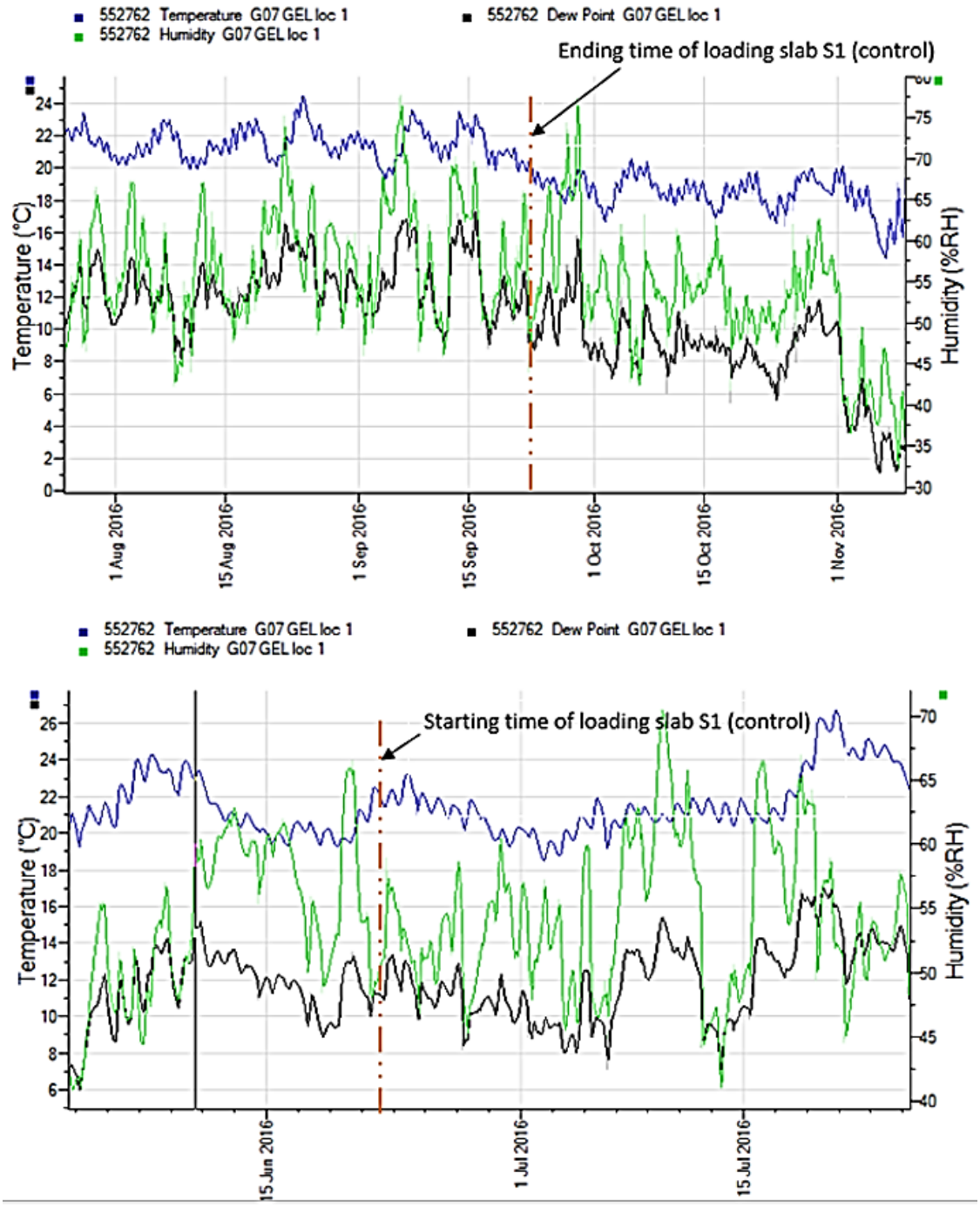

Figure 3-14. Relative humidity and temperature for solid slab S1

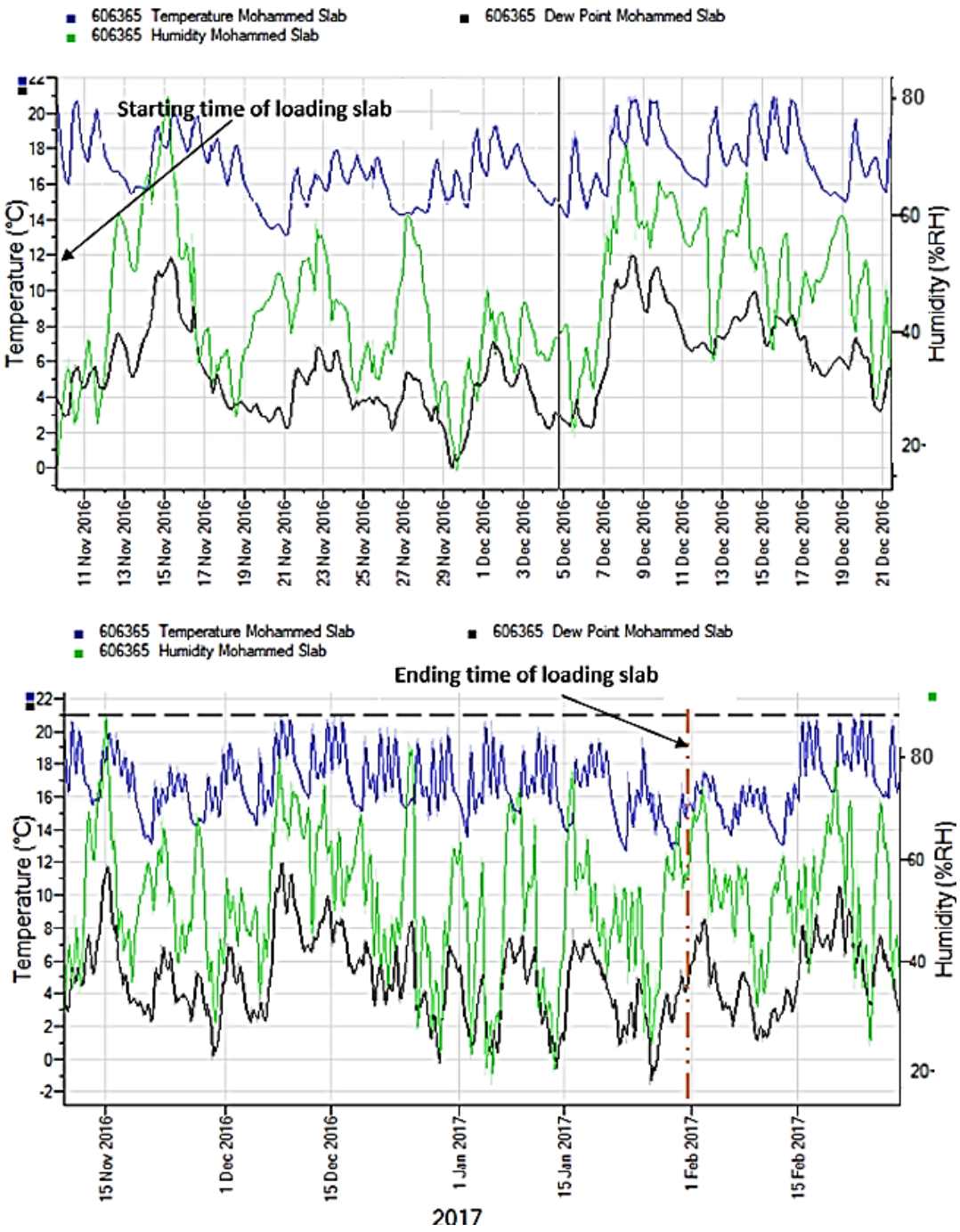

Figure 3-15. Relative humidity and temperature for all slabs containing opening

3.6.1 Compressive Strength of Concrete

The compressive strength of concrete is one of its important properties. Many other properties such as tensile strength, modulus of elasticity and modulus of rupture can be approximately related to the mean compressive strength which is influenced by many factors. As stated earlier, three cylinders (150x300mm) and three cubes (100x100x100mm) were tested from three batches for each slab.

Before testing, the surface of the samples was wiped clean. The samples were tested to obtain the compressive strength of concrete according to the procedure specified in BS EN 12390-3 (2009). The load was increased at a constant rate of 3 kN/sec and the failure loads were recorded. From the failure loads, the cylinder and cube strengths were calculated. The average cylinders and cubes compressive strength were obtained for each slab is given in Table 3-4 at ages corresponding to the age of slabs at loading.

Table 3-4: Experimental results for concrete compressive strength test

Slab specimens	Cylinder compressive strength at slab loading age (MPa)	Cube compressive strength (MPa)	Age of concrete at slab loading age (days)
S1	37.45	47	75
S0	36	45.23	62
S2	36.65	46.14	41
S3	36.25	45.6	43
S4	36.8	46.3	51
S5	35.95	45.17	28

3.6.2 Modulus of Elasticity of Concrete

Another important parameter for concrete specification is modulus of elasticity. It is dependent on several factors such as the age of concrete and strength, the properties of the cement and aggregates, and the rate of load application. The elastic modulus is needed in the analysis to estimate the stiffness of each member and to calculate the internal actions. It is also required to estimate the initial deformations caused by internal actions and the stresses. In the present study, three cylinders were tested from three batches for each reinforced concrete slab as shown in Figure 3-16.

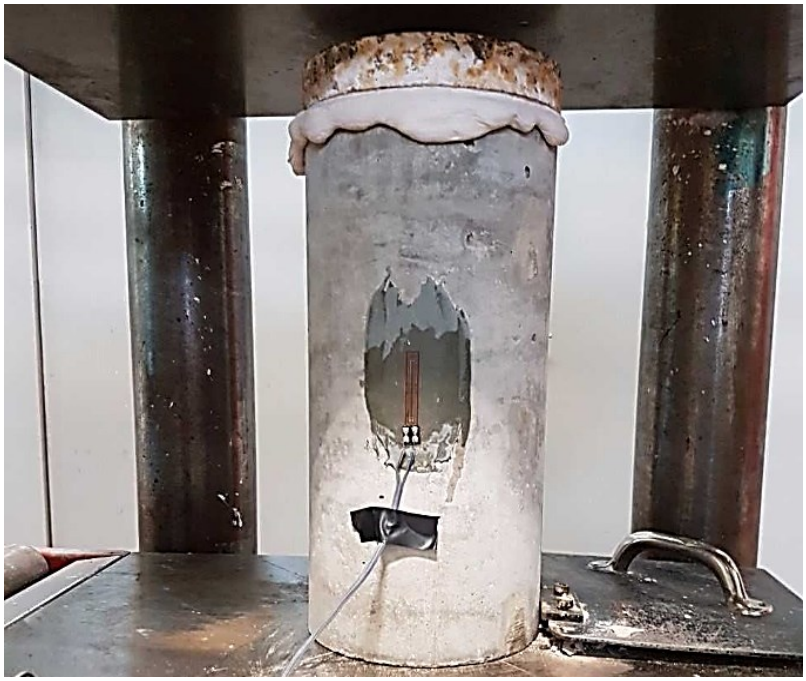

Figure 3-16. Modulus of elasticity test of cylinder

The static modulus of elasticity was determined according to ASTM C469 (2014). Two electrical resistance strain (ERS) gauges were placed on the surface of each cylinder to record the axial deformation corresponding with applied stress. The modulus of elasticity was calculated according to the following equation and the average values are given in Table 3-5 corresponding to the age of slabs at loading.

$$\mathrm{E_c} = (\sigma_2 - \sigma_1)/(\varepsilon_2 - 50 \times 10^{-6}) \qquad (3\text{-}1)$$

Where σ_2 is the stress corresponding to 40% of the failure load, σ_1 is the stress is the stress corresponding to a longitudinal strain of 50×10^{-6} ,and ε_2 is the longitudinal strain due to an applied stress of σ_2. Several equations are available to estimate the modulus of elasticity of concrete. For normal weight concrete, the modulus of elasticity of concrete E_{ct0} at any time of loading can be determined using the following equation which is adopted by (ACI-209.2R, 2008) and the values are given in Table 3-5:

$$\mathrm{E_{ct0}} = 0.043\ \gamma_c{}^{1.5}\ \sqrt{\mathrm{f_{ct0}}}\ \ (\mathrm{MPa}) \qquad 3\text{-}2)$$

Table 3-5: Measured and calcuated results for concrete modulus of elasticity

Slab specimens	Measured Modulus of elasticity strength at slab loading age (MPa)	Estimated Modulus of elasticity strength Eq. (3-2) at slab loading age (MPa)	Age of concrete at slab loading age (days)
S1	29560	29882	75
S0	29850	29297.7	62
S2	29450	29561	41
S3	29170	29399.28	43
S4	29700	29621.47	51
S5	29300	29277.37	28

3.6.3 Splitting Tensile Strength of Concrete

The tensile strength of concrete is an important property because a reinforced concrete member greatly affected when the tensile stress in the extreme fibre exceeds the tensile strength of concrete; the cracking of concrete is then expected and, thereby, the nonlinear behaviour of reinforced concrete begins. Tensile strength of concrete is always expressed in terms of a specific test procedure. The direct tension test, the modulus of rupture test, and the split cylinder test are the three kinds of tests that have been usually used. However, direct uniaxial tensile tests are difficult to perform. Basically, the modulus of rupture has been found to overestimate the tensile strength of concrete (L'Hermite, 1959; Young & Mindness, 1981). In the present study, three cylinders (150x300mm) from each batche were tested for each slab as shown in Figure 3-17.

Figure 3-17. Splitting tensile strength test

The samples were tested to obtain the average splitting tensile strength of concrete according to the procedure specified in BS EN 12390-6 (2009). The load was increased at a constant rate (0.25kN/sec) up to the failure load. The splitting tensile strength f_{spt} was calculated corresponding to the age of slabs at loading according the following equation and the average values are given in Table 3-6.

$$\mathrm{f'_{tsp}} = \frac{2\,\mathrm{p}}{\pi\,\mathrm{L}\,\mathrm{D}} \qquad 3\text{-}3)$$

Where L is the length of the tested specimen in mm, D is the diameter of the tested specimens, and p is the failure load. Several equations are available to estimate the tensile strength of concrete. In 1990 (Gardner, 1990), derived best-fit mathematical relationship based on entire test results on normal concrete. The correlation between splitting cylinder tensile strength and compressive strength can be estimated by the following equation and the estimated values are given in Table 3-6.

$$\mathrm{f'_{tsp}} = 0.34\,\mathrm{f'_c}^{0.66}\ \ (\mathrm{MPa}) \qquad 3\text{-}4)$$

Table 3-6: Measured and estimated results for concrete spitting tensile strength

Slab specimens	Measured Splitting tensile strength Eq. (3-3) at slab loading age (MPa)	Estimated Splitting tensile strength Eq. (3-4) at slab loading age (MPa)	Age of concrete at slab loading age (days)
S1	4.25	3.72	75
S0	3.8	3.62	62
S2	4	3.66	41
S3	3.9	3.64	43
S4	4.1	3.67	51
S5	3.75	3.61	28

3.7 Creep and Shrinkage Deformations

Due to the properties of concrete, under sustained stress, the concrete specimen exhibits an immediate strain at the time of loading; then a long-term strain, which gradually increases with time. In the period immediately after first loading, creep strain develops quickly while shrinkage strain is developed in the absence of tress when drying starts at end of moist curing. The reduction in the volume of concrete caused by the loss of water during the drying known as drying shrinkage. The shrinkage and creep were predicted according to the CEB FIP 2010 and ACI 209.2R-08 models. The actual environmental conditions, i.e. relative humidity and temperature, compressive strength and curing time was used as input parameters. Figure 3-18,Figure 3-19,Figure 3-20, and Figure 3-21 show the results of predicted and measured creep and shrinkage deformations. It can be seen that the experimentally measured creep in all specimens was accurately predicted by both CEP-FIP 2010 model. Nevertheless, the measured shrinkages strains lie between CEP-FIP 2010 and ACI209.2R models. Generally, it can be seen that the CEB-FIP 2010 model was most appropriate. Hence, it was decided to predict the creep coefficients and unrestrained shrinkage strains for the tested

slabs using the method given in CEP-FIP 2010. The predicted creep coefficient and shrinkage strain were based on notional size of the slab and not on small cylinder and prism.

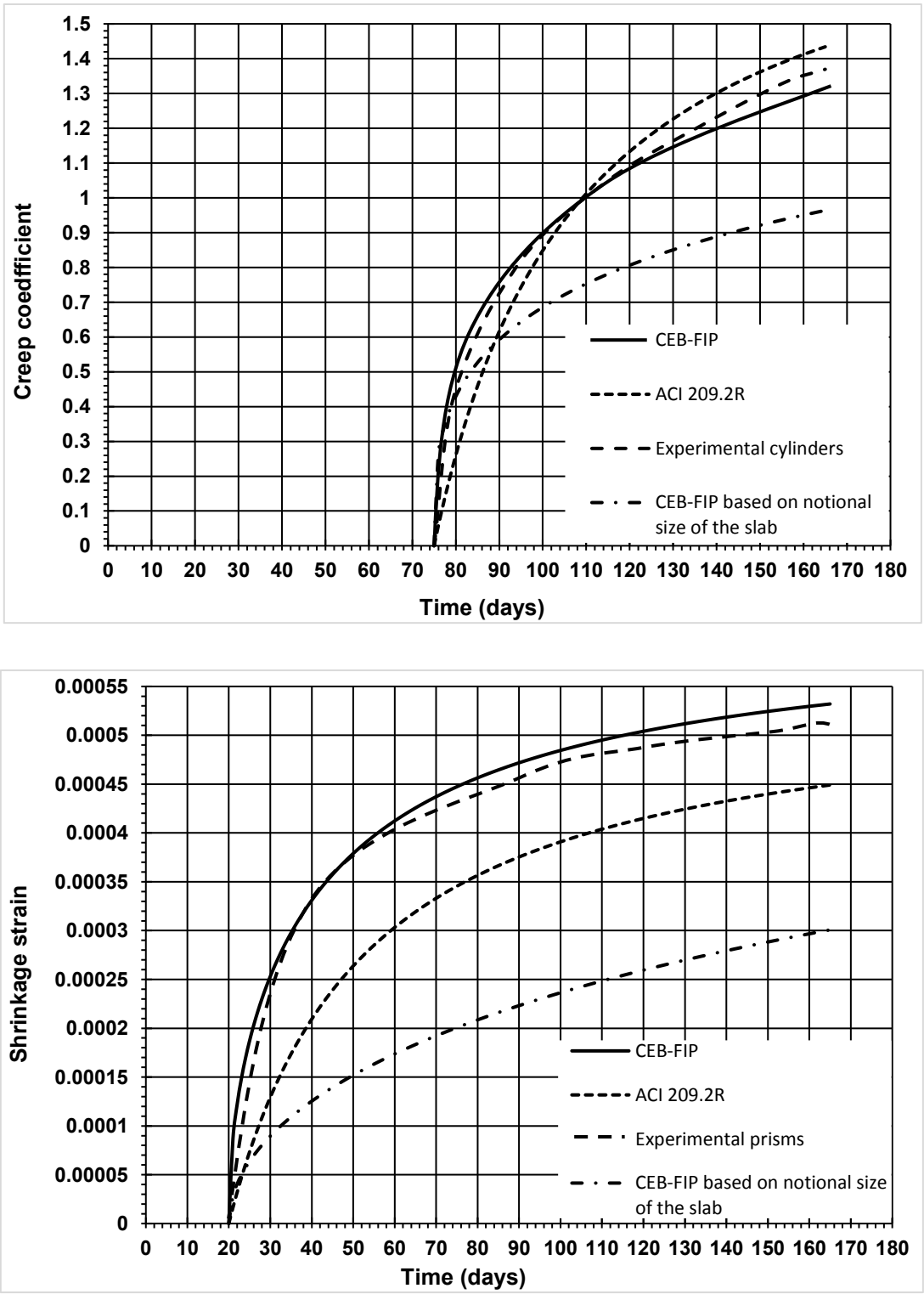

Figure 3-18. Comparison of measured and predicted long-term deformation of shrinkage and creep of solid slab S1

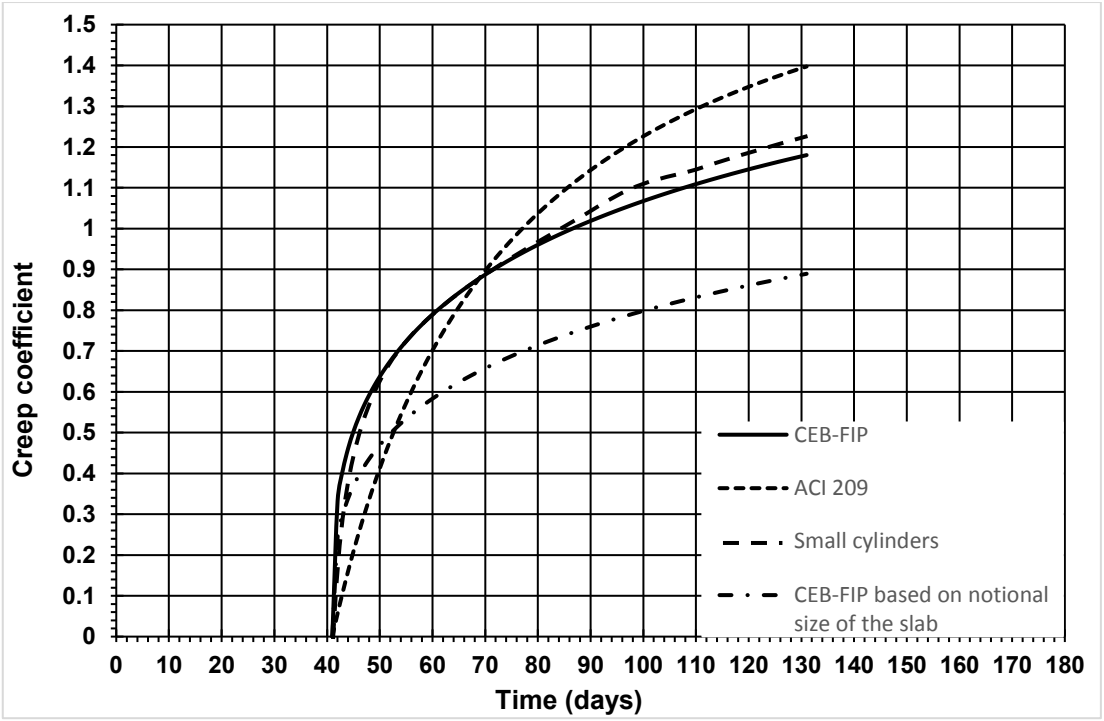

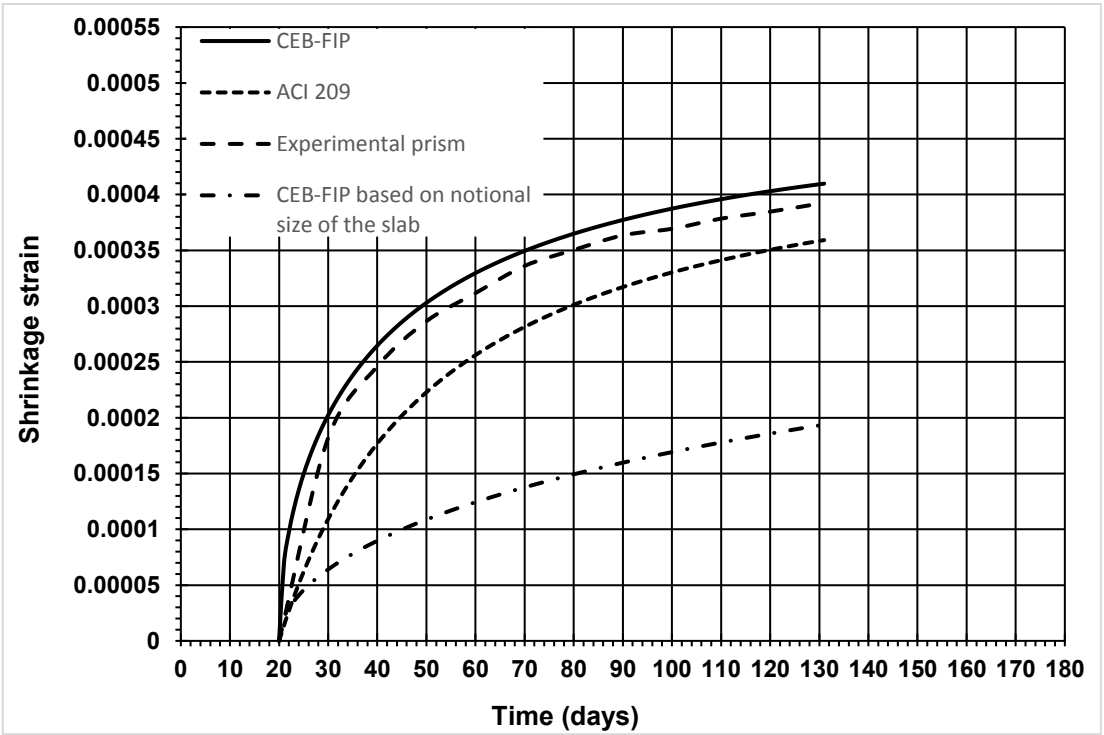

Figure 3-19. Comparison of measured and predicted long-term deformation of shrinkage and creep of slab S2

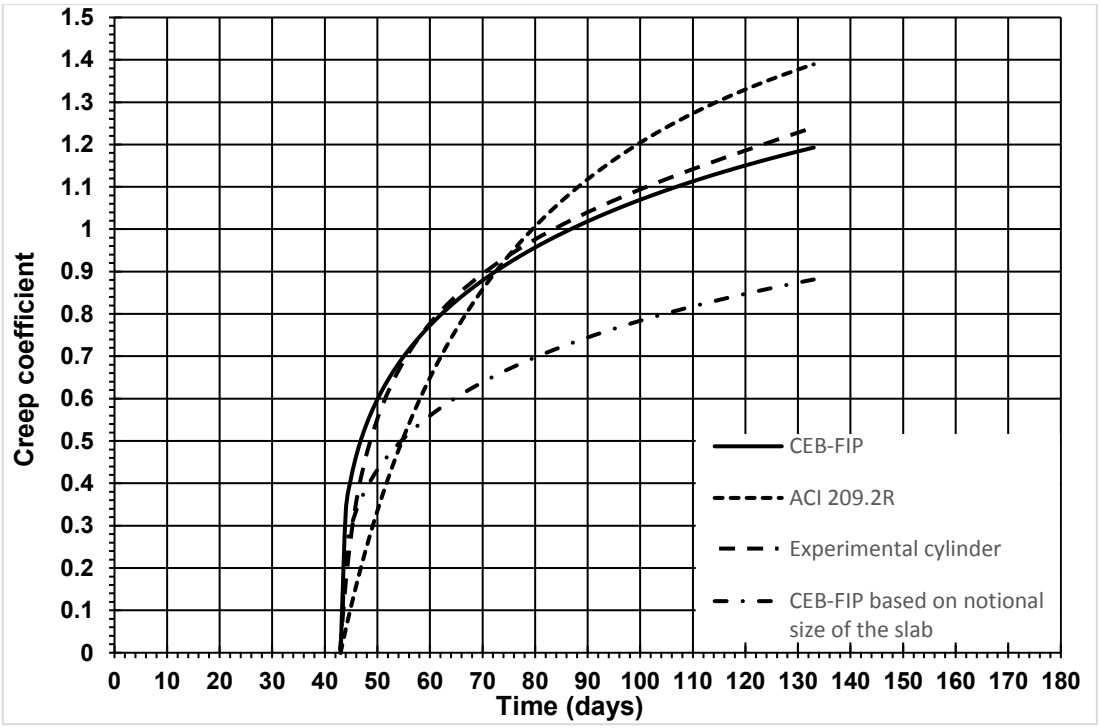

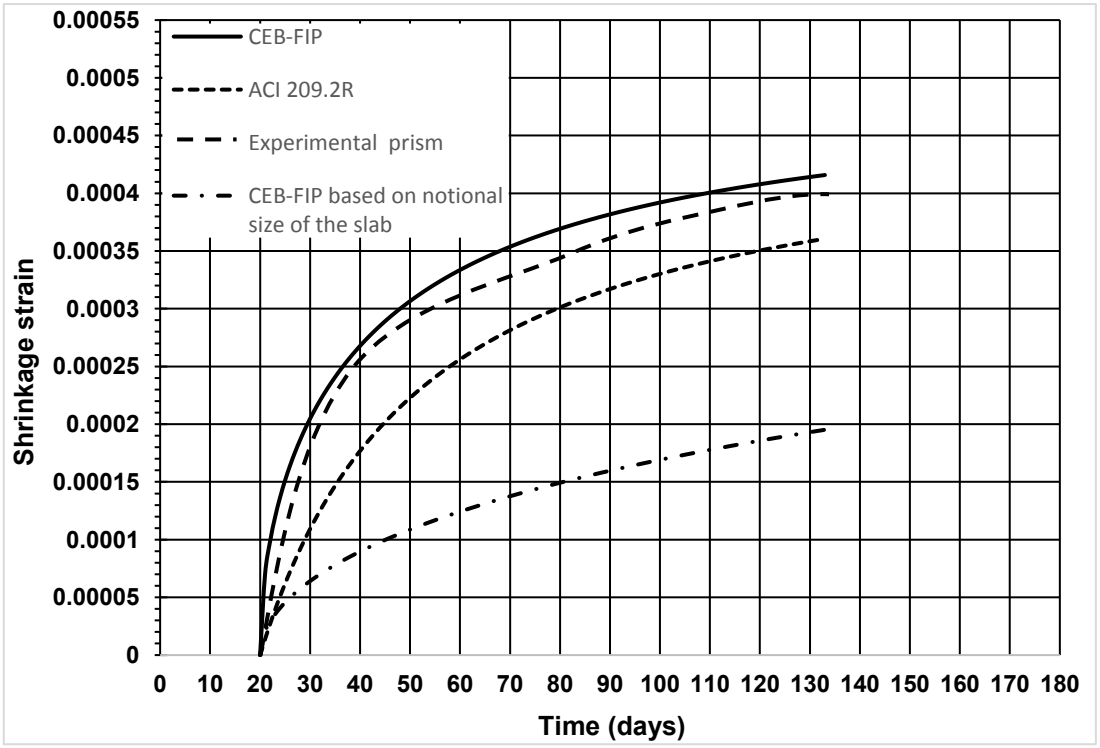

Figure 3-20. Comparison of measured and predicted long-term deformation of shrinkage and creep of slab S3

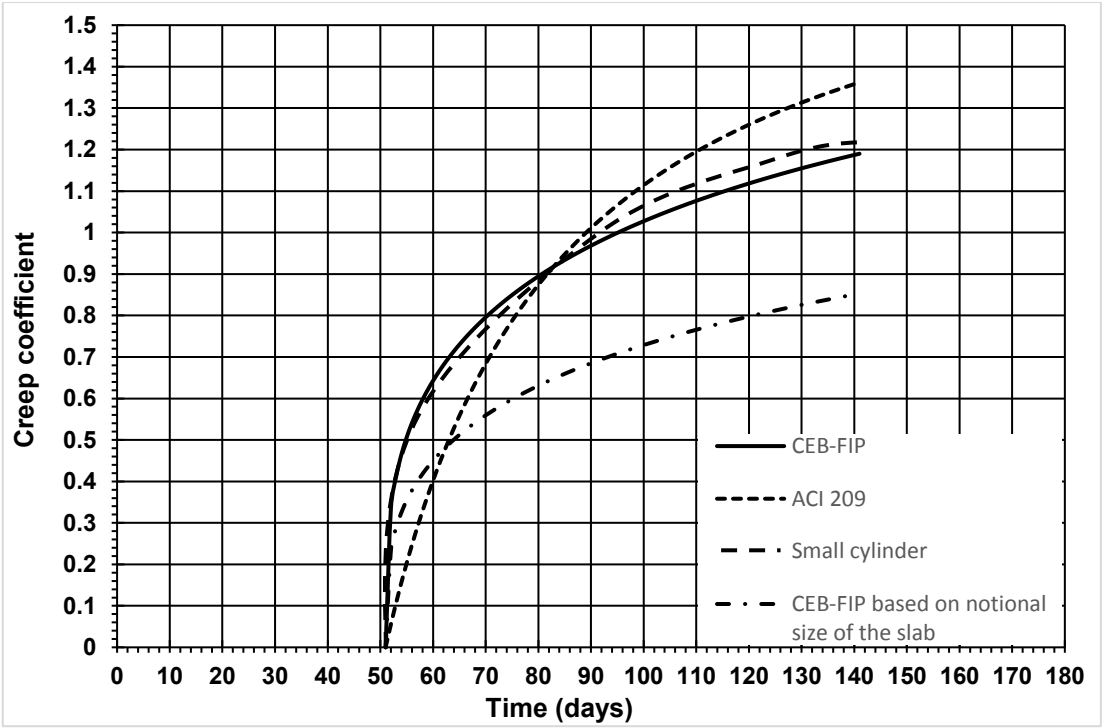

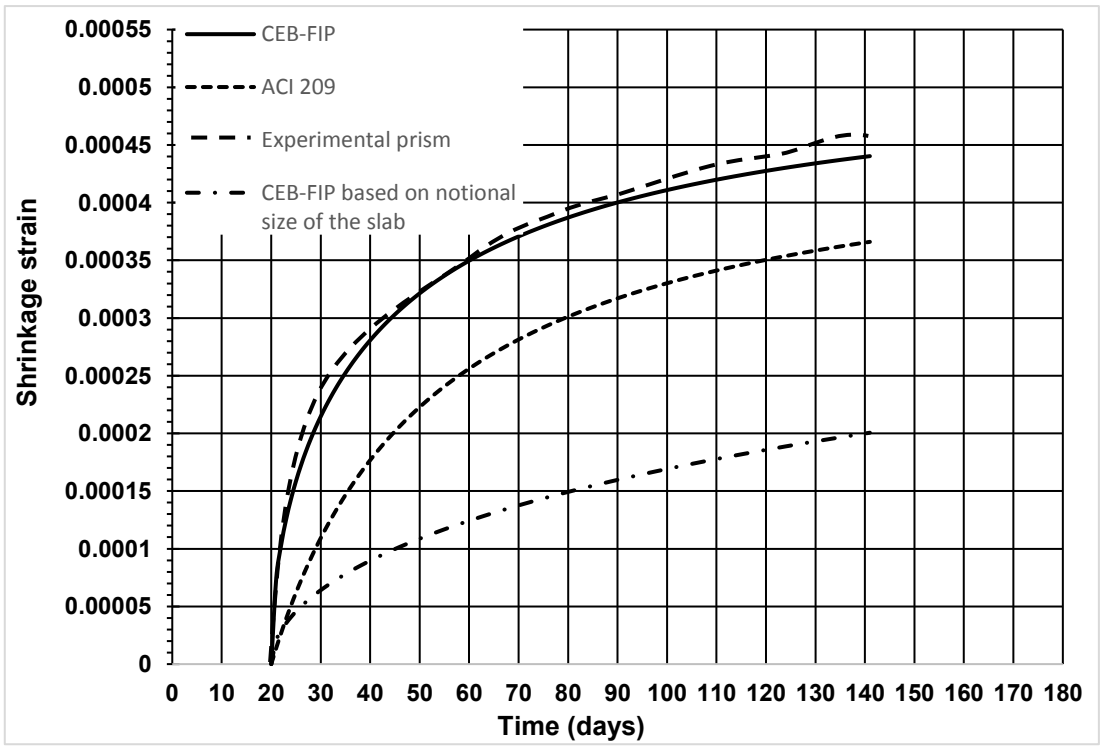

Figure 3-21. Comparison of measured and predicted long term deformation of shrinkage and creep of slab S4

3.8 Summary

This chapter has provided all details of the experimental methodology for the tested slabs that have been carried out at laboratory of Leeds University as part of this research. Testing program was aimed to conduct two experimental series. First series consists of two short-term large scale slabs in order to ensure the predictive capability of the proposed numerical analysis procedure and to decide the suitable sustained load level. Second series consists of four large scale slabs tested for a period of 90 days. Of these, one slab is reference and other four slabs contain different sizes of openings. The objective of the second series is divided into two parts; first to ensure the reliability of the proposed procedure, second to identifying the influence of the tensile/compressive creep ratio on the long-term movements of the slab at potential design situations where the experimental test alone does not helpful.

Test set up and loading for reinforced concrete slab specimens were described. Details of the slab geometry and steel reinforcement arrangements were presented. Instruments used in the tested slabs in order to measure deflections, steel strains, and surface strain of concrete were also included. Tests carried out to determine the mechanical properties of concrete were described. Measured and predicted long-term properties of concrete were also provided. Results obtained from these large scale tests are presented and critically evaluated with numerical findings in Chapter 5.

Chapter 4 Numerical Modelling of Reinforced Concrete Slabs

4.1 Introduction

As it has already been stated, the experimental investigations alone will not therefore sufficiently distinguish the influence of each relevant parameter on the long-term behaviour. The investigation of the behaviour of reinforced concrete slabs is often undertaken by gathering test data from experiments and then following up with a detailed theoretical study. This method is often viable for the study of instantaneous behaviour of the slabs. It is, however, expensive and time consuming for the investigation of long-term behaviour of slabs. Unfortunately, analytical solutions are limited to simple problems. Otherwise, the numerical procedures provide good option to accurately simulate structural behaviour if the appropriate modelling approach and material laws are effectively utilized. The major aim of this study is to construct a numerical analysis procedure for modelling the slab response.

Therefore, a numerical nonlinear layered cross-sectional analysis procedure has been proposed in this study to predict the response of partially cracked reinforced concrete slabs. The numerical analysis was performed using finite difference method. The procedure is based on the layered approach in a rational way to deal with complex problems such as concrete cracking, tension stiffening, concrete creep and shrinkage.

This chapter mainly describes the methodology of the numerical analysis procedure. The material constitutive models are included. The modelling of the slab components such as boundary conditions, mesh size and load is described. Finally, the procedure for modelling cracking, tension stiffening, creep and shrinkage in reinforced concrete is described.

4.2 Finite Difference Method

As explained earlier in section 2.3.2, the finite difference method is one of the efficient available methods for numerical solution of partial deferential equations

(PDEs). It is very simple and effective. Furthermore, it is the most general and clear, particularly, in the problems of plate bending analysis, which is a classical field of finite difference method (Szilard, 2004). Moreover, it is easy to obtain higher order solutions by using this method. A more useful application of finite differences is in cases when the bending moment is not easy to determine. It operates directly on the differential equations, which requires replacing the differential equations by a series of linear algebraic equations, i.e. difference expressions, at a finite number of points on the plate. These points are located at the intersection joints of a rectangular, triangular or other mesh network, called finite difference mesh as shown in Figure 4-1.

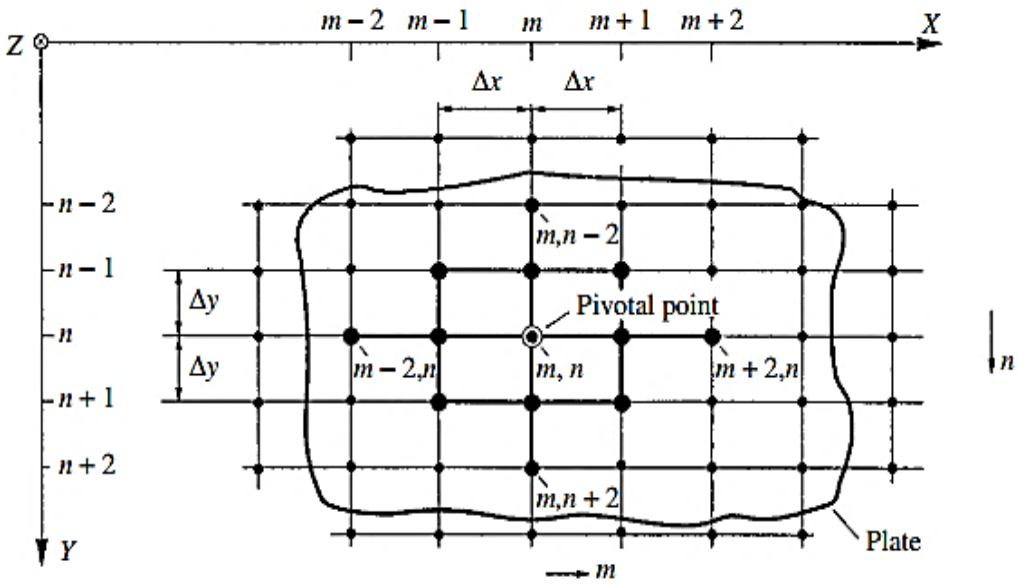

Figure 4-1. Finite difference mesh and nodes

The finite difference method applies a mathematical discretization of the plate continuum by yielding a set of algebraic equations, therefore, the deflections at these points can be obtained. By considering this method, the fourth order derivative of governing differential equation at nodes of plate can be obtained approximately from the following expressions:

$$\left(\frac{\partial^4 w}{\partial x^4}\right)_{m,n} \approx \frac{1}{\lambda^4}(w_{m+2,n} - 4\,w_{m+1,n} + 6\,w_{m,n} - 4\,w_{m-1,n} + w_{m-2,n} \qquad (4\text{-}1)$$

$$\left(\frac{\partial^4 w}{\partial y^4}\right)_{m,n} \approx \frac{1}{\lambda^4}(w_{m,n+2} - 4\,w_{m,n+1} + 6\,w_{m,n} - 4\,w_{m,n-1} + w_{m,n-2} \qquad (4\text{-}2)$$

$$\left(\frac{\partial^4 w}{\partial x^2\,\partial y^2}\right)_{m,n} \approx \frac{1}{\lambda^4}\left[4\,w_{m,n} - 2\left(w_{m+1,n} - w_{m-1,n} + w_{m,n+1} + w_{m,n-1}\right)\right.$$
$$\left. + w_{m+1,n+1} + w_{m+1,n-1} + w_{m-1,n+1} + w_{m-1,n-1}\right] \qquad (4\text{-}3)$$

Once the deflection at these grid points are obtained, internal forces and deformations can be obtained at these points by differentiation. Since only the deflection represents the unknowns, the size of the coefficient matrix is much smaller in comparison to that of the finite element method (Szilard, 2004). Owing to these advantages, it was decided to select this method in the present study.

4.3 Materials Modelling

The reliability of the predicted behaviour depends on the accuracy of modelling the structure components, the loading and the material properties. The material modelling will be presented in this section; the other components will be presented in the next sections. To describe the response of reinforced concrete, constitutive models are required for concrete response in tension and compression. Reinforced concrete members are usually made up of steel and concrete, which have different behaviour. The modelling of concrete and reinforcement are given in the next subsections.

4.3.1 Uniaxial Compression of Concrete

As a composite material, normal concrete is consisted of cement, fine and coarse aggregates. The mechanical properties are very complex since it is heterogeneous. Concrete exhibits many micro-cracks at the interface between mortar and coarse aggregate, even before any load. These micro-cracks have a great influence on the mechanical behaviour and nonlinear behaviour of concrete. Under uniaxial compressive stress, concrete exhibits linear elastic behaviour up to 30-40% of the compressive strength. In the next stage, the stress-strain curve is no longer linear as shown in Figure 4-2.

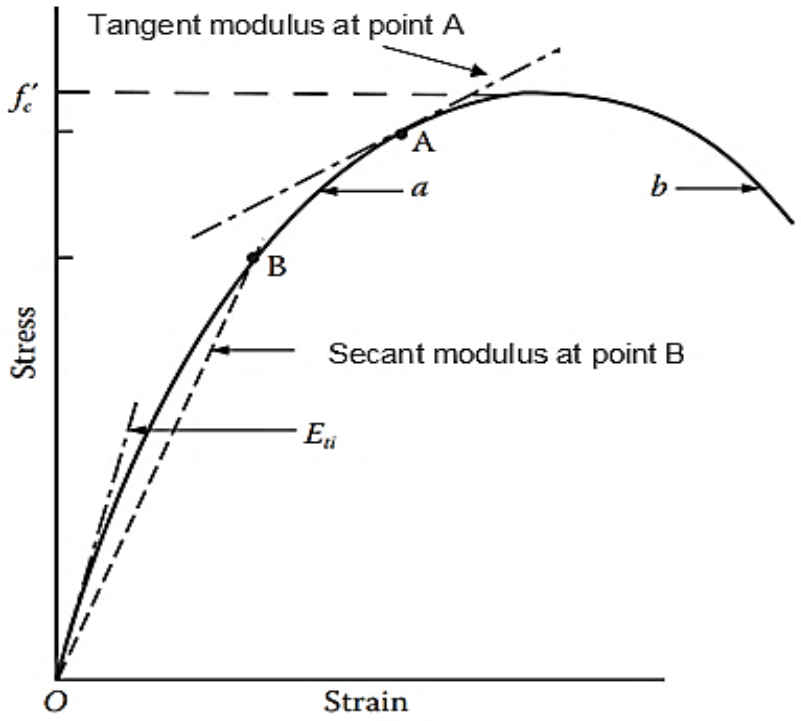

Figure 4-2. Typical uniaxial compressive stress-strain curve and modulus of concrete

In the nonlinear analysis of reinforced concrete structures, the response is governed by consideration of nonlinear behaviour of concrete stress-strain curves. However, the material stiffness of concrete can be estimated by secant modulus or tangent modulus as shown in Figure 4-2. In the present study, the secant modulus is adopted to represent the stiffness of stress-strain curve of concrete. There are several mathematical models have been derived to estimate the uniaxial stress-strain curve of concrete. Some of earlier better known models for normal strength concrete are derived by (Hognestad, 1951) and (Kent & Park, 1971). In 1951, (Hognestad, 1951) proposed a parabolic curve that is shown in Figure 4-3. It can be divided into three portions. The first portion represents linear elastic branch and material stiffness can be easily estimated. The second portion describes the ascending portion (nonlinear relation between stress and strain) from linear point to the peak strength point at the corresponding strain. The third portion represents the post peak stress until the ultimate strain value. The complete stress-strain behaviour is given by the following expression:

$$\sigma_c = f'_c \left[2\left(\frac{\varepsilon_c}{\varepsilon_o}\right) - \left(\frac{\varepsilon_c}{\varepsilon_o}\right)^2 \right] \qquad (4\text{-}4)$$

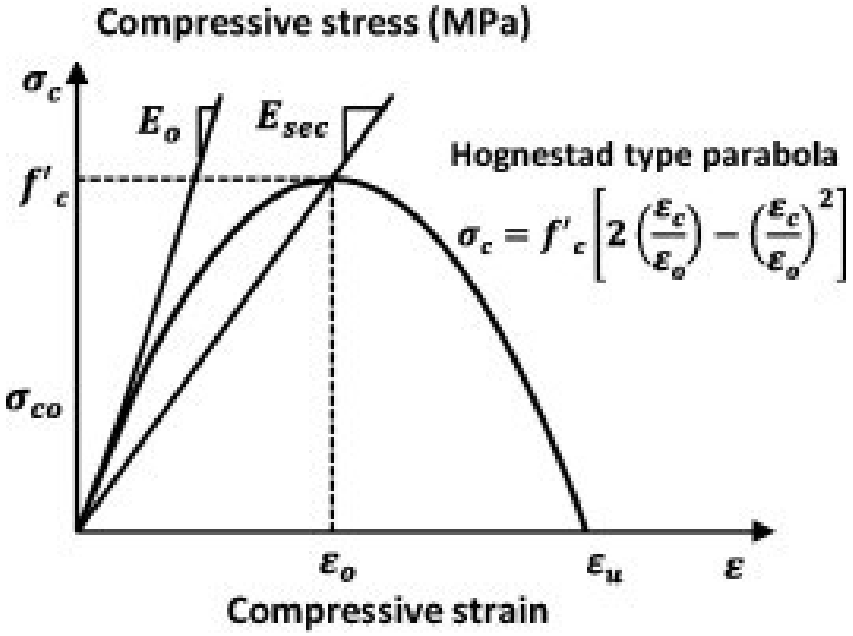

Figure 4-3. Uniaxial stress-strain curve for concrete proposed by (Hognestad, 1951)

Reinforced concrete members are rarely stressed with pure uniaxial state, however, the current available models of uniaxial stress-strain curves can be modified to represent realistic situation of loading. For concrete in a biaxial compression state, stress and strength enhancement is justified by using a relationship proposed by (Kupfer & Hilsdorf, 1969) model. This approach stated that the strength enhancement factor for concrete in two directions, arising from the stress acting in the one direction as shown in Figure 4-4.

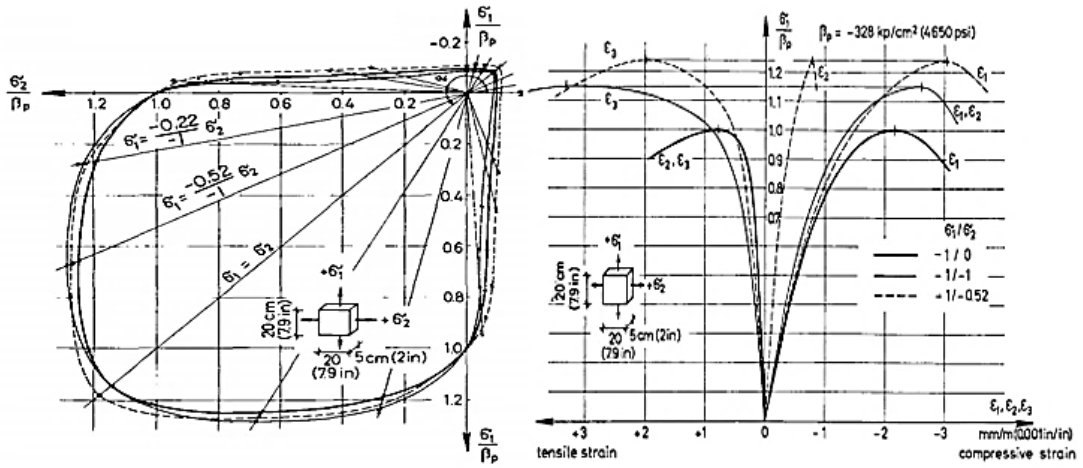

Figure 4-4. Biaxial strength and stress-strain enhancement factor of concrete (Kupfer and Hilsdorf, 1969)

4.3.2 Uniaxial Tension of Concrete

The nonlinear response of concrete is often governed by progressive tensile cracking, resulting in localized failure zones. Thus, tensile cracking must be taken into consideration in predicting their service behaviour as well as ultimate load capacity. The uniaxial tensile stress-strain response of plain concrete is nearly linear until its tensile strength. Thus, the material stiffness can be found easily. After fracture, the behaviour is no longer linearly, and the stress gradually decreases while the strain increases (softening zone), as shown in Figure 4-5.

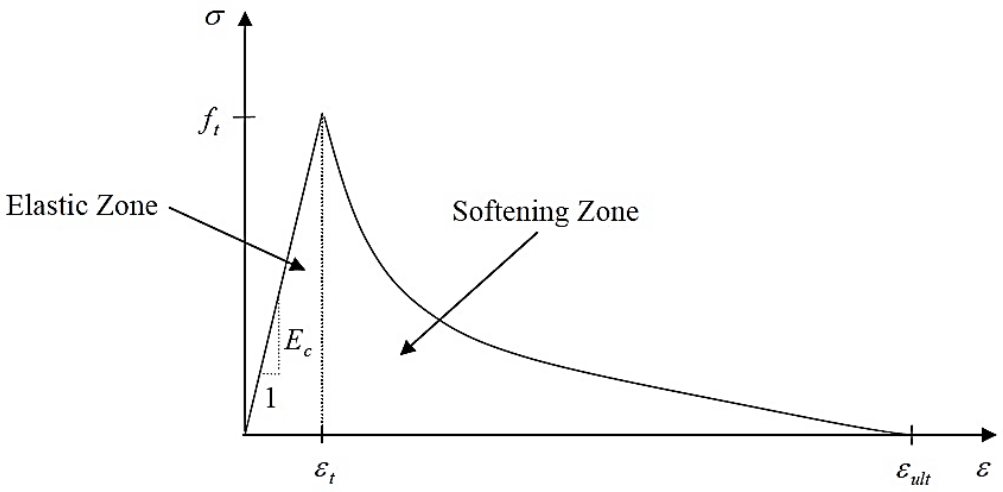

Figure 4-5. Uniaxial tensile stress-strain curve of concrete

A more commonly adopted method for dealing with post-cracking response is proposed by (Hordijk, 1991). Hordijk model has been adopted in most finite element software for modelling post-cracking tensile behaviour. In this model, the first segment of stress-strain curve is linear while the second part of the stress-strain curve is nonlinear as shown in Figure 4-5. The model provides a nonlinear descending softening curve for simulating the post-cracking tensile behaviour. The nonlinear part is based on the fracture energy G_f to reflect the cracking behaviour. Unlike the strain softening response, tension stiffening does not drop off until the steel reinforcement has yielded. As a result, the descending branch of the uniaxial stress-strain curve of pain concrete should not be used as a basis for developing a tension stiffening model (Fields and Bischoff, 2004). In the present study, therefore, the tensile fracture of concrete is considered as brittle.

The strength of concrete in tension is much lower than the strength in compression. The strength of concrete under biaxial tension is nearly equal to its uniaxial tensile strength (Kupfer and Hilsdorf, 1969). More recently, concrete researchers have been shown that the splitting tensile strength test of cylinder gives a more reasonable tensile strength predictions than the modulus of rupture test or direct tensile test (Efsen & Glarbo, 1956; Peltier, 1954; Wright, 1955). Several equations are available to estimate the splitting tensile strength of concrete.

In addition to model derived by Gardner, (ACI318, 2014) proposed an empirical equation based on laboratory tests to determine the relationship between average splitting tensile strength f'_{tsp} and the average compressive strength f_c' for normal weight concrete as following:

$$\mathrm{f'_{tsp}} = 0.56\sqrt{\mathrm{f_{cm}}}\ \ (\mathrm{MPa}) \qquad (4\text{-}5)$$

In the present study, for convenience, the experimental obtained values from laboratory for the splitting tensile strength of concrete were used directly as input in the numerical analysis procedure. Therefore, a brittle tensile strength had to be assumed and hence the concrete layer contribution has set to zero when the principal tensile stress in the concrete layer reaches the splitting tensile strength of concrete (see section 4.9.1).

4.3.3 Modelling of Long- term Properties of Plain Concrete

As the properties of concrete, the strain in the member changes for a long period of time. Among the time dependent properties of concrete that are of interest to the structural engineer are the shrinkage and creep. While the concrete creeps under sustained stress, the shrinkage is stress independent. For analysis of the time-dependent movements, it is necessary to employ time functions models for strain in the materials. Creep and shrinkage are influenced by several factors, among these factors are ambient relative humidity, load level, age of concrete at loading, curing conditions, mix proportions and properties, shape and size of member. There are several analytical models derived for predicting creep and shrinkage deformations such as (CEB-FIP-MC2010, 2010) and (ACI-209.2R,

2008). In the present study, it was decided to select (CEB-FIP-MC2010, 2010) model for prediction creep and shrinkage deformation.

The concrete strength of concrete develops with time. The development of compressive strength at age t depends on the type of cement, curing conditions and temperature. The development of compressive strength of concrete at various ages may be estimated by (CEB-FIP-MC2010, 2010) as the following:

$$\mathrm{f_{cm}(t)} = \beta_{cc}.\beta_{as}(t) \tag{4-6}$$

$$\beta_{cc} = \exp\left\{s.\left[1 - \left(\frac{28}{t}\right)^{0.5}\right]\right\} \tag{4-7}$$

Where $f_{cm}(t)$ is the mean compressive strength in MPa at an age t in days, f_{cm} is the mean compressive strength of concrete at the age of 28 days (MPa), β_{cc} is a function to describe the development with time, and s is a coeffiecient with depends on the strength class of cement (for the cement type used in the current study $s = 0.2$).

The development of tensile strength with time is strongly influenced by curing and drying conditions as well as by of the dimensions the structural members. It may be assumed that for a duration of moist curing $t_s \leq 7$ days and a concrete age $t > 28$ days the development of tensile strength is similar to that of compressive strength (CEB-FIP-MC2010, 2010). In this study, the development of tensile strength was ignored, since the moist curing duration was $t_s \cong 20$ days > 7

The concrete modulus of elasticity also develops with time due to the properties of concrete. Thus, the modulus of elasticity of concrete at an age $t > 28$ days may be estimated from formula adopted by (CEB-FIP-MC2010, 2010) as following:

$$\mathrm{E_{ci}(t)} = \beta_{E}(t).\mathrm{E_{ci}} \tag{4-8}$$

$$\beta_{E}(t) = [\,\beta_{E}(t)\,]^{0.5} \tag{4-9}$$

Where $E_{ci}(t)$ is modulus of elasticity in (MPa) at an age t in days and E_{ci} is modulus of elasticity in (MPa) at an age of 28 days.

In the reinforced concrete, creep and aging $\chi(t, t_0)$ are important parameters for creep analysis of any structure where $\chi(t, t_0)$ is the ageing coefficient. The coefficient $\chi(t, t_0)$ depends on the age of concrete at first loading, the size and shape of the member, and the duration of load (R.I. Gilbert & Ranzi, 2010). The coefficient $\chi(t, t_0)$ was called by (Trost, 1967) the relaxation coefficient but was later renamed by Bazant the aging coefficient. The values of $\chi(t, t_0)$ are usually less than 1, with 0.8 to 0.85 as the mean estimate. In 1988, (Z. Bazant, 1988) stated that Coefficient $\chi(t, t_0)$ does not really introduce a correction for the stress relaxation. Rather, it introduces a correction for aging. Hence, the stress history and the effect of aging coefficient must be included to predict the deformation of reinforced concrete (RC) members accurately (R.I. Gilbert & Ranzi, 2010).

4.3.4 Steel Reinforcement

Steel reinforcement is used in concrete construction to increase the stiffness of member since it is relatively strong and stiff compared with concrete. In reinforced concrete structures, the response of reinforcing steel bar severely affects the behaviour of the member, particularly, near the ultimate load stages (nonlinear zone). The typical engineering stress-strain curve for steel reinforcement subjected to tensile loading is shown in Figure 4-6.

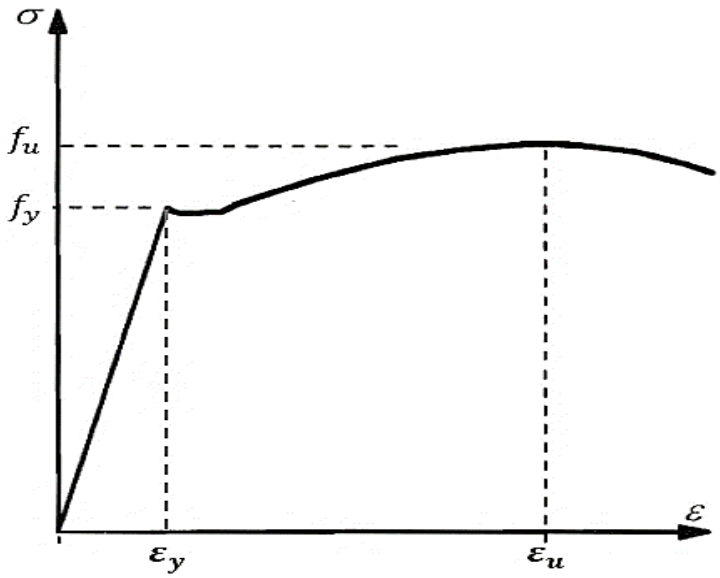

Figure 4-6. Uniaxial stress-strain curve for typical reinforcement

The stress at yield point f_y refer to yield tensile strength of steel with corresponding yield strain $\boldsymbol{\varepsilon_y}$. In this region, the modulus of elasticity can be found by the slope of the linear elastic portion of the curve. After the yield stress-strain point, the behaviour of steel reinforcement is no longer linear and behaves as elastic material, thus, the stress slightly decreases while the strain increases. In the service load range, the tensile reinforcement behaves typically linear-elastic.

Adequate analysis of the member usually requires realistic stress-strain relationships for modelling of steel reinforcement. There are several constitutive models have been proposed for response of steel reinforcement. Therefore, the most common approach for modelling the reinforcement is the elastic-strain hardening through simplified and idealized the shape of the stress-strain curve. For convenience, it is commonly necessary to idealize the stress-strain curve through consider bi-linear or tri-linear approach depending on the accuracy required. In the present study, the idealization of stress-strain curve has been derived from uniaxial tensile stress-strain tests at laboratory of University of Leeds as shown in Figure 4-7. The idealization of stress-strain curve depends mainly on the slop of the experimental stress-strain curve after yield point. Accordingly, the proposed line has been derived to represent the stress-strain relationship of steel reinforcement. Moreover, the secant modulus of steel can be found at each point on the idealized curve.

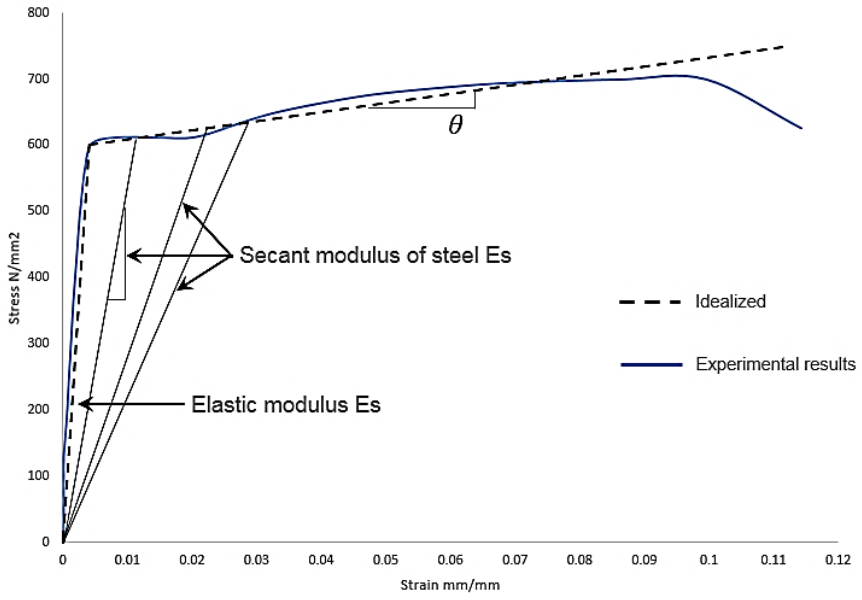

Figure 4-7. Idealized of stress-strain curves of steel

4.4 Creep Superposition of Concrete

When the member subjected to a constant stress $\sigma_c(t_0)$ applied at time t_0 , the total strain, including shrinkage, can be determined from:

$$\varepsilon(t, t_0) = \frac{\sigma_{c t0}}{E_c(t_0)} + \emptyset(t, t_0).\frac{\sigma_{c t0}}{E_c(t_0)} + \varepsilon_{sh}(t) \qquad (4\text{-}10)$$

Then

$$\varepsilon(t, t_0) = \frac{\sigma_{c t0}}{E_c(t_0)} + [1 + \emptyset(t, t_0)] + \varepsilon_{sh}(t) \qquad (4\text{-}11)$$

The equation (4-11) indicates the assumption that the total strain, instantaneous plus creep, is proportional to the applied stress. The stresses in reinforced concrete members usually varies with time for many reasons (as explained in the literature section 2.15) even if the load is constant. In the singly reinforced concrete flexural member, the neutral axis moves downward as a result of creep and shrinkage strains. Accordingly, the compressive area increases, and the stress decreases significantly. For analysis of such a section, equation (**4-11**) cannot be used directly since the stress within the cross-section varies with time even though the bending moment constant. The concrete creep caused by variable stress is generally calculated using the principle of superposition. The principle of superposition was first applied to concrete by (McHenry, 1943). Using this method, the total strains at time t may be expressed as the sum of the strain produced by $\sigma_{c_{t0}}$, the strain produced by the gradually stress increment $\Delta\sigma_{c_t}$, and shrinkage strain as shown in the following expression:

$$\varepsilon(t, t_0) = \frac{\sigma_{c t0}}{E_c(t_0)}.[1 + \emptyset(t, t_0)] + \frac{\Delta\sigma_{c t}}{E_c(t_0)}.[1 + \chi(t, t_0).\emptyset(t, t_0)] + \varepsilon_{sh}(t) \qquad (4\text{-}12)$$

In the present study, the varying in the flexural stress due to creep and shrinkage effects was assumed only in the compressive zone (details about the dealing with this problem are given in the section 4.9.2).

4.5 Modelling of Creep and Shrinkage in Reinforced Concrete Sections under Flexural

Over time, the deformation of reinforced concrete member attains values several times larger its initial values due primarily to creep and shrinkage effect. The inclusion of the reinforcement increases the instantaneous flexural stiffness, so that the instantaneous curvature reduces. The reinforcement provided in the section restrains the free development of shrinkage and creep. As explained earlier in section 2.15 , if the reinforcement is not symmetrically or just placed in the tension side, shrinkage would be expected to induce a curvature in the cross section. Furthermore, shrinkage induces tension stresses in the concrete due to the restraining action of the reinforcement, which effectively reduces the crack resistance. Similarly, creep also induces a curvature with time in the cross section. In such a case, the restraint to movement due to reinforcements will reduce the creep in the tension zone and lead to drop in the position of the neutral axis. Typically, in the singly reinforced sections the curvature, neutral axis movement and tensile restraint stresses are important while in symmetrically reinforced sections the tensile stresses are predominant rather than neutral axis movement and curvature. The estimation of creep and shrinkage deformations in reinforced concrete member is not straightforward. Accordingly, available analytical methods consider the creep and shrinkage actions are independently and derived based on the uncracked or fully cracked conditions with simple assumptions.

Therefore, in the present study, an extensive attempt has been made to deal with creep and shrinkage as dependently in the partially cracked reinforced concrete members. The reliability of analysis must be able to take into consideration the possible design scenario, particularly here is the existence of openings. Thus, new model is suggested in this research to deal with creep and shrinkage in reinforced concrete sections. The method is based on restraint concept that provided from reinforcement. Consider the section properties of unreinforced and reinforced concrete as shown in Figure 4-8. Assume that the external moment on the section is applied just before cracking moment, thus, the initial strain and curvature are occurred. Hence, the restraint ratio R is then defined as the ratio of the strain in reinforced concrete at the level of reinforcement bars to the strain in

unreinforced concrete corresponding to the level of reinforcement bars. The ratio can be obtained according to the following expression:

$$R = \frac{\bar{\varepsilon}}{\varepsilon_c} \tag{4-13}$$

Where R is the restraint ratio, ε_c is the strain at t_0 in the unreinforced concrete at the level corresponding to the reinforcement bars, and $\bar{\varepsilon}$ is the strain at t_0 in the reinforced concrete at the level of reinforcement. Typically, the restraint ratio R decreases as reinforcement ratio increases. This ratio also depends on the reinforcement position and whether the section is singly reinforced or doubly. By taking the sectional properties of the current work, this ratio typically ranged from 0.171 to 0.947 in the fully cracked and uncracked sections, respectively. For the unreinforced concrete members, the restraint ratio is equal to one and the internal stresses due to restraint to shrinkage will vanish.

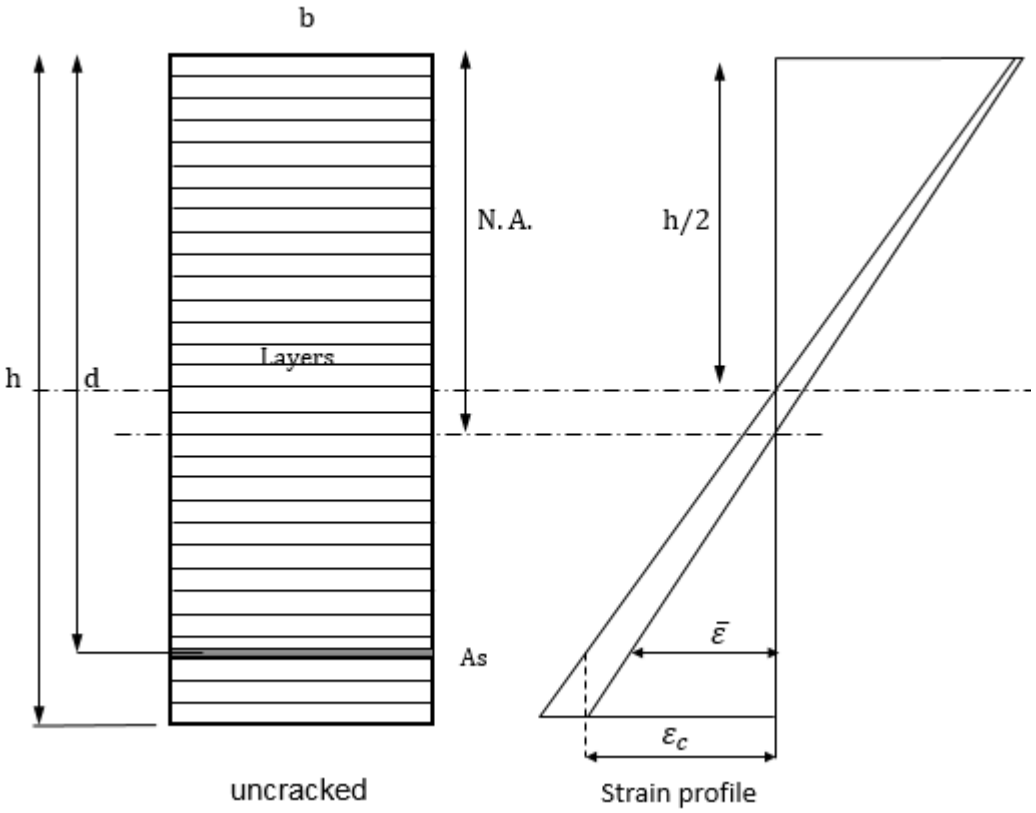

Figure 4-8. Sectional properties of unreinforced and reinforced concrete

To model shrinkage action, assume that cracking occurs instantly immediately at a section of a slab, but much of the slab remains uncracked, after the load is applied at age t_0 and the concrete has initial shrinkage at biaxial directions as shown in Figure 4-9a. After the load is applied, the initial strain and curvature are occurred. However, the reinforcement does not shrink, hence, the shrinkage of the concrete surrounding the reinforcement will be constrained and this will cause tensile strains to develop in the concrete and compressive strain in the reinforcement as shown in Figure 4-9b.

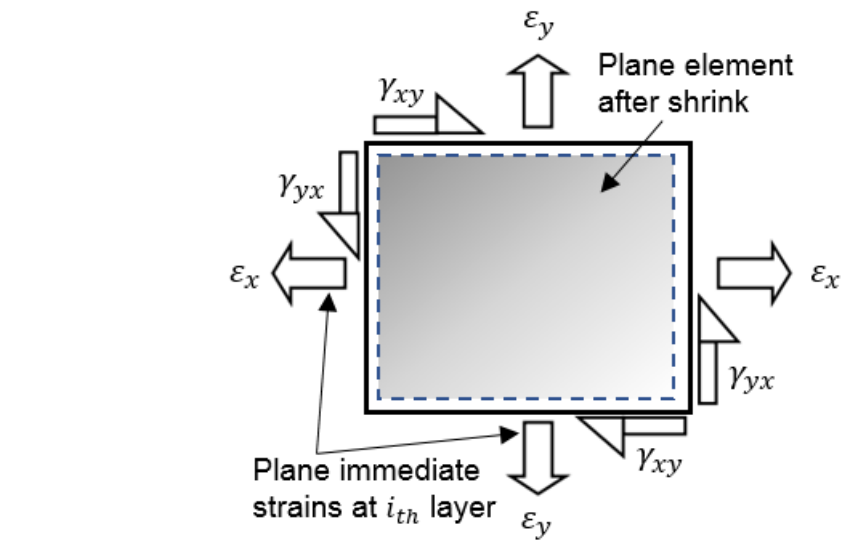

(a)

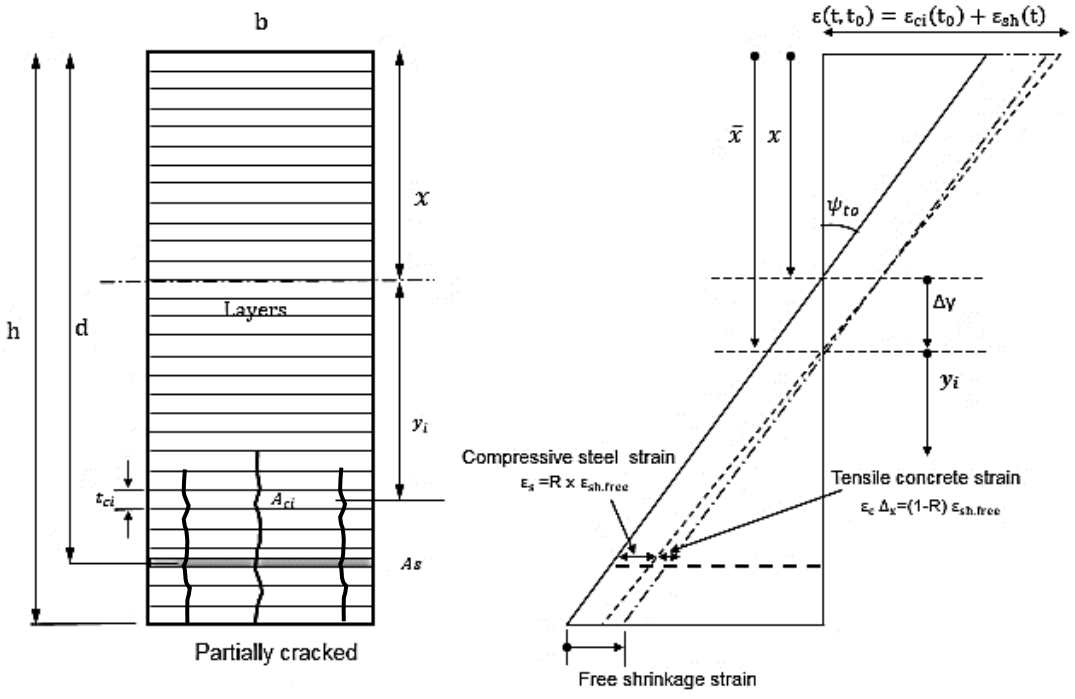

(b)

Figure 4-9. Shrinkage action at plane element (a), and restraint to shrinkage provided by reinforcement (b)

The tensile stresses of concrete in the level of reinforcement are then obtained from restraint ratio according to the following expressions:

$$\sigma_{cs} = (1 - R)\varepsilon_{sh.free} * E_c \quad (4\text{-}14)$$

$$\sigma_{ss} = R * \varepsilon_{sh.free} * E_s \quad (4\text{-}15)$$

Where σ_{cs} is the tensile stresses of concrete, σ_{ss} is the compressive stress of reinforcement, and $\varepsilon_{sh.free}$ is the free shrinkage strain.

On the other hand, to model creep and shrinkage actions, consider that the cracking occurs at a section of a slab, whenever the tensile stress in the concrete reaches the tensile strength of concrete but much of the slab remains uncracked, instantly after the load is applied at age t_0. Immediately after the load is applied the initial strain and curvature are occurred, and the concrete has initial shrinkage. At age t, some creep and shrinkage have taken place with time. Due to the presence of reinforcement, the neutral axis position is shifted downward as shown in Figure 4-10. To model this problem, the restraint ratio is also required, therefore, the total restraint strains (shrinkage and creep) is then calculated. Then, the new neutral axis position and curvature are obtained by similar triangle option. In such a case, where the bending strain profile distribution is comparatively small, the creep strain would be expected to be small, thus, in this case the shrinkage strains govern the total strains and will cause some reduction in tensile stresses of the reinforcing bar. In contrast, in the high bending zones, the creep strain would be anticipated to be higher than shrinkage strains and thereby the creep will govern the total strain and, hence, will lead to induce tensile tresses in the reinforcement bar over time. Therefore, the method proposed in this study is appropriate to deal with such interaction. This method also is appropriate for different material properties within the layered section.

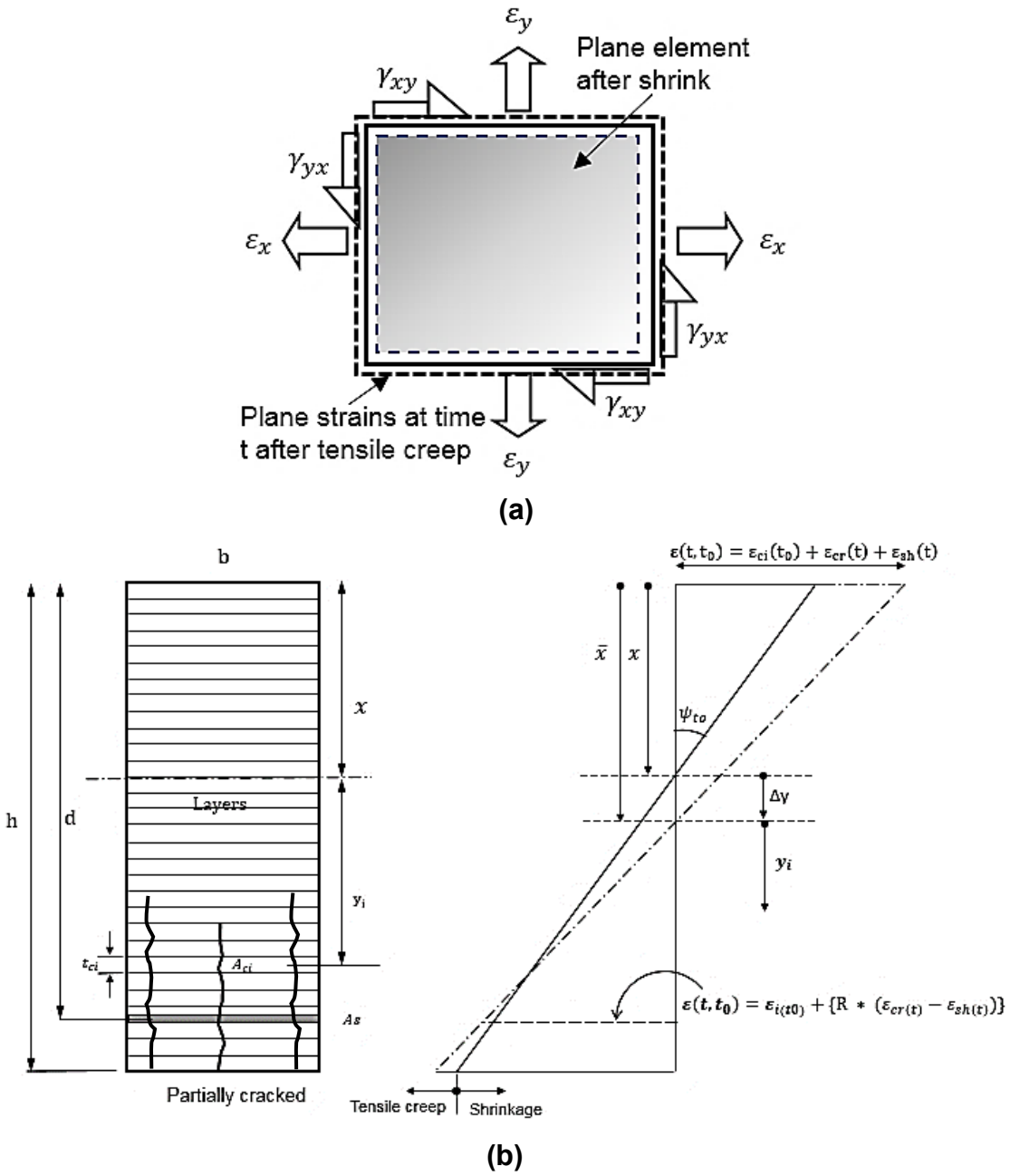

Figure 4-10. Shrinkage and creep action of plane element (a) and changes in curvature and neutral axis at age t (b)

4.6 Modelling of Boundary Conditions and Loads

Setting up a proper boundary conditions is necessary for accurate analyses. The boundary conditions are the known conditions on the surfaces and supports. The rigorous solution of the governing differential equation must satisfy simultaneously the boundary conditions and differential equation of any given problem. There are three available boundary conditions such as geometrical boundary conditions, mixed boundary conditions and statical boundary

conditions (Szilard, 2004). For geometrical boundary conditions, certain boundary conditions provided by the magnitude of displacements. In the bending theory of plates, the displacement components to be used in formulating the boundary conditions are slope and lateral deflections. Solution of the differential equation by using finite differences method requires appropriate representation of the boundary conditions. When central finite differences method is used to solve fourth order differential equation, the introduction of fictitious points outside of the slab is required. In such a case, the fictitious points outside the slab boundaries are expressed in terms of deflections of the mesh points located inside the slab boundaries as shown in Figure 4-11. In the present study, slabs were supported at four sides on stiff supports (I-sections). Therefore, no differential settlements are occurred. In the case of the slab contains an opening, special boundary conditions at the opening edges are needed. Therefore, settings up proper boundary conditions are necessary. At the edges of the opening the bending moments are set to zero whereas the deflections along its boundary are not.

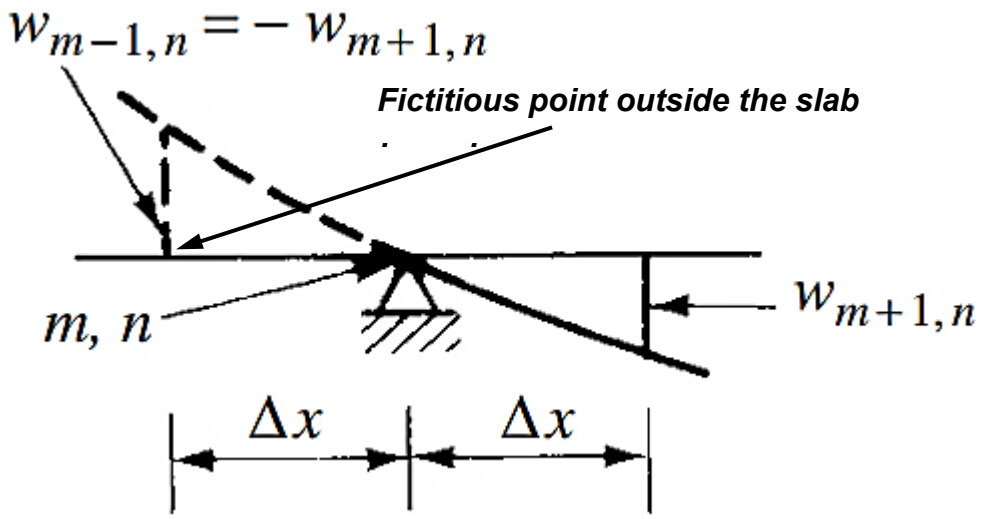

Figure 4-11. Representation of boundary conditions for finite differences method by (Szilard, 2004)

In reinforced concrete members subjected to load, five different types of loading conditions can occur: concentrated forces and moments acting at a point; prescribed boundary displacements; distributed loads; body force loadings and; thermal loadings. Correctly modelling the load in the finite difference method is

an important aspect for solving governing differential equation. Thus, to apply the loads to the slab in the model, the load representation is required. Node locations that coincide with the location of concentrated forces is required. In the present study, the slab was subjected to partial area loading of 200x200 mm. For modelling such load, the force was divided properly on the finite nodes, which is located under the loaded area.

4.7 Mesh Sizes and Convergence Analysis

The most important step in the numerical analysis procedure is the convergence analysis. While the use of an ordinary finite difference technique is very simple, and the method is quite general, it is characteristics by slow convergence. Thus, when higher order derivatives and a large number of mesh points are involved, the solution due to machine errors may convergence to a wrong number that adversely affects its accuracy. Therefore, the use of an iterative approach is recommended. Moreover, extremely fine mesh resulting large number of simultaneous equations and hence may create additional errors in solutions. In 2004, (Szilard, 2004) carried out a series of convergence analysis for square plate supported on four sided as shown in Figure 4-12. As can be seen from the figure, when the change of the mesh size is ranged from $(a/4)$ to $(a/8)$, the error is decreased from 28% to 2%, respectively. It is clear that the error decreases significantly when the number of elements (finer mesh) increases. This can confirm that the finite difference method gives good results with a little discretization in continuum.

In this study, the convergence study was done to optimize the mesh size and numerical model reliability with respect to elastic deflection. In the nonlinear cracking analysis, the development of crack produces convergence issues. This is attributed by the local softening after fracture of the concrete material. This issue can be resolved efficiently by selecting a proper model for the post-cracking tensile behaviour. In this study, however, the softening post-cracking part is ignored as it has been mentioned in section 4.3.2. Therefore, the concrete was modelled as a linear brittle material when the concrete stress exceeds the tensile strength. Moreover, the convergence problem can be treated by increasing the number of load steps (small increments) in the analysis. The convergence

analyses were performed as a basic evaluation for the numerical model in order to obtain the optimal results. In this study, square element type was chosen, and different mesh sizes of 25 mm, 50 mm, 75 mm and 100 mm were tested, with all other parameters kept constant.

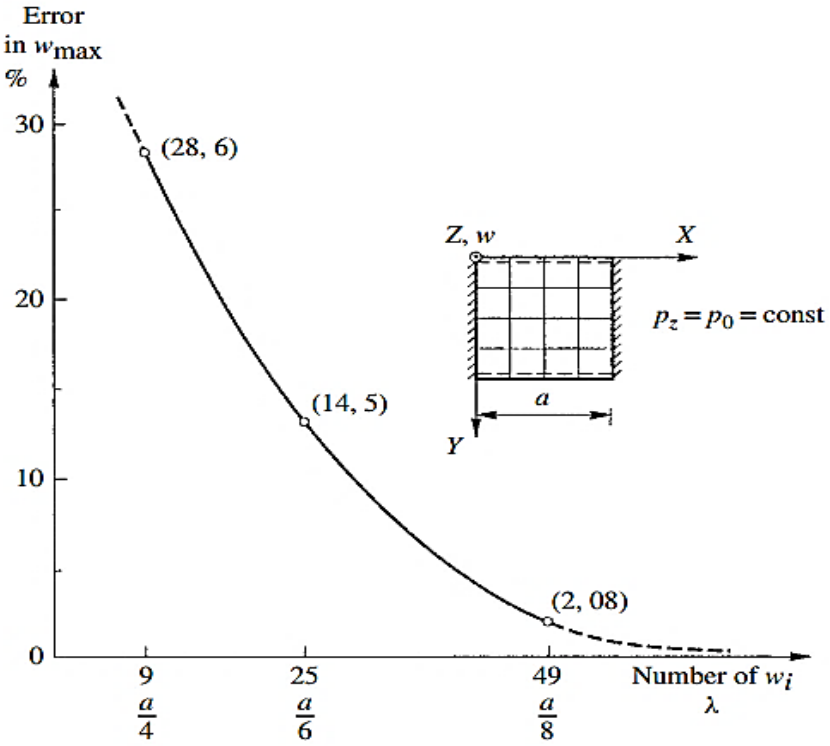

Figure 4-12. Convergence of FDM (Szilard, 2004)

4.8 Assumptions

Reinforced concrete members are typically made up of steel and concrete, which have different behaviour. Steel reinforcement can be considered as homogeneous material with properties can be defined. On the other hand, concrete is anisotropic non-homogenous material and its mechanical properties is complex. The modelling of reinforced concrete structural members depends on separate material models for the concrete and steel, which makes the reliable analysis is impossible. However, during the nonlinear modelling of reinforced concrete members, an appropriate assumption is usually the critical key factor for accurate and successful analysis.

4.8.1 Assumptions of Short-term Analysis

The basic assumptions adopted in the present study are as following:

- Plane sections remain plane before and after deformation.
- The plane cross section is perpendicular with horizontal mid plane=90^0.
- The slab is thin. Thus, the out-of-planeside, i.e. the shear stress is ignored.
- The cracking of concrete was assumed fixed smeared and is formed orthogonally within in-plane principal directions.
- Redistribution of elastic moments due to flexural stiffness cracking is ignored.
- The tensile behaviour of concrete is modelled as linear brittle.
- The geometric nonlinearity is not considered in the analysis.
- As the smeared crack model was adopted, reinforcing steel was modelled as additional smeared stiffness over the concrete plane stress elements.
- Perfect bond between concrete and steel was assumed. Hence, the loss of bond stress after cracking is ignored.
- The reinforcing steel is assumed to carry stress along its axis only and the effect of dowel action is neglected (this is reasonably specifically in the case of small reinforcing bar diameters).
- Perfect shear stress transfer between layers is assumed.

4.8.2 Assumptions of Long-term Analysis

- The creep strain (tension and compression) is proportional to the stress.
- The restraint to shrinkage by the end supports is not considered.
- The temperature effect is ignored.
- The creep and shrinkage strain profiles are considered linearly through the section.
- Shrinkage is assumed uniform throughout the depth of slab sections.
- Creep and shrinkage strains were assumed as not separated phenomena acting on reinforced concrete flexural sections.
- Neutral axis changes due to creep and shrinkage are considered in the numerical analysis procedure.
- Creep induced from restraint to initial shrinkage stresses prior to loading is ignored since it is relatively small.
- The reduction in concrete tensile strength due to sustained loading was ignored.

- Loss of tension stiffening due to internal cracking was ignored. This is reasonable since the loss of tension stiffening is largely dependent on the reduction of concrete tensile strength under sustained loading. This is reasonable since all slabs were loaded over 28 days and, hence, the concrete has gained much strength.
- However, it is suggested that the loss of beneficial stiffness only due to cracks caused by restraint to shrinkage.
- Loss of tension stiffening with time due to tensile creep was ignored. This is reasonable since creep plays an insignificant part in such changes (see section 2.13).
- The effect of member size on concrete creep and shrinkage are considered by using notional size member expression h.
- Average ageing coefficient $\chi(t, t_0)$ was assumed to be 0.85.

4.9 Numerical Analysis Procedure

The numerical analysis of a reinforced concrete structure is complicated by the nonlinear material stress-strain relationships. This section describes the major components of the numerical analysis procedure adopted in this research. The procedure described is solved by the computational system using Visual Basic for Applications (VBA), which was used to obtain the numerical solutions. VBA is the programming language for advanced users to automate computing operations and extend multi functionalities. VBA programming can establish and formulate complicated engineering multi models (such as concrete cracking and material nonlinearity) in one task. It is very efficient for solving fourth order differential equations. These advantages are not provided in the MATLAB. Thus, it was decided to solve the numerical procedure using VBA programming.

Usually, the first step in prediction of long-term movements for partially cracked members is to perform instantaneous nonlinear cracking analysis; the long-term deformations is then incorporated. The analysis of partially cracked members is not straightforward. The difficulties of prediction the complete behaviour of such analysis is caused by the nonlinearity of the moment-deformation relationships of the sections due to cracking and nonlinear stress-strain relationship at high level of compressive stresses. Therefore, the step by step method with load increment

procedure is necessary. The step by step method is not subject to many of the simplifying assumptions contained in other methods of analysis and generally leads to reliable results. Based on the approach described above, a VBA (Visual Basic for Applications) programme was developed. Using the program, the sectional properties such as stresses of materials, neutral axis position and curvature of sections can be determined. To analyse the effect of creep and shrinkage, their effects are treated as dependent and applied to the strain profile as additive with respect to restraint ratio. The results of analysis will be presented with experiment together. The algorithms used in this work for both short and long-term analysis are included in the following sections:

4.9.1 Short-term Analysis.

The analysis of a flexural members involves the determination of stresses, strains, curvatures, and deflections at different points. The first step in the analysis is usually to determine bending and torsional moment distributions M_x, M_y, and M_{xy} ; then the internal deformations are computed once the flexural rigidity of slab $[D]$ is given (see graphical examples Figure A-1 in appendix A). For each element, an estimation of the flexural rigidity is required. Reinforced concrete members is usually made up from two materials with different properties, namely, steel and concrete. In the section 2.4, it was always assumed that the plate material is homogeneous and isotropic in all directions. In many practical applications for instance reinforced concrete slabs, however, it is often necessary to consider directional dependent bending stiffness since the slab in this case is described as orthotropic. In the present study, the reinforcement properties and spacing were the same in both directions. Thus, the flexural rigidity in both directions D_x and D_y are nearly equal. As stated earlier, the reinforcement is modelled as an additional smeared stiffness over the concrete plane stress elements in a state of uniaxial stress. The reinforcing steel is treated as being equivalent smeared steel layers (whose equivalent thickness is $t_s = A_s / b$, where A_s is the area of total reinforcing bar and b is the total length of the member). It is assumed that each layer is in a state of plane stress, as illustrated in Figure 4-13a, that compatibility between the steel layers and the concrete layers is maintained through the analysis, including perfect bond. The material properties

of each layer are assumed constant throughout the layer thickness, and the contribution of material properties are obtained by summing algebraically of each layer. In each layer of the element, the stress points are taken as Gauss points at its mid-point, and the stress components at these Gauss points are assumed to be constant over the thickness of each layer. The theoretical load steps were applied at each 5kN. Prior to cracking the section material properties behave as a linear elastic isotropic. In this stage, the neutral axis position coincides with the centroid of the section, and hence the whole concrete layers and reinforcement layer are contributed to the stiffness. Once the concrete cracks at specific layers, wherever the tensile stress in the concrete reaches the tensile strength, the contribution of cracked layers has set to zero as shown in Figure 4-13b. Then, the effective flexural stiffness is recomputed depending on the contribution of effective concrete layers and their properties according to the following equation:

$$D = \sum_{i=1}^{ith} (E_i . A_i . y_i^{\,2}) \qquad (4\text{-}16)$$

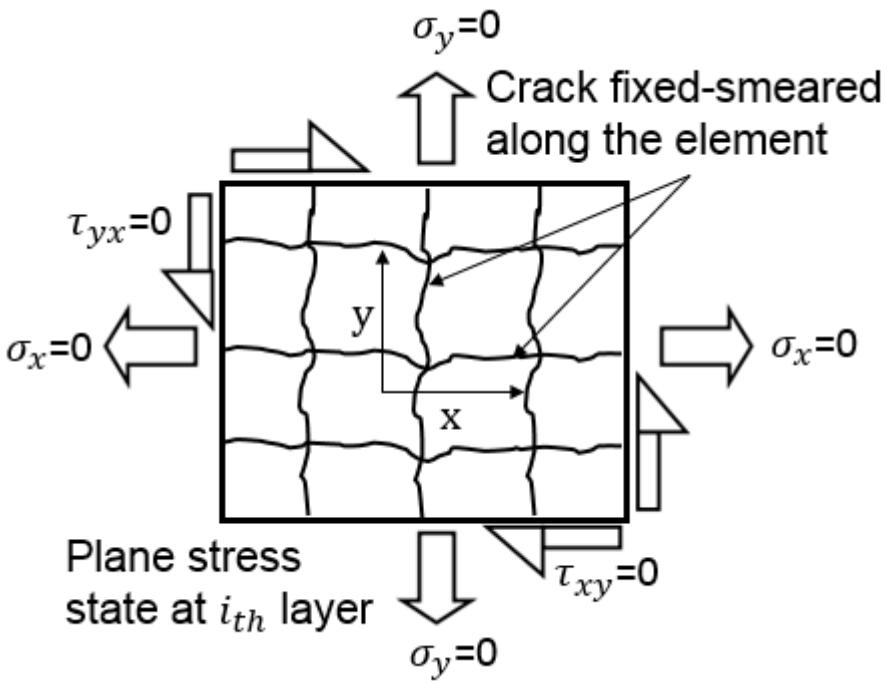

(a)

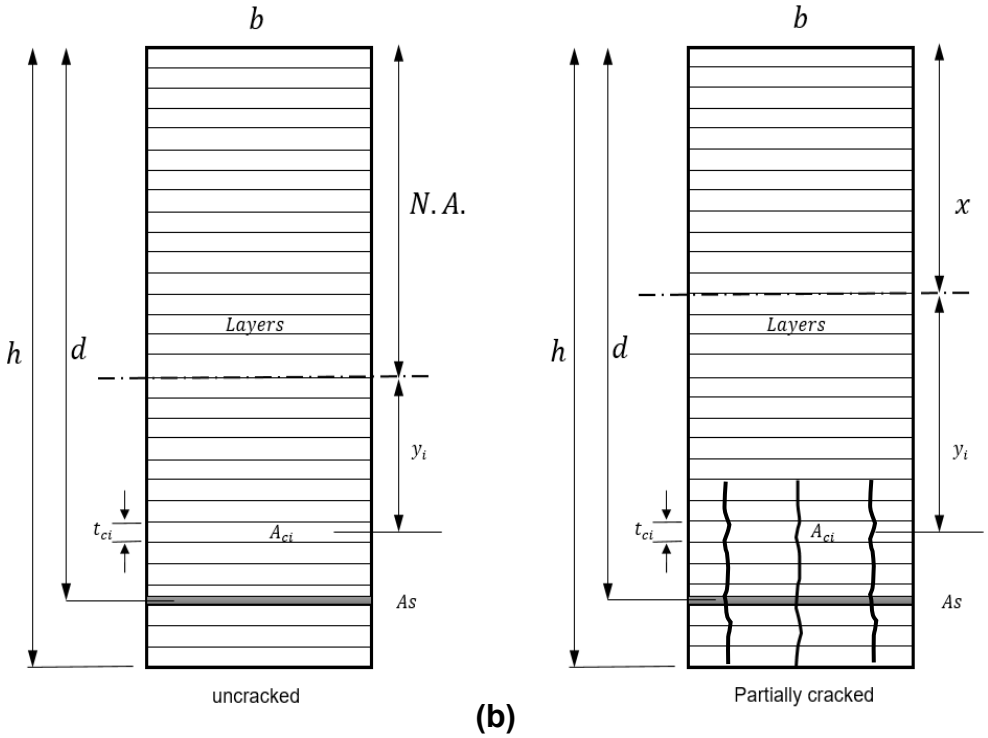

Figure 4-13. Plane stress state of i_{th} element (a), and associated layered transformed cross-section subjected to biaxial bending moment (b)

Again, cracks in reinforced concrete members occur wherever and whenever the tensile stress in the concrete reaches its tensile strength. To reflect the reduction in stiffness due to cracking, the moment-curvature relationship (see equations (**4-17**) is used to modify the stiffness. The bending and torsional moment at each local principal direction are added up to reflect the correct sense of moment-curvature relationship which is used to trace the cracking of concrete. This procedure is successful to reflect the reduction in torsional rigidity due to cracking. Once the layer had cracked theoretically, the contribution of this layer to the torsional stiffness has set to zero and hence the modified torsional rigidity of an element is considered. At each loading stage, the principal strains ($\varepsilon_x, \varepsilon_y, \gamma_{xy}$) for each layer are computed from curvature and neutral axis; and then the orthotropic tensile and in-plane shear stresses are obtained at each layer using relationships given in equation (4-18). The distribution of stresses in the slab can be seen in Figure A-2 and A-3 in appendix A).

$$\begin{Bmatrix} M_x \\ M_y \\ M_{xy} \end{Bmatrix} = \begin{bmatrix} \frac{E_x\, h^3}{12(1-\upsilon_x\upsilon_y)} & \upsilon_y \frac{E_x\, h^3}{12(1-\upsilon_x\upsilon_y)} & 0 \\ \upsilon_x \frac{E_y\, h^3}{12(1-\upsilon_x\upsilon_y)} & \frac{E_y\, h^3}{12(1-\upsilon_x\upsilon_y)} & 0 \\ 0 & 0 & \frac{\sqrt{E_x E_y}\, h^3}{12\,(1+\sqrt{\upsilon_x\upsilon_y})} \end{bmatrix} \begin{Bmatrix} \frac{\partial^2 w}{\partial x^2} \\ \frac{\partial^2 w}{\partial y^2} \\ \frac{\partial^2 w}{\partial x\ \partial y} \end{Bmatrix} \quad (4\text{-}17)$$

$$\begin{Bmatrix} \sigma_x \\ \sigma_y \\ \tau_{xy} \end{Bmatrix} = \begin{bmatrix} \frac{E_x}{(1-\upsilon_x\upsilon_y)} & \upsilon_y \frac{E_x}{(1-\upsilon_x\upsilon_y)} & 0 \\ \upsilon_x \frac{E_y}{(1-\upsilon_x\upsilon_y)} & \frac{E_y}{(1-\upsilon_x\upsilon_y)} & 0 \\ 0 & 0 & G_{xy} \end{bmatrix} \begin{Bmatrix} \varepsilon_x \\ \varepsilon_y \\ \gamma_{xy} \end{Bmatrix} \quad (4\text{-}18)$$

If the computed stress at the other layers exceeds its tensile strength, a crack is introduced by setting the stress to zero in the corresponding direction. Thereafter, concrete at that point is modelled as elastic orthotropic material with directions fixed parallel and normal to the crack direction and, hence, the new local flexural stiffness (see graphical examples in Figure A-4 and A-5 in appendix A) is recomputed. At this stage, the mesh topology is assumed as a continuum as the smeared crack concept do not account for discontinuities in the topology of mesh. Then, the deflections are then obtained for the differential equations relating the external load with the deflection along the member domain using finite differences forms, corresponding to the new stiffness and curvature values. As the load increases further, more cracks develop and the flexural stiffness decreases. To predict the crack condition, the statement (if...then), which is provided by VBA, is used to check whether the stress in the concrete reaches to its tensile strength. Once the tensile stress exceeds the tensile strength, the layer contribution to the stiffness is assumed zero according to the following expression:

$$\mathrm{IF}(\mathrm{curvature} * (x - y_i) * E_i <= f_t, (x - y_i)^2 * E_i * A_i, 0) \quad (4\text{-}19)$$

Where x is neutral axis, y_i layer axis, E_i modulus of elasticity of layer, f_t concrete tensile strength, and A_i area of layer.

At higher load level, the stress-strain relationships for compressive concrete and steel begin to enter the nonlinear range, thus, the material stiffness of such

elements are also reduced and hence the local material stiffness matrix becomes orthotropic. Accordingly, the moment-curvature relationship of the section becomes nonlinear. At each loading stage, the principal compressive strains are computed from curvature; and material secant stiffness (E_x and E_y) is then computed using steel and concrete models as shown in Figure 4-3 and Figure 4-7, respectively. A possible algorithm for such analysis is illustrated in Figure 4-14.

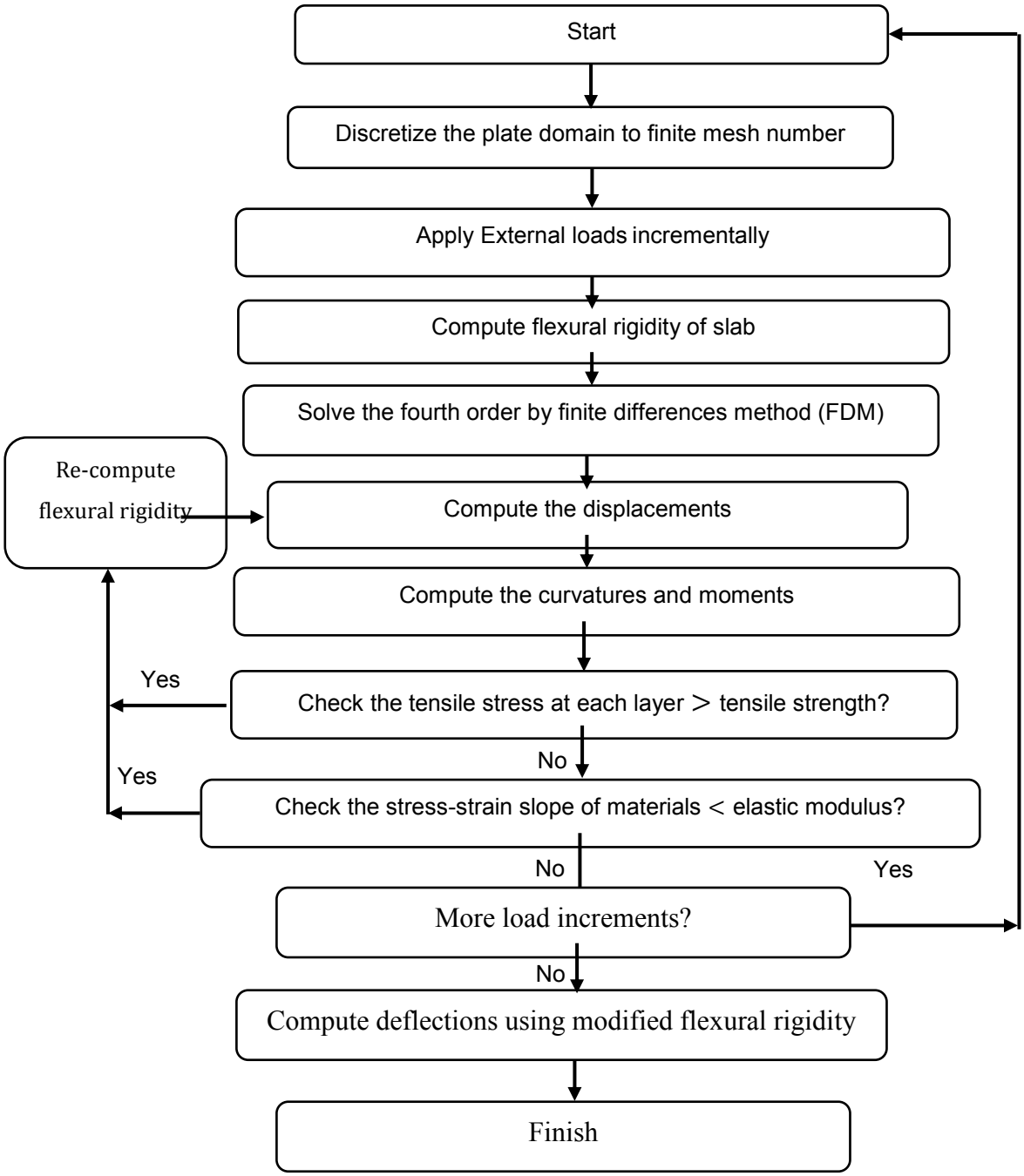

Figure 4-14. Algorithms of current numerical analysis (short-term)

4.9.2 Long-term Analysis.

As the properties of concrete, develop with time, the deformation of reinforced concrete (RC) member gradually increases several times greater than its instantaneous values, and certainly it can cause a redistribution of internal stresses. Usually, there are three basic phenomena that lead to an increase in movements with time. These are shrinkage, creep of the concrete, and loss of tension stiffening. Modelling of these phenomena in reinforced concrete members is not straightforward. The procedures for modelling creep and shrinkage actions in reinforced concrete sections are presented in section 4.5. In reality, it is not possible to distinguish whether the change in the flexural movements is affected mainly from the loss of tension stiffening or shrinkage or creep or is the result of creep variations (compressive and tensile). Therefore, attempts have been made in this research to incorporate these phenomena in a rational and reliable approach; then the outputs will be analysed and discussed with experimental data as given in the Chapter 5, to ascertain the parameter that governs the analysis.

The analysis of a flexural members with time involves the determination of long-term movements at different points. At time of loading t_0, the sectional properties are computed without effect of concrete creep and shrinkage properties. When the initial load increases up to desired sustained load level, the slab cracks at several sections. Therefore, the initial effective flexural stiffness and curvature are computed. At age t, the shrinkage and creep of concrete have taken place, leading to a change in the curvature and neutral axis position depending on the restraint ratio, and this may result in additional movements with time. The most important factor in the analysis of concrete structures with time is time discretization. To trace the behaviour of reinforced concrete structures, the time domain needs to be discretized into several time step. An effective time discretization should introduce a nearly constant change in displacement. In 1979, (Gilbert, 1979), suggested to discretize the time on a creep-time curve such that the same magnitude of creep strain occurs in each time step. To minimize the error during the early stages after loading when the development of creep and shrinkage strains are noticeable, the suitable time discretization is required. In this research, the time discretization is assumed to be constant at each 5 days

interval for both creep and shrinkage-time curves. This time interval would be accepted, particularly for creep and shrinkage strains predicted by using notional size member. Once the creep and shrinkage strains are calculated, their effects added to the initial strains with respect to the restraint ratio; then the long-term movements are obtained depending on the new flexural stiffness. Once the updated flexural stiffness is computed, a solution is then obtained for the fourth order differential equation relating the external load to the deflection by using finite differences form along the slab domain. Due to the ageing nature of concrete, the rate of deformation of concrete under a sustained load is no longer increases as in effective modulus method (EMM). In many cases, the flexural compressive stress varying with time and hence the strain rate is no longer increases as the same rate of constant stress. In this research, the creep superposition is employed to trace the long-term behaviour of reinforced concrete slab reliably. The ageing coefficient factor is assumed constant through 90 days. Moreover, the reduction in concrete compressive stress is also computed with respect to new neutral axis position. The complete procedure is illustrated in the algorithm provided in Figure 4-15.

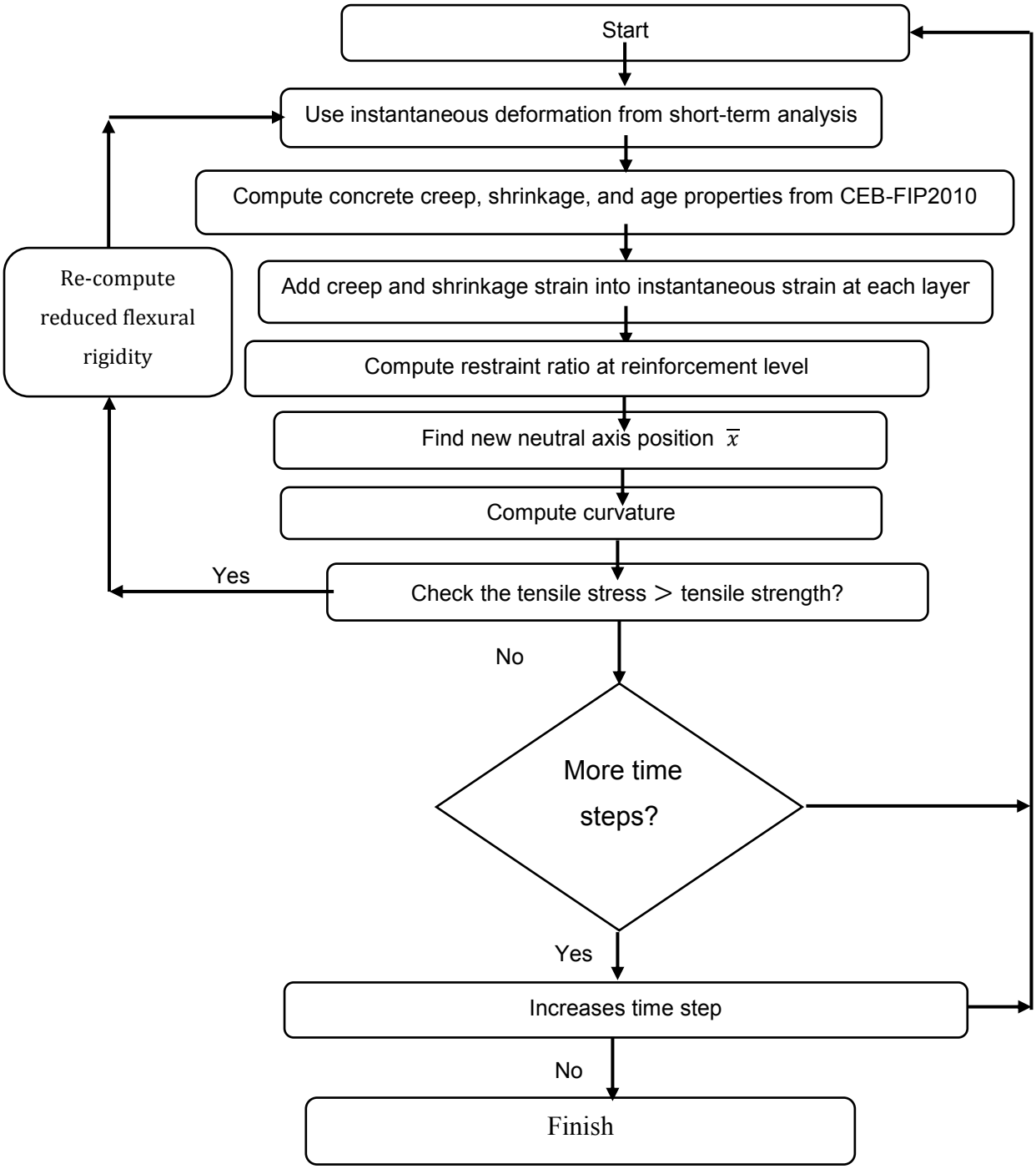

Figure 4-15. Computation algorithms for current numerical analysis (long-term)

Chapter 5 Results and discussion

5.1 Introduction

Experimental investigations alone will not sufficiently distinguish the influence of relevant parameter on the long-term behaviour. Therefore, a numerical nonlinear layered cross-sectional analysis procedure described in Chapter 4 has been used to analyse the slabs tested experimentally and the results are presented in this Chapter. The slabs tested in Chapter 3 are modelled first. The numerical results are then compared with the experimental data in order to verify the proposed analysis procedure for worst design situations. The models proposed by CEB-FIP 2010 and Eurocode 2 (BSI, 2004) for prediction of the mean average short-term and long-term movements have been adopted in this study to analyse the reinforced concrete slabs under both short-term and long-term loading.

This chapter provides two main objectives. The first objective is to examine the outcomes of the numerical analysis procedure. The second objective is to identify mainly the influence of tensile to compressive creep ratio on the long-term behaviour of slabs at potential design situations. The results drawn from these objectives have been critically assessed and discussed. In addition to these objectives, the results obtained from the code-based models have been presented and critically discussed. Later on, the parametric study was conducted based on the verified numerical capability to investigate the influence of opening sizes on the deflections under sustained loading.

5.2 Experimental Results of Load- Steel Strain

Among the available methods that are reliable to understand the behaviour of reinforced concrete slabs is experimental testing. Steel strain readings represent one of the best parameters that is reliable to identify the influence of opening on the slab behaviour. Thus, two reinforced concrete slabs with the same properties and dimensions were poured and tested until failure, and the data were measured from zero until collapse load. The first slab is solid S0 while the second slab S5 contains opening with size 150x250 mm next to the column. The strain gauges

were placed at six different locations, as given in Figure 3-3, to measure the strains in the reinforcement.

The steel strain readings for each test are plotted in Figure 5-1 (a) to Figure 5-1 (f). These results illustrate the effect of existence of the opening on the tensile steel strains. From the measured data, it can be clearly observed that the strains of reinforcements are small and behave linearly at a low load levels, and the slop of the lines are proportional to the external applied load, as a result of the uncracked section properties. Once the load increases further, it can be noted that the strain readings are no longer proportional to the external applied load. The changes in the slope of the load-strain curves of both slabs reflect the formation and extension of the internal and external cracks; these cracks then cause a drop in the average tensile stress carried by the concrete, which effectively increases the stresses in the tensile steel reinforcement.

From Figure 5-1 (a), (d), (e), and (f) It is obvious that the slope of the load-strain curves of the slab containing opening S5 are lower than the solid slab S0, except for Figure 5-1 (b) and Figure 5-1 (c). The difference in the behaviour is mainly attributed to the existence of the opening in the slab, where the overall slab stiffness is several times lower than the solid slab, and hence a higher curvatures and stresses in the slab containing opening would be expected to occur, specifically in the high bending moment zones, which concentrate around the opening. Thus, more cracks form in these high stress zones. In such a case, it can be concluded that the average tensile stress of the concrete in the slab containing opening is less than the average tensile stresses in the solid slab.

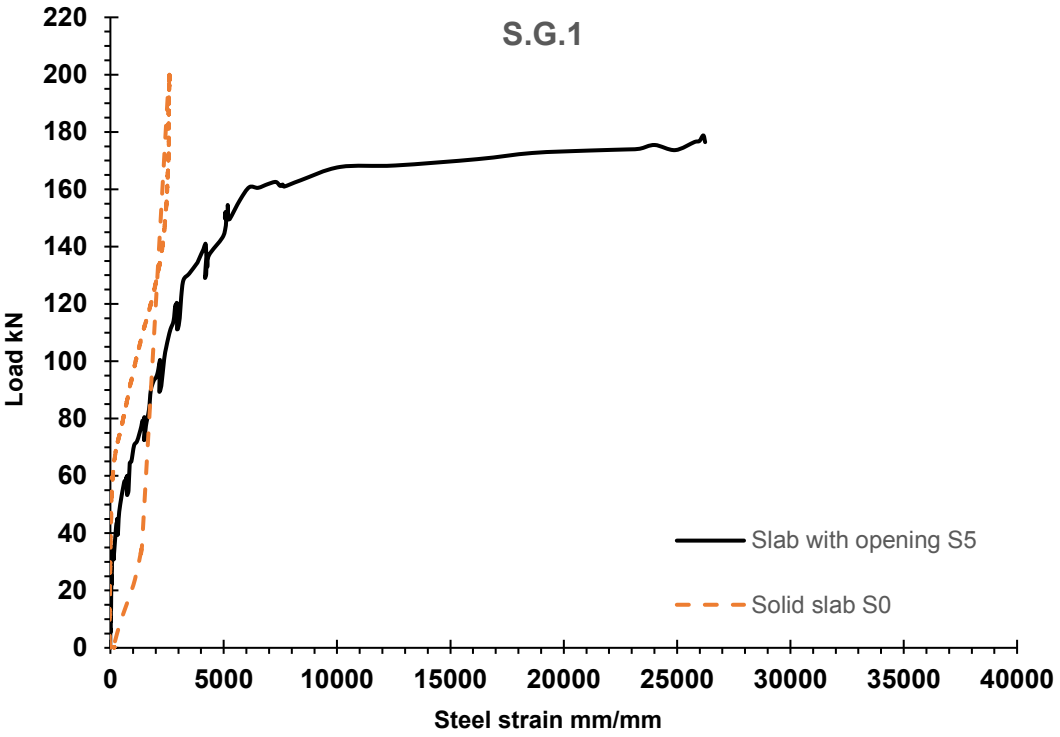
S.G.1
Load kN
Steel strain mm/mm
Slab with opening S5
Solid slab S0

(a)

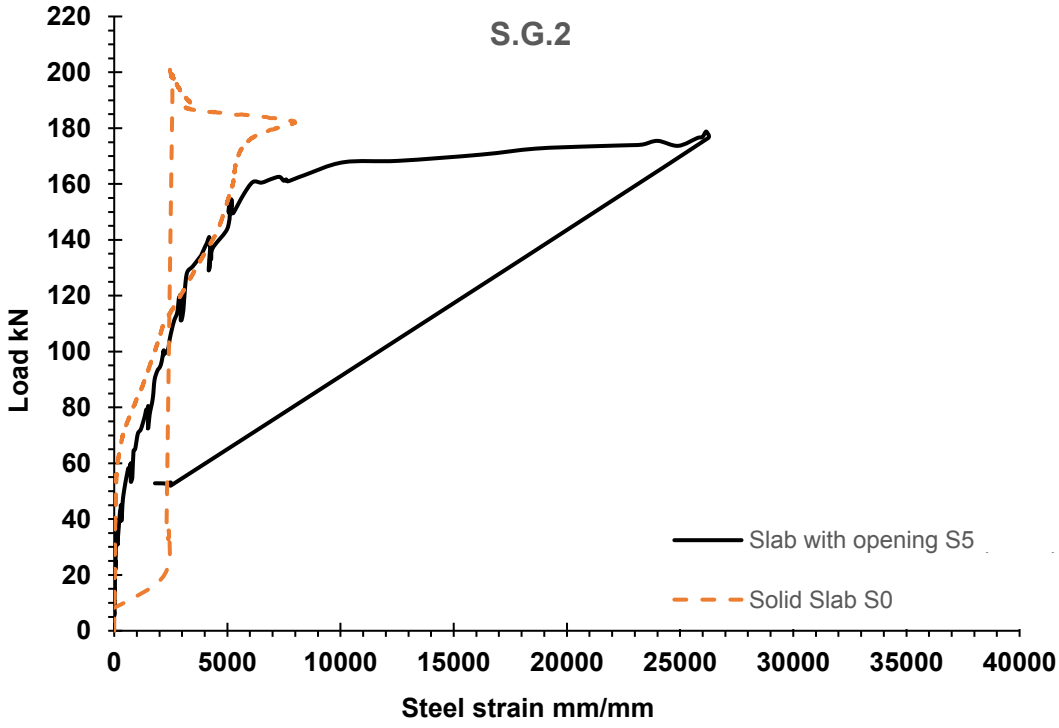
S.G.2
Load kN
Steel strain mm/mm
Slab with opening S5
Solid Slab S0

(b)

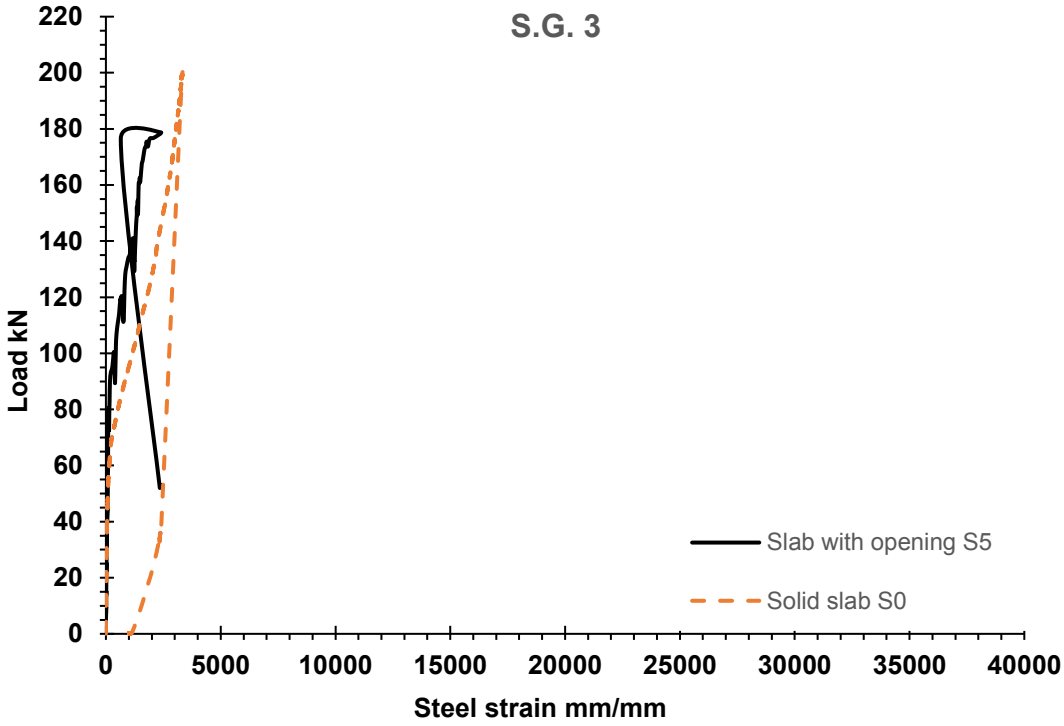
S.G. 3
Load kN
Steel strain mm/mm
Slab with opening S5
Solid slab S0

(c)

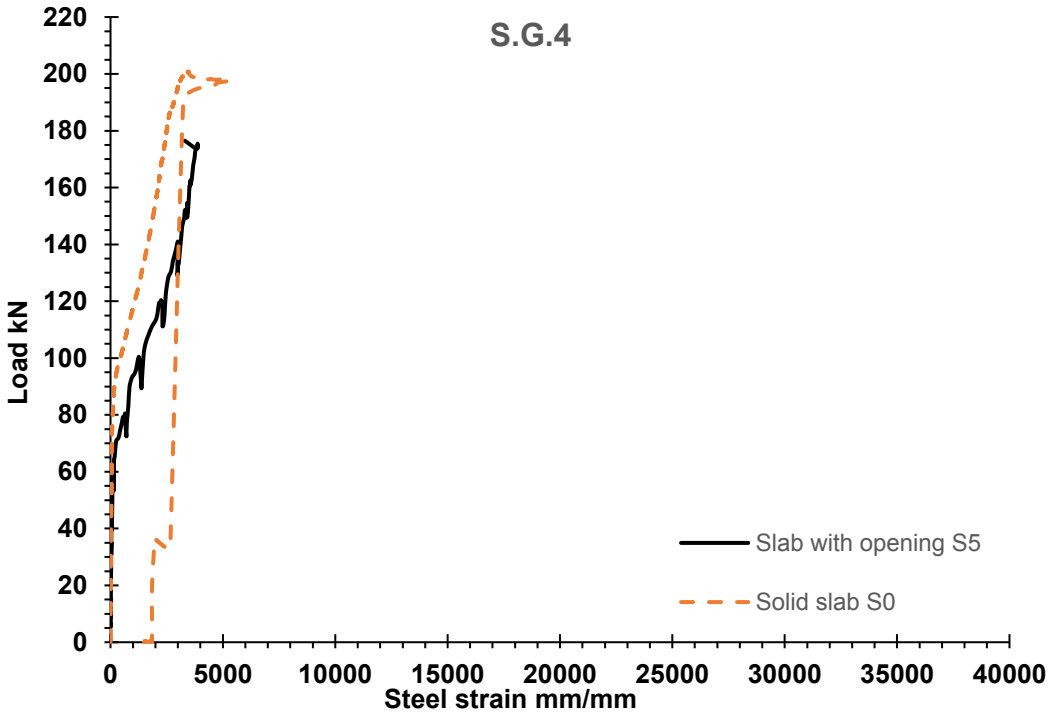
S.G.4
Load kN
Steel strain mm/mm
Slab with opening S5
Solid slab S0

(d)

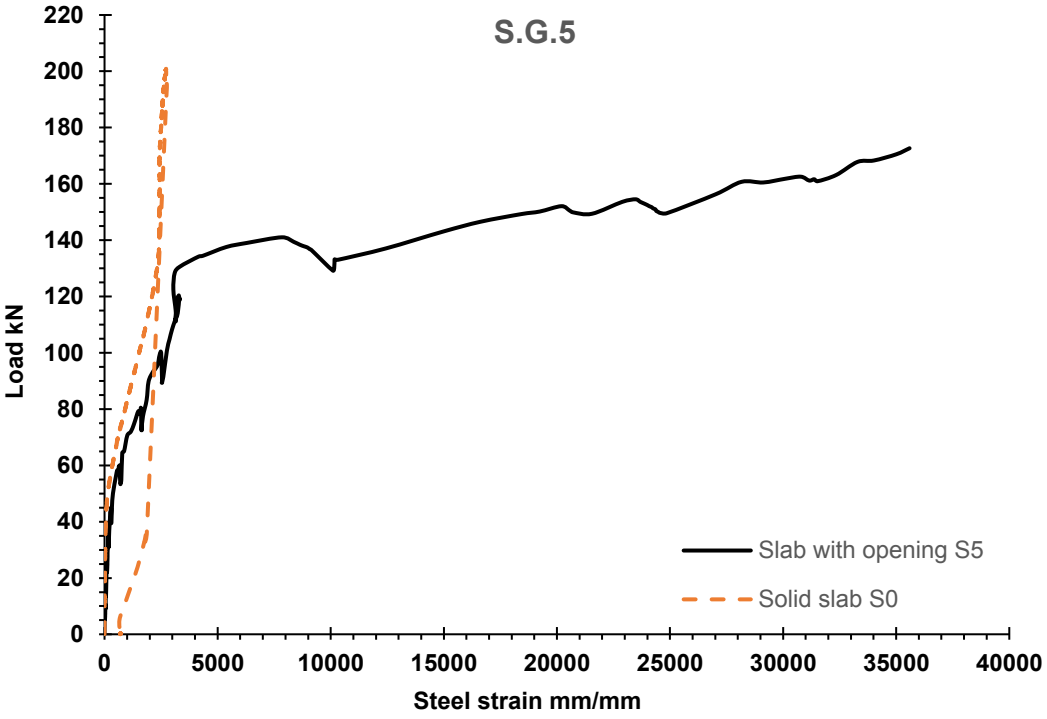

(e)

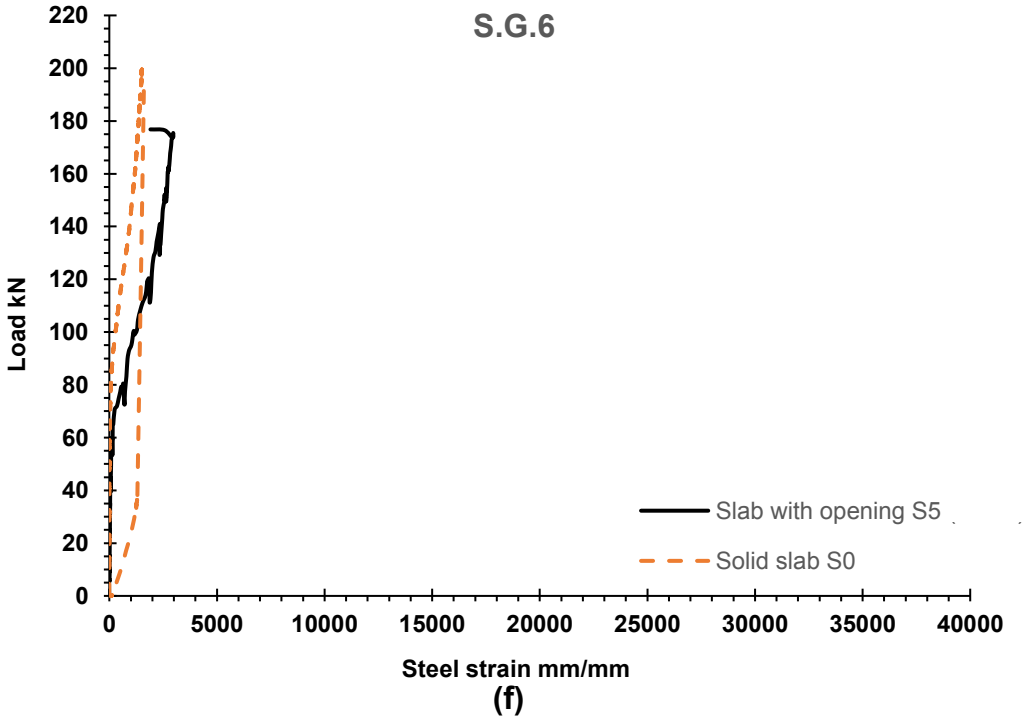

(f)

Figure 5-1. Measured tensile steel strains for slabs with and without opening

5.3 Convergence Analysis

As explained earlier, the most important step in the numerical analysis procedure is the convergence analysis. It is well known that that mesh sensitivity analysis should be performed by starting from coarse mesh and then monitoring the convergence of one of the variables until a suitable mesh size is reached. In this section, convergence analysis is presented to optimize the mesh size and numerical model reliability with respect to the load-elastic deflection relationship for solid slab model and for slab with opening 400x400 mm, to obtain more accuracy. As explained earlier in section 4.7, when higher order derivatives and a large number of mesh points are involved, the use of an iterative approach is recommended.

Visual basic for applications gives an option to solve the equations with a maximum number of iterations. Thus, in this study, the maximum iteration number is used with maximum differences 0.00001. The solution will converge when there is no change in the deflection. In this study, however, the analysis is terminated when the load is reached the failure load. Square element type is selected, and different mesh sizes of 25 mm, 50 mm, 75 mm and 100 mm were tested, with all other parameters kept constant. From observations on Figure 5-2 (a), it can be seen that the mesh sizes have slight impact on the deflection optimization for solid slab. However, the results show that the difference is clear for slab with opening when the mesh size has been changed from 100 mm to 25 mm as shown in Figure 5-2(b). It can be noticed, although, that there is no change in the results when the mesh size refined from 50 mm to 25 mm. Thus, it was decided to select 50mm mesh size for all slab models to minimize the large number of simultaneous equations.

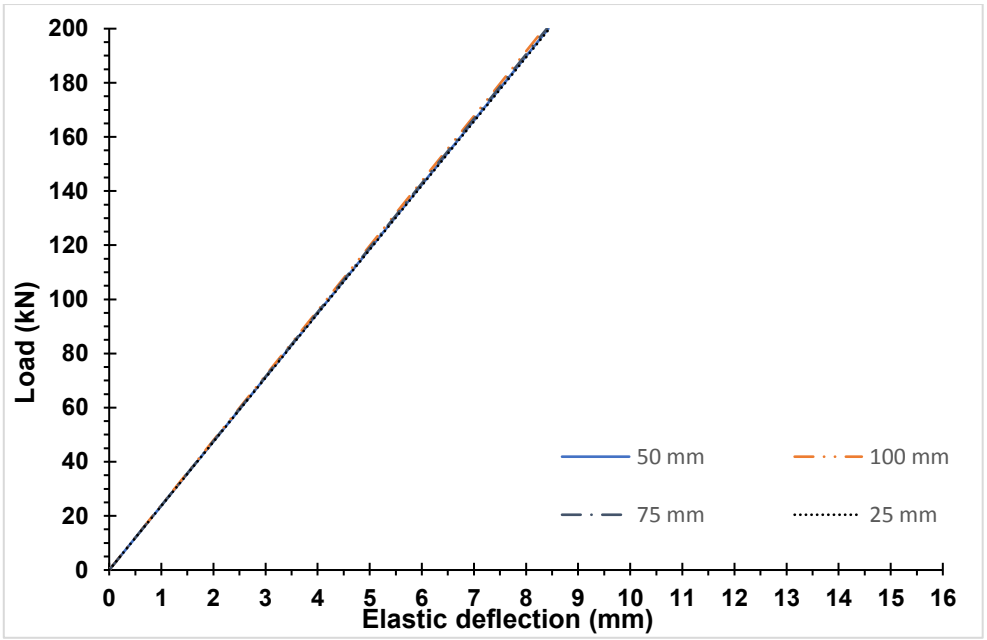

(a)

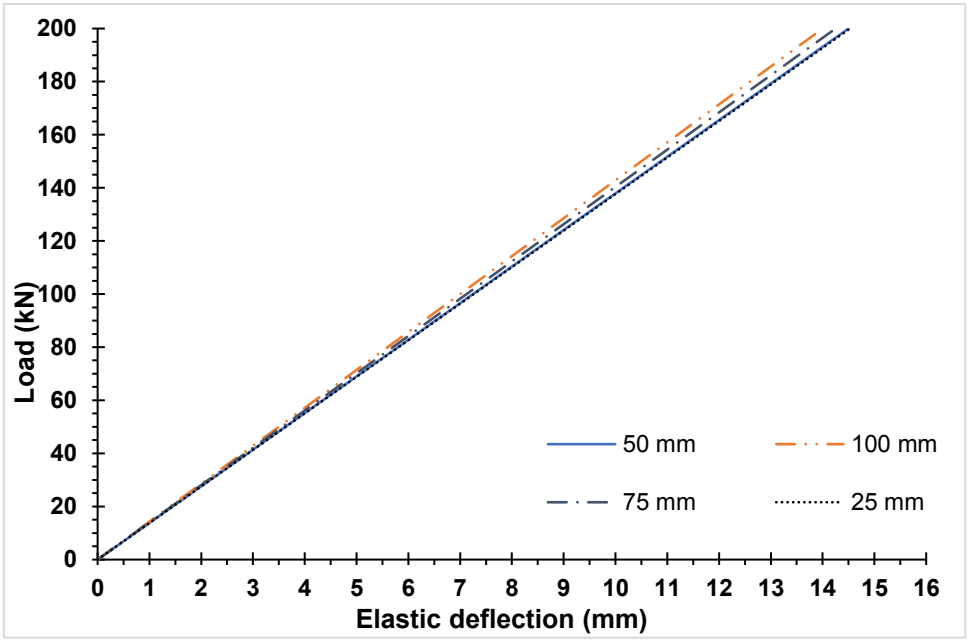

(b)

Figure 5-2. Load-deflection relationship for different mesh sizes of slab with opening 400x400

5.4 Verification of Short-term Deformation Results with the Proposed Procedure

Cracking and material nonlinearities are the main sources that influence the load-deformation response. As stated earlier, the first step in the prediction of long-term movements in partially cracked members is usually to perform the instantaneous nonlinear analysis. In this section, the analysis of the reinforced concrete slabs based on the proposed procedure will be compared with the

experimental results in terms of load-deflections and load- steel strains curves. Two reinforced concrete slabs with the same properties and dimensions were poured and tested until failure as shown in Figure 3-1, and the data were measured and collected from zero until collapse load. The first slab is solid while the second slab contains opening with size 150x250 mm next to the column. In the sections 5.4 and 5.6 ,the detailed behaviour of each slab will be presented individually first; this will be followed by a comparison between the experimental and numerical results.

5.4.1 Solid Slab S0

Deflections were recorded using LVDT at three different locations. In addition, tensile steel strains were measured at six different locations. The measured data were compared with the numerical findings. The following subsections display the comparisons of the results.

5.4.1.1 Load-deflection Results.

From the measured data shown in Figure 5-3 (a), 5-4 (b), and 5-4 (c) it can be noted that the response of the slab behaves linearly, and the slop of the load-deflection plot is proportional to the uncracked section properties. The load-deflection curves are linear up to 20%, 22%, and 25% of the ultimate load for LVDT1, LVDT2 and LVDT3, respectively. The recorded first cracking load was about 20% of the ultimate load, when the allowable extreme fibre tensile stress of the concrete is exceeded. As the load increases further, it is obvious that the measured deflections are no longer proportional to the external applied load, with some changes in the slope that reflect the successive cracking of the concrete. Thereafter, the sudden change in the local stiffness due to cracking leads to change in the response of the slab dramatically. This behaviour is obviously in line with the observations provided in the literature with respect to the formation of cracks under increasing loading and their effects on the bending stiffness and curvatures. As the load approaches the ultimate load, the load-deflection curves show high nonlinearity due to the severe cracking of concrete as well as the nonlinearity of stress-strain curves of materials, specifically in the high bending moment zones.

From a comparison between the numerical and experimental results of the load-deflection curves, it can be seen that the computed deflections show good estimation at each load level as shown in Figure 5-3 (b) and 5-3 (c), except for Figure 5-3 (a) where the computed deflections give good results from onset of loading up to 60% of the ultimate load. Beyond this value, the experimental response is stiffer than the numerical load-deflection response, which can be attributed to the perfect bond assumption where it does not allow for the modelling of realistic bond stress loss after cracking. This will lead therefore to overestimate the theoretical cracking in concrete and thereby further loss of the beneficial tensile concrete to the member stiffness. This confirms the conclusion reported in the literature by (Bischoff,2001). He concluded that the amount of tension transferred to the concrete between cracks depends to a large extent on the bond between steel and concrete. The second reason that comes into play is that the adoption of the smeared crack model, which causes a significant drop in the overall stiffness of the model, particularly in the high bending regions, i.e. in the centre of the slab. This in line with the conclusion reported by (Bhatti et a.,1996).

.

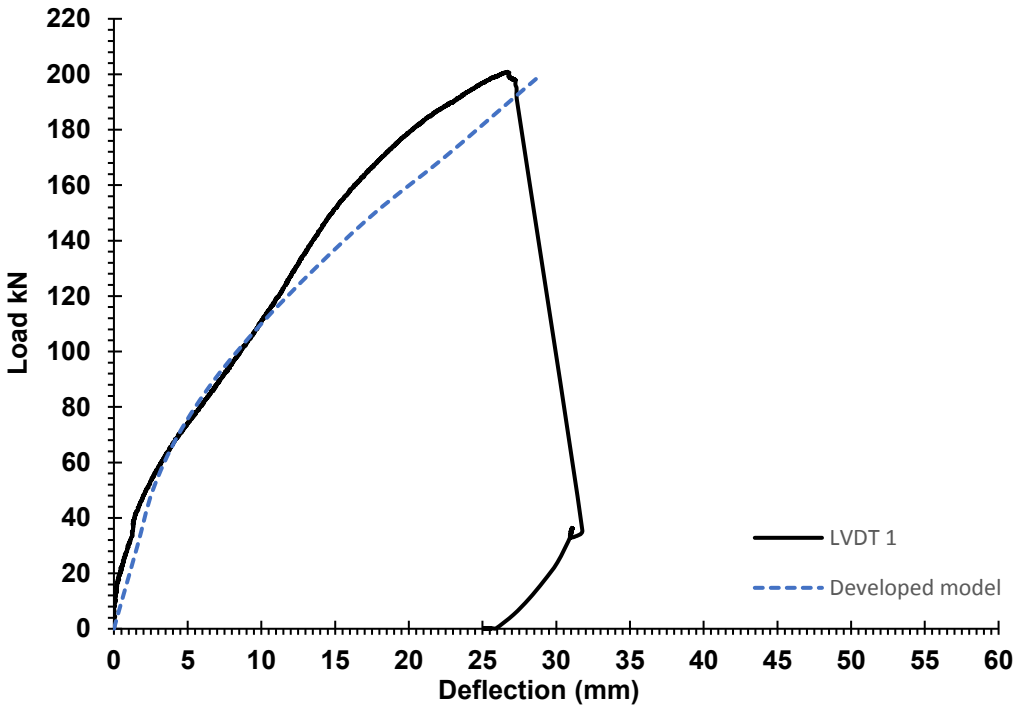

(a)

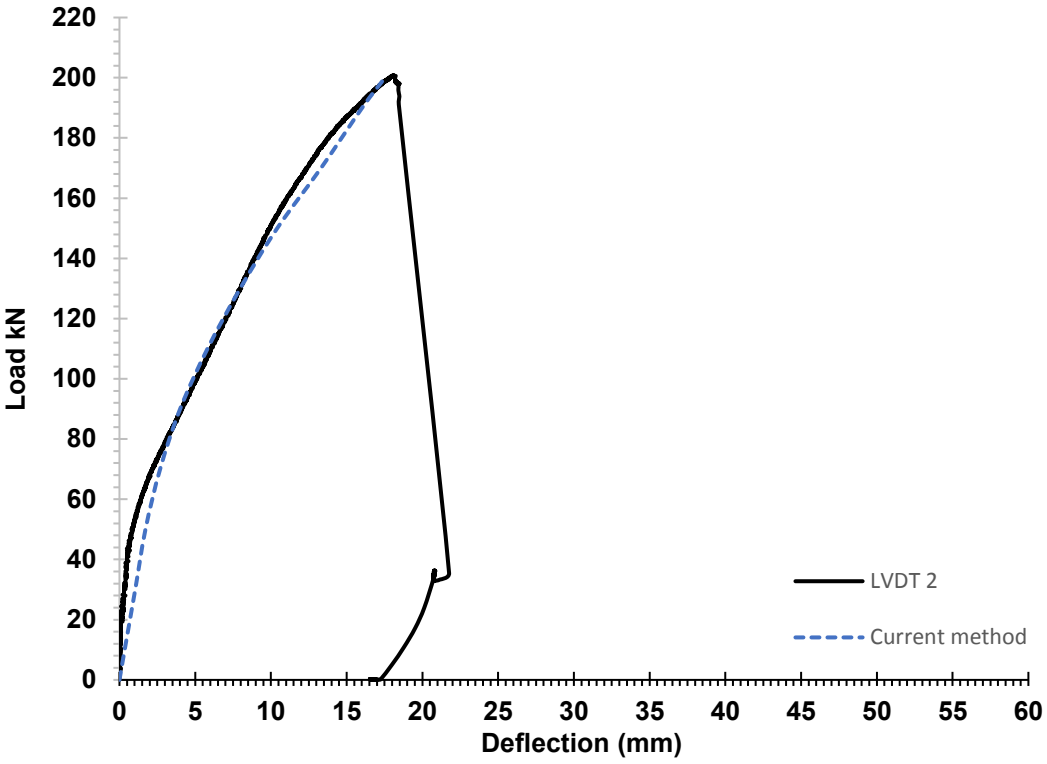

(b)

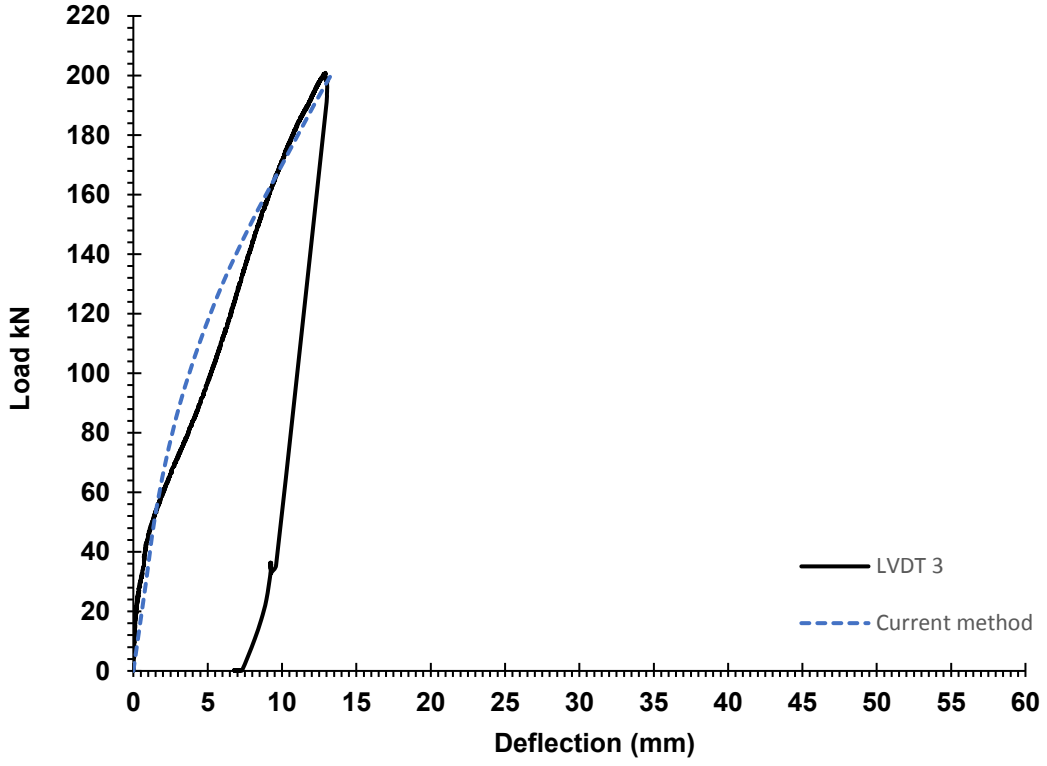

(c)

Figure 5-3. Comparison of measured and predicted deflections of solid slab S0

5.4.1.2 Load- Steel Strain Results

From the recorded data shown in Figure 5-4 (a) to 5-4 (f), it is clear that the load-strain relationships are linear up to 22.5%, 27.5%, 27.5%, 40%, 22.5%, and 42.5% of the ultimate load for S.G.1, S.G.2, S.G.3, S.G.4, S.G.5, and S.G.6, respectively. Thereafter, there are noticeable increases in the steel strains under increasing load and the strains are then no longer proportional to the applied load. This behaviour is attributed to the loss of bond stresses post cracking, which leads to increase the steel stresses and decrease the average tensile stresses carried by concrete as more cracks form. Overall, when the load reaches the ultimate load, it can be seen that the load increased but the strains of the steel reinforcement remained constant, which indicates the progressive damage of the bond between the concrete and reinforcing steel as well as the progressive of punching shear cracking.

From the test data, it is clear that the steel strain readings of S.G.1 and S.G. 5, i.e. placed on the reinforcement in both directions at the mid of the slab, have the same readings, which reveals that the distribution of bond stresses is equal in both directions. Furthermore, it is worth noting that the steel experiences a jump in strains, i.e. beyond 22.5% of the ultimate load for S.G.1 and S.G.5, while the first cracking load for this slab was recorded at about 20% of the ultimate load. This indicates that the first crack formed at the extreme bottom face, when the allowable extreme fibre tensile stress of the concrete is exceeded, then the crack propagated toward the reinforcing steel position. Hence, the tensile stresses of concrete below the neutral axis is gradually carried by the reinforcing steel, which indicates a direct relationship between the tensile stress drop after cracking and the steel stress development.

Figure 5-4 (a) to 5-4 (f) also display a comparison between the numerical and experimental load-steel strain curves. It is obvious that the average numerical results coincide well with the measured results up to 40% of the ultimate load. Beyond this level, it is clear that the computed strains are considerably lower than the experimental values with a small change in the slope of the load-strain curves, which can be attributed to the perfect bond assumption where the theoretical tensile steel stresses after cracking will be underestimated. This coincides with

the reported bond-slip behaviour as presented in section 2.9. This points out to the fact that the perfect bond assumption does not realistically model the gradual loss of bond stress after cracking at high service load levels; and this explains why there is no jump in the theoretical tensile steel strains.

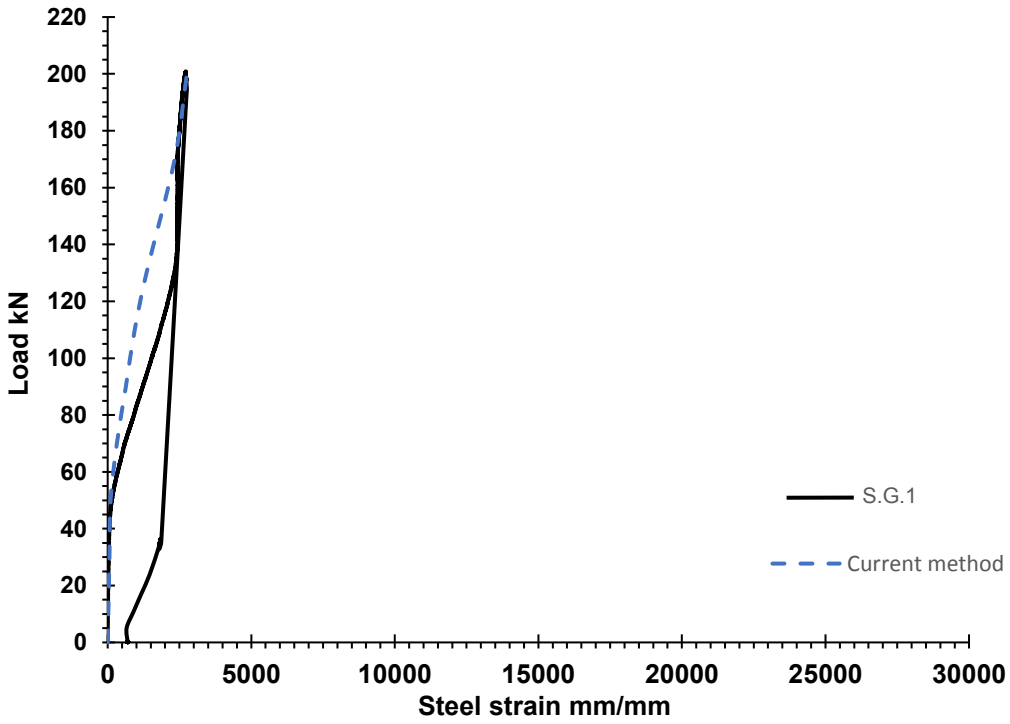

(a)

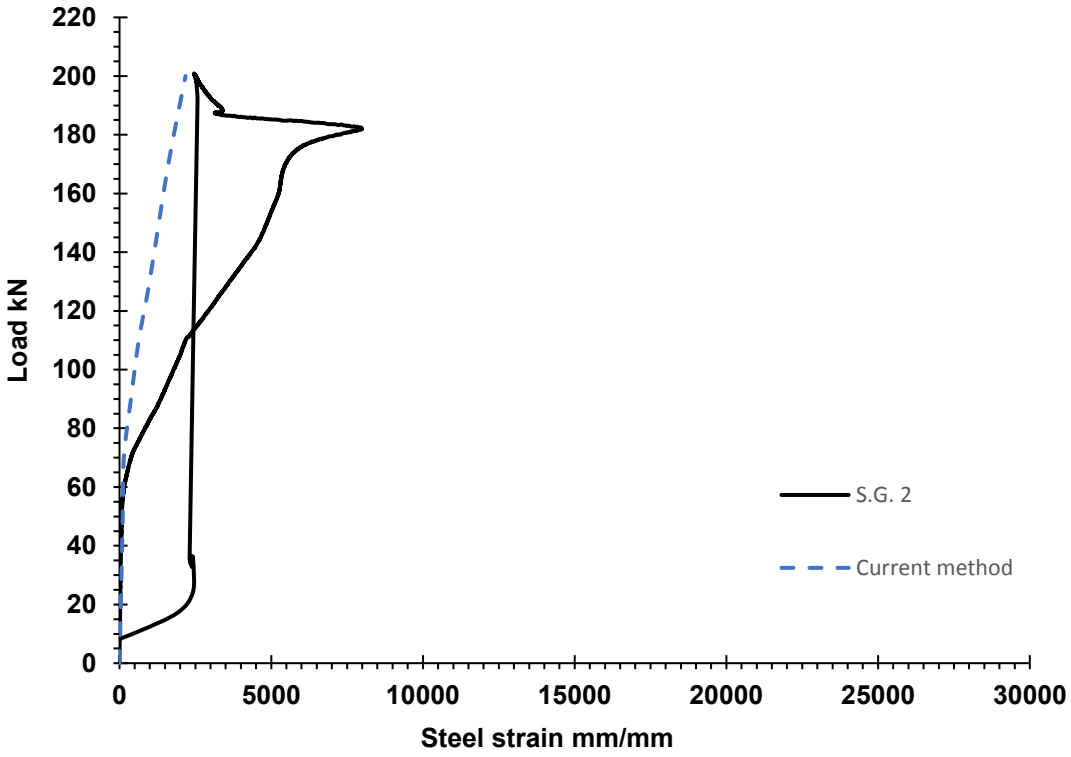

(b)

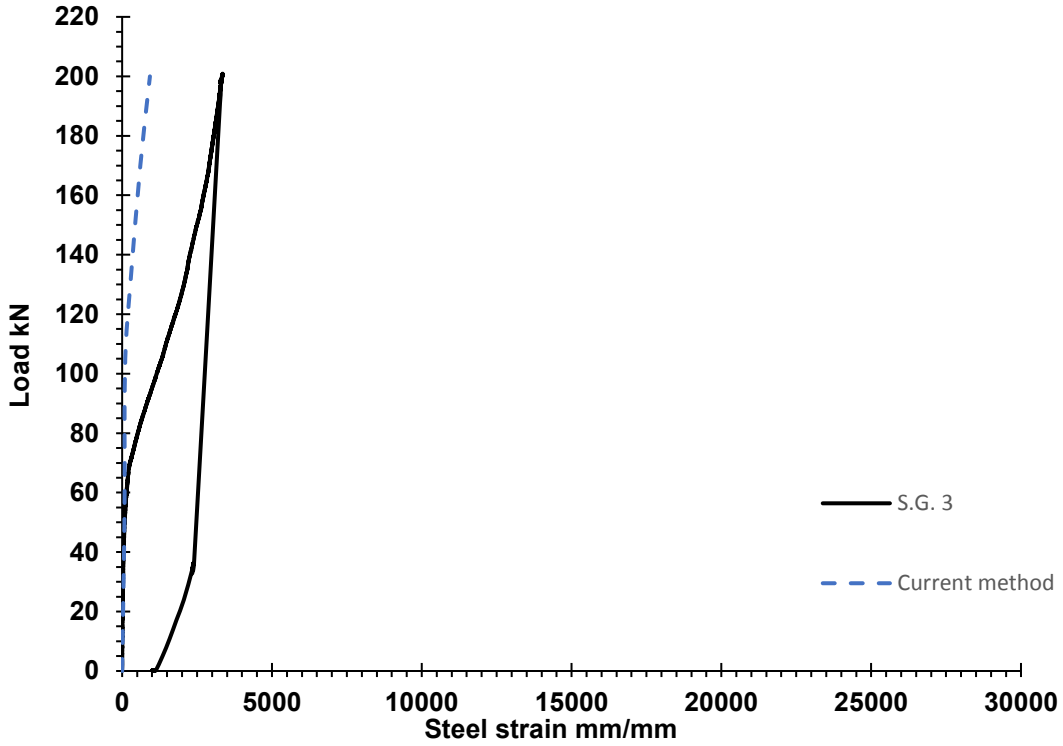
Load kN
220
200
180
160
140
120
100
80
60
40
20
0
0
5000
10000
15000
20000
25000
30000
Steel strain mm/mm
S.G. 3
Current method

(c)

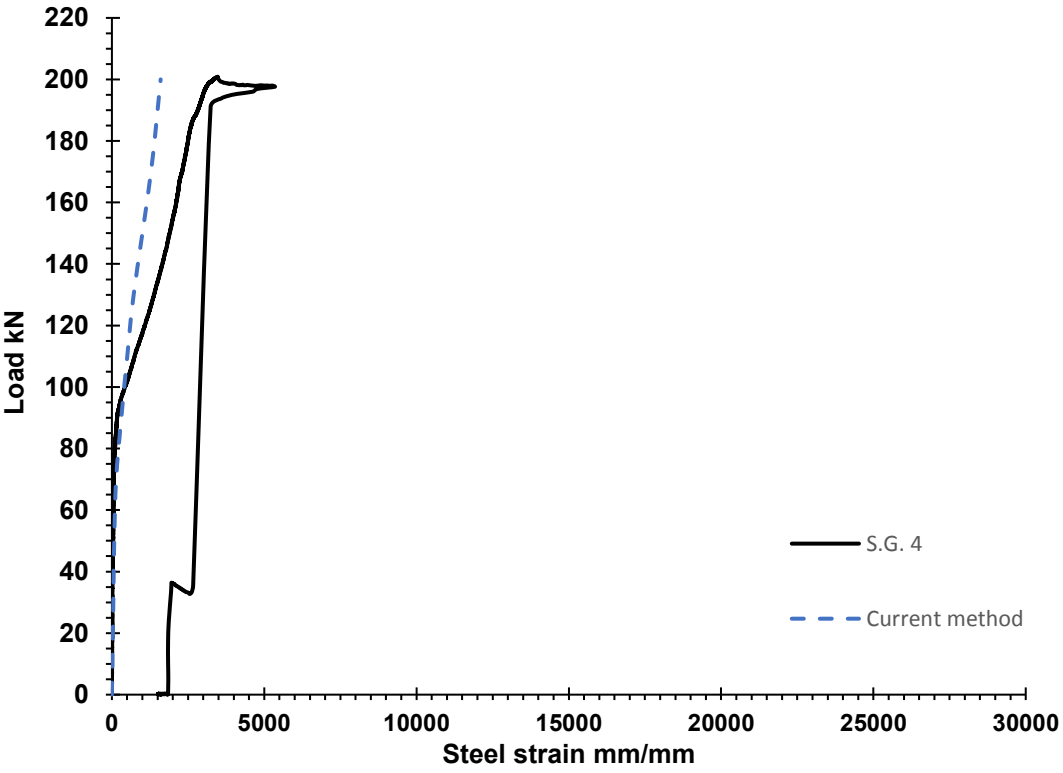
Load kN
220
200
180
160
140
120
100
80
60
40
20
0
0
5000
10000
15000
20000
25000
30000
Steel strain mm/mm
S.G. 4
Current method

(d)

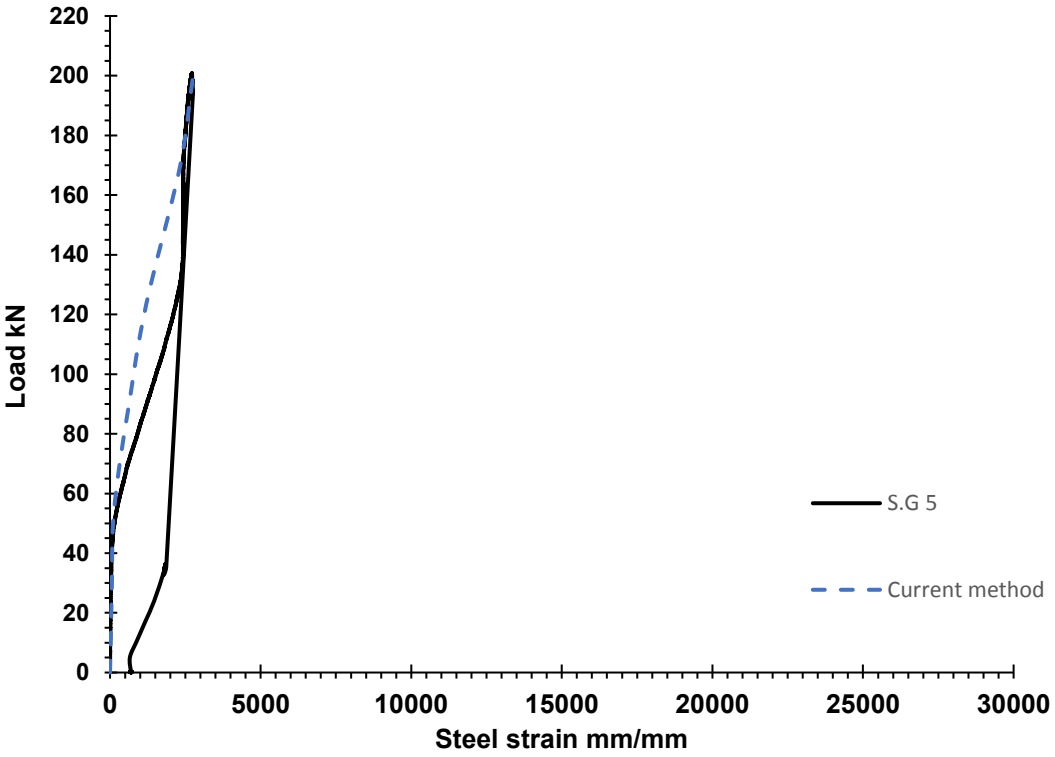

(e)

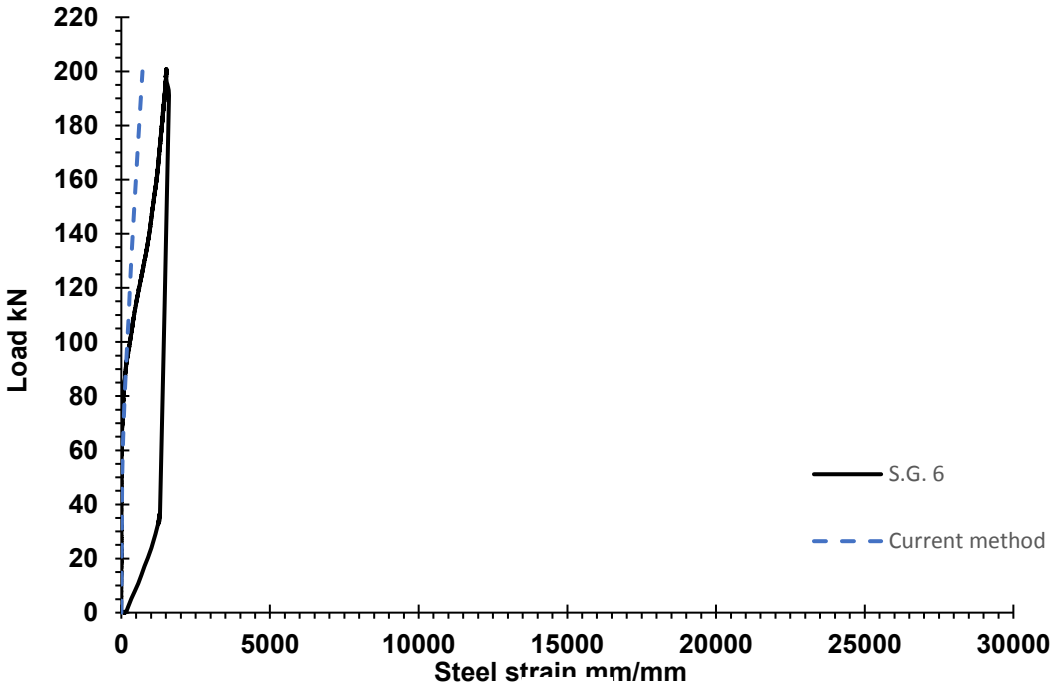

(f)

Figure 5-4. Comparison of measured and predicted steel strains of solid slab S0

5.4.2 Slab S5

For the slab S5, deflections were recorded using LVDT at six different locations and were compared with the numerical outcomes. In addition, tensile steel strains were measured at six different locations and the data were compared with numerical findings. The following subsections present the comparisons of the results of the proposed numerical procedure and the experimental data in terms of load-deflection and load-steel strain curves.

5.4.2.1 Load-deflection Result

From the test readings shown in Figure 5-5 (a) to 5-5 (f) it can be noted that the response of the slab behaves linearly at the initial load levels due to high stiffness pre-cracking, and the slop of the load-deflection plot is high and proportional to the uncracked section properties. As shown in Figure 5-5 (a) to 5-5 (f), the load-deflection curves are linear up to 11.17%, 12.5%, 13.48%,14%,11.17% and 13.9% of the ultimate load for LVDT1, LVDT2, LVDT3, LVDT4, LVDT5 and LVDT6, respectively. The recorded first cracking load was about 11% of the ultimate load, when the extreme fibre tensile stress of the concrete at the section with high bending moment exceeds its tensile strength. Under further loading, it is obvious that the measured deflections are no longer proportional to the external applied load, and the slope of the load-deflection curves decreased. The changes in the slope of the load-deflection curves reflect the growth and development of the cracks in the slab. Consequently, the sudden change in the local stiffness due to cracking alters the response of the slab dramatically. However, the active concrete still continuous to carry tensile stresses between the cracks due to the bond stresses between the reinforcing steel and the surrounding concrete. Furthermore, the active concrete below the neutral axis position, for partially cracked sections, also contributes to carry some tensile stresses. As the load approaches the ultimate load, the load-deflection curves show some nonlinearity due to the severe cracking of concrete as well as the nonlinearity of material relationships. This agrees with the reported post cracking behaviour of the slab under increasing load as presented in Chapter 2.

A comparison between the load-deflection curves of the slab was tested experimentally and the numerical analysis results is presented in Figure 5-5 (a) to 5-5 (f) below. As in the previously modelled slabs, it is obvious that the computed load-deflection curves based on theoretical assumptions are initially linear and identical well with the measured results in the elastic range up to 47.5%, 58.6%, 58.6%, 61.45%, 44.7% and 55.86% of the ultimate load for LVDT1, LVDT2, LVDT3, LVDT4, LVDT5 and LVDT6, respectively. Thereafter, the response of experimental load-deflection curves is significantly stiffer than the response of numerical load-deflection curves. As previously stated, the difference in the response of experimental and numerical load-deflection curves is strongly attributed to the assumptions of the perfect bond and smeared cracking model. The adoption of these assumptions will lead therefore to overestimate the theoretical cracking in concrete and thereby further loss in the beneficial tensile concrete to the member stiffness, which causes a significant drop in the overall stiffness of the model, particularly in the high bending regions, i.e. in the centre of the slab and around the opening region. This evidently refers to the fact that the modelling of the slab behaviour is very complex, particularly when the opening exists, and the adoption of these assumptions leads to overestimate the theoretical deflections at high service load levels.

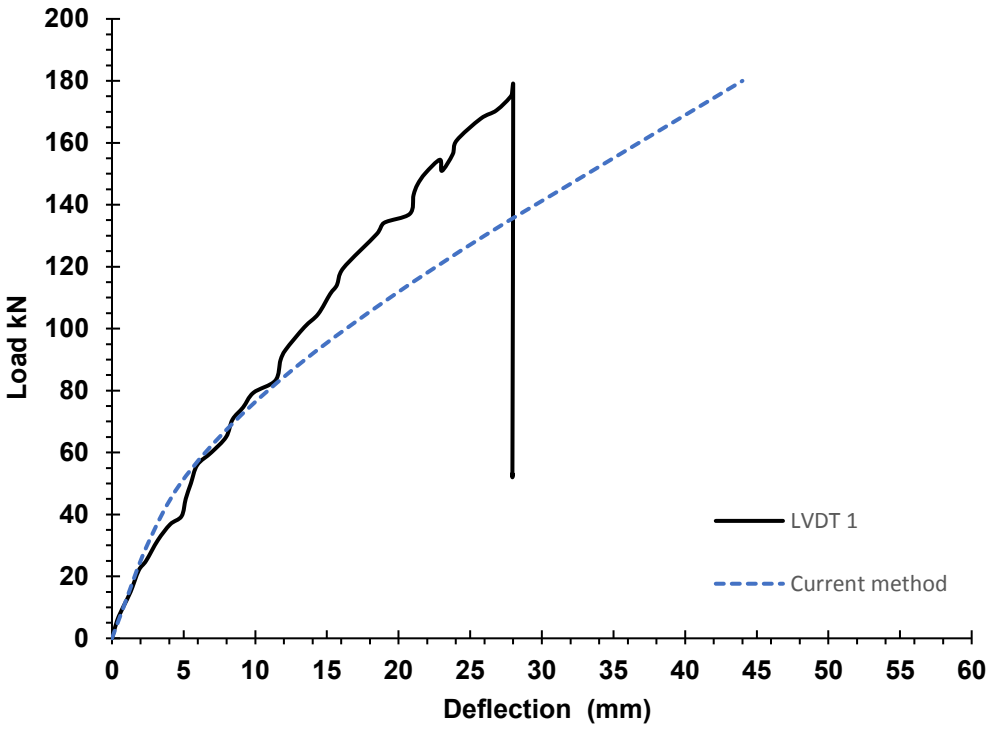

(a)

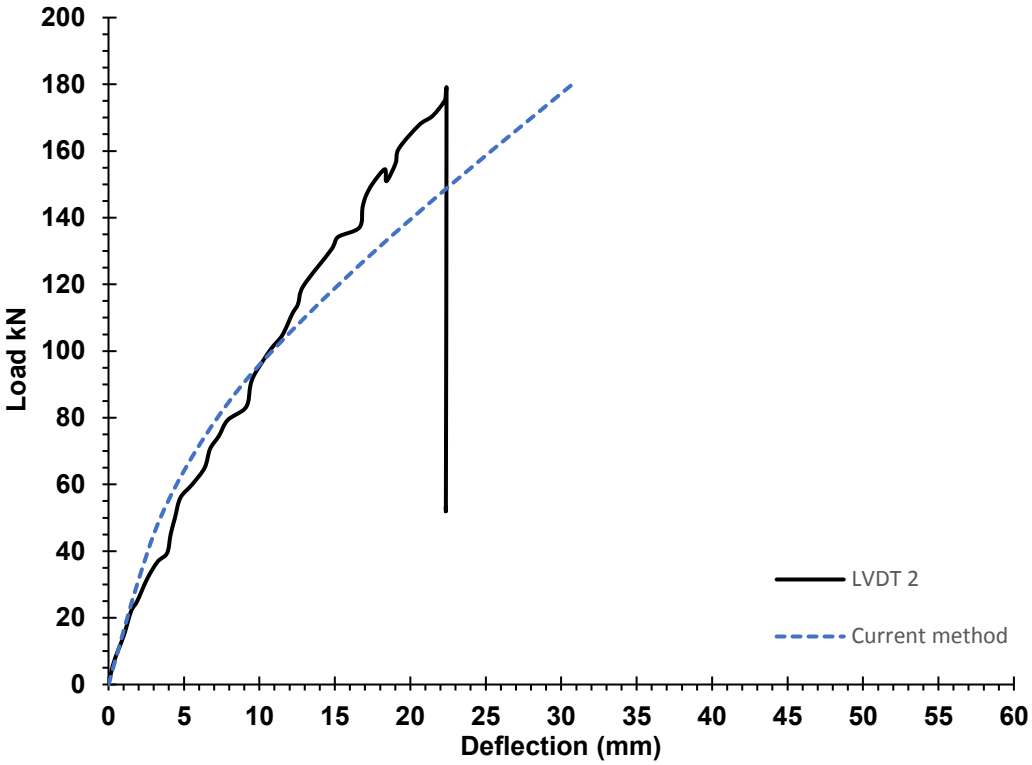
Load kN
Deflection (mm)
LVDT 2
Current method

(b)

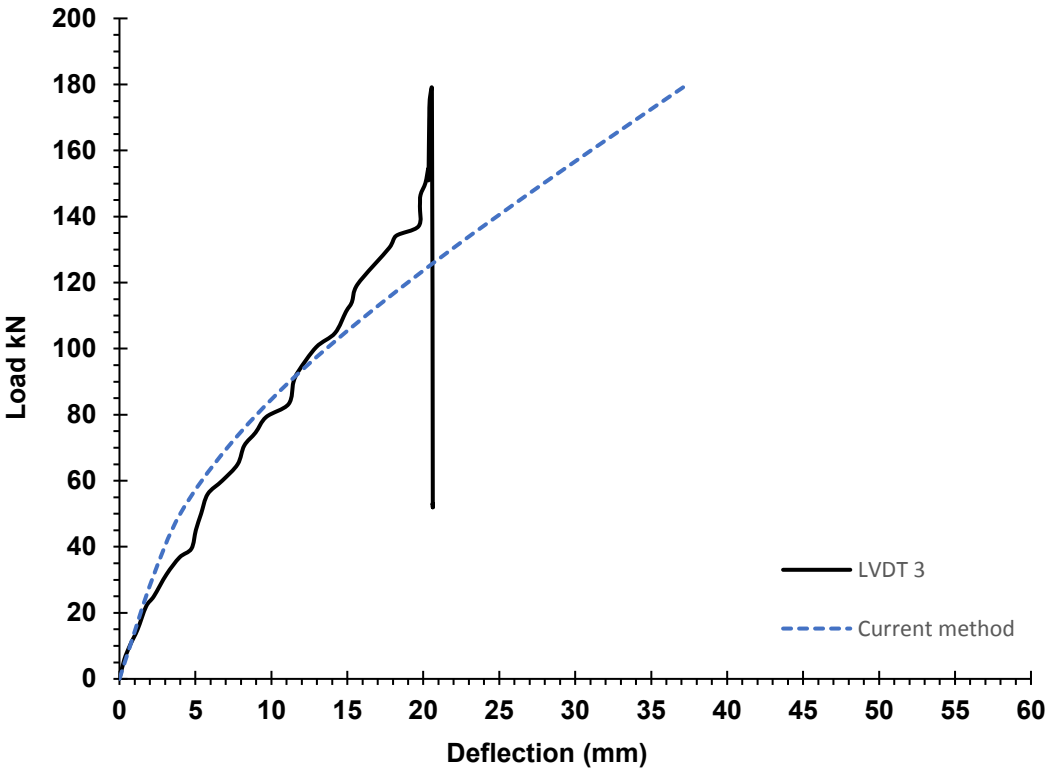
Load kN
Deflection (mm)
LVDT 3
Current method

(c)

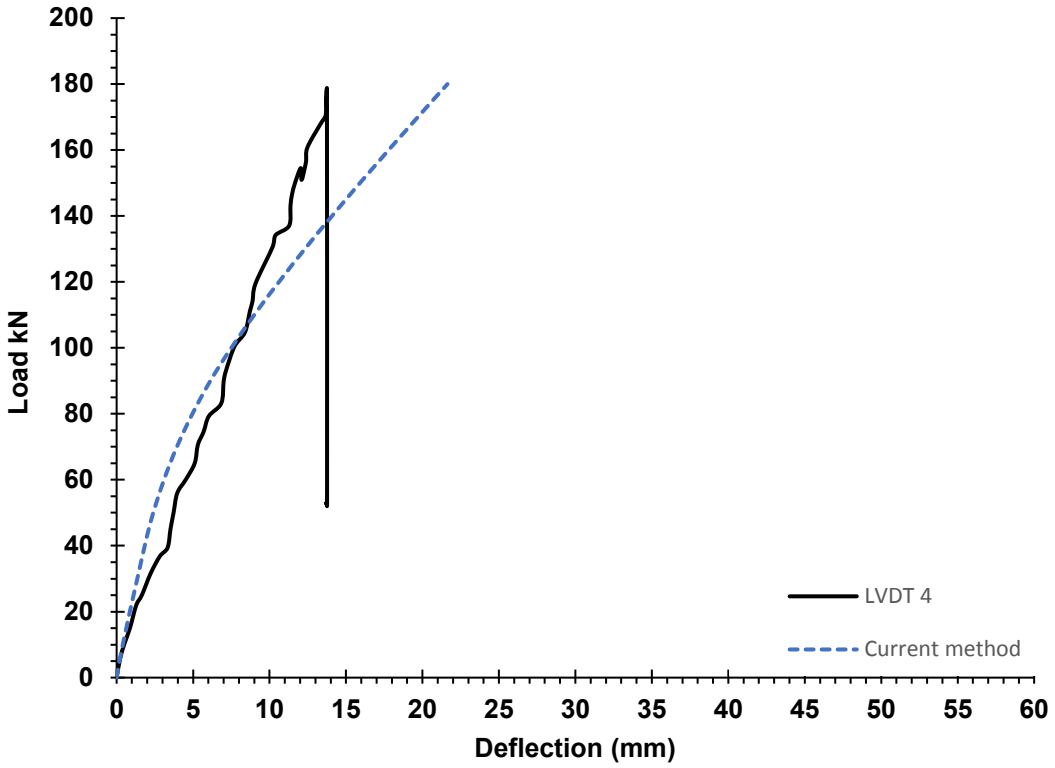
Load kN
Deflection (mm)
LVDT 4
Current method

(d)

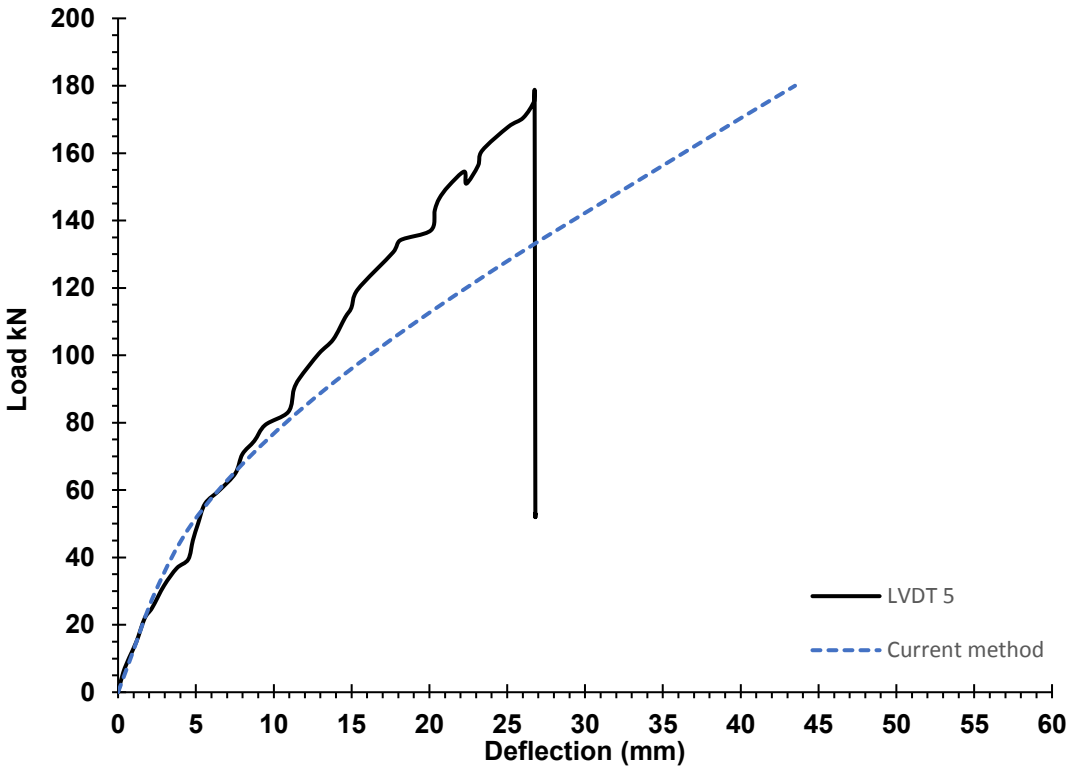
Load kN
Deflection (mm)
LVDT 5
Current method

(e)

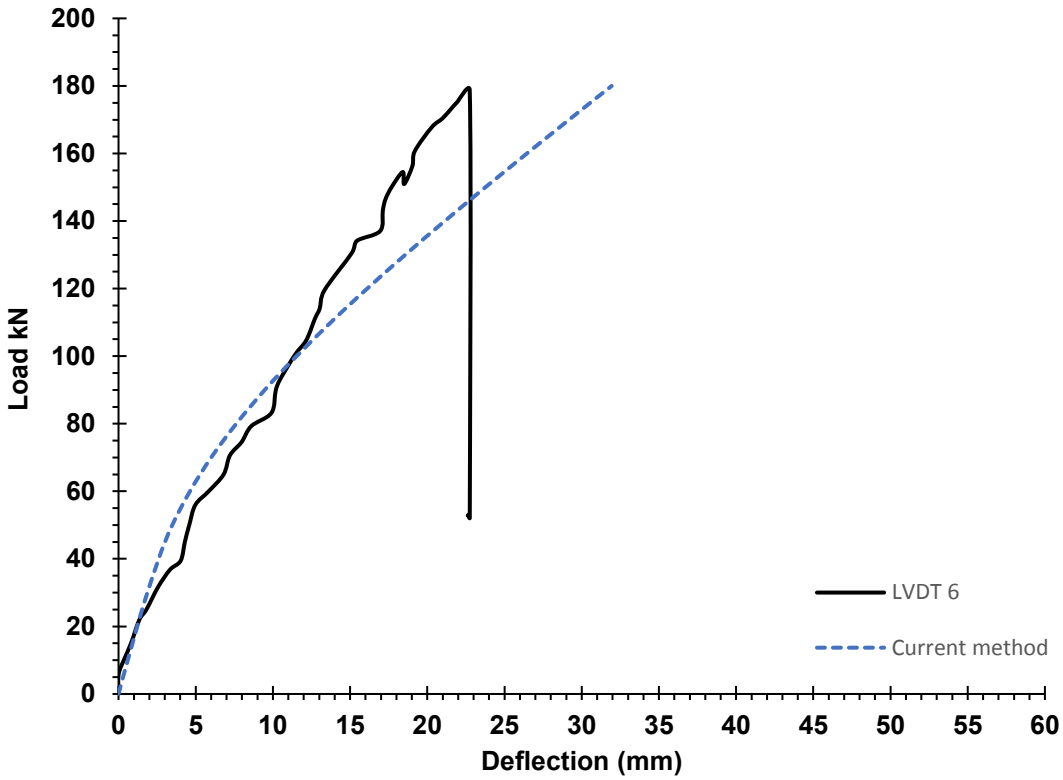

(f)

Figure 5-5: Comparison of measured and predicted deflections of slab S5.

5.4.2.2 Load- Steel Strain Results

Figure 5-6 (a) to 5-6 (b) show the experimentally recorded load-steel strain data where it can be seen that the strain readings are linear and proportional to the external applied load during the initial load stages up to 15.76%, 15.7%, 22.34%, 25.14%, 11.17, and 24.6% of the ultimate load for S.G.1, S.G.2, S.G.3, S.G.4, S.G.5, and S.G.6, respectively. As the load increases further, it is obvious that the steel experiences a jump in stress and then the load-strain relationships are no longer linearly, with a noticeable reduction in the slope of the curves that reflect the gradual loss of beneficial tensile stresses of the concrete after cracking. When the load approached the ultimate load, it can be noticed that the steel strains developed significantly with little change in the carried load, except for Figure 5-6 (c), 5-6 (d) and 5-6 (f), which indicates that the steel reinforcement reached the yielding stress and thereafter the strain increases at a relatively constant stress.

Figure 5-6 (a) to 5-6 (b) also compares the measured steel strains where recorded experimentally with the numerical results based on theoretical approaches. Overall, it is clear that the precision of the computed theoretical

strains is in good agreement with the strains measured experimentally during the elastic range up to 39.1% of the ultimate load. Beyond this level, it is seen that the numerical procedure underestimated the steel strains with a small change in the slope of the load-strain curves, which can be attributed to the perfect bond assumption where the theoretical tensile steel stresses after cracking will be underestimated. As it has been explained, this confirms that the perfect bond assumption does not realistically model the gradual loss of bond stress after cracking and it does not work well at high service load levels; and this explains why there is no jump in the theoretical tensile steel strains.

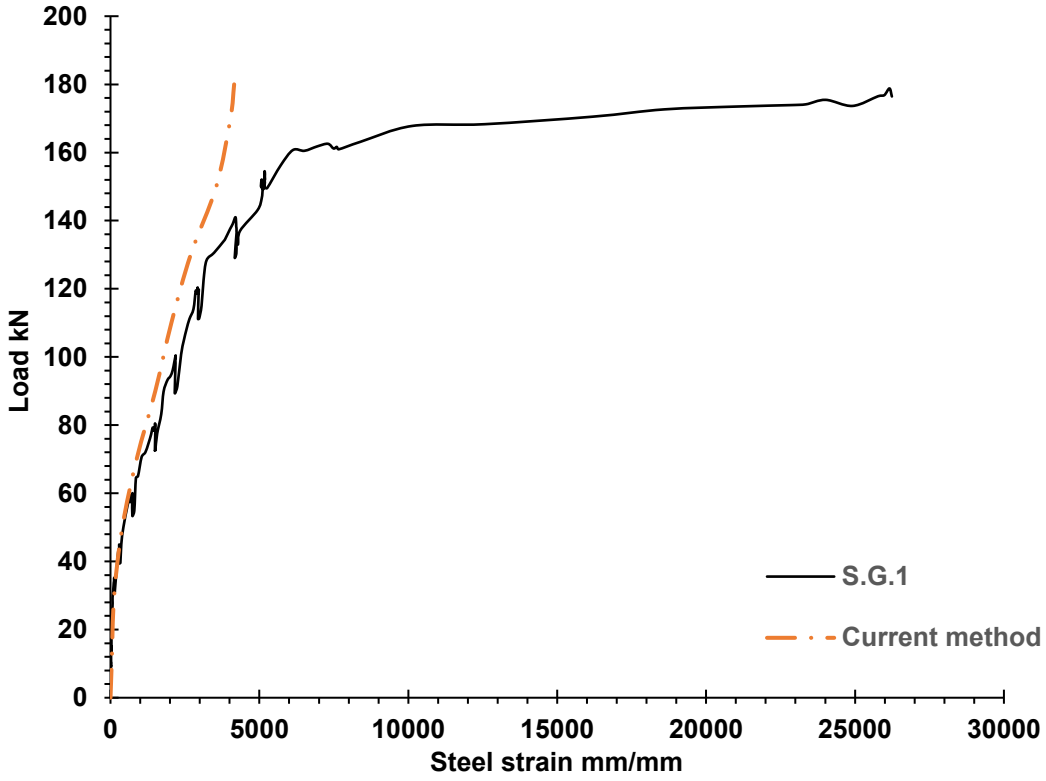

(a)

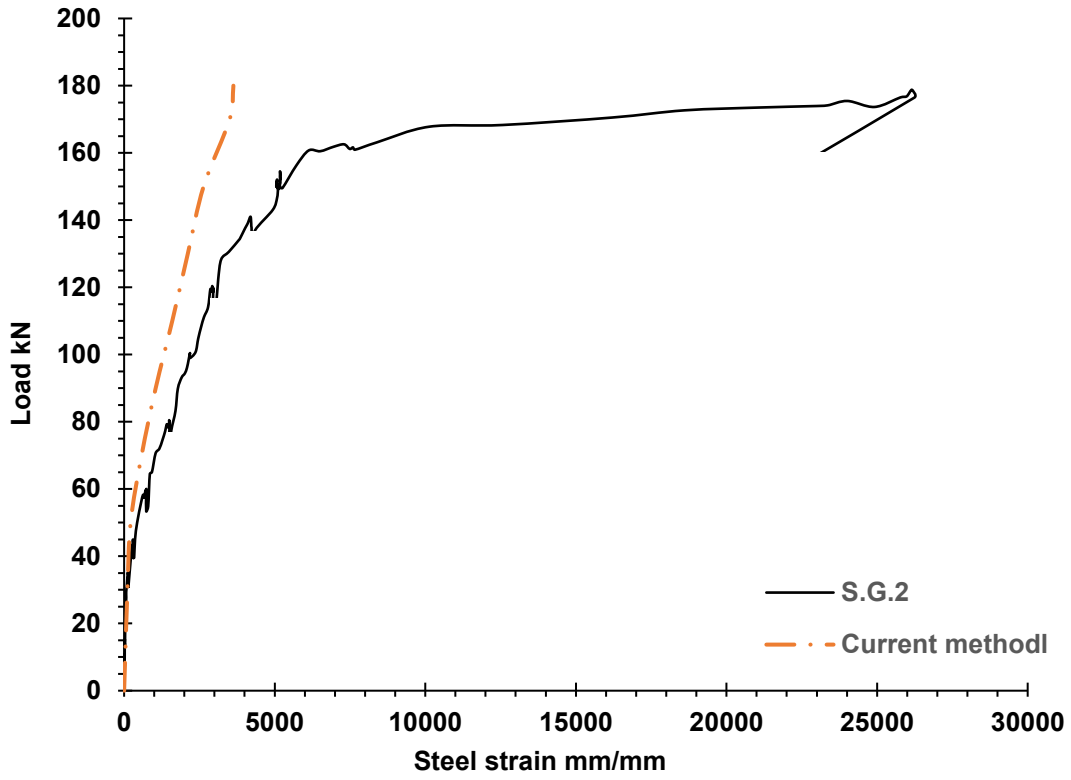
Load kN
200
180
160
140
120
100
80
60
40
20
0
0
5000
10000
15000
20000
25000
30000
Steel strain mm/mm
S.G.2
Current methodl

(b)

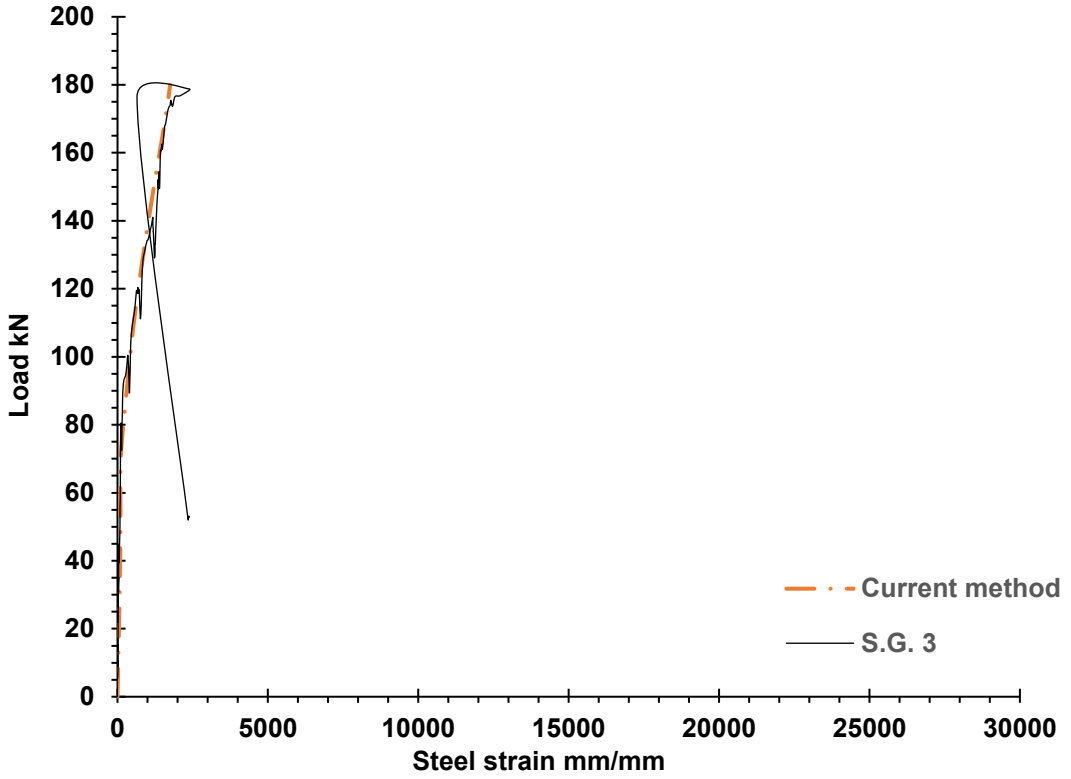
Load kN
200
180
160
140
120
100
80
60
40
20
0
0
5000
10000
15000
20000
25000
30000
Steel strain mm/mm
Current method
S.G. 3

(c)

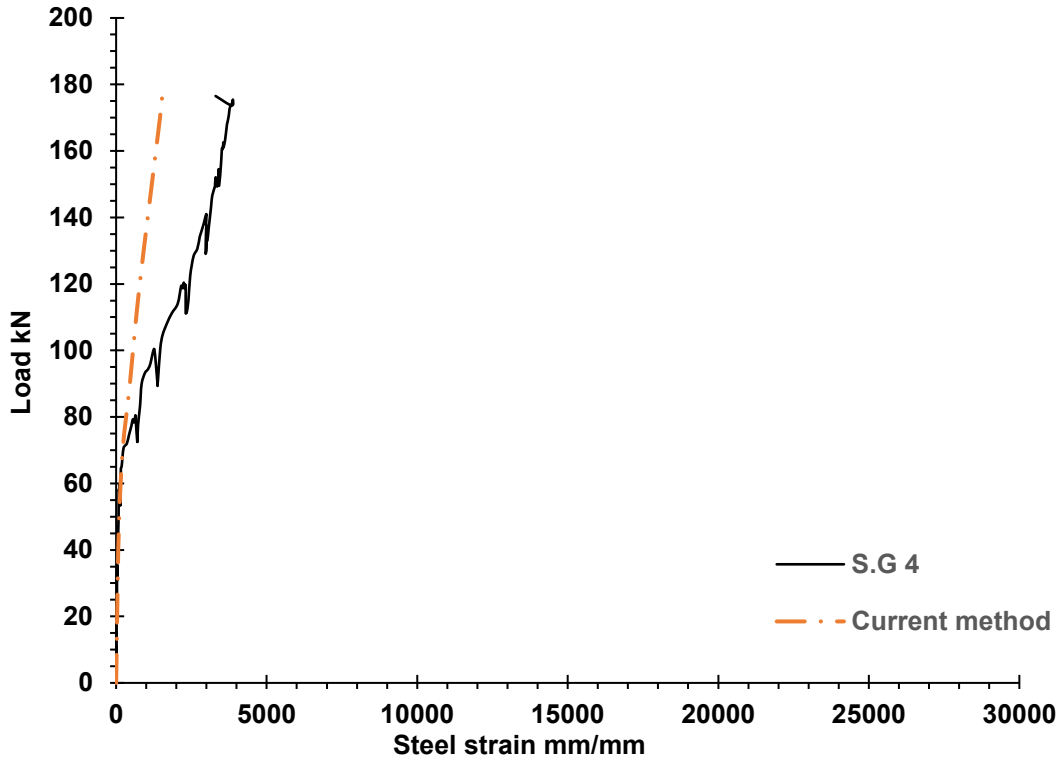
Load kN
200
180
160
140
120
100
80
60
40
20
0
0
5000
10000
15000
20000
25000
30000
Steel strain mm/mm
S.G 4
Current method

(d)

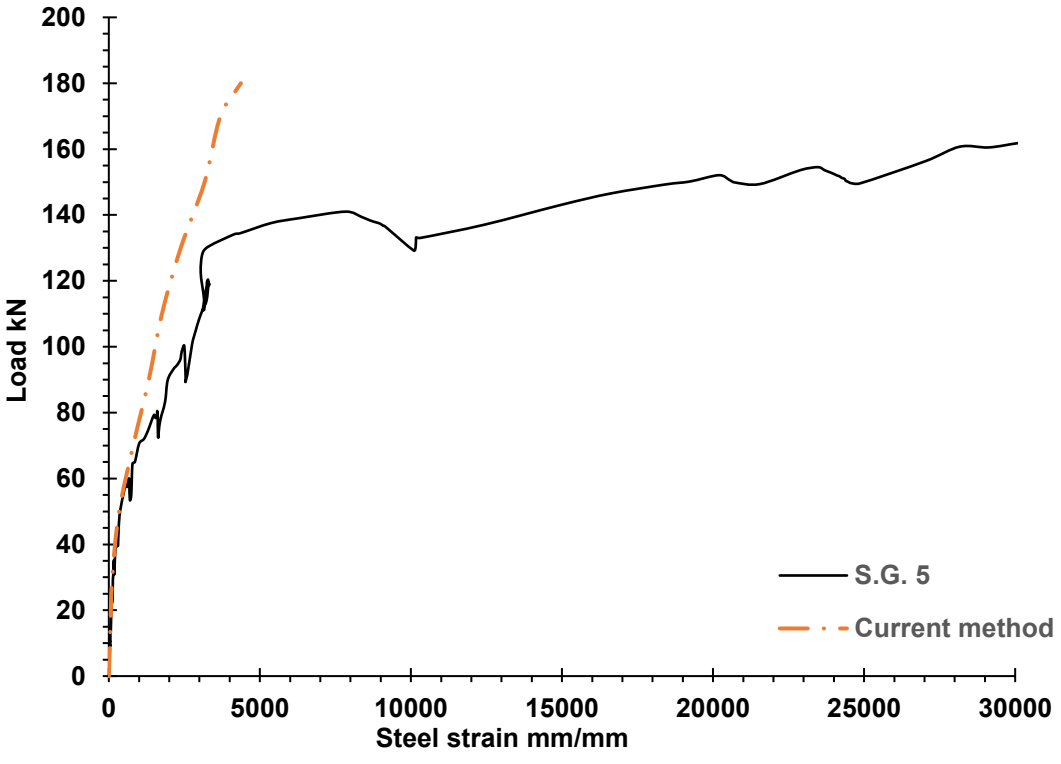
Load kN
200
180
160
140
120
100
80
60
40
20
0
0
5000
10000
15000
20000
25000
30000
Steel strain mm/mm
S.G. 5
Current method

(e)

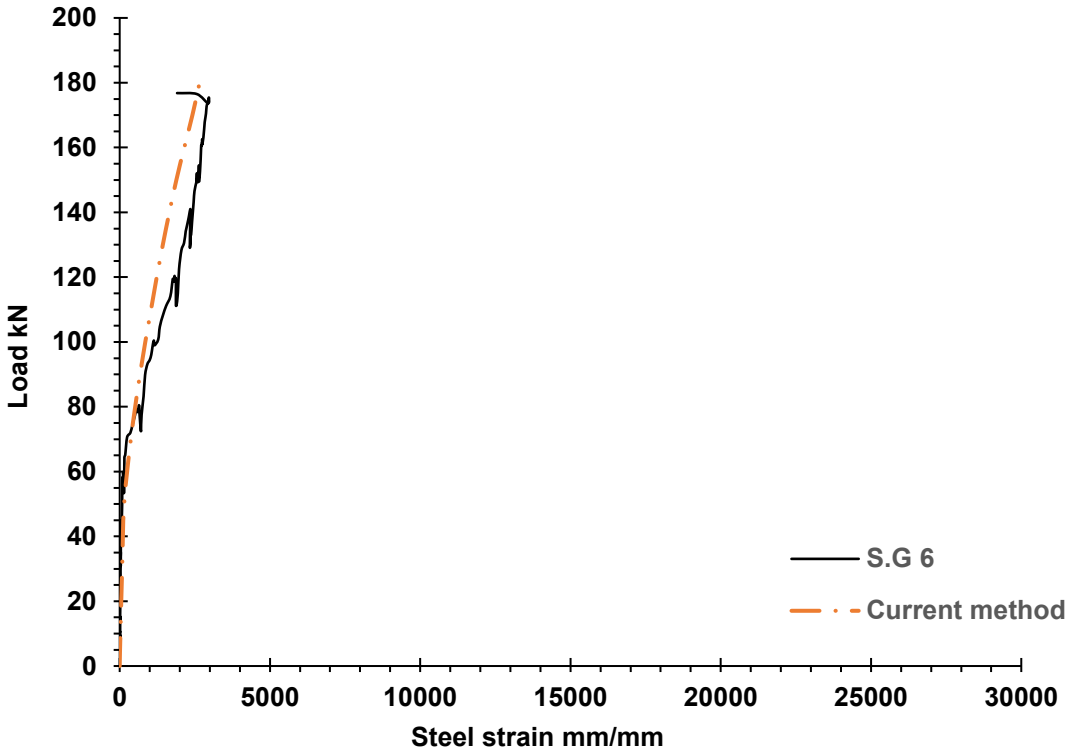

(f)

Figure 5-6. Comparison of measured and predicted tensile steel strains of slab S5.

5.5 Sustained Load Level

Often members can be partially cracked, thus, the response is very complex and shared between the concrete and reinforcement. Due to the properties of concrete, typically creep and shrinkage, develop with time, the deformation of reinforced concrete member gradually increases over time. Creep can be expected to be greater in members loaded at a level only just above cracking load since the tensile stresses will be higher than for members loaded at higher levels. In contrary, the shrinkage curvature can be expected to be greater in fully cracked sections than uncracked sections. Thus, selecting an appropriate sustained load is the key to a successful analysis. As already mentioned, the first step in the long-term analysis is usually to perform the instantaneous nonlinear analysis.

Therefore, the analysis results presented in section 5.4 have been offered a clear picture to ensure that under specific load level the precision of the proposed procedure will be in good agreement with the actual behaviour. Based on these comparisons presented in section 5.4, it was decided to select the theoretical sustained load level of 80 kN for solid slab while the theoretical sustained load

level of 60 kN is suggested for slabs containing an opening in order to minimize the expected errors arising from higher levels of load.

5.6 Verification of Long-term Movements with the Proposed Procedure.

As stated in section 2.11, there are three main phenomena that lead to an increase in deformation with time under sustained loads. These are shrinkage, creep, and time-dependent cracking which particularly affects the magnitude of tension stiffening with time. Therefore, an extensive attempt is made for modelling these phenomena in the current numerical analysis procedure. The analysis procedure is examined under different design conditions, i.e. different sustained loading and age of concrete at loading as well as the existence of the opening with different aspect ratios. Four reinforced concrete slabs with the same properties and dimensions were poured and tested and the data were measured and collected from zero until 90 days. Of these, one slab without opening S1 and other three slabs S2, S3, and S4 with different sizes of openings. The experimental results were then compared with the numerical results in terms of time-deflections and time- surface strains of tensile concrete.

5.6.1 Deflection Development with Time

Deflections were recorded with time using LVDT at two different locations and compared with outcomes from analytical and numerical results for solid slab S1. For slabs containing an opening, deflections and steel strains were monitored with time at six different locations and the data were compared with numerical findings. In this section, the results of partially cracked slabs with and without opening under sustained loading is presented and discussed.

5.6.1.1 Solid Slab S1

As the properties of concrete develop with time, the deformation of reinforced concrete member gradually increases several times greater than its instantaneous values. As shown in Figure 5-7(a) and 5-7(b) the results indicate that there are significant increases of measured deflection values with time. As can be seen, deflections calculated using numerical analysis procedure, underestimate the results when the tensile creep is equal to one-time

compressive creep. The calculated deflections exhibit fit better results when the tensile creep is equal to seven times compressive creep. This behaviour could be attributed to the stress/strength ratio where the compressive stress/strength ratio in the solid slab usually is small compared with tensile stress/strength ratio and, hence, the development of tensile creep strain is much larger than the compressive creep strain. This agrees with the observations reported in the literature by (Forth, 2014; Z.P. Bazant & Oh, 1984; Branson, 1977; Chu & Carreira, 1986). This is sufficient evidence to suggest that the ratio of tensile to compressive creep is not unity.

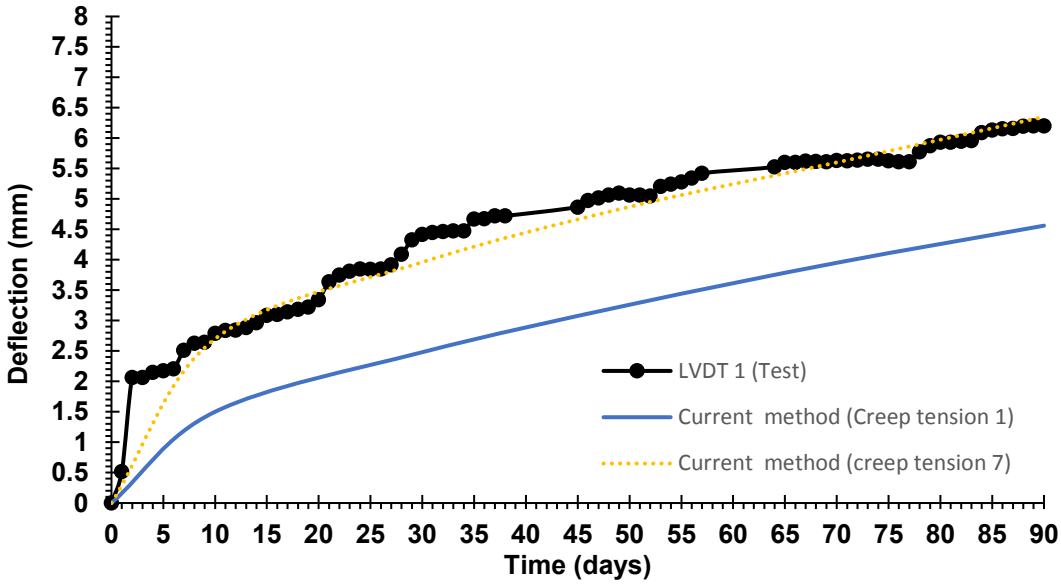

(a)

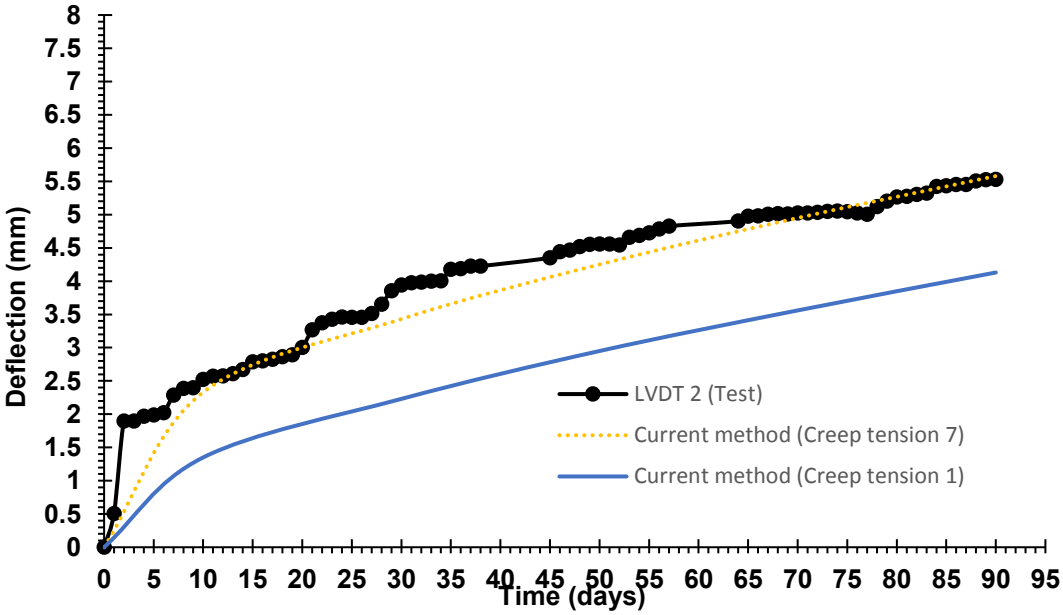

(b)

Figure 5-7. Comparison of long-term deflections of solid slab S1

5.6.1.2 Slabs Contain an Opening (S2, S3 and S4)

A comparison between numerical and experimental results for slabs with openings is illustrated in Figure 5-8, Figure 5-9 and Figure 5-10 for slabs S2, S3, and S4, respectively. In all slabs, it is clear from the results that the long-term deflections calculated using numerical analysis procedure provides good estimation when the tensile creep coefficient equal to compressive creep coefficient. This could be attributed to the equality of stress/strength ratio in tensile and compressive area. As it has been explained in the literature, the amount of tensile stress transferred to the concrete depends to a large extent on the bond stress between the reinforcing bar and surrounding concrete. Due to presence of opening, there is a reduction in bending stiffness and this, in turn, will lead to more tension stiffening decay in comparison with solid slab and, hence, less tensile stresses in the concrete portions between cracks, specifically around the opening zones. This would be expected to reduce the tensile stress/strength ratio and will be much closer to the compressive stress/strength ratio and, hence, quite similar development of tensile and compressive creep strain. This agrees with observations by (Forth,2014). He stated that it is possible for the actual compressive creep to be equal to the actual tensile creep when similar stress/strength ratios exist in tensile and compressive zones. This may explain why the numerical deflection values show good agreement with the experimental values when tensile creep coefficient is equal to compressive creep coefficient. In such a case, there is evidence to suggest that the stress/strength ratios in the tension and compression zone of sab with opening are equal. It is of interest to note that there is a similar trend with experimental behaviour for all slabs that contain opening. Therefore, this strongly points to the fact that the long-term analysis of members depends on the stress levels in the compression and tension zone. Hence, this inequality between tensile/compressive creep should be considered in the analysis.

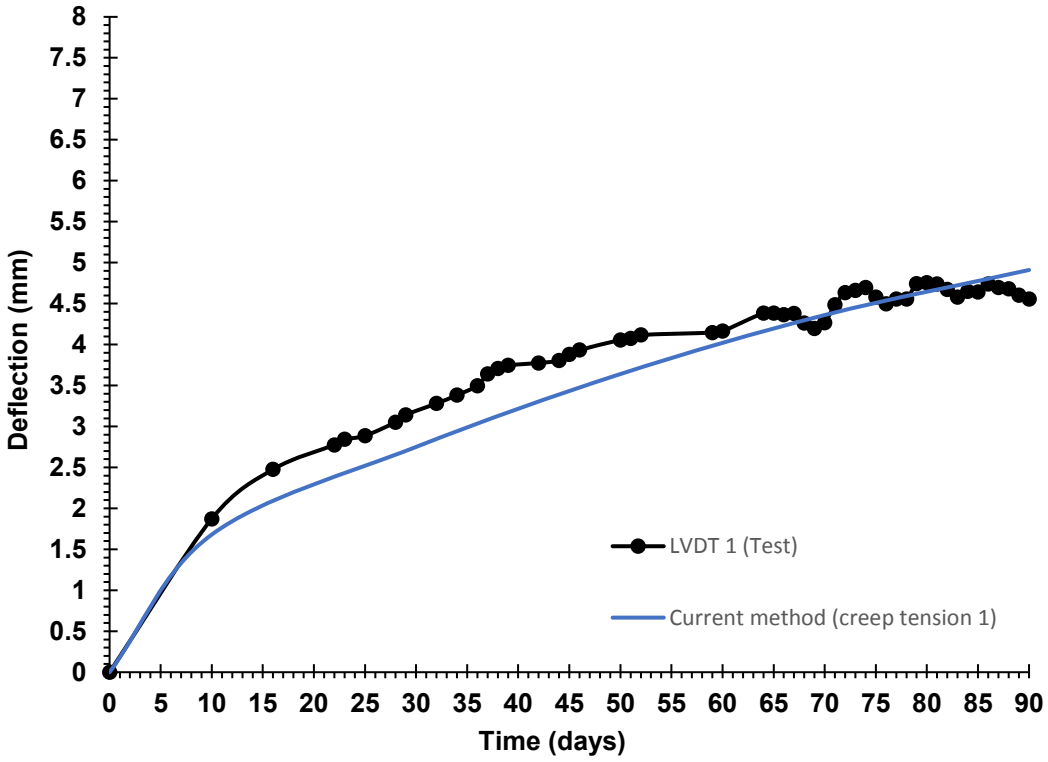
Deflection (mm)
Time (days)
LVDT 1 (Test)
Current method (creep tension 1)

(a)

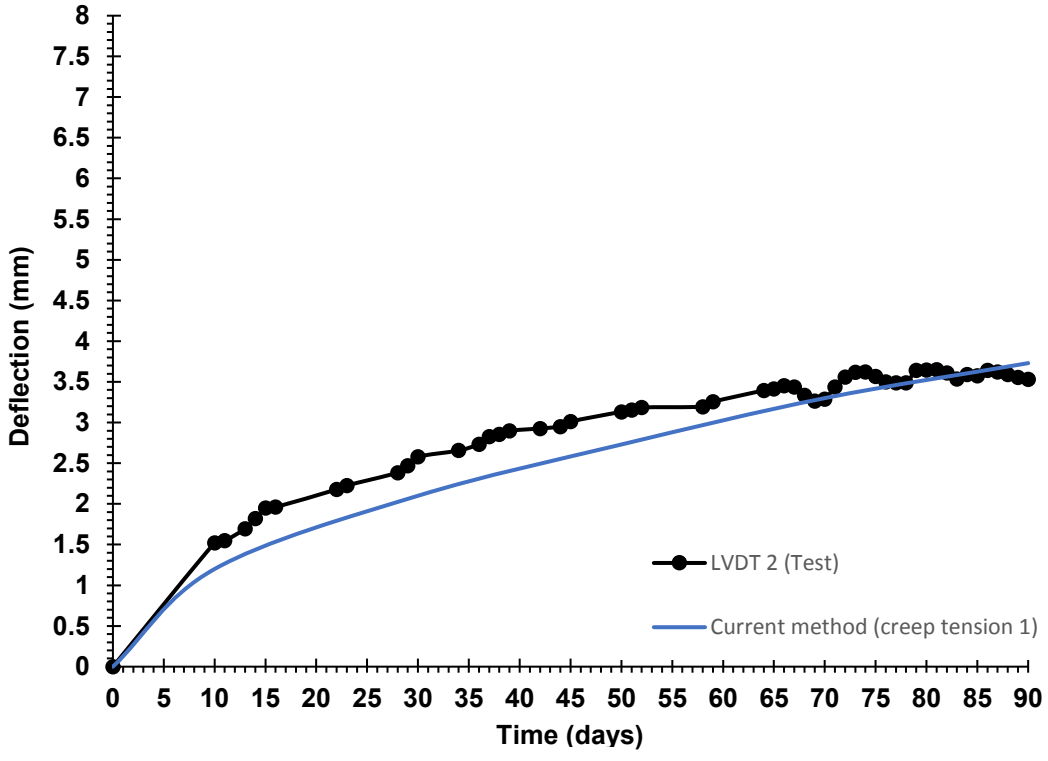
Deflection (mm)
Time (days)
LVDT 2 (Test)
Current method (creep tension 1)

(b)

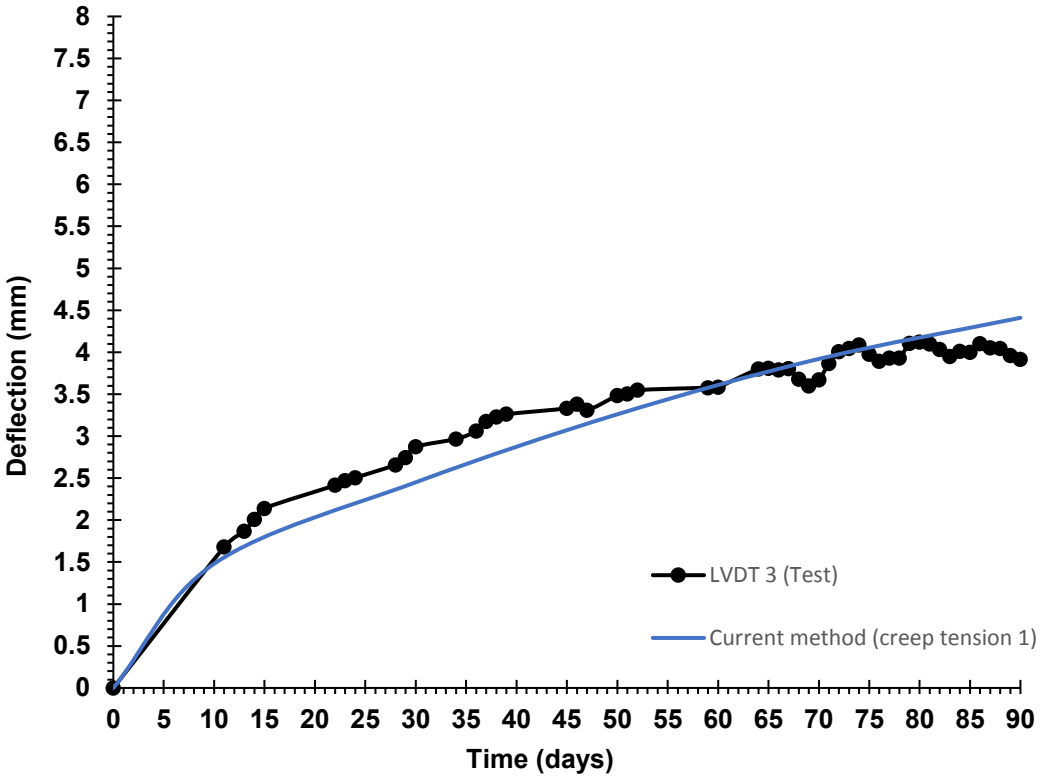
Deflection (mm)
Time (days)
LVDT 3 (Test)
Current method (creep tension 1)

(c)

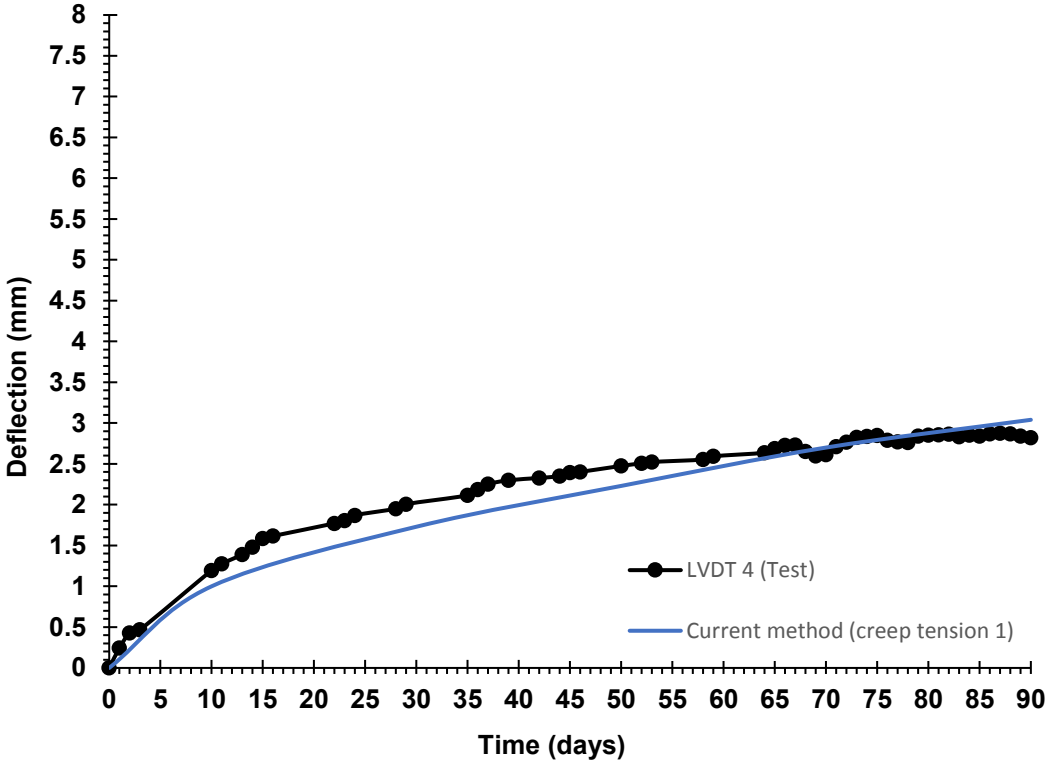
Deflection (mm)
Time (days)
LVDT 4 (Test)
Current method (creep tension 1)

(d)

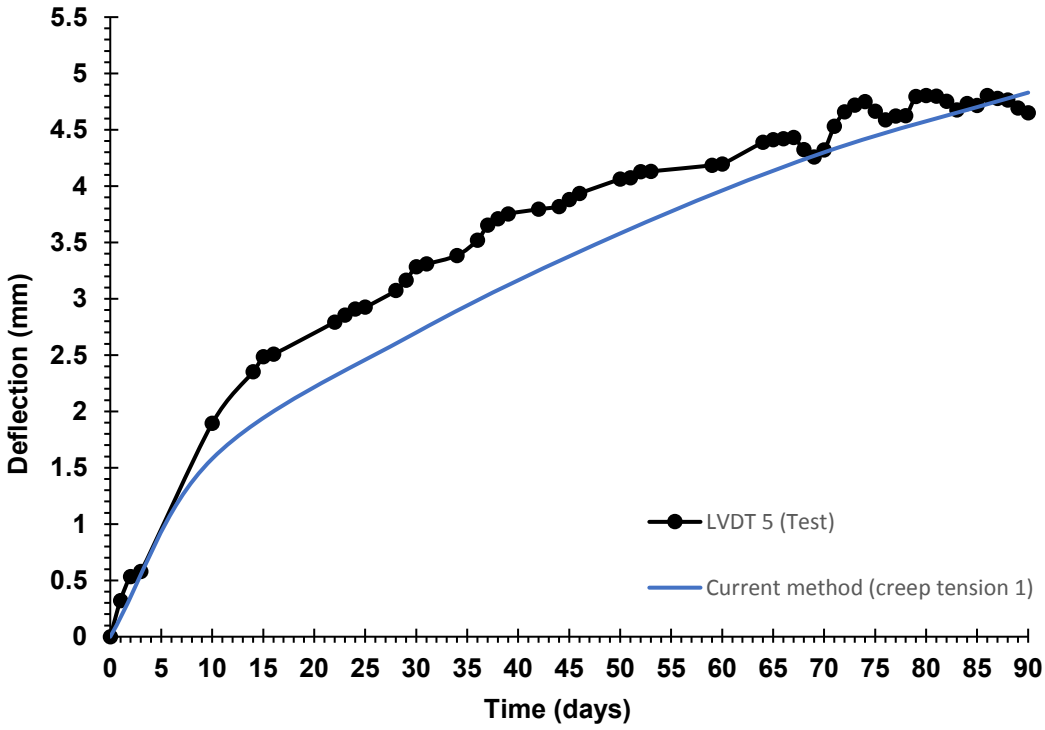

(e)

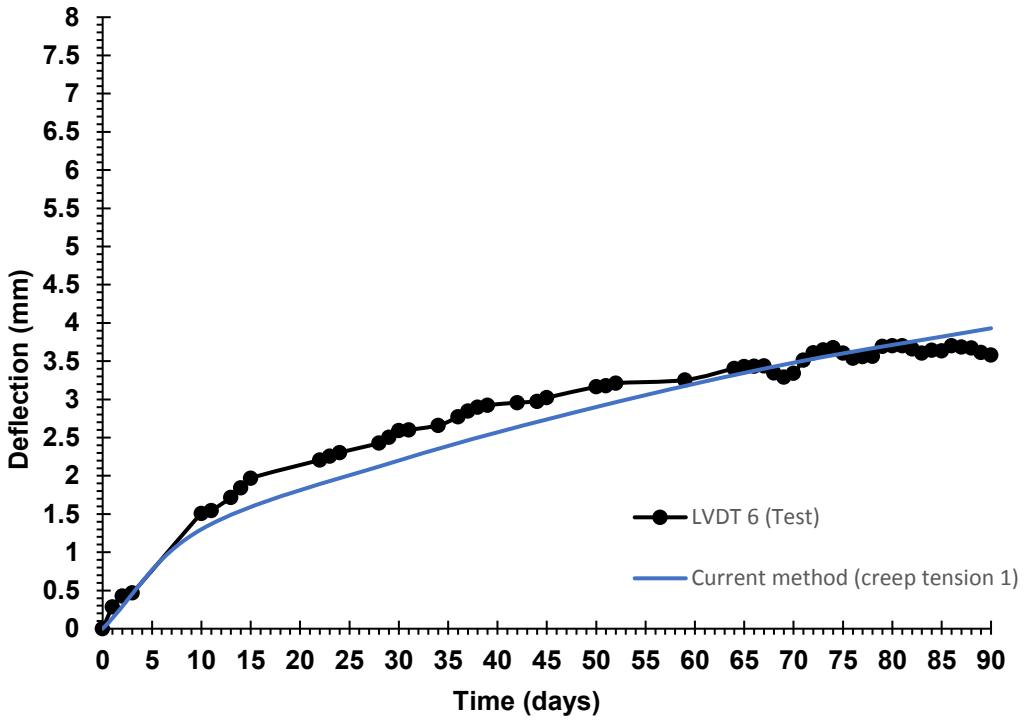

(f)

Figure 5-8. Comparison of measured and predicted long term deflections of slab S2

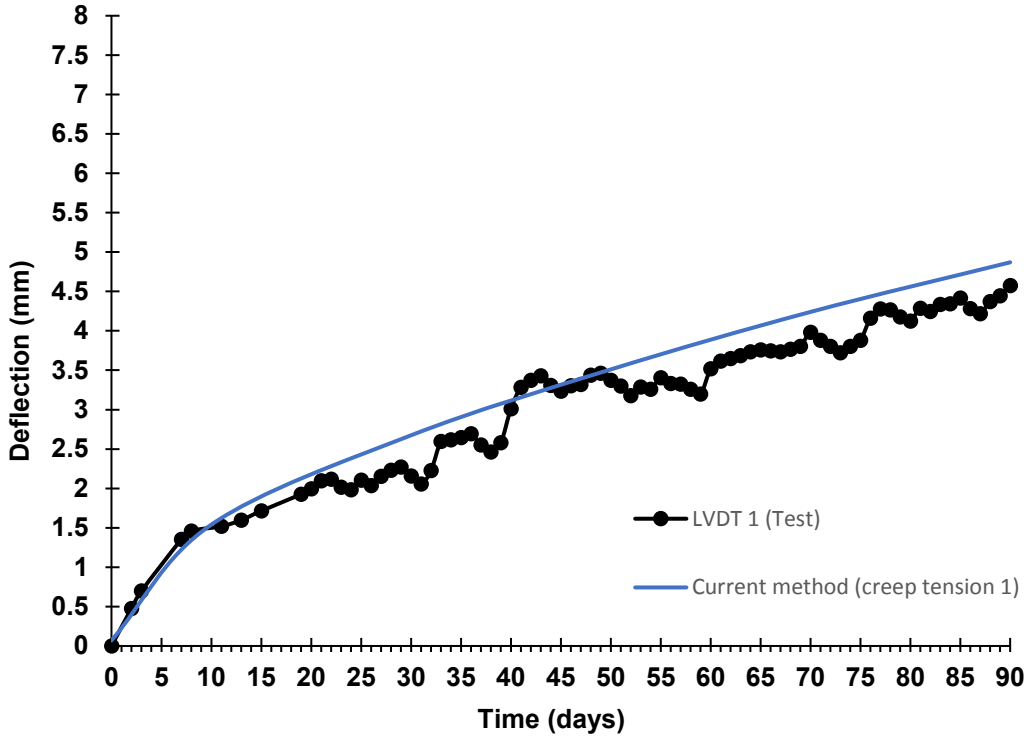
Deflection (mm)
Time (days)
LVDT 1 (Test)
Current method (creep tension 1)

(a)

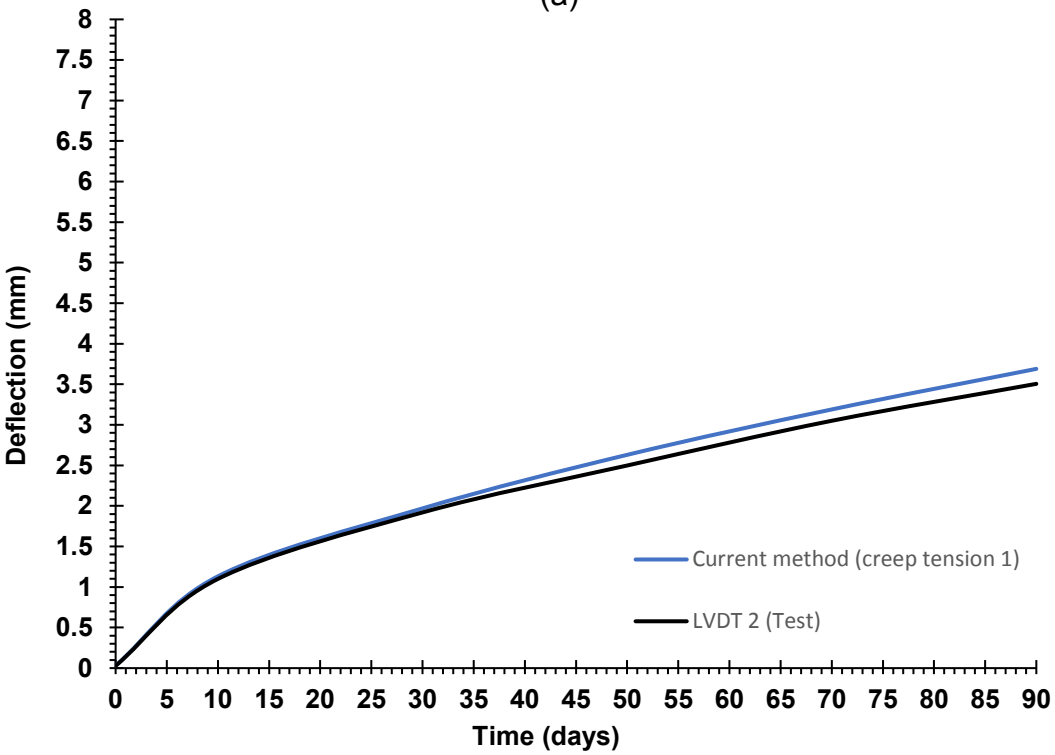
Deflection (mm)
Time (days)
Current method (creep tension 1)
LVDT 2 (Test)

(b)

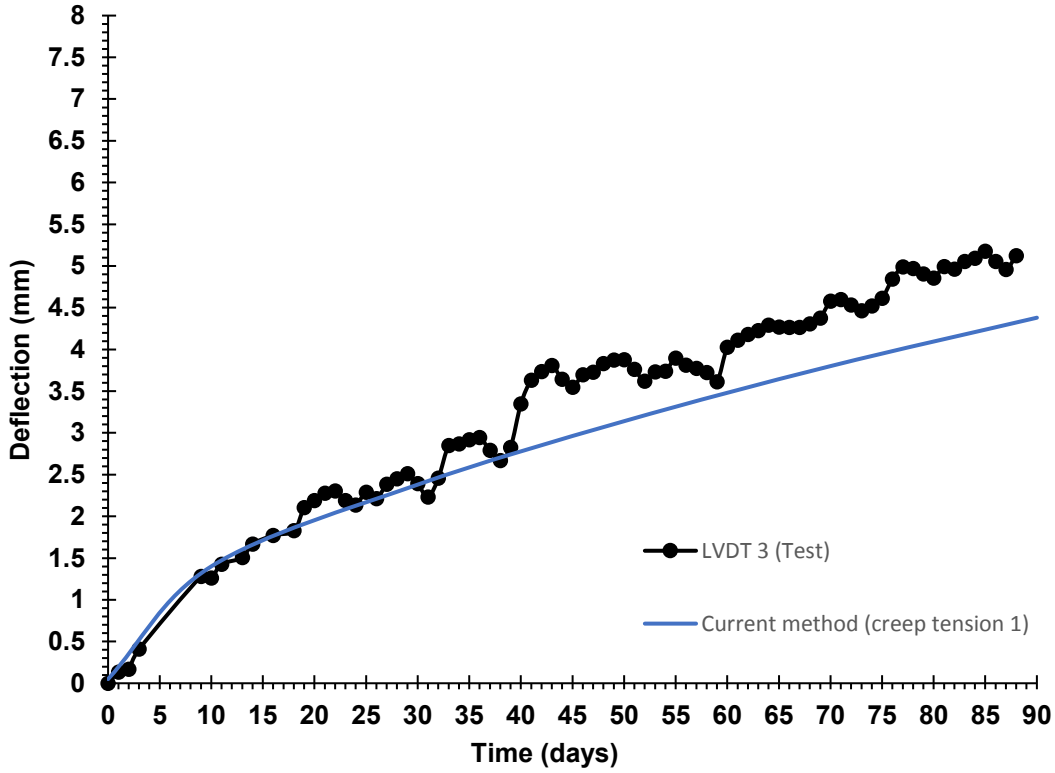
Deflection (mm)
Time (days)
LVDT 3 (Test)
Current method (creep tension 1)

(c)

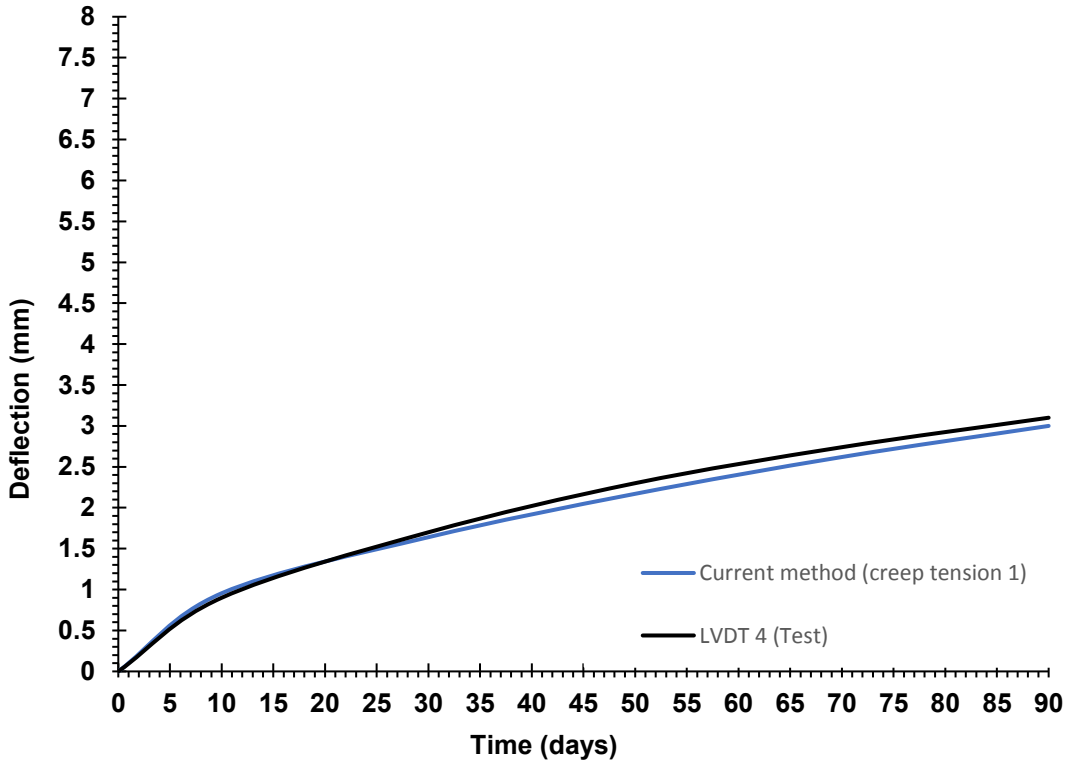
Deflection (mm)
Time (days)
Current method (creep tension 1)
LVDT 4 (Test)

(d)

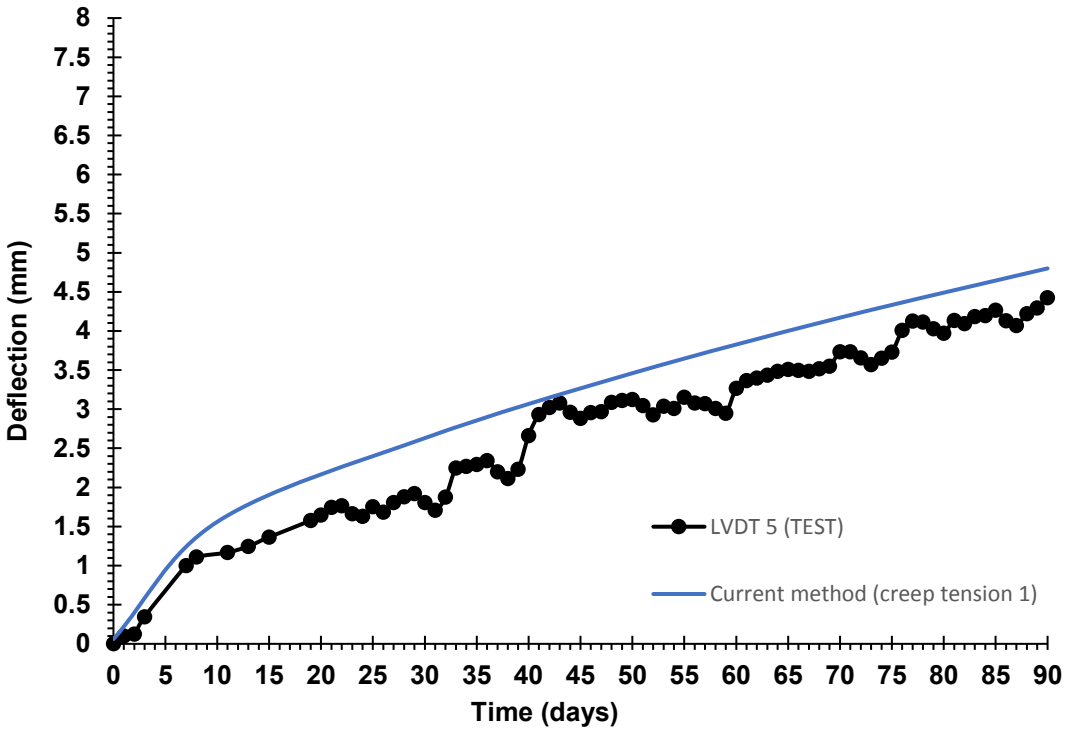

(e)

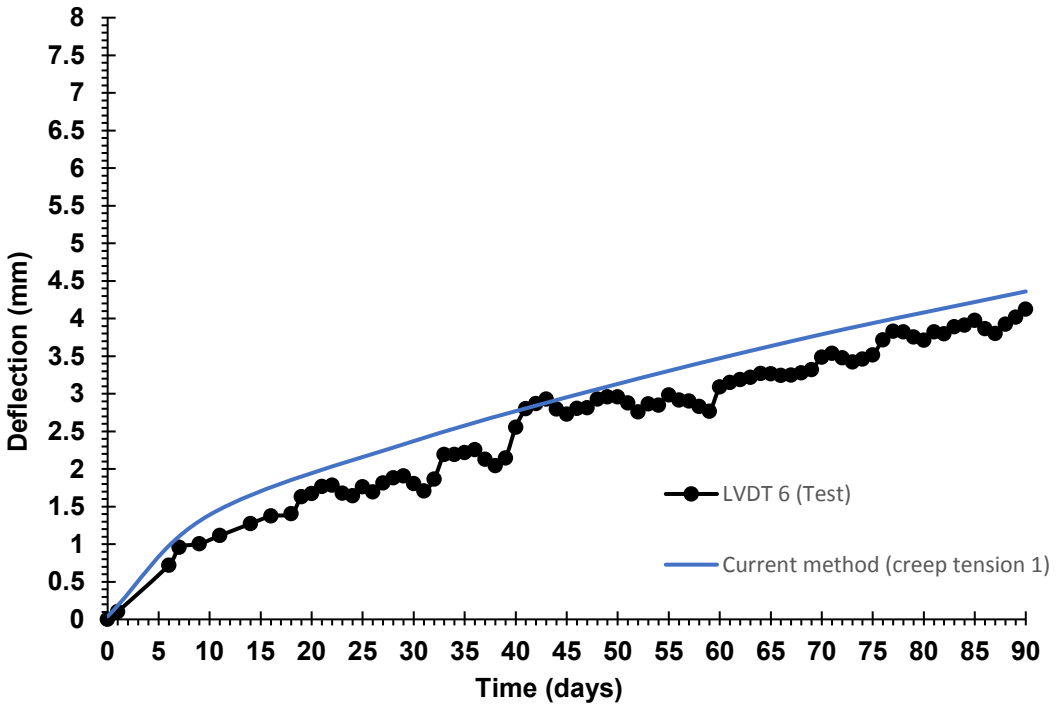

(f)

Figure 5-9. Comparison of measured and predicted long term deflections of slab S3

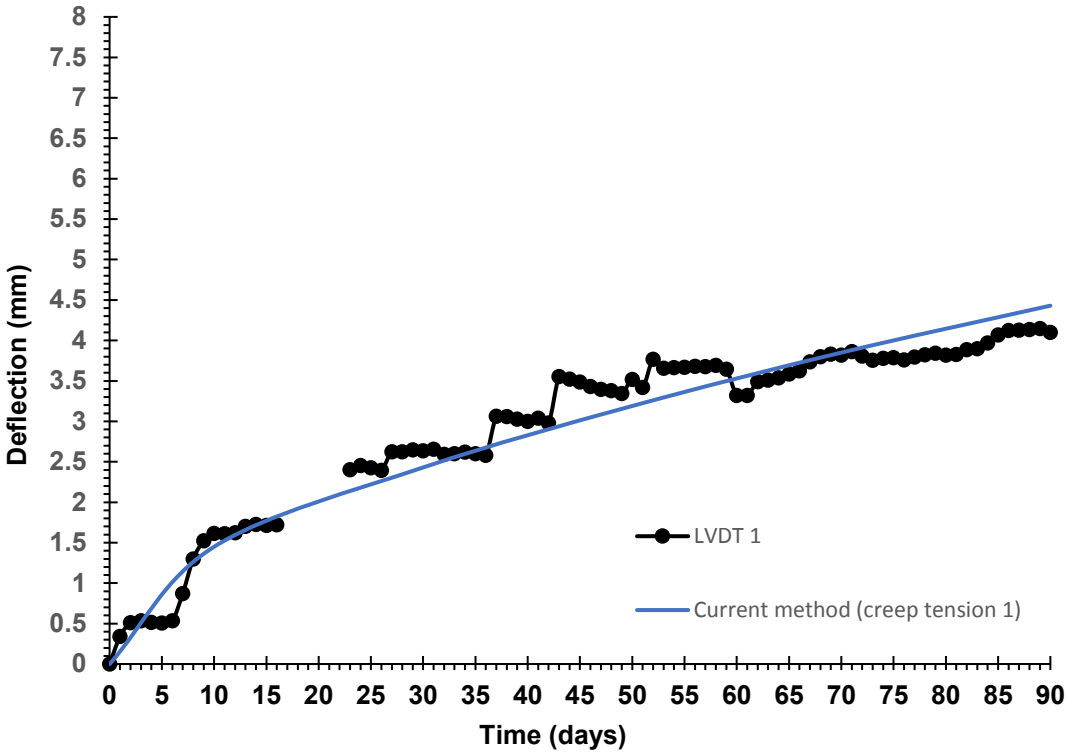
Deflection (mm)
Time (days)
LVDT 1
Current method (creep tension 1)

(a)

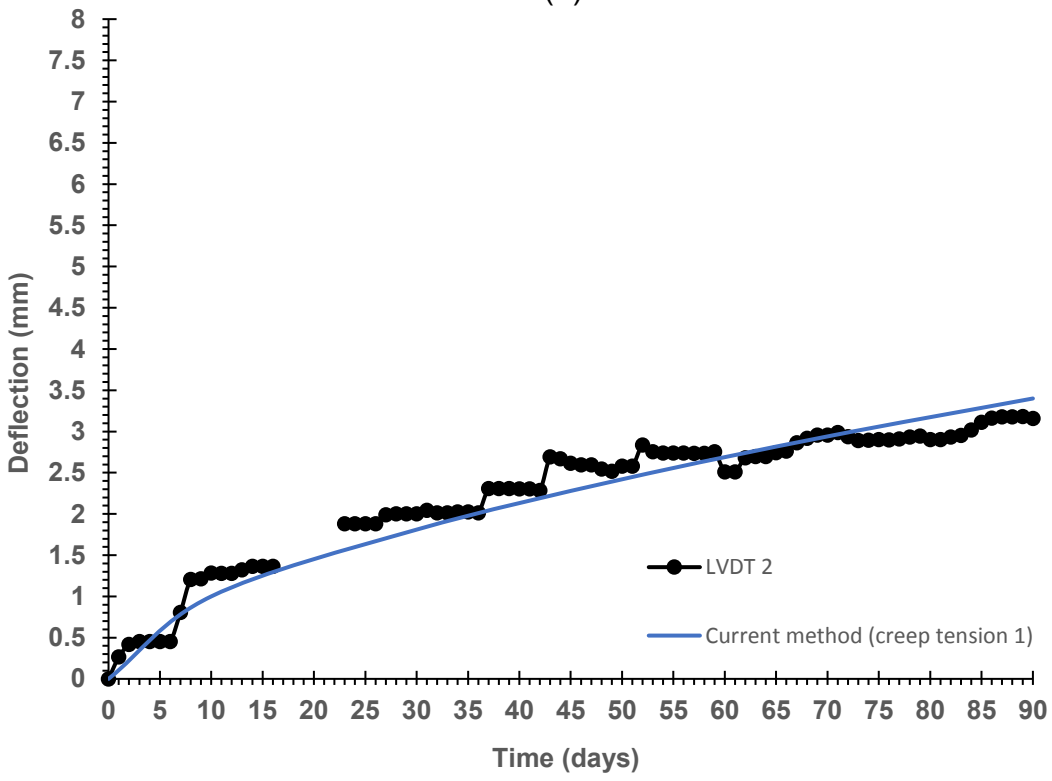
Deflection (mm)
Time (days)
LVDT 2
Current method (creep tension 1)

(b)

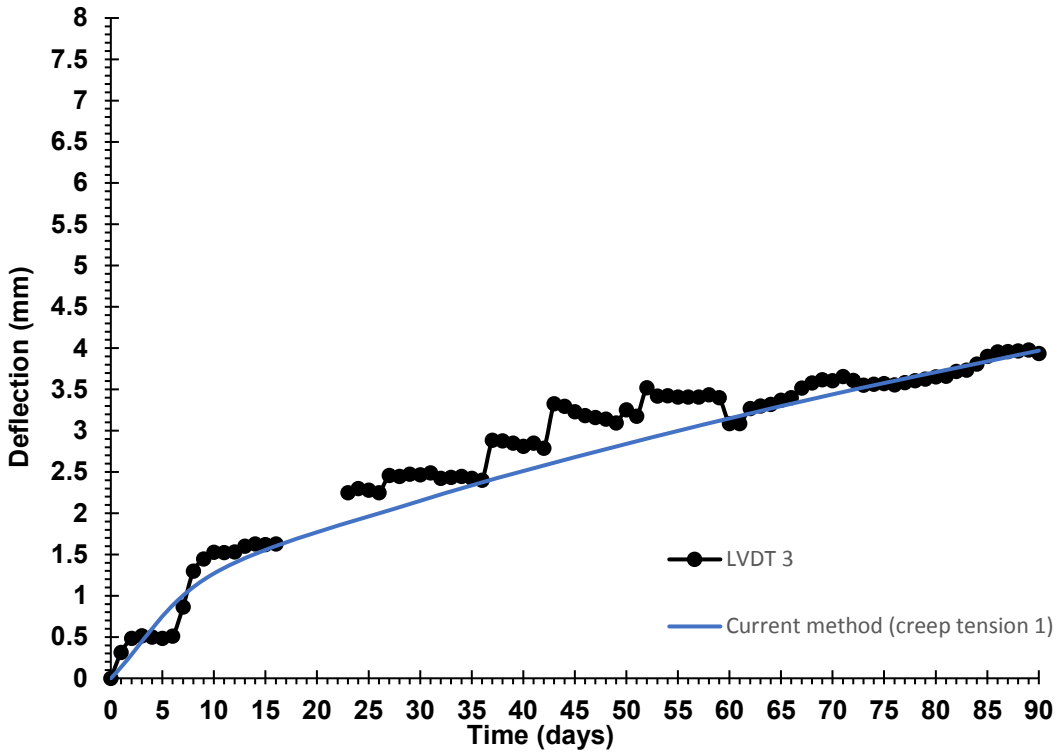
Deflection (mm)
Time (days)
LVDT 3
Current method (creep tension 1)

(c)

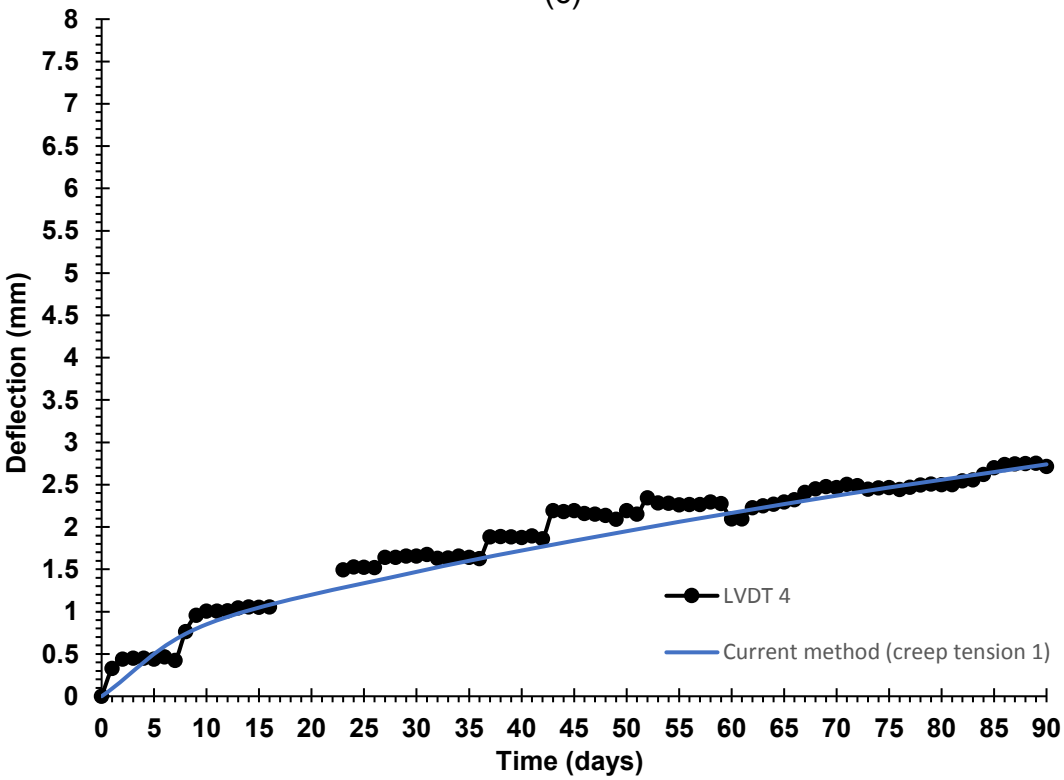
Deflection (mm)
Time (days)
LVDT 4
Current method (creep tension 1)

(d)

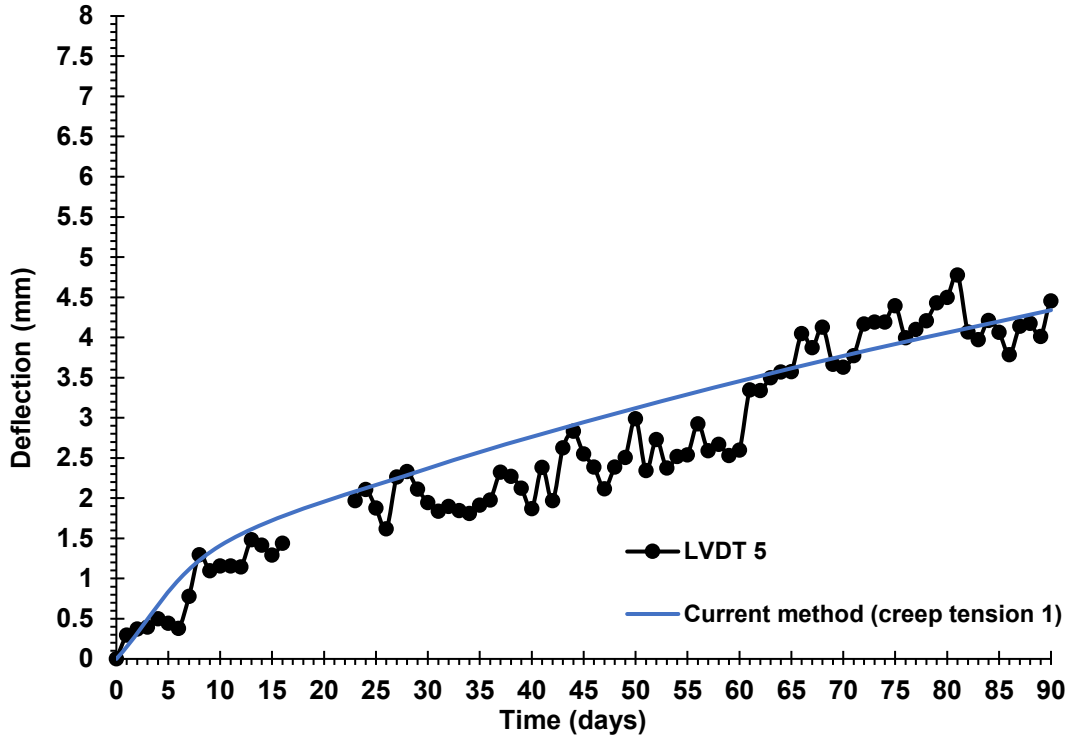

(e)

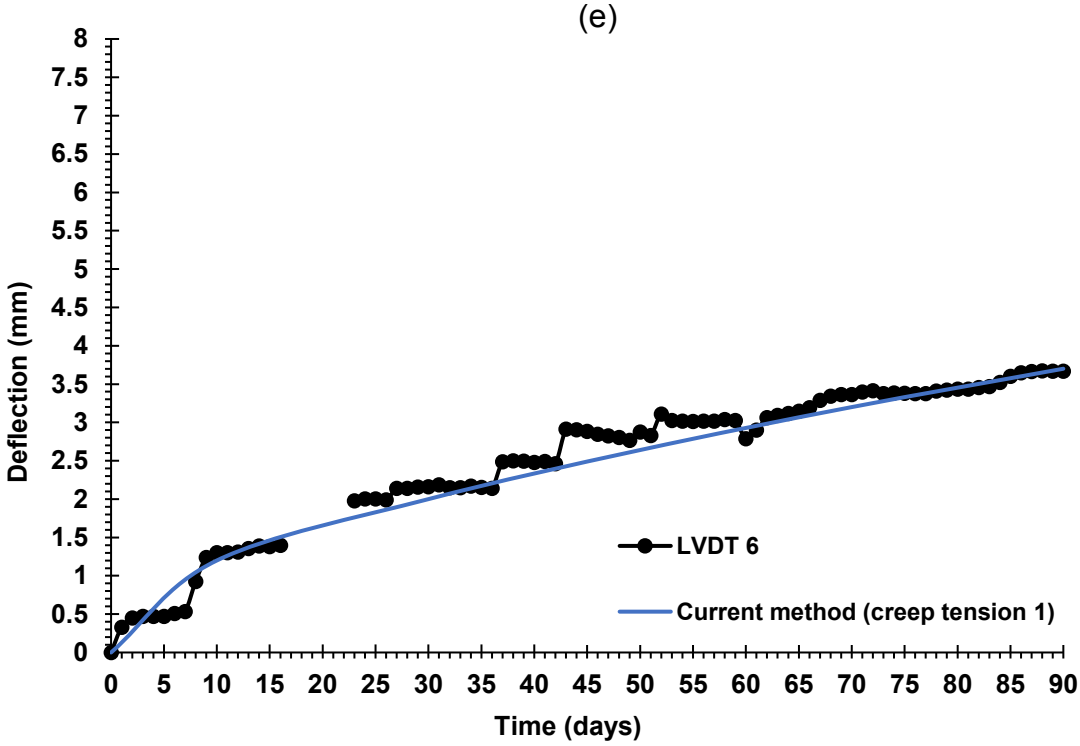

(f)

Figure 5-10. Comparison of measured and predicted long term deflections of slab S4.

5.6.2 Concrete surface tensile strain development with time

Strains were recorded with time using VWG at two locations (as given in Figure 3-4) and compared with outcomes from numerical results. For solid slab S1, As can be seen from Figure 5-11, it is obvious that the strains estimated using numerical analysis procedure underestimate the results compared with the experimental data when the tensile creep coefficient is equal to one time compressive creep coefficient, whereas the computed strains exhibit reasonable results when the tensile creep coefficient is equal to seven times compressive creep coefficient. As stated earlier this indicates again that the compressive stress/strength ratio in the solid slab is small compared with tensile stress/strength ratio and hence the development of tensile creep strain is much larger. It should be noted that, even though the tensile creep coefficient is equal to seven times compressive creep coefficient, the computed tensile strains of concrete show a slight underestimation as shown. This could be attributed to the shrinkage effect, which causes significant increases in crack widths with time. This in line with findings reported by (Gilbert, 2017; Chong, 2004). Another reason that come into play may be resulted from cracks widening as a result of internal events, and formation of surface microcracks. Furthermore, this likely as a result of local events caused by an internal crack breaking through into the face of the crack or from the extension of cracks nearest to the primary cracks and there will thus the cracks widen without transfer of stress between the reinforcing bar and the concrete within this zone. This may confirm why the time-deflection curves of solid slab show reasonable agreements when the tensile creep is equal to seven times compressive creep, while the predicted tensile surface strains shows slight underestimation of results.

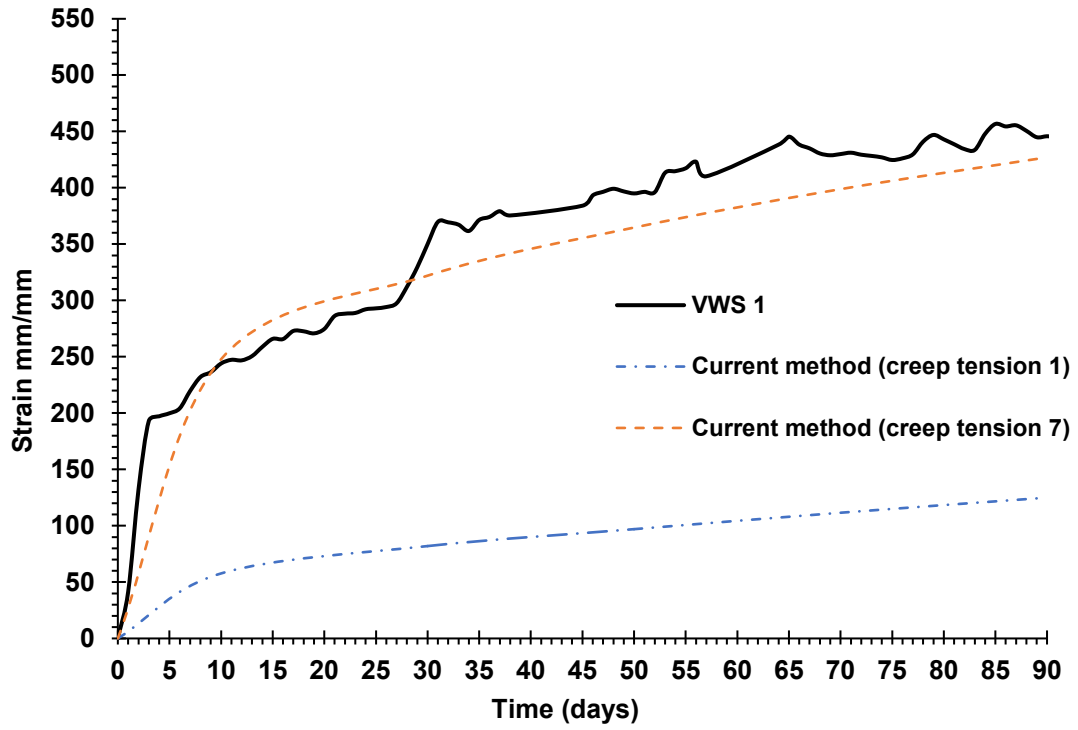

(a)

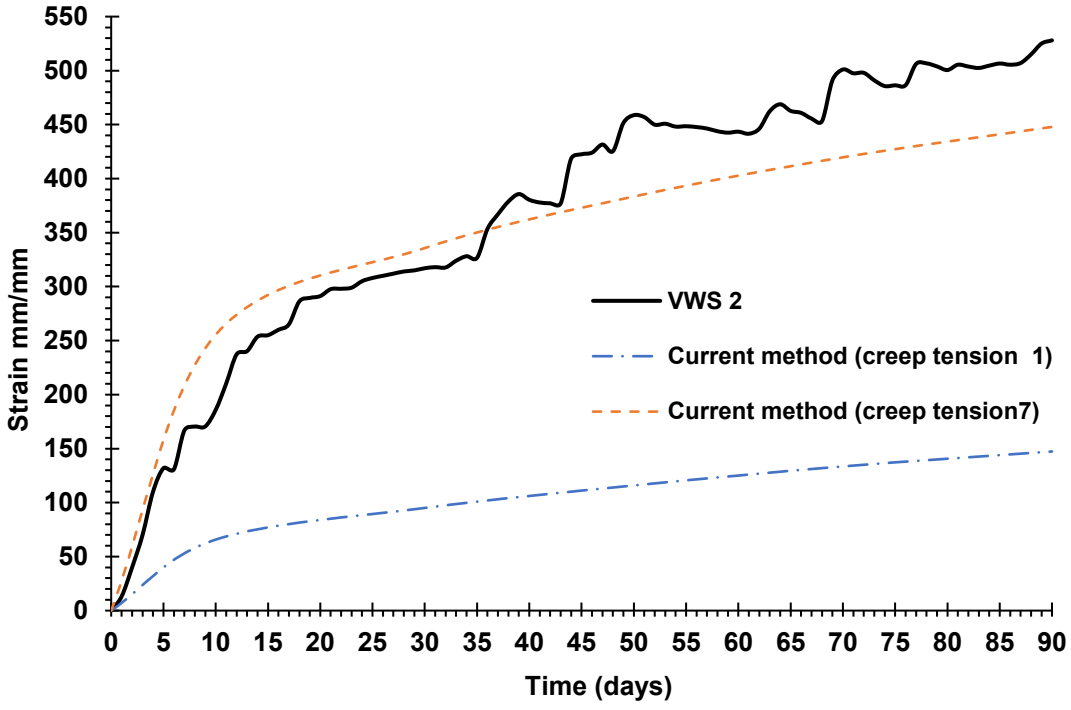

(b)

Figure 5-11. Comparison of measured and predicted long-term concrete surface tensile strain of solid slab S1.

For slabs contain openings, strains were monitored with time using VWG at two locations, as given in Figure 3-5, and compared with findings from numerical results. As can be seen from Figure 5-12,Figure 5-13and Figure 5-14, it can be noted that the strains calculated using numerical analysis procedure underestimates the results compared with the experimental data when the tensile creep coefficient is equal to one time compressive creep coefficient. This is usually attributed to main three possibilities: cracks widening due to shrinkage, formation of surface microcracks, and as a result of local events caused by an internal crack breaking through into the face of the crack or from the extension of cracks nearest to the primary cracks and there will thus the cracks widen without transfer of stress between the reinforcing bar and the concrete within this zone. This explains why the time-deflection curves of slab with opening show reasonable trend when the tensile to compressive creep is equal, while the predicted tensile surface strains show quite underestimation of results. Therefore, it is worth noting that the variation between the experimental and predicted tensile surface strains of concrete is quite remarkable for slabs with opening than solid slab, as given in Figure 5-11, where the presence of opening leads to more tension stiffening decay in comparison with solid slab and hence less tensile stress in concrete portions between cracks, specifically around the opening zones.

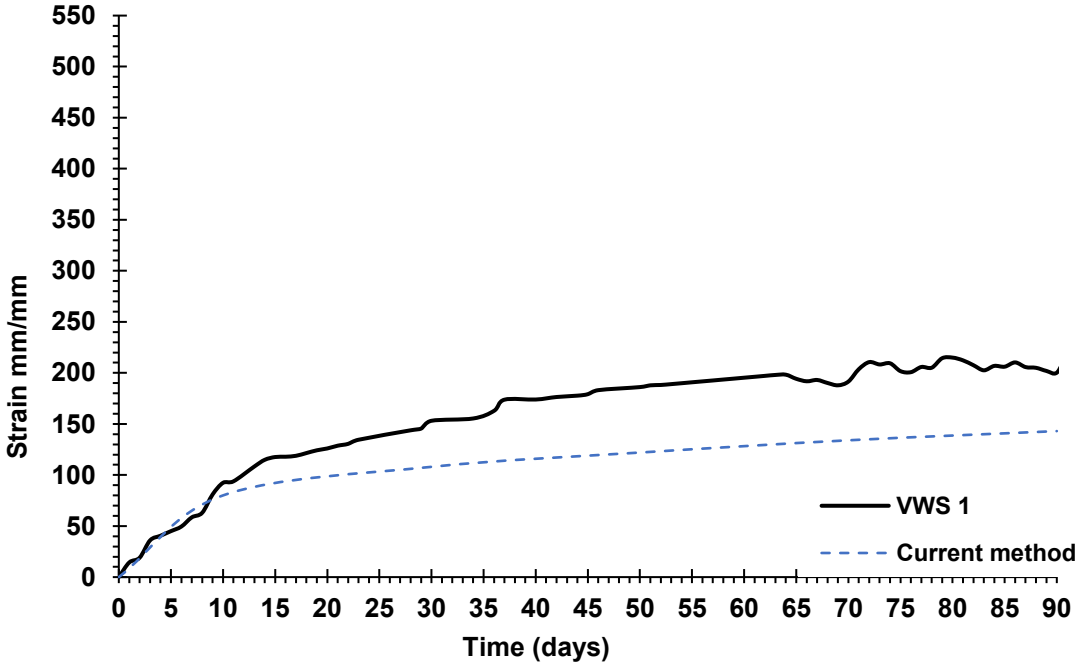

(a)

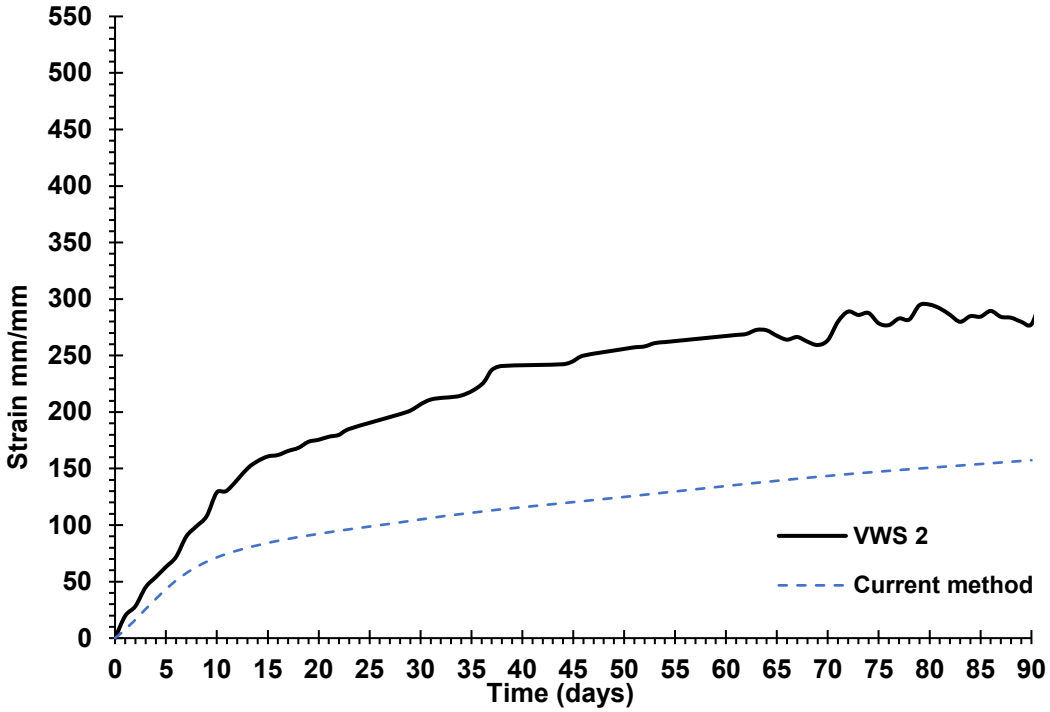

(b)

Figure 5-12. Comparison of measured and predicted long-term concrete surface tensile strain of slab S2

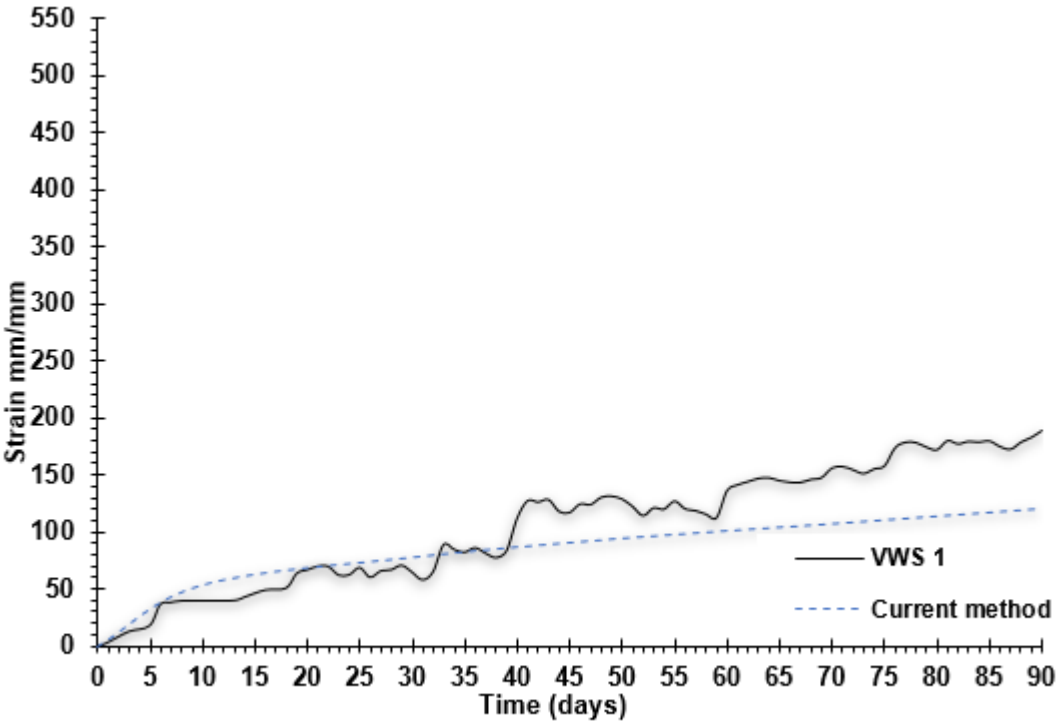

(a)

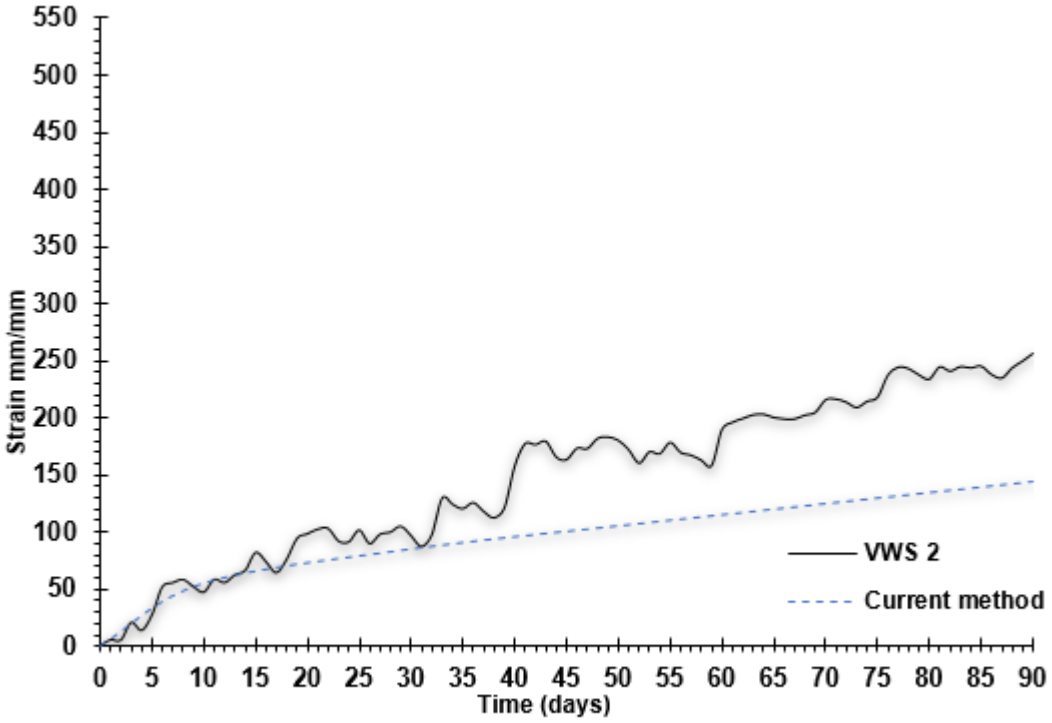

(b)

Figure 5-13. Comparison of measured and predicted long-term concrete surface tensile strain of slab S3

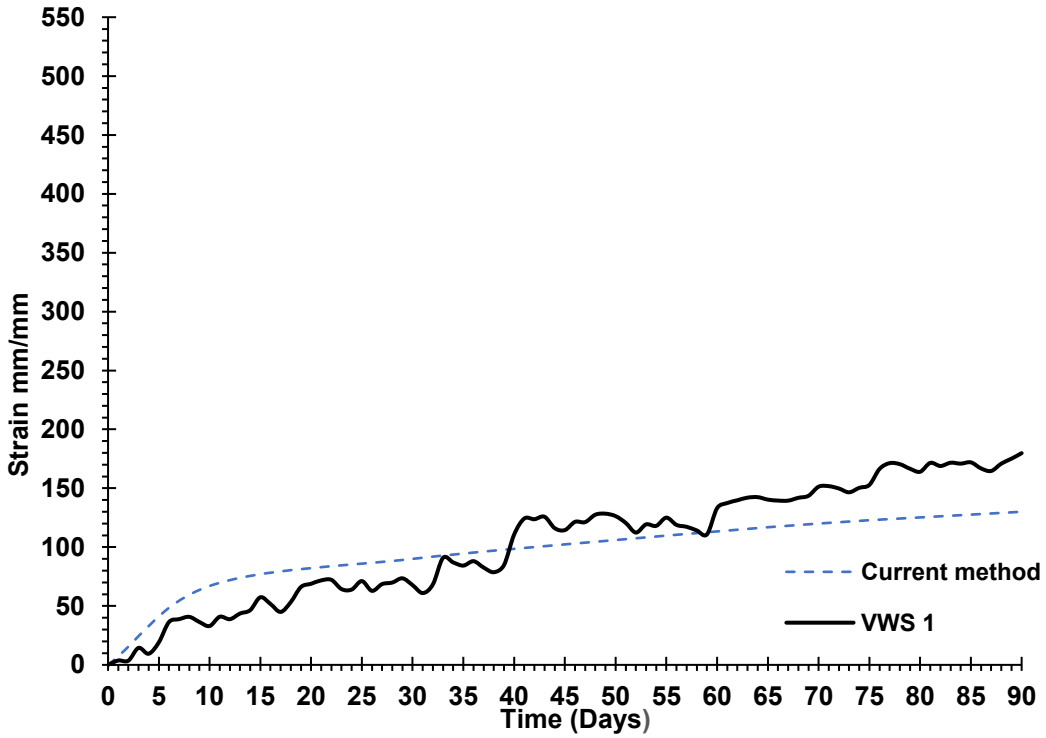

(a)

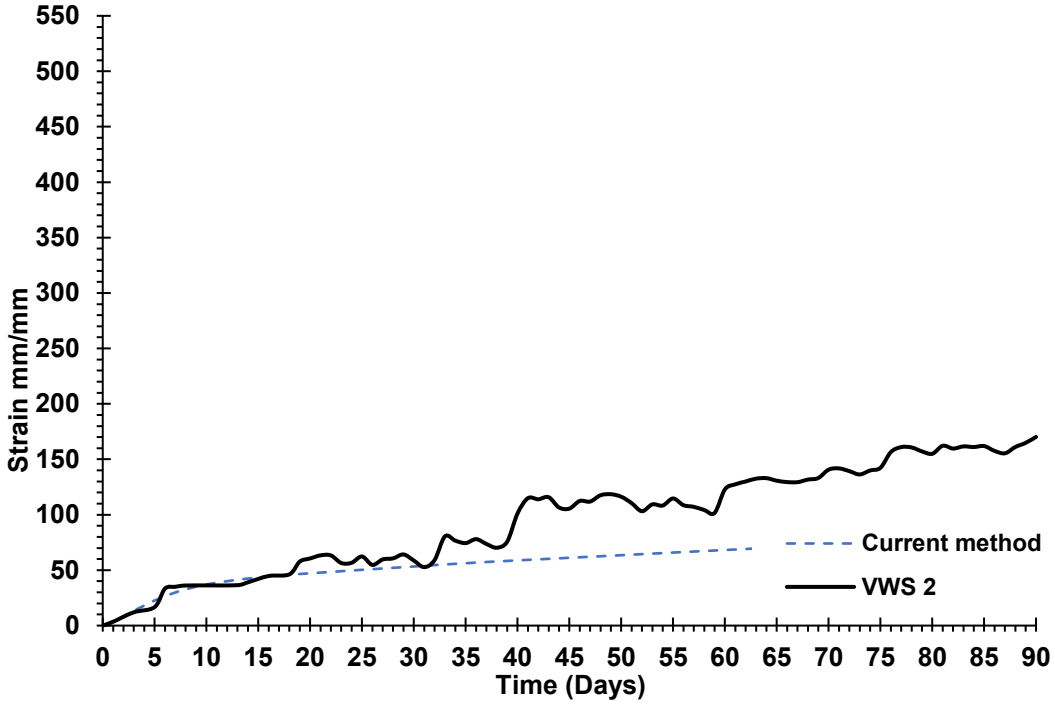

(b)

Figure 5-14. Comparison of measured and predicted long-term concrete surface tensile strain of slab S4

5.7 Summary

Before proceeding to the next sections, the summary about the proposed analysis procedure is presented in this section. This chapter has presented the numerical analysis technique that has been used to analyse the response of slabs with and without opening under short-term and long-term loading. The finite difference method is usually efficient and easy to model the response of reinforced concrete slabs. The perfect bond and smeared cracking approaches are the simplest models and require the least computational resources since they simulate reinforced concrete in an average manner. However, the shortcoming of the proposed procedure is that, it only offers average results for a reinforced concrete slab, such as average stress and average strain, where the determination of a localized mechanism of the slab is not possible.

A comparison of the numerical and the experimental results is included in sections 5.4 and 5.6. Obviously, the proposed procedure overestimates the defections and underestimates the steel strains when the load approaches the

ultimate load; however, it gives good correlation with the measured data in the service load range. For the slabs were subjected to sustained loading, the proposed procedure gives good estimation of deflection for solid slab when the tensile creep coefficient is equal to seven times compressive creep coefficient. However, for slabs contains an opening, the proposed procedure gives a fairly good estimation when the tensile creep is equal to compressive creep. This is attributed to the reason discussed in subsections 5.6.1.1 and 5.6.1.2.

5.8 Code-based Models

Deflection of the slab is considered the most important design consideration. It was mentioned in Chapter 2 that all the available models have been derived originally for beams and one-way spanning slabs. Design codes usually provide methods that are based on the calculation of effective stiffness or effective curvature of the members between uncracked and fully cracked states. In the present study, the effectiveness of the models proposed by CEB-FIP 2010 and Eurocode 2 (BSI, 2004) for the prediction of short-term and long-term deflections have been adopted and evaluated with available experimental data.

The elastic bending moments M_x and M_y are calculated at each element by solving the second order differential equation, based on plate bending element, using finite difference method. The torsional moment has been ignored. The reduced flexural stiffness due to cracking in each direction are computed by using a distribution coefficient expression offered by the above-mentioned codes. The restraint to early drying shrinkage provided by embedded reinforcement is considered by reduces the modulus of rupture. The value of $0.33\sqrt{f'_c}$ was used for the reduced effective modulus of rupture. The effect of creep of concrete is taken into account by modifying the elastic modulus of concrete. The shrinkage curvature recommended by the CEB-FIP 2010 and Eurocode 2 (BSI, 2004) has been used; a solution by finite-difference form is then obtained for the second derivatives relating the deflection at node points to the shrinkage curvatures in both directions.

5.8.1 Short-term Deflection

The analysis results based on the code model were compared with the experimentally tested slabs in term of load-deflection relationship. The first slab is solid S0, while the second slab S5 contains opening with size 150 mmx 250 mm. The measured deflection at mid-span of slab was used only.

The comparison between the experimental results and the code model results is illustrated in Figure 5-15 and Figure 5-16. It is clear that the response of the slab is identical in the elastic range up to 58% and 35.75% of the ultimate load for slabs S0 and S5, respectively. After this load, the experimental response of the slabs is stiffer than the model response, which can be attributed to the approximation introduced in the expressions adopted by codes, i.e. the average load-deformation response of tension member after cracking. The code model shows a high change in the slope of the load-deflection curve as can be seen in Figure 5-16 , which reveals a severe reduction in flexural stiffness of the slab after cracking. This seems likely that the introduction of the opening leads to overestimate the theoretical cracking in concrete, based on code models, in comparison with the solid slab. Although the models recommended by building codes have been derived from the experimental tests based on the average behaviour of uniaxial tension members post cracking, it is obvious that the model overestimates the theoretical deflections of the slab when the load approaches the ultimate load capacity. On the other hand, there is evidence to prove that the value of $0.33\sqrt{f'_c}$, which has been used to reflect the reduced effective modulus of rupture, shows good agreements with the experimental recodes in term of cracking load.

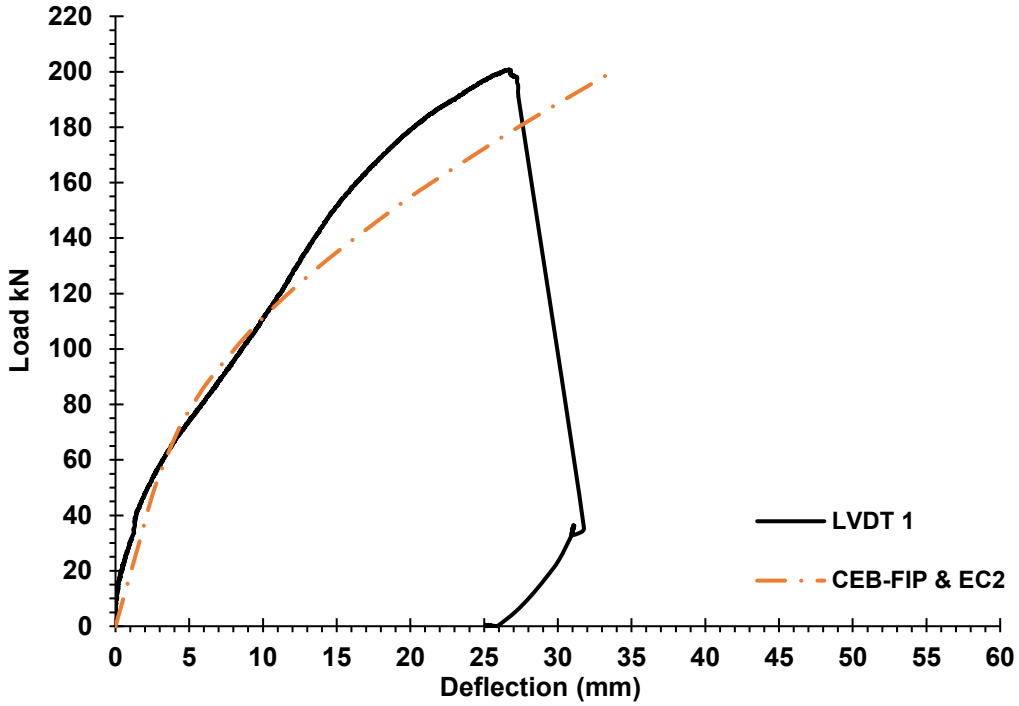

Figure 5-15. Comparison between measured and calculated short-term deflections for slab S0.

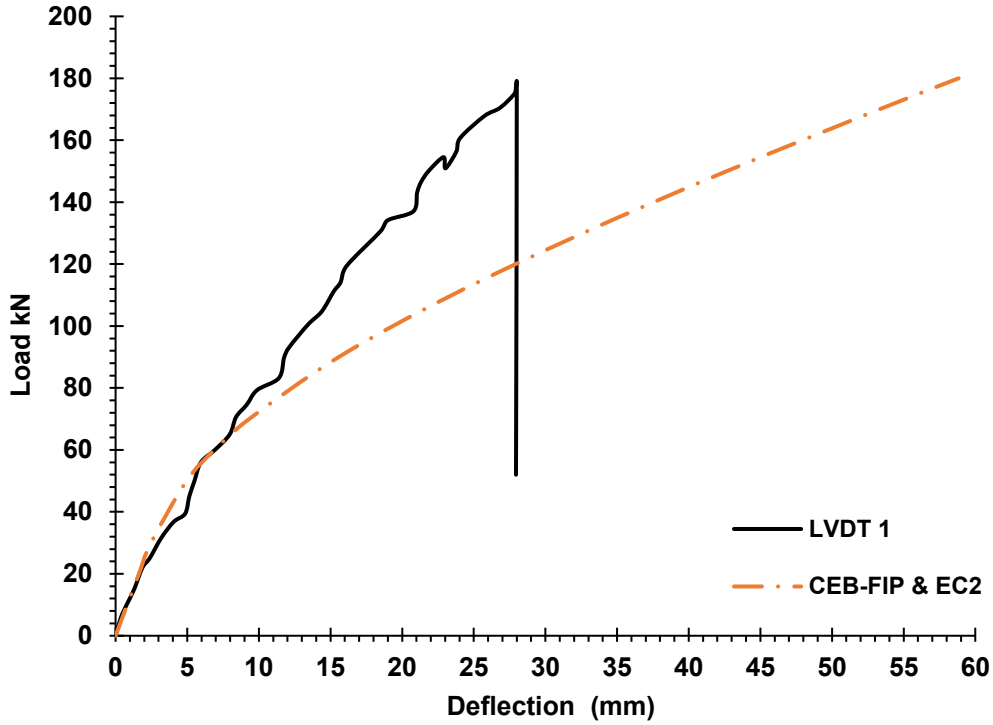

Figure 5-16. Comparison between measured and calculated short-term deflections for slab S5.

5.8.2 Long-term Deflection

The analysis results based on the code model were compared with the experimentally tested slabs in term of time-deflection relationship. The first slab is solid S1 under sustained loading of 80 kN, while other slabs (S2, S3 and S4) contain opening with different aspect ratios under sustained loading of 60 kN. The measured deflection at mid-span of slab was used only. The results are presented and discussed in the following paragraphs.

Figure 5-17 presents a comparison between the experimental results and the code model results for the solid slab S1. Although the models proposed by the code for estimation the long-term deflections have been originally derived based on the assumptions that the neutral axis position and bending stress history is fixed as well as the creep coefficient in compression and tension are the same, however, the results indicated that the calculated deflections obtained by CEB-FIP 2010 and Eurocode 2 (BSI, 2004) showed good agreement with the experimental data.

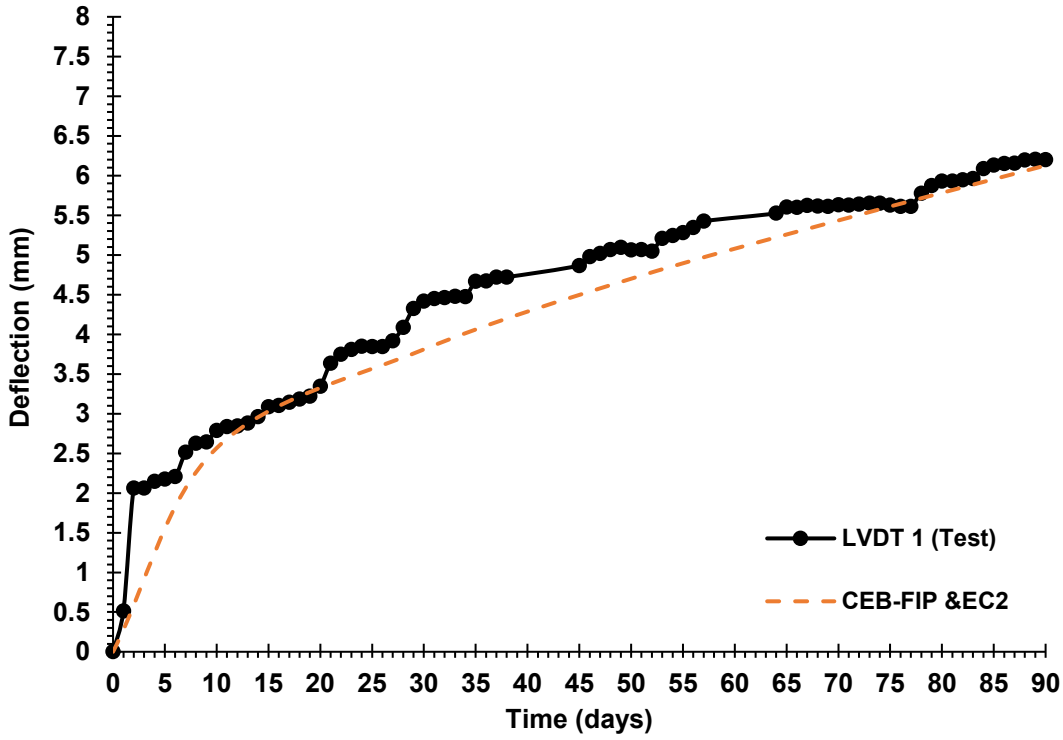

Figure 5-17. Comparison between measured and calculated long-term deflections for slab S1.

For slabs contain an opening (S2, S3 and S4), a comparison between the experimental results and the theoretical results is presented in Figure 5-18, Figure 5-19 and Figure 5-20. As it has already been explained, the models have been derived based on crude assumptions; this could lead to overestimate the deformation with time. Although the model showed good estimation for the solid slab S1, as shown in Figure 5-17, it is seen that the predictions based on the code model greatly overestimated the long-term deflections for all slabs with the opening under sustained loading of 60 kN; however, the calculated instantaneous deflections based on the code model showed good estimation up to 35.75% (64 kN) of the ultimate load. It is of interest to note that there is a similar trend for all slabs that contain the opening. This is usually attributed to two reasons: firstly, the assumption of fixing the neutral axis position wherein the bending stress history is being fixed and, secondly, the influence of creep and shrinkage where their effects are treated as separate and independent. This leads to the fact that the long-term deflections calculated using above-mentioned code models will considerably overestimate the actual deflections for the slabs with opening.

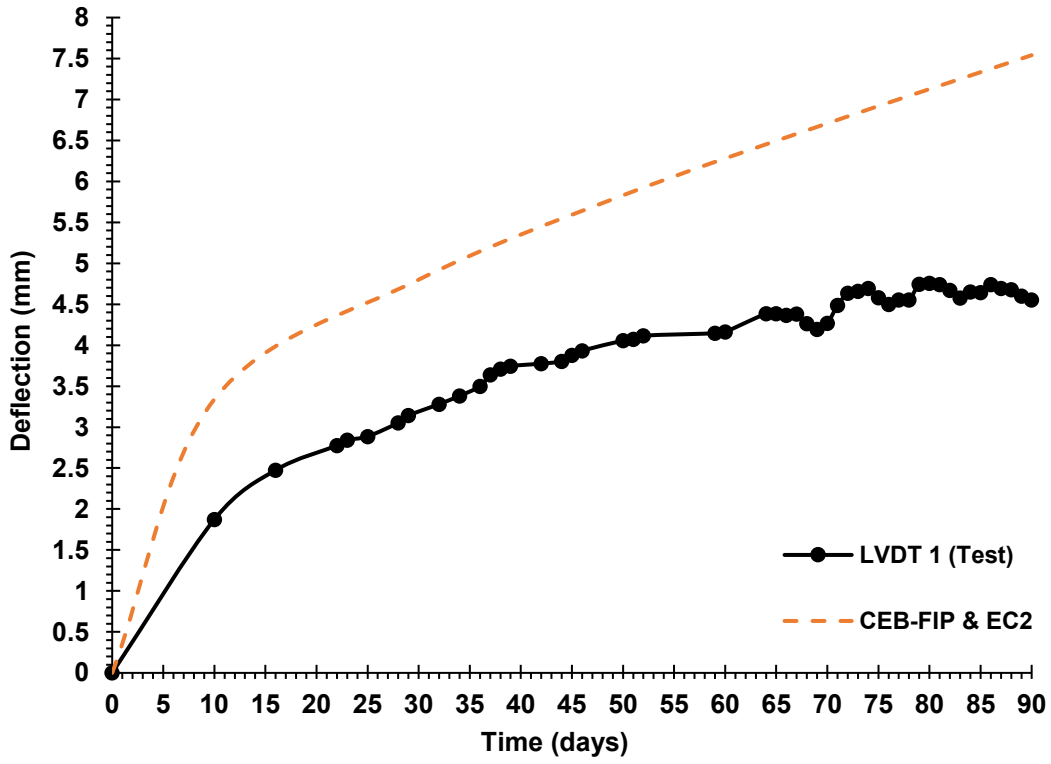

Figure 5-18.Comparison between measured and calculated long-term deflections for slab S2.

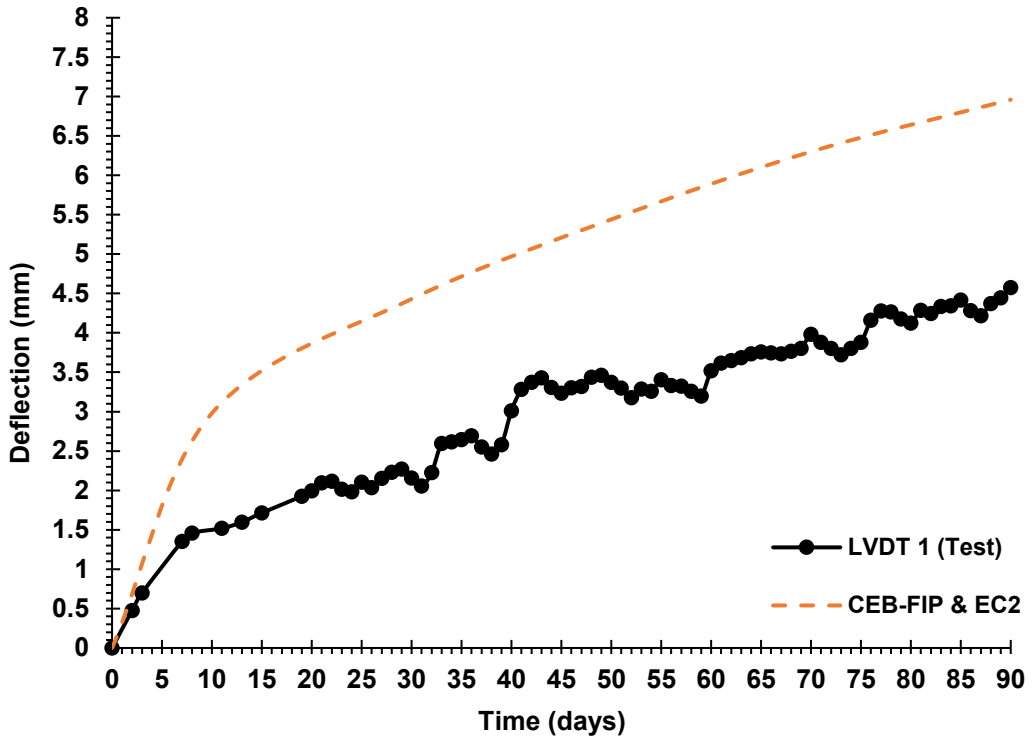

Figure 5-19. Comparison between measured and calculated long-term deflections for slab S3.

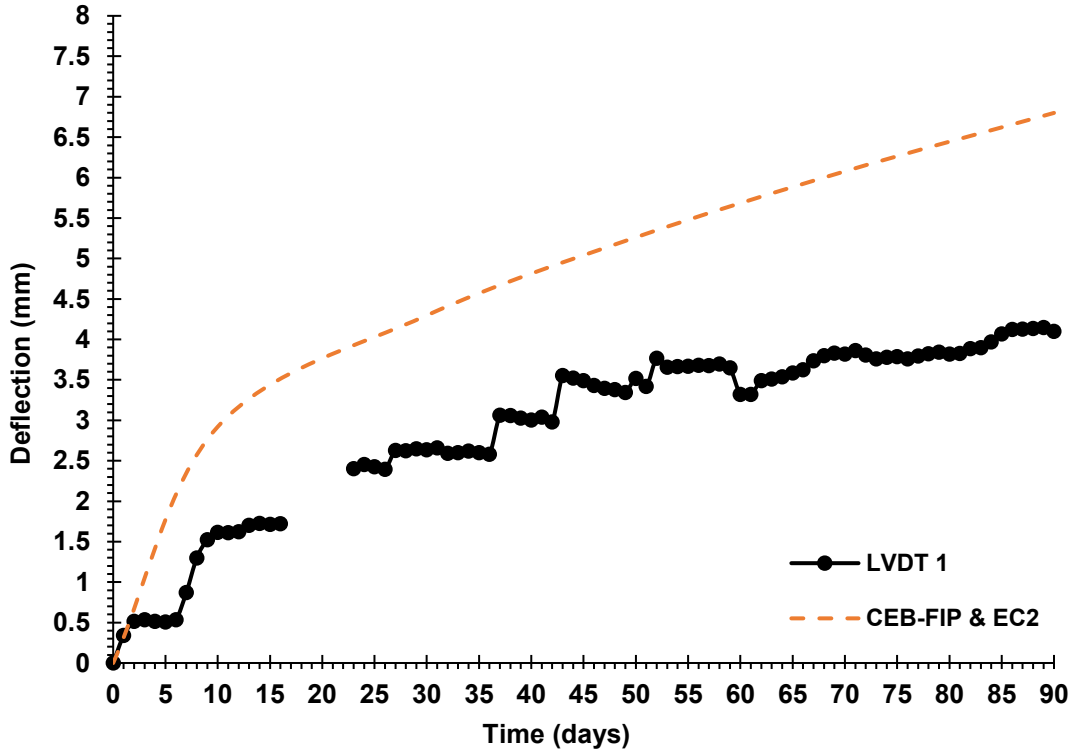

Figure 5-20. Comparison between measured and calculated short-term deflections for slab S4.

5.9 Parametric Studies

The last objective in this research was to perform a series of numerical experiments. Thus, in this section the parametric study based on verified numerical analysis procedure is presented. In many cases, however, the serviceability limit state of deflection is usually critical, rather than the ultimate limit states, specifically, in the case of flat plates and flat slabs. The final deflections, including instantaneous, depend primarily on the development of creep and shrinkage, tension stiffening, and time-dependent cracking that affect the magnitude of tension stiffening. This section aims to offer a clear picture of the variation of instantaneous and long-term deflection for slabs with and without openings, and hence give better evidence to understand the behaviour.

Therefore, the parametric study was carried out to investigate the influence of different opening sizes on the long-term deflections of partially cracked reinforced concrete slabs which could not be covered experimentally. There are several factors that influence the instantaneous load-deformation response. Of these, cracking and material nonlinearity are more predominant. Although it is possible to compute deflections using elastic theory of plates, the extent of cracking affects the stiffness and hence accurate predictions of deflections are not possible (Adan, et al. 2010). Under constant load, as the properties of concrete, the curvatures and flexural stiffness of the members is also influenced with time. Thus, the deflection attains values several times larger than the instantaneous deflection. As explained earlier, the first step in the prediction of long-term movements in partially cracked sections is usually to perform instantaneous nonlinear cracking analysis.

5.9.1 Parameters Considered

It is not reasonable to study all parameters that influencing the behaviour of the members. Obviously, the scope of any experimental program conducted in the laboratory remains restricted by the different aspects. In the present study, an attempt is made extensively to experimentally verify the proposed procedure to investigate the predictive capability of the analysis procedure that can be used to investigate the slab behaviour with different design situations, particularly the presence of opening. It was decided to select 60kN as a sustained loading in the

parametric study. The main investigated parameter in the present study is the size of openings with all other parameters kept constant. This is reasonable since there are wide range of researches in literature concern with the effect of material properties on the reinforced concrete slab behaviour.

As the properties of concrete, typically creep and shrinkage, develop with age, the deformation of a slab is affected. Thus, the CEB-FIP MC-90 was used for modelling creep and shrinkage deformations with time based on notional size of slab as shown in Figure 5-21 and Figure 5-22. The curing duration was assumed t_s =28 days and the age at loading was assumed t_0 =28 days. Moreover, the average relative humidity was assumed 60%.

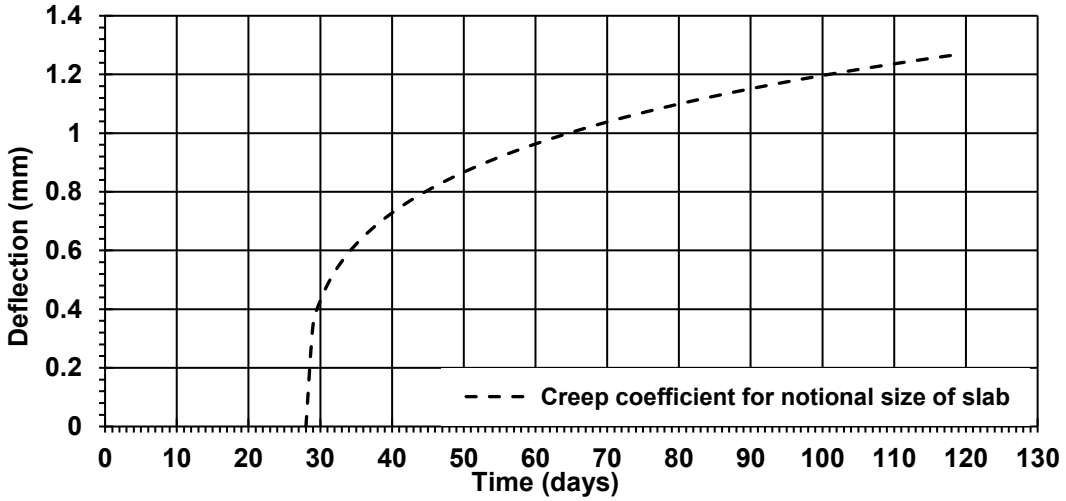

Figure 5-21. Creep coefficient based on CEB-FIP MC-90

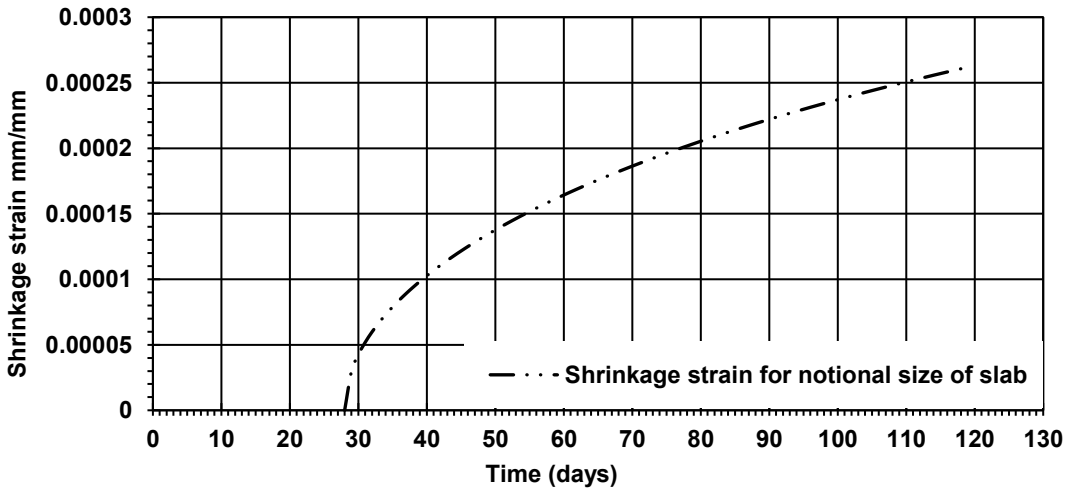

Figure 5-22. Shrinkage strain based on CEB-FIP MC-90

The concrete compressive strength was assumed 35 MPa. The analytical model derived by (Gardner, 1990) was used to predict the splitting tensile strength. Moreover, the modulus of elasticity of concrete E_c was predicted using (ACI-209.2R, 2008). The long- and short-term material properties are listed in Table 5-1.

Table 5-1: Parametric study considerations.

Sustained load (kN)	60
Modulus of concrete elasticity (MPa)	29000
Splitting tensile strength (MPa)	3.55
Compressive strength (MPa)	35
R.H. %	60
Age at loading $\boldsymbol{t_0}$ (days)	28
Curing duration $\boldsymbol{t_s}$ (days)	28

All slabs had the same dimensions with clear span of 1500x1500x125 mm. The loaded area had a dimension 200 x 200 mm. The details of slab geometry and opening sizes are illustrated in Figure 5-23 and Figure 5-24. Totally five slabs with different opening sizes are introduced. Of these, one slab as reference. The flexural reinforcement for all slabs were assumed orthogonal and comprised of 8 mm diameter with clear spacing 95 mm c/c deformed bars. The same analysis procedure which described in the section 4.9 is followed in the parametric analysis.

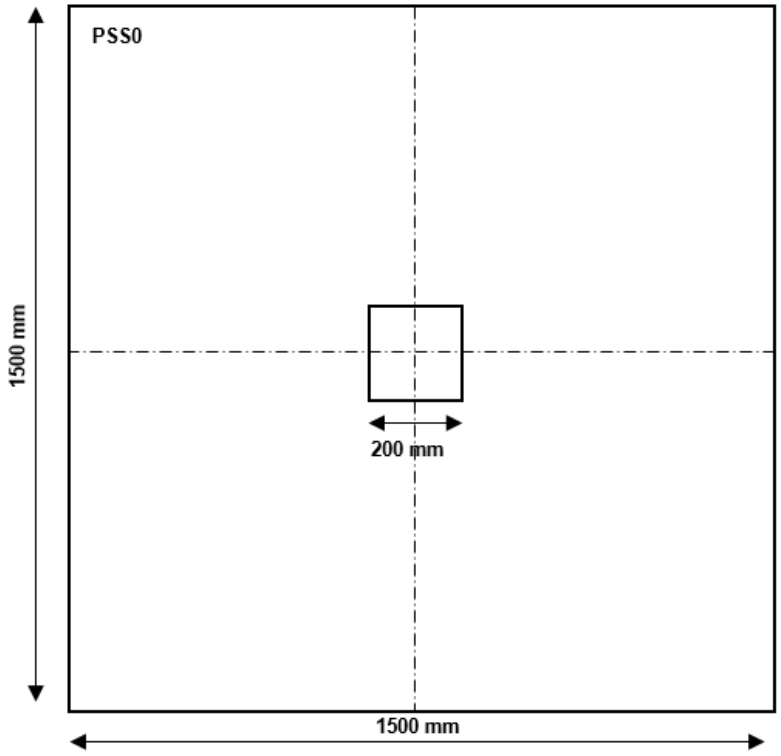

Figure 5-23. Schematic of reference slab

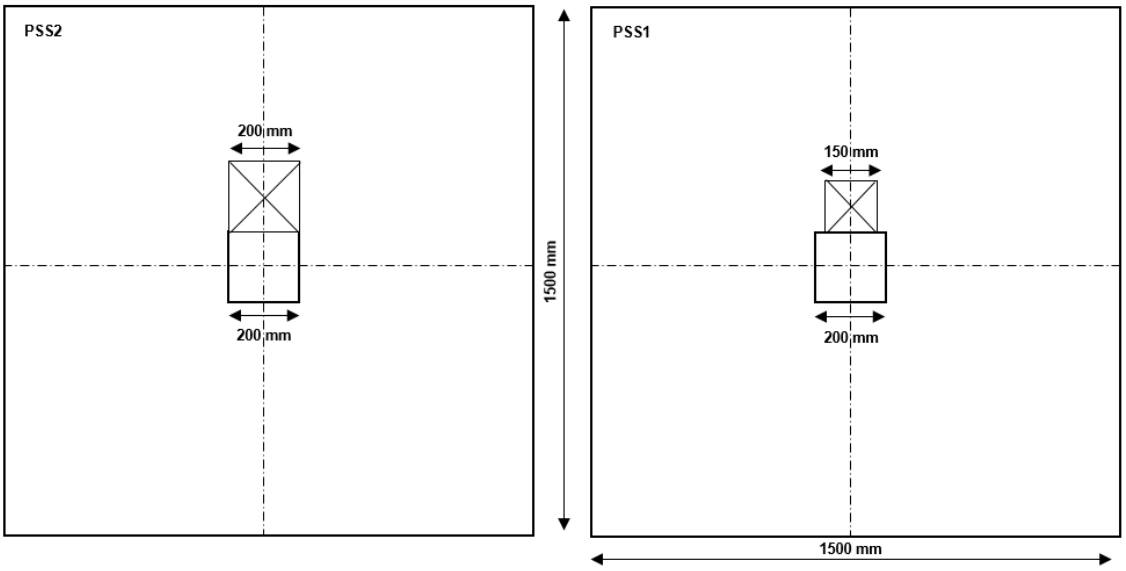

(a)

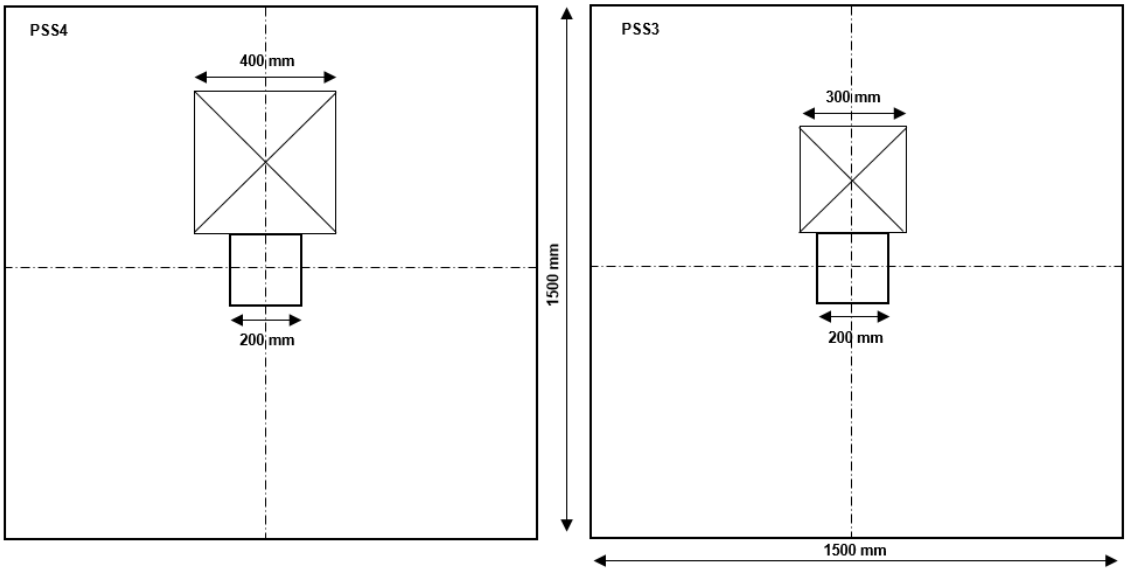

(a)

Figure 5-24: Schematic of slabs with different opening sizes

5.9.2 Influence of Opening Sizes on Deflections

In this section, the calculated deflections at the centre for five slabs are presented and discussed. Figure 5-25 shows the computed long-term deflection curves for slabs PSS0, PSS1, PSS2, PSS3, and PSS4, respectively. It has already been noted earlier that the solid slab gives good agreements when the tensile creep coefficient is equal seven times compressive creep coefficient. From the observations on the curves, it can be noted that the deflection increases with time for all slabs. From the comparison, it is evident that the long-term deflections of slabs with opening are greater than solid slab PSS0. This would be expected since the presence of openings reduces the bending stiffness and hence the instantaneous and long-term curvatures are influenced. As can be seen, there were significant differences in the time-deflection curves when the opening sizes increases further. This is sufficient evidence to suggest that the influence of openings on the long-term deflection with time is not minor.

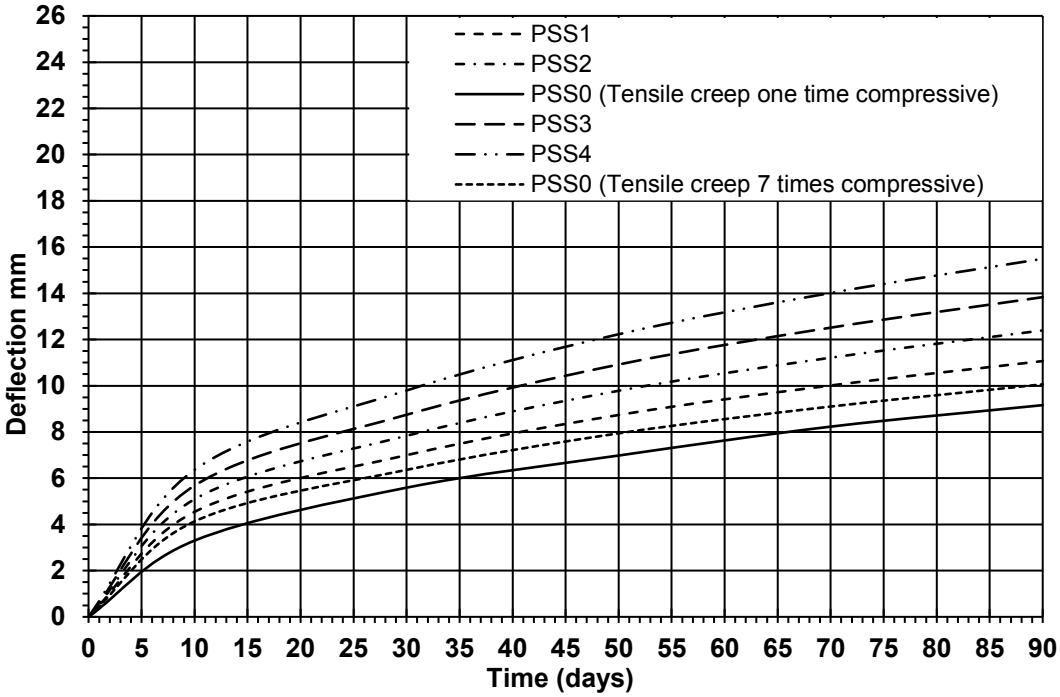

Figure 5-25. long-term deflections of slabs

Comparison of the variation of instantaneous and long-term deflections for different opening sizes is also shown in Figure 5-26. In all cases, it can be noted that the deflection increases with time for all slabs. From the comparison, it is obvious that the deflections for slabs with openings are greater than solid slab PSS0. As explained earlier, this would be expected since the presence of openings reduces the bending stiffness and hence the instantaneous and long-term curvatures are influenced. It is seen that the presence of openings influences both instantaneous and long-term deflections significantly. As the opening sizes increased, it starts to affect the behaviour of time- deflection curves. Again, from observations on parametric study, it can be noted that the instantaneous deflections increased when the opening size increases. This in line with observations in literature provided by (Bhatti et a.,1996).

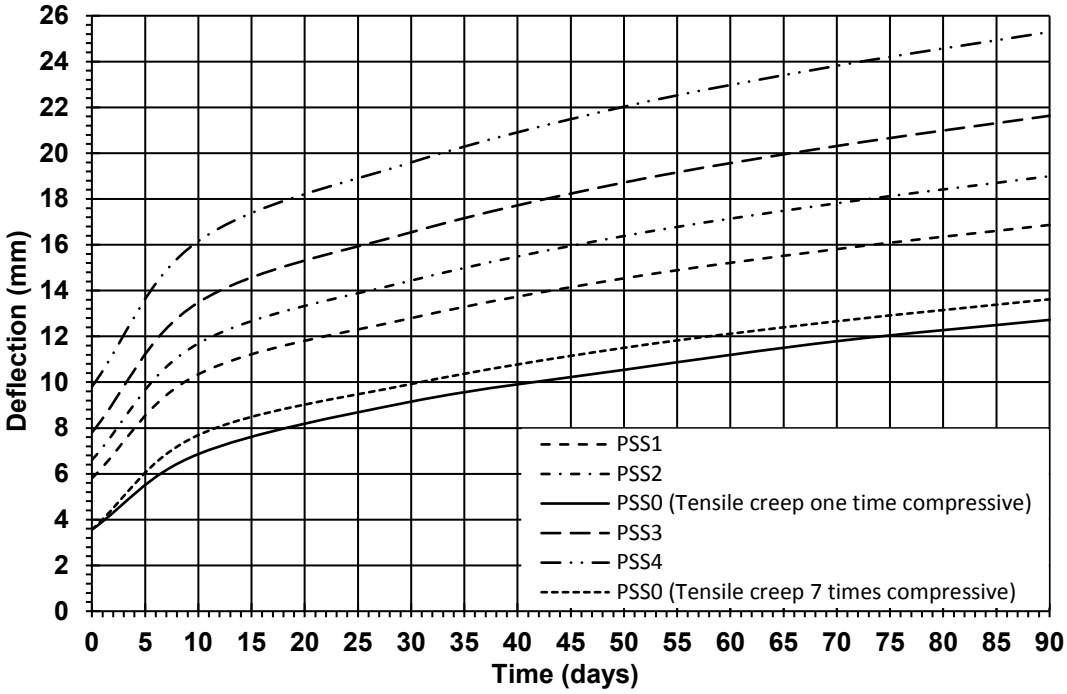

Figure 5-26. Instantaneous and long-term deflections of slabs

Chapter 6 Conclusions and Recommendations

6.1 Summary

A literature review on the available research was carried out to develop the numerical analysis method. The method of analysis was developed to estimate short- and long-term flexural deformations in partial cracked slabs. In Chapter 4, the numerical method developed in this study have been demonstrated to compute reasonably accurate quantitative results. In Chapter 5, the method has been employed to verify the process of analysis procedure through a series of large full-scale of experiments. Thereafter, the parametric study has been carried out to investigate the influence of openings on instantaneous and long-term deflections. Furthermore, the analytical models have been evaluated critically through a series of experimental tests. Based upon the work presented in this research, the following conclusions and recommendations have been summarized.

6.2 Conclusions

From presented figures and curves, general conclusions and observations of this research are summarized in the following three sections:

6.2.1 Conclusions Based on the verifications of the numerical method

- In general, based on the finite difference approach, the mesh size refinement has a relatively slight difference on the convergence of load-elastic deflection results of solid slab while it has relatively significant difference for slabs with openings when the mesh size larger than 50 mm.
- In general, the finite differences method has simplified the solving of higher order differential equations of plate by replaces them into algebraic linear simultaneous equations with high efficiency. It has simplified boundary condition representations in terms of forces and displacements.
- Layered analysis approach offered good option to trace the change of sectional properties.

- While the perfect bond assumption with smeared crack model does not consider the loss of bond stress after cracking, it has usually provided good estimation of deflections for solid slab.
- The presence of the opening in the slab next to column affected the estimation of deflections compared with solid slab.
- In general, the calculated steel strains showed lower values than measured values for all slabs.
- While there are no criteria to evaluate the combined effects of creep, shrinkage, cracking and tension stiffening, it can be concluded that the current proposed procedure has successfully modelled these phenomena.
- The ratio of tensile to compressive creep was not unity and it was dependent on the level of applied stress/strength ratio.
- While it is impossible to distinguish between the flexural deformations caused by creep, shrinkage, and time-dependent cracking. However, it can be concluded that the current method is able to compute the long-term deflections reasonably.

6.2.2 Conclusions Based on the Evaluation of Code-based models

- The model for effective curvature incorporated in CEB-FIP2010 and Eurocode 2 (BSI, 2004) for cracked members have been presented and their applicability has been evaluated critically against experimental data. The effective curvature method has been shown to accurately model the shape of the load-deflection response of slabs in the service load levels.
- A proposed value of $0.33\sqrt{f'_c}$,which has been suggested to estimate the reduction in effective modulus of rupture due to restraint stresses, showed good agreements in term of cracking load for both solid slab and slabs with opening.
- The model provided by CEB-FIP2010 and Eurocode 2 (BSI, 2004) for prediction of long-term defections of cracked members have been introduced. Although the model considers a constant stress with time, the model showed good agreement in terms of the long-term deflections. While the model has been shown to highly overestimate the long-term deflections for slabs with openings.

6.2.3 Conclusions Based on the Parametric Study

- A parametric study was carried out to investigate the influence of opening on the deflections of slabs with and without opening by using the verified numerical analysis procedure. The results showed that the presence of the opening increases the instantaneous deflection values in comparison with the solid slab.
- The results showed that the increasing of the opening sizes leads to increasing the instantaneous deflections.
- The results confirmed that the presence of the opening increases the long-term deflections in comparison with solid slab.
- The results gave clear evidence to conclude that the increasing of opening sizes leads to increase in the long-term deflection of slabs.

6.3 Recommendations and Future Research

The following are recommendations areas for further research.

- During this study, the cracking was modelled as smeared fixed as well as the reinforcing steel was assumed as smeared with perfect bond assumption. Thus, advanced approaches for discrete crack and bond-slip are needed with combination of creep and shrinkage effects. This if confirmed by further research, may have significant practical consequences.
- Further analyses are needed with different boundary conditions that can be supported by experimental programme to study the effect of end conditions on the response of partially cracked slabs.
- In the future, the FEA commercial software could be improved to consider the creep and shrinkage effects with cracking nonlinear analysis.
- During this study the loss of tension stiffening due to internal damage were not considered in the modelling of the time-depending cracking. Thus, more developments are needed to include these phenomena.
- Further investigations for evaluation the inequality between the tensile and compressive creep should be examined with more design scenario.
- The influence of other parameters that affect the short- and long-term flexural behaviour such as different opening geometries, adding flexural reinforcement in compression requires more investigation.
- Universal models for biaxial tension stiffening tests that incorporates longitudinal and transverse reinforcement bar are strongly required.
- Appropriate treatments on concrete stress-strain relationships are needed to deal with creep and shrinkage phenomena as pre-strains in the nonlinear cracking analysis.

6.4 References

Abrishami, H. H., & Mitchell, D. (1996). Influence of splitting cracks on tension stiffening. ACI Structural Journal, 93(6), 703-710.

ACI318. (2014). Building Code Requirements for Structural Concrete and Commentary.

ACI-207.2R. (2002). Effect of Restraint, Volume Change, and Reinforcement on Cracking of Mass Concrete. *American Concrete Institute*.

ACI-209.2R. (2008). Guide for modeling and calculating shrinkage and creep in hardened concrete. *American Concrete Institute,ACI Committee 209 , Farmington Hills,Michigan.*

ACI-318. (2014). *ACI 318-14 Building Code Requirements for Structural Concrete and Commentary (Metric)*: American Concrete Institute.

ACI-435.9R-91. (1991). State of the art report on conctrol of two way slab deflections. *ACI Structural Journal, 88*(4), 501-514.

ACI-209.1R. (2005). Report on factors affecting shrinkage and creep of hardned concrete. ACI Committee 209.

224.2R-92 (1992). Cracking of concrete members in direct tension. Re approaved 1997.

ACI-ASCE-Committee-326. (1962). ACI-ASCE Committee 326 (now 426) .Shear and Diagonal Tension. Journal of ACI, Vol. 59, No.1–3, pp. 1–30, 277–334, 352–396; also discussion and closure Vol. 59, No.10, pp.1323–49.

Aikaterini, S., Genikomsou, & Polak, M. A. (2017). Effect of Openings on Punching Shear Strength of Reinforced Concrete Slabs—Finite Element Investigation. *ACI Struct J., 114*(5), 1249-1262.

Anil, O., Kina, T., & Salmani, V. (2014). Effect of opening size and location on punching shear behaviour of two-way RC slabs. *Magazine of Concrete Resarch, 66*(18), 955--966.

ASCE-Task-Committee. (1982). ASCE Task Committee on Finite Element Analysis of Reinforced Concrete Structures. Finite Element Analysis of Reinforced Concrete. American Society of Civil Engineers, New York, 533.

Bazant, Z. (1988). Mathematical Modeling of Creep and Shrinkage of Concrete. *1988 John Wiley & Sons Ltd, New York*.

Bazant, Z. P., & Baweja, S. (1995). Creep and Shrinkage Prediction Model for Analysis and Design of Concrete Structures. *-Model B3," Materials and Structures, 28*, 357-365, 415-430, 488-495. .

Bazant, Z. P., & Baweja, S. (2000). Creep and Shrinkage Prediction Model for Analysis and Design of Concrete Structures. *: Model B3," The Adam Neville Symposium: Creep and Shrinkage-Structural Design Effects, SP-194*.

Bazant, Z. P., & Oh, B. H. (1984). Deformation of progressively cracking reinforced. *concrete beams.ACI Journal, 81*(3), 268-278.

Bach, C., & Graf, O. (1915). Tests of square and rectangular reinforced concrete slabs supported on all sides. Berlin, 30, 1-309.

Balazs, G. L. (1993). Cracking analysis based on slip and bond stresses. ACI Materials Journal, 90(4), 340-348.

Bhatti, M.A., Lin, B. and Vega, J.I.M., 1996. Effect of openings on deflections and strength of reinforced concrete slabs. Special Publication, 161, pp.149-164.

Bazant, Z. P., & Xi, Y. (1994). Drying creep of concrete: constitutive model and new experiments separating its mechanisms. Materials and structures, 27, 3-14.

Beeby, A. W., & Scott, R. H. (2006). Mechanisms of long-term decay of tension stiffening. Magazine of Concrete Research, 58(5), 255-266.

Bergan, P. G. (1978). Finite Elements in Nonlinear Mechanics. *Norwegian Institute of Technology, Trondheim, Norway*.

Bischoff, P. H. (2001). Effects of shrinkage on tension stiffening and cracking in reinforced concrete. *Canadian Journal of Civil Engineering, 28*(3), 363-374.

Bischoff, P. H. (2005). Reevaluation of deflection prediction for concrete beams reinforced with steel and fiber reinforced polymer bars. Journal of Stuctural Engineering ASCE, 131(5), 752-767.

Bischoff, P. H., & Paixao, R. (2004). Tension stiffening and cracking of concrete reinforced with glass fiber reinforced polymer (GFRP) bars. Canadian Journal of Civil Engineering, 31, 579-588.

Bischoff, P. H., & Scanlon, A. (2007). Effective moment of inertia for calculating deflections of concrete members containing steel reinforcement and fiber-reinforced polymer reinforcement. ACI Structural Journal, 104(1), 68-74.

Blaauwendraad, J., & Grootenboer, H. J. (1981). Essentials for discrete crack analysis. *IABSE Colloquium on Advanced Mechanics of Reinforced Concrete*, 263-272.

Blakey, F. A. (1961). Deformations of an Experimental Lightweight Fiat Plate Structure. *Civ. Engg. Trans., Institution of Engineers,Australia, Vol. CE3, No. 1, March, 1961., CE3*(1).

Borg, S. F. (1962). Fundamentals of engineering elasticity. *Van Nostrand Reinhold Company, New York*.

Borgas, L., Melo, G., & Gomas, R. (2013). Punching shear of reinforced concrete flat plates with openings. *ACI Struct J., 110*(4), 547-556.

Boon, K. H., Diah, A. M., & Loon, L. Y. (2009). FLEXURAL BEHAVIOUR OF REINFORCED CONCRETE SLAB WITH OPENING. Malaysian Technical Universities Conference on Engineering and Technology, Proceedings of MUCEET2009.

Branson, D. E. (1965). Instantaneous and time-dependent deflections on simple and continuous reinforced concrete beams. *Alabama Highway Department, Bureau of Public Roads, HPR Report No. 7, Part 1,*, 1-78.

Branson, D. E. (1977). Deformation of Concrete Structures, *McGraw Hill Book Co., New York.*

Brooks, J. J. (2005). 30-year creep and shrinkage of concrete. *Magazine of Concrete Research,University of Leeds, 57*(9), 545-556.

BS8110-1:1997. British Standard Institute. 1997. BS 8110-1: 1997 Structural Use of Concrete – Part 1: Code of Practice for Design and Construction. London: British Standard Institute.

BS8110-2:1985. (1985). British Standard Institute. 1985. BS 8110-2: 1985 Structural use of concrete – Part 2: Code of Practice for Special Circumstances. London: British Standard Institute.

BS EN 206, A. 2013. Concrete: Specification, performance, production and conformity.

BS EN 197-1. 2011. BS EN 197-1: 2011. Cement, Composition, Specifications and Conformity Criteria for Common Cements. London, England: British Standard Institution (BSI).

BS EN 12390-3. 2009. 12390-3: 2009, 2009. Testing Hardened Concrete. Compressive Strength of Test Specimens. British Standards Institution.

BS EN 12390-6. 2009. 12390-6 (2009)"Testing Hardened Concrete. Tensile Splitting Strength of Test Specimens". British Standard Institution, London

BS EN 1008 2002. Mixing Water for Concrete. Specification for Sampling, Testing and Assessing the Suitability of Water.

BS 882:1992 Specification for aggregate from natural sources for concrete. London: British Standard Institution

Bubnov, I. G. (1914). Theory of Structures of Ships. *St. Petersburg, 2*.

Cauchy, A. L. (1828). Sur l'equilibre le mouvement d'une plaque solide. *Exercises Math, 3*, 328.

CEB-FIP-MC2010. (2010). FIP (fédération internationale du béton) (fib),2010. *Lausanne, Switzerland*.

CEB-FIP. (1990). CEB-FIP90 model code 1990. *Comitee Euro-Internationale Du Beton*.

Cervera, M., & Chiumenti, M. (2006). Smeared crack approach: back to the original track. International Journal for Numerical and Analytical Methods in Geomechanics, 30, 1173-1199.

Chu, K. H., & Carreira, D. J. (1986). Time-dependent cyclic deflections in RC beams. *Journal of Structural Engineering, 112*(5), 943-959.

Chong, K. T. (2004). Numerical modelling of time-dependent cracking and deformation of reinforced concrete structures. (PhD thesis), The University of New South Wales, Sydney, Australia, School of Civil and Environmental Engineering,

Clough, R. W. (1962). The stress distribution of Norfolk Dam. *Structures and Materials Research, 100*(19).

Clough, R.W., 1965. The finite element method in structural mechanics. Chapter 7 of Stress analysis, pp.85-119.

Clark, L. A., & Cranstown, W. B. (1979). The influence of bar spacing on tension stiffening in reinforced concrete slabs. Advances in concrete slab technology, Pergammon Press, London.

Collins, M. P., & Mitchell, D. (1980). Shear and torsion design of prestressed and non-prestressed concrete beams. *PCI Journal, 25*(4), 32-100.

Collins, M. P., & Mitchell, D. (1991). Prestressed concrete structures. Prentice-Hall Inc., Englewood Cliffs, N.J.

Concrete-Society. (2005). Deflections in concrete slabs and beams: report of a joint project of the British Cement Association, The Concrete Society and The Concrete Centre. Concrete Society technical report(58).

Crisfield, M. A. (1982). Local instabilities in non-linear analysis of reinforced concrete beams and slabs *Proceedings Institution of Civil Engineers*, 135-145.

Darwin, D. (1993). "Reinforced Concrete." Finite Element Analysis of Reinforced Concrete Structures II: Proceedings of the International Workshop, J. Isenberg, ed., ASCE, New York, pp. 203-232.

Dilger, W., & Neville, A. M. (1971). Method of creep analysis of structural members. *.ACI, SP 27-17, 349–379.*

Efsen, A., & Glarbo, O. (1956). Tensile Strength of Concrete Determined by Cylinder Splitting Test. *Benton Og Jernbeton (Copenhagen), 1*, 33-39.

El-Salakawy, E. F., Polak, M. A., & Soliman, M. H. (1999). Reinforced Concrete Slab-Column Edge Connections with Openings. *ACI Structural Journal 96*(1), 79-87.

Elstner, R. C., & Hognested, E. (1956). Shearing strength of reinforced concrete slabs. *American Concrete Institute, 53*(2), 29-58.

Eurocode2. (2004). British Standard Institute. 2004. BS EN 1992-1-1: 2004 Eurocode 2: Design of concrete structures – Part 1-1: General rules and rules for buildings. London: British Standard Institute.

Faber, O. (1927). Plastic yield, shrinkage and other problems of concrete and their effects on design. *Proceedings of the Institution of Civil Engineers, 225, Part I, London, 27–73.*

Fernandez, R. M., & Muttoni, A. (2009). Applications of the critical shear crack theory to punching of RC slabs with transverse reinforcement *American Concrete Institute Structural Journal, 106*(4), 485-494.

fip-Model-Code. (2010). Fib model code for concrete structures 2010.

Fields, K., & Bischoff, P. H. (2004). Tension stiffening and cracking of high-strength reinforced concrete tension members. ACI Structural Journal, 101(4), 447-456.

Flugge, W. (1962). Handbook of Engineering Mechanics. *McGraw-Hill Book Company, New York*.

Fluhr, W. E., Ang, A., & Siess, C. P. (1960). Theoretical analysis of the effects of openings on the bending moments in square plates with fixed edges. *University of Urbana Illinois, Structural Research Series No. 203, Carried out in part under National Science Foundation*.

Foppl, A. (1951). Vorlesungen uber technische Mechanik

Verlag R., Oldenburg, Munich, 1944, 1951. *Verlag R., Oldenburg, Munich, 1 & 2*.

Forth, J. P. (2014). Predicting the tensile creep of concrete. *Cement & Concrete Composites, 55*, 70-80.

Forth, J. P., Mu, R., Scott, R. H., Jones, A. E., & Beeby, A. W. (2013). Verification of cracked section shrinkage curvature models. *Structures and Buildings,Proceedings of the Institution of Civil Engineers*.

Galerkin, B. G. (1933). Thin Elastic Plates. *Gostrojisdat Leningrad*.

Gardner, N. J. (1990). Effect of Temperature on the Early-Age Properties of Type I, Type III, and Type I/Fly Ash Concretes. *ACI Materials Journal, 87*(1), 68-78.

Gardner, N. J., & Lockman, M. J. (2001). Design Provisions for Drying Shrinkage and Creep of Normal Strength Concrete. *ACI Materials Journal, 98*(2), 159-167.

Gardner, N. J. (2011). Span/Thickness Limits for Deflection Control. ACI Structural Journal, American Concrete Institute,Farmington Hills, 108(4), 453-460.

Genikomsou, A. (2015). Nonlinear Finite Element Analysis of Punching Shear of Reinforced Concrete SlabColumn Connections. thesis,Waterloo, Ontario, Canada.

Ghali, A., Favre, R., & Elbadry, M. (2002). Concrete structures: Stresses and deformations. *London and New York*(Third edition).

Ghali, A. (1987). Prediction of deflections of two-way floor systems. presented at 1987 ACI Fall Convention, Seattle, Washington.

Ghali, A. (1993). Deflection of Reinforced Concrete Members: A Critical Review. ACI Structural Journal, American Concrete Institute, Farmington Hills,, 90(4), 463-473.

Ghali, A., Favre, R., & Elbadry, M. (2011). Concrete Structures: Stresses and Deformations: Analysis and Design for Sustainability, 4th edition, CRC Press, Boca Raton, p. 646.

Gilbert, R. I. (1979). Time-dependent behaviour of structural concrete slabs. (PhD thesis), The University of New South Wales, Sydney, Australia.,

Gilbert, R. I. (2004). Cracking and crack control in reinforced concrete structures subjected to long-term loads and shrinkage. 18th Australasian conf. on the Mechanics of structures and Materials (ASMSM18), University of W.A., Perth, Balkema, the Netherlands, 803-809.

Gilbert, R. I. (2007). Tension stiffening in lightly reinforced concrete slabs. Journal of Structural Engineering, ASCE, 133(6), 899-903.

Gilbert, R. I. (2011). The serviceability limit states in reinforced concrete design. Procedia engineering, The Twelfth East Asia-Pacific Conference on Structural Engineering and Construction, 14, 385–395.

Gilbert, R. I. (2017). Cracking caused by early-age deformation of concrete prediction and control. Procedia Engineering, Modern Building Materials, Stuctures and Techniques, MBMST 2016, 172, 13-22.

Gilbert, R. I., & Warner, R. F. (1978). Tension Stiffening in Reinforced Concrete Slabs. Proceedings, Structural Engineering Division, ASCE, Vol. 104, No. ST12, pp. 1885–900

Gilbert, R. (2008). Calculation of Long-Term Deflection. *In CIA Seminar*.

Gilbert, R. I. (1988). Time effects in concrete structures. *Amsterdam ; New York : Elsevier, 1988.*

Gilbert, R. I. (2001). Deflection Calculation and Control -Australian Code Amendments and Improvements. *ACI international Special Publication SP 203, Code Provisions for Deflection Control in Concrete Structures, Chapter 4, American Concrete Institute. Editors E.G. Nawy and A. Scanlon, Detroit*, 45–78.

Gilbert, R. I., & Guo, X. H. (2005). Time-dependent deflection and deformation of reinforced concrete flat slabs—An Experimental Study. *ACI Structural Journal, 102*(3), 363-373.

Gilbert, R. I., & Ranzi, G. (2010). Time-dependent behaviour of concrete structures. *London and New York : CRC Press*.

Gillbert, R. I., & Wu, H. Q. (2009). Time-dependent stiffness of cracked reinforced concrete elements under sustained actions. *Australian Journal of Structural Engineering, Taylor and Francis, 9*(2).

Gilbert, R.I. and Warner, R.F., 1977. Nonlinear analysis of reinforced concrete slabs with tension stiffening. UNICIV Rep. No. R-167, Studies from the School of Civil Engineering, Univ. of New South Wales, Kensington, Australia.

Goto, Y. (1971). Cracks formed in concrete around deformed tension bars. ACI Journal, 68(4), 244-251.

Graf, O. (1933). Tests of reinforced concrete slabs under concentrated load applied near one support. Berlin, 73.

Guan, H., & Loo, Y. C. (1997). Flexural and shear failure analysis of reinforced concrete slabs and flat plates. *Advances in Structural Engineering, 1*(1), 71-85.

Hatt, W. K. (1907). Notes on the Effect of Time Element in Loading Reinforced Concrete Beams *Proc. ASTM 7*, 421-433.

Ha, T., Lee, M., Park, J., & Kim, D. (2015). Effects of openings on the punching shear strength of RC flat-plate slabs without shear reinforcement. The Structural Design of Tall and Special Buildings, 24(15), 895-911.

Hand Jr, F.R., Pecknold, D.A. and Schnobrich, W.C., 1972. A layered finite element nonlinear analysis of reinforced concrete plates and shells. University of Illinois Engineering Experiment Station. College of Engineering. University of Illinois at Urbana-Champaign.

Hand, F.R., Pecknold, D.A. and Schnobrich, W.C., 1973. Nonlinear layered analysis of RC plates and shells. Journal of the structural division, 99(7), pp.1491-1505.

Hansen, T. C., & Mattock, A. H. (1966). Influence of size and shape of member on the shrinkage and creep of concrete. Journal of the American Concrete Institute, 63(2), 267-290.

Hencky, H. (1921). Der spanngszustand in rechteckigen platten. *Z Andew Math und Mech, 1*.

Hillerborg, A. (1985). Numerical methods to simulate softening and fracture of concrete. *In Fracture mechanics of concrete: structural application and numerical calculation.Springer, Dordrecht*, 141-170.

Hobbs, D. W. (1979). Shrinkage-induced Curvature of Reinforced Concrete Members. *Cement and Concrete Association,London, UK.*

Hognestad, E. (1951). A study on combined bending and axial load in reinforced concrete members. *Univ. of Illinois Engineering Experiment Station, Univ. of Illinois at Urbana-Champaign*, 43-46.

Hognestad, E. (1953). Shearing strength of reinforced concrete column footings. ACI Journal, 50, 189-208.

Hognestad, E., Elstner, R. C., & Hanson, J. A. (1964). hear Strength of Reinforced Structural Lightweight Aggregate Concrete Slabs. *American Concrete Institute, 61*(6), 643-655.

Hordijk, D. A. (1991). Local Approach to Fatigue of Concrete. . ***PhD thesis, Delft University of Technology*****.**

Huber, M. T. (1929). Probleme der Static Techish Wichtiger Orthotroper Platten. ***Warsawa***

Jiang, J. and Mirza, F.A., 1997. Nonlinear analysis of reinforced concrete slabs by a discrete finite element approach. Computers & structures, 65(4), pp.585-592.

Jofriet, J. C., & McNeice, G. M. (1971). Finite Element Analysis of RC Slabs. ***Journal of Structural Division, ASCE, 97*****(ST3), 785-806.**

Jones, J., Wua, C., Oehlers, D. J., Whittaker, A. S., Sun, W., Marks, S., & Coppola, R. (2009). Finite difference analysis of simply supported RC slabs for blast loadings. Engineering Structures, 31, 2825-2832.

Kaklauskas, G., & Gribniak, V. (2011). Eliminating shrinkage effect from momentcurvature and tension-stiffening relationships of reinforced concrete members. Journal of Structural Engineering,, 137(12), 1460-1469.

Kaklauskas, G., Gribniak, V., Bacinskas, D., & Vainiunas, P. (2009). Shrinkage influence on tension stiffening in concrete members. Eng Struct 2009;31:1305–12., 31, 1305-1312.

Kent, D. C., & Park, R. (1971). Flexural members with confined concrete. ***Journal of the Structural Division, Proc. of the American Society of Civil Engineers, 97*****, 1969-1990.**

Kinnunen, S., & Nylander, H. (1960). Punching of Concrete Slabs Without Shear Reinforcement. . ***Transactions of the Royal Institute of Technology, No. 158, Stockholm, Sweden*****, 112.**

Kirchhoff, G. R. (1850). Uber das gleichgewichi und die bewegung einer elastishem scheibe. ***J Fuer die Reine und Angewandte Mathematik, 40*****, 51-88.**

Kupfer, H., & Hilsdorf, H. K. (1969). Behaviour of Concrete under Biaxial Stress. ***Concrete institute, 66*****(8), 656-666.**

L'Hermite, R. (1959). Actual Ideas About the Technology of Concrete. , ***Annals, Technical Institute of Building and Public Works, Paris*****, 115-116.**

Lee, J., & Fenves, G. L. (1998). Plastic-Damage Model for Cyclic Loading of Concrete Structures. ***Journal of Engineering Mechanics, 124*****(8), 892-900.**

Levy, M. (1899). Memoire sur la theorie des plaques elastiques planes,. ***J Math Pure Appl, 3*****, 219.**

Lima, M.V.A., Lima, J.M.F. and Lima, P.R.L., 2014. Finite Difference Energy Method for nonlinear numerical analysis of reinforced concrete slab using simplified isotropic damage model. Revista IBRACON de Estruturas e Materiais, 7(6), pp.940-964.

Lin, C.S. and Scordelis, A.C., 1975. Nonlinear analysis of RC shells of general form. Journal of the Structural Division, 101(3), pp.523-538.

Loo, Y. C., & Guan, H. (1997). Cracking and punching shear failure analysis of RC flat plates. *Journal of Structural Engineering, ASCE, 123*, 1321-1330.

Lubliner, J., Oliver, J., Oller, S., & Onate, E. (1989). A Plastic-Damage Model for Concrete. *International Journal of Solids and Structures, 25*(3), 299-326.

Marti, P., Alvarez, M., Kaufmann, W., & Sigrist, V. (1998). Tension chord model for structural concrete. Structural Engineering International, 98(4), 287-298.

McHenry, D. (1943). A new aspect of creep in concrete and its application to design. *Proceedings of the ASTM, 43*, 1069–1084.

McNeice, G. M.,1967. Elastic-plastic bending analysis of plates and slabs by the finite element method. Ph.D. Thesis presented to the University of London, London, England.

McCormac, J.C. and Brown, R.H., 2015. Design of reinforced concrete. John Wiley & Sons.

Moe, J. (1961). Shearing strength of reinforced concrete slabs and footings under concentrated

loads. *Development Department Bulletin D47, Portland Cement Association, Skokie, Illinois.*

Mowrer, R. D., & Vanderbilt, M. D. (1967). Shear Strength of Lightweight Aggregate Reinforced Concrete Flate Plates. *ACI Journal Proceedings, 64*(11), 722-729.

Mu, R., Forth, J. P., & Beeby, A. W. (2008). Modelling of shrinkage induced curvature of cracked concrete beams. *Tailor Made Concrete Solutions (Walraven JC and Steelhurst D (eds)). Taylor & Francis, Abingdon, UK, 573–578*.

Mu, R., Forth, J. P., Beeby, A. W., & Scott, R. (2008). Modelling of shrinkage induced curvature of cracked concrete beams. *Tailor Made Concrete Solutions (Walraven JC and Steelhurst (eds). Taylor & Francis, Abingdon, UK* 573-578.

Muttoni, A. (2008). Punching shear strength of reinforced roncrete slabs without transverse reinforcement,. *ACI Structural Journal 105*(4), 440-450.

Neville, A. M., & Brooks, J. J. (1975). Estimating long-term creep and shrinkage from short-term tests. *Magazine of concrete research, 27*(90), 3-12.

Neville, A. M., Dilger, W. H., & Brooks, J. J. (1983). Creep of Plain and Structural Concrete. *Construction Press (Longman Group Ltd).*

Ngo, D., & Scordelis, A. C. (1967). Finite Element Analysis of Reinforced Concrete Beams. *ACI Journal, 64*(14).

Ng, C. K., Edward, T. J., & Lee, D. K. T. (2008). Theoretical Evaluation on Effects of Opening on Ultimate Load-carrying Capacity of Square Slabs. Electronic Journal of Structural Engineering, 8.

Nilson, A. H. (1968). Nonlinear analysis of reinforced concrete by the finite element method. ACI Journal, 65(9), 757-776.

Ouyang, C., Wollrab, E., Kulkarni, S. M., & Shah, S. P. (1997). Prediction of cracking response of reinforced concrete tensile members. Journal of Structural Engineering, ASCE, 123(1), 70-78.

Park, R., & Gamble, W. L. (2000). Reinforced concrete slabs. John Wiley & Sons.

Peltier, R. (1954). Theoretical Investigation of the Brazilian Test,. *RILEM Bulletin (Paris), 19* 31-69.

Phuvoravan, K., Sotelino,E.D. (2005). Nonlinear finite element for reinforced concrete slabs. Journal of Structural Engineering,131 (4), 643-649.

Phillips, D.V., 1973. Non-Linear Analyses of Structural Concrete by Finite Element Methods (Doctoral dissertation, University of Wales ,Swansea).

Poisson, S. D. (1829). Memoire sur l'equilibre et le mouvement des corps elastique. *Mem Acad Sci, 8*, 357.

Prescott, W. S., Ang, A., & Siess, C. P. (1961). Analysis of clamped square plates containing openings with stiffened edges. *University of Illinois Urbana , Illinois, Research Program Carried out in part under National Science Foundation Grant No. G-6572*.

Prakash, S. (2018). Nonlinear Finite Element Analysis of Shrinking Reinforced Concrete Slabs-on-ground. MSc thesis in Concrete Structures.

Rashid, Y. R. (1968). Analysis of Pre-Stressed Concrete Pressure Vessels. *Nuclear Engineering, 7*(4), 334-355.

Rao, P.S., 1966. Die Grundlagen zur Berechnung der bei statisch unbestimmten Stahlbetonkonstruktionen im plastischen Bereich auftretenden Umlagerungen der Schnittkräfte. (Basic Laws Governing Moment Redistribution in Statically Indeterminate Reinforced Concrete Structures)," DAfStb, Ernst & Sohn, Berlin, Heft 177,1966, 99 pp.

Regan, P. E. (1974). Design for punching shear. The Structural Engineer, 52 No.6, 197.

Richart, F. E. (1948). Reinforced concrete wall and column footings. ACI Journal, 45, 97-127 and 237-260.

Rizkalla, S. H., Hwang, L. S., & El-Shahawi, M. (1983). Transverse reinforcement effect on cracking behaviour of reinforced concrete members. Canadian Journal of Civil Engineering, 10, 566-581.

Roknuzzaman, M., Haque, M. R., & Ahmed, T. U. (2015). Analysis of Rectangular Plate with Opening by Finite Difference Method. *American Journal of Civil Engineering and Architecture, Vol. 3, No. 5*, 165-173.

Rots, J. G., Nauta, P., Kuster, G. M. A., & Blaauwendraad, J. (1985). Smeared crack approach and fracture localization in concrete.

Rostasy, F.S., Koch, R., Leonhardt, F. and Patzak, M., 1976. Zur Mindestbewehrung für Zwang von Außenwänden aus Stahlleichtbeton: Versuche zum Tragverhalten von Druckübergreifungsstößen in Stahlbetonwänden. (Minimum Reinforcement for Restrained External Lightweight Reinforced Concrete Walls)," DAfStb, Ernst & Sohn, Berlin, Heft 267, 1976, 83 pp

Rusch, H., Hilsdorf, H. K., & Jungwirth, D. (1983). Creep and Shrinkage-Their Effect on the Behaviour of Concrete Structures. *by Springer-Verlag New York Inc.*

S.P.Timoshenko, & Woinowsky-Krieger, S. (1959). Theory of Plates and Shells. *2nd edn,McGraw-Hill, New York*.

Scanlon, A., 1971. Time dependent deflections of reinforced concrete slabs. Thesis presented at the university of Alberta in 1971 in partial fulfilment of the requirements for the degree of Doctor of Philosophy.

Scanlon, A., & Murray, D. W. (1982). Practical calculation of two-way slab deflections. *Concrete International Magazine*, 43-50.

Scanlon, A., & Murray, D. (1982). Practical calculation of two-way slab deflections. Concrete International: Design & Construction, 43-50.

Scott, R. H., & Beeby, A. W. (2005). Long-term tension stiffening effects in concrete. ACI Journal, 102(1), 31-39.

Scott, R. H., & Beeby, A. B. (2004). Procedures for long term tension stiffening of reinforced concrete tension specimens. *Applied Mechanics and Materials, 1*(2), 239-244.

Scott, R. H., & Beeby, A. B. (2005). Long-term tension-stiffening effects in concrete. *ACI Structural Journal*.

Sheetal, G., & Itti, S. V. (2014). Study on Two way RC Slab using ANSYS with and without central opening. *International Journal of Scientific Engineering and Technology, 3*(8), 1108-1110.

Shehzad, M.K., 2018. Influence of vertical steel reinforcement on the behaviour of edge restrained reinforced concrete walls Ph.D. Thesis presented to the University of Leeds, Leeds, UK).

Sooriyaarachchi, H., Pilakoutas, K., & Byars, E. (2005). Tension stiffening behaviour of GFRPreinforced concrete. ACI Special Publications, 2(230), 975-990.

Subramanian, N. (2013). Design of reinforced concrete structures. Oxford University Press.

Stevens, N. J., Uzumeri, S. M., Collins, M. P., and Will, G. T. (1991). "Constitutive model for reinforced concrete finite element analysis." ACI Structural Journal, 88(1), pp. 49-59.

Szilard, R. (2004). Theories and Applications of Plate Analysis: Classical, Numerical and Engineering Methods. *John Wiley & Sons*.

Talbot, A. N. (1913). Reinforced concrete wall footings and column footings. *University of Illinois Engineering Experiment Station, Bulletin, 67*, 114.

Taylor, P. J. (1969). Initial and Long-Term Deflections of a Reinforced Concrete Flat Plate Structure. *Conference on the Deformation of Concrete and Concrete Structures, Brisbane, Institution of Engineers, Australia*.

Taylor, P. J., & Heiman, J. L. (1977). Long-Term Deflection of Reinforced Concrete Flat Slabs and Plates *ACJ Journal, 74*(11), 556-561.

Tam, K. S. S., & Scanlon, A. (1986). Deflection of two-way slabs subjected to restrained volume change and transverse loads. ACI Journal, Proceedings, 83(5), 737-744.

Teng, S., Cheon, H., Kuang, K., & Geng, J. (2004). Punching shear strength of slabs with openings and supported on rectangular columns. *ACI Struct J., 10*(5), 678-687.

Timoshenko, S., & Goodier, J. N. (1951). Theory of elasticity, 2nd ed. *McGraw-Hill Book Company, New York*.

Timoshenko, S. P. (1913). Sur la stabilite des systemes elastiques. *Ann des Points et Chaussees, 13*, 496-566.

Timoshenko, S. P. (1915). On large deflections of circular plates. *Mem Inst Ways Commun, 89*.

Trost, H. (1967). Auswirkungen des Superpositionsprinzips auf Kriech- und RelaxationsProbleme bei Beton und Spannbeton. *Beton- und Stahlbetonbau, 62*(10), 261-269.

Vecchio, F. J., & Collins, M. P. (1986). The modified compression field theory for reinforced concrete elements subjected to shear. *ACI Journal, 83*(2), 219-231.

Vecchio, F. J., & Selby, R. G. (1991). Toward compression field analysis of reinforced concrete solids. *ASCE Journal of Structural Engineering, 117*(6), 1740-1758.

Vollum, R. L. (2002). Influences of shrinkage and construction loading on loss of tension stiffening in slabs.

Weiss, W.J., 1999. Prediction of early-age shrinkage cracking in concrete elements. Ph.D. Dissertation, Northwestern University, Evanston.

Wright, P. J. F. (1955). Comments on an Indirect Tensile Test on Concrete Cylinders. *Magazine of Concrete Research (London), 7*(20), 87-96.

Wu, M. H. Q. (2010). Tension stiffening in reinforced concrete-instantaneous and time-dependent behavior. (PhD thesis), The University of New South Wales, Sydney, Australia, School of Civil and Environmental Engineering,

Young, J. F., & Mindness, S. (1981). Concrete. *Prentice Hall, New Jersey*.

Zienkiewicz, O.C. and Cheung, Y.K., 1965. Finite element procedures in the solution of plate and shell problems. Chapter 8 of Stres3 Analysis, John Wiley and Sons Ltd., pp.120-144.

Zienkiewicz, O.C. and Cheung, Y.K., 1967. The finite element method in structural and continuum mechanics. McGraw-Hill.

Appendix A

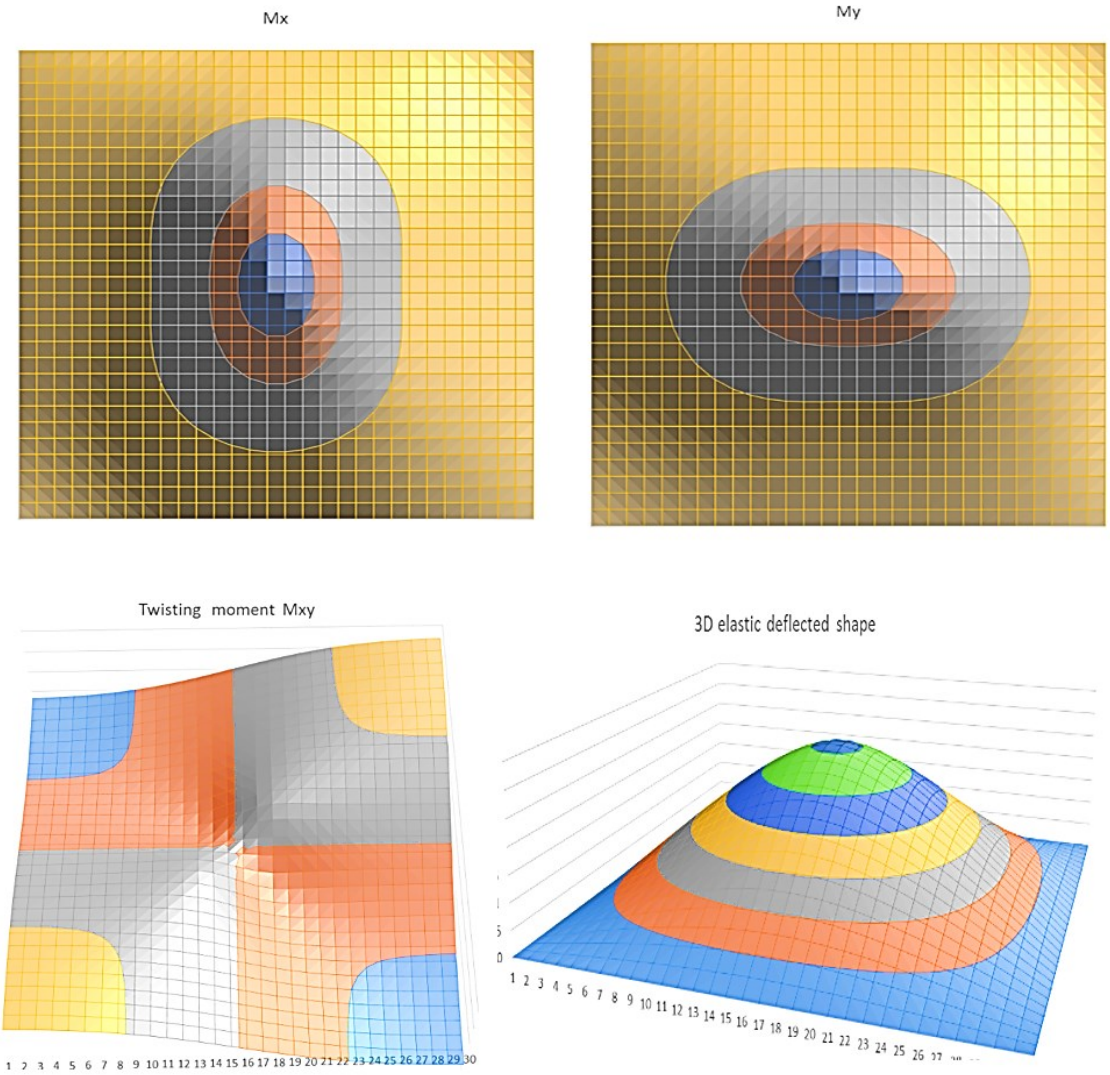

Figure A-1. Contour maps of internal moments and deflections of solid slab at theoretical loading.

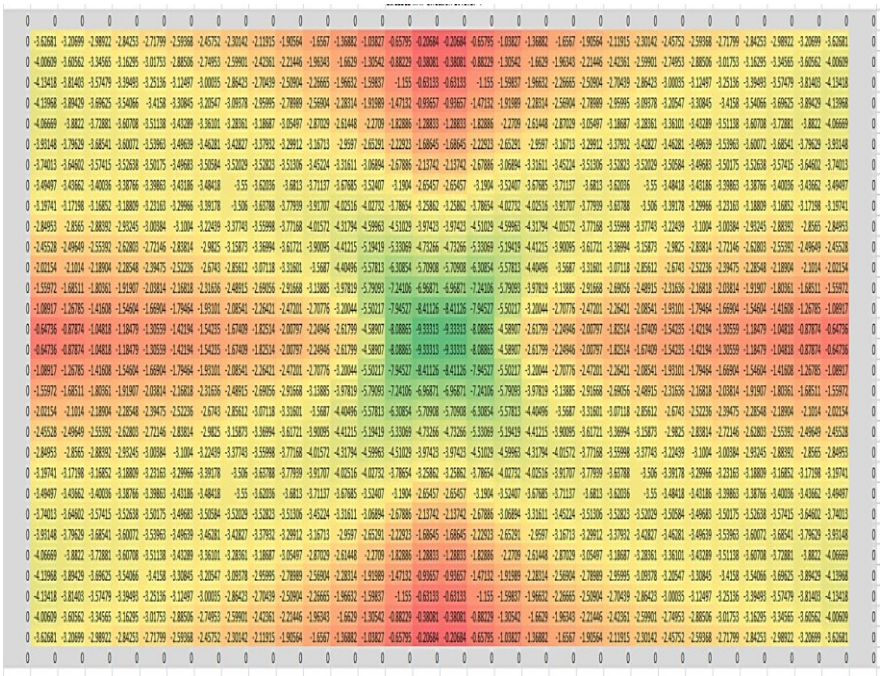

Figure A-2. Stress distribution of extreme compression fibre of the slab S1 under theoretical load 80 KN.

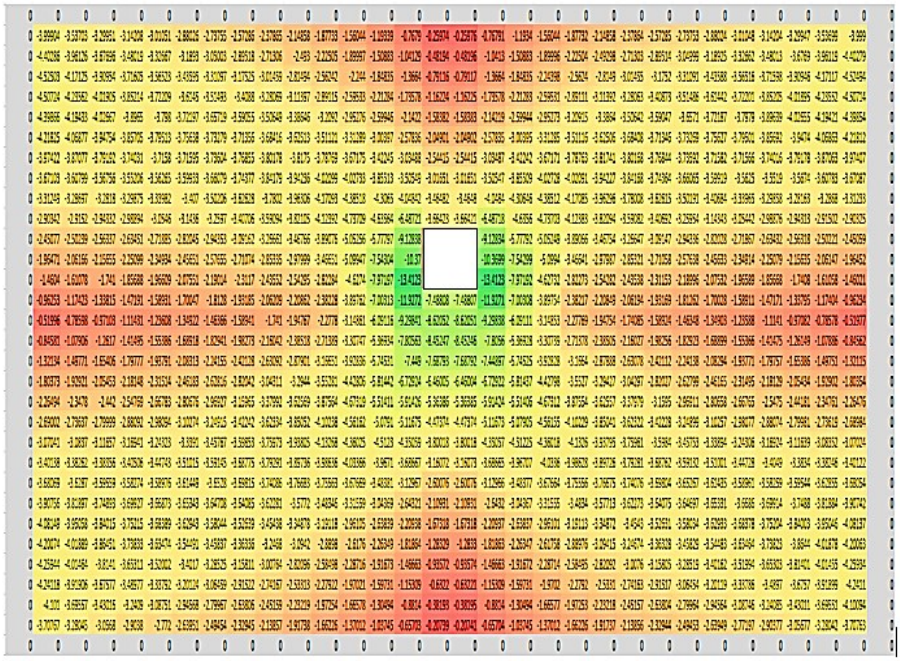

Figure A-3. Stress distribution of extreme compression fibre of the slab S3 under theoretical load 60 KN.

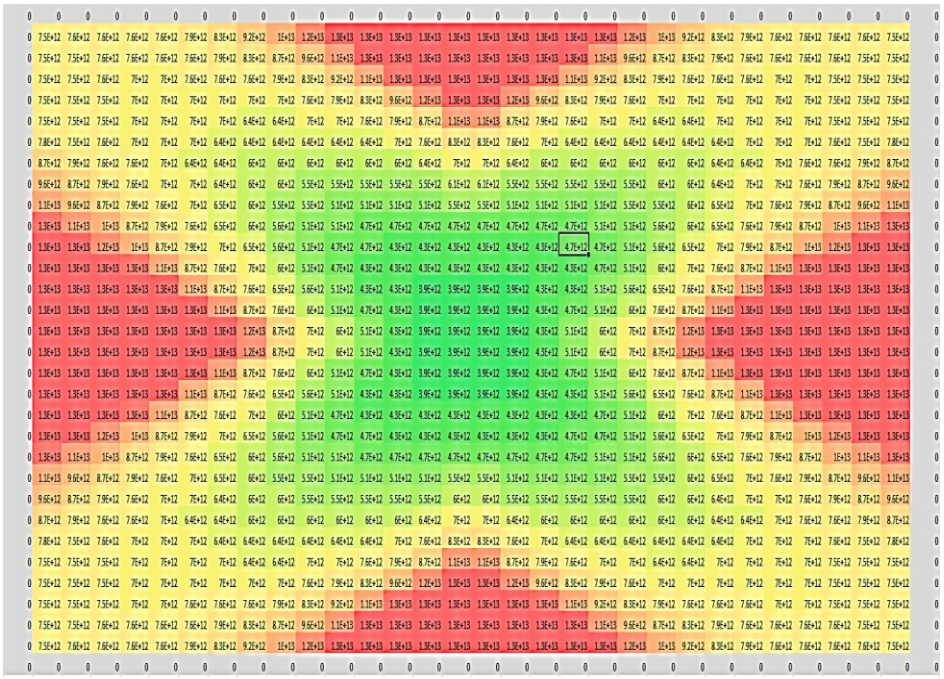

Figure A-4. Reduction in flexural rigidity of the slab S0 under theoretical load 200 KN.

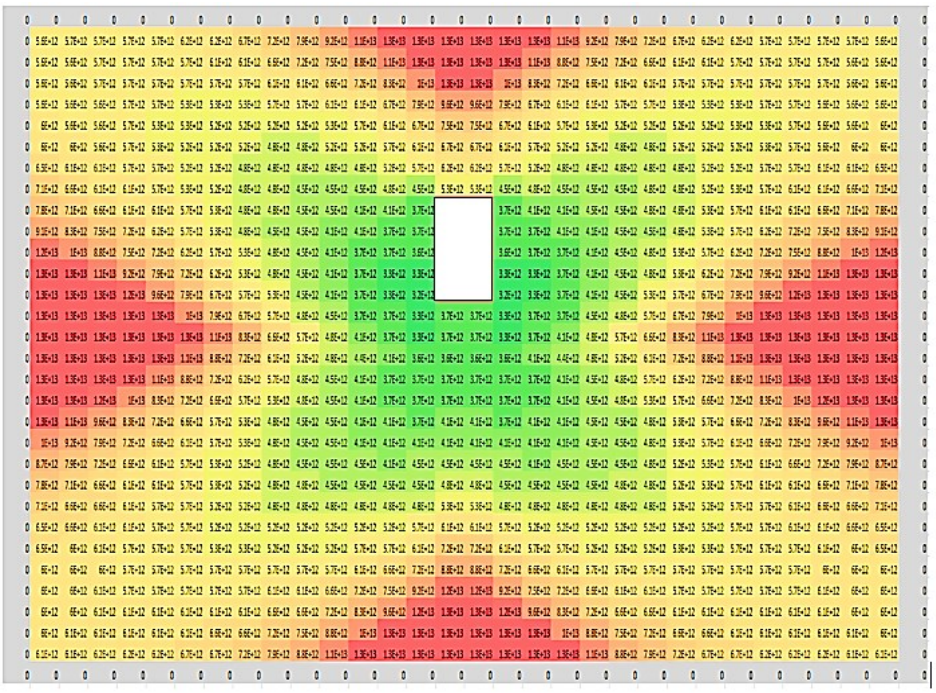

Figure A-5. Reduction in flexural rigidity of the slab S5 under theoretical load 180 KN.